CORTICAL PLASTICITY AND TINNITUS

CORTICAL PLASTICITY AND TINNITUS

By Michal Chrostowski, BASc

A Thesis

Submitted to the School of Graduate Studies
In Partial Fulfillment of the Requirements
for the Degree Doctor of Philosophy

McMaster University

DOCTOR OF PHILOSOPHY (2012)
(Neuroscience)
McMaster University
Hamilton, Ontario

TITLE: Cortical Plasticity and Tinnitus
AUTHOR: Michal Chrostowski, BASc (University of Toronto)
SUPERVISOR: Dr. Suzanna Becker
CO-SUPERVISOR: Dr. Ian C. Bruce
NUMBER OF PAGES: xii, 221

Abstract

Tinnitus is an auditory disorder characterized by the perception of a ringing, hissing or buzzing sound with no external stimulus. Because the most common cause of chronic tinnitus is hearing loss, this neurological disorder is becoming increasingly prevalent in our noise-exposed and ageing society. With no cure and a lack of effective treatments, there is a need for a comprehensive understanding of the neural underpinnings of tinnitus. This dissertation outlines the development and validation of a comprehensive theoretical model of cortical correlates of tinnitus that is used to shed light on the development of tinnitus and to propose improvements to tinnitus treatment strategies.

The first study involved the development of a computational model that predicts how homeostatic plasticity acting in the auditory cortex responds to hearing loss. A subsequent empirical study validated a more biologically plausible version of this computational model. The goal of these studies was to determine whether and how a form of plasticity that maintains balance in neural circuits can lead to aberrant activity in the auditory cortex. The final study extends the validated computational model to develop a comprehensive theoretical framework characterizing the potential role of homeostatic and Hebbian plasticity in the development of most major cortical correlates of tinnitus.

These theoretical and empirical studies provide a novel and complete description of how neural plasticity in adult auditory cortex can respond to hearing loss and result in the development of tinnitus correlates. Furthermore, the final model provides important insights into how tinnitus treatments may benefit from taking into account the behaviour of cortical plasticity after hearing loss.

Preface

This thesis contains a total of five chapters. Chapter 1 provides background and context for the body of work, as well as outlining its contribution to the field. Chapters 2 through 4 are written as empirical journal articles. Chapter 5 discusses the importance of the work along with limitations and future work.

Chapter 2 has been published in the *Journal of Computational Neuroscience*[1] and Chapter 3 has been submitted to and is under review by the *Journal of Neurophysiology*[2]. Material from Chapter 2 is used with permission from Springer Science and Business Media through a License Agreement for use of material in a thesis/dissertation. Material for Chapter 3 is used with consent from the editor of the *Journal of Neurophysiology*.

This research was supported by operating grants from the Natural Sciences and Engineering Research Council of Canada (NSERC) awarded to Dr. Suzanna Becker. During years 2 and 3, this research was also supported by a Tinnitus Research Initiative (TRI) grant awarded to me through Dr. Suzanna Becker. The research was also supported by an Alexander Graham Bell scholarship from NSERC to me during years 4 and 5.

[1] Chrostowski M, Yang L, Wilson HR, Bruce IC, Becker S (2011). Can homeostatic plasticity in deafferented primary auditory cortex lead to traveling waves of excitation? *J Comput Neurosci* 30:279-299.
[2] Chrostowski M, Stolzberg D, Becker S, Bruce IC, Salvi RJ (in revision). A potential role for homeostatic plasticity in adult primary auditory cortex. *J Neurophys* JN-00205-2012.

Acknowledgements

First and foremost, I wish to express my utmost gratitude to Suzanna Becker and Ian Bruce, without whom this body of work would not have been achievable. Their guidance during my doctoral studies has been instrumental in my development as a scientist. It is my belief that the best scientific mentors are those that foster independent scientific inquiry while offering guidance when it is needed. In this respect, my supervisors have excelled as mentors, and have my sincerest thanks. I am also grateful to Daniel Goldreich and Jim Reilly for their assistance during my doctoral studies.

I would like to thank Richard Salvi for allowing me to gain experience in empirical research in his lab space, and for being a truly supportive mentor over the last three years. My thanks are also extended to Daniel Stolzberg and Guang-Di Chen for their friendship and willingness to teach and share ideas.

My time at McMaster would not have been so fulfilling had it not been for those I have met here. In particular, I am grateful to Michael Wong for his friendship, insights, and mutual interest in staying active, and to Nick Déry, for his encouragement and advice over the last four years.

I could not have succeeded in this endeavour without the unwavering support of my parents and brother. In addition, I benefited from the motivation and positive outlook provided to me by my good friend Maxim. Most importantly, I am forever grateful to my wife Julie, whose love and support helped see me through the most challenging moments of the last five years.

All of you have provided me with the inspiration needed to get to this point.

Contents

List of Tables

List of Figures

List of Abbreviations

AI or A1 - primary auditory cortex

AN - auditory nerve

CF - characteristic frequency

CNS - central nervous system

DCN - dorsal cochlear nucleus

HSP - homeostatic plasticity

IC - inferior colliculus

MGB - medial geniculate body

STDP - spike timing-dependent plasticity

Declaration of Academic Achievement

For Chapter 2, the idea behind the original computational model was conceived by Dr. Suzanna Becker, Dr. Ian Bruce and Le Yang, a former doctoral student working with Dr. Becker. I was responsible for implementing the final (published) version of the model, developing the novel results on travelling waves, analyzing and interpreting simulations, and writing the manuscript.

For Chapters 3 and 4, I was responsible for all aspects of research including model conception and implementation, experimental design, data collection and analysis, and writing. For Chapter 3, Drs. Becker, Bruce and Salvi assisted with revising the manuscript while Daniel Stolzberg assisted with the development of software for data analysis.

Background and General Introduction

1.1 Background: The Auditory System

There are several peripheral and central stages in the auditory system at which the sounds that enter our ears are processed before these sounds are represented within the auditory cortex. Furthermore, auditory nuclei throughout the central auditory system have been implicated in tinnitus, which is investigated in this body of work. Figure 1 outlines the ascending pathway of the central auditory system and provides context for the auditory structures discussed in this chapter. These structures include the dorsal cochlear nucleus (DCN), the inferior colliculus (IC) and the primary auditory cortex (AI); the proceeding sections provide an introduction to the auditory periphery and these three auditory centers.

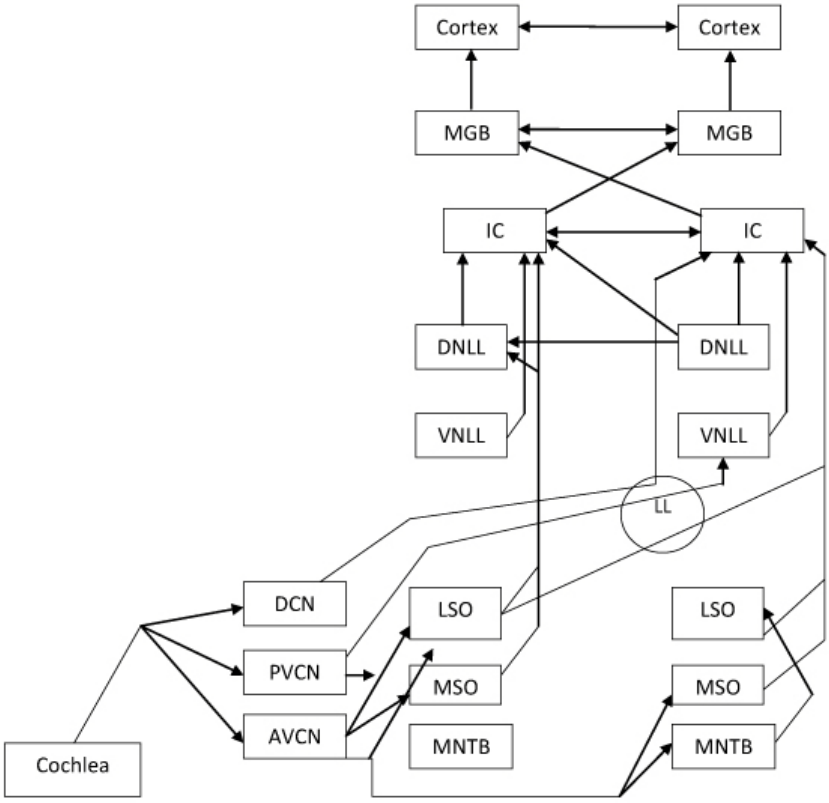

Figure 1.1: The central auditory system. The central auditory pathway begins with the earliest nuclei innervated by auditory nerve fibers originating from the peripheral auditory system. The figure captures major pathways but minor pathways and cortical feedback projections are not included. DCN, dorsal cochlear nucleus; PVCN, posteroventral cochlear nucleus; AVCN, anteroventral cochlear nucleus; LSO, lateral superior olive; MSO, medial superior olivary nucleus; MNTB, medial nucleus of the trapezoid body; LL, lateral lemniscus; VNLL, ventral nucleus of the lateral lemniscus; DNLL, dorsal nucleus of the lateral lemniscus; IC, inferior colliculus; MGB, medial geniculate body.

1.1.1 Auditory Periphery

Sound is first processed by the peripheral auditory system when sound waves enter through the outer ear via the pinna and the external auditory canal (Figure 2). As vibrations impinge on the tympanic membrane (the ear drum), energy is transferred to bony ossicles (the malleus, incus and stapes) in the middle ear. The ossicles are connected to the oval window of the cochlea coupling this window with the tympanic membrane. Thus, the various frequency components and amplitudes characterizing sound are effectively conveyed to the inner ear where vibrations can be encoded as electrical signals (Yost, 2007).

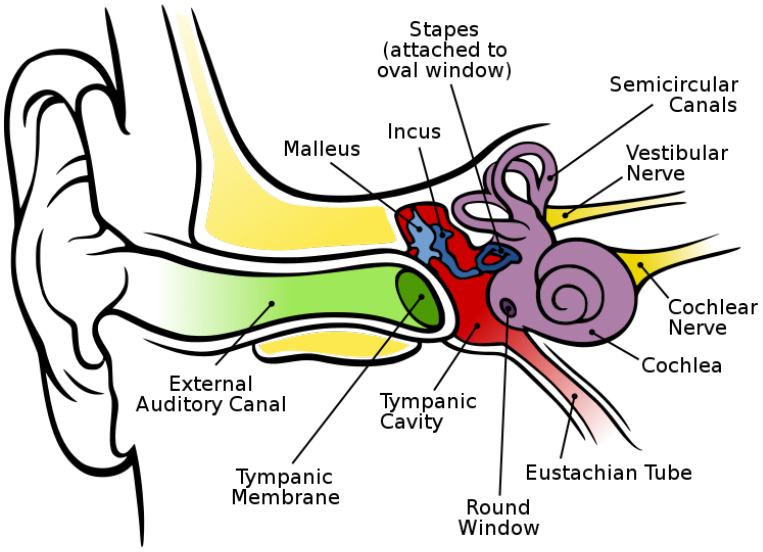

Figure 1.2: A diagram of the peripheral auditory system. The transformation of sound waves entering the ear begins in the auditory canal, eventually becoming encoded as neural firing in the auditory (cochlear) nerve, which drives higher auditory structures.

This figure was adapted from Chittka and Brockmann (2005) and is used in accordance with the PLoS Creative Commons Attribution License.

Within the cochlea, vibrations of the oval window are transferred to a fluid called perilymph. These vibrations move along a membrane called the basilar membrane (see Figure 3) as a traveling wave, which displaces the membrane maximally at different points. The maximum displacement of the basilar membrane is dependent on the membrane's physical properties; these physical properties determine the cochlear tonotopy (i.e. the mapping of frequency components to different points along the basilar membrane) illustrated in Figure 3. A simplified explanation of what follows is that through an interaction between the vibrating basilar membrane and another (tectorial) membrane, hair cells that are found throughout the coiling cochlea are depolarized (Yost, 2007). This depolarization occurs due to a shearing force exerted on stereocilia attached to the hair cells. Louder sounds produce greater displacement at the location of the basilar membrane that is most responsive to the frequency content in that sound, which leads to a greater shearing force on stereocilia and a larger depolarization in the hair cell to which the stereocilia are attached (Yost, 2007). Auditory nerve fibers are connected to hair cells called inner hair cells, and the depolarization of these hair cells leads to spiking in auditory nerve fibers. Thus, nerve fibers that innervate hair cells present throughout the cochlea can encode frequency and amplitude information for an incoming sound.

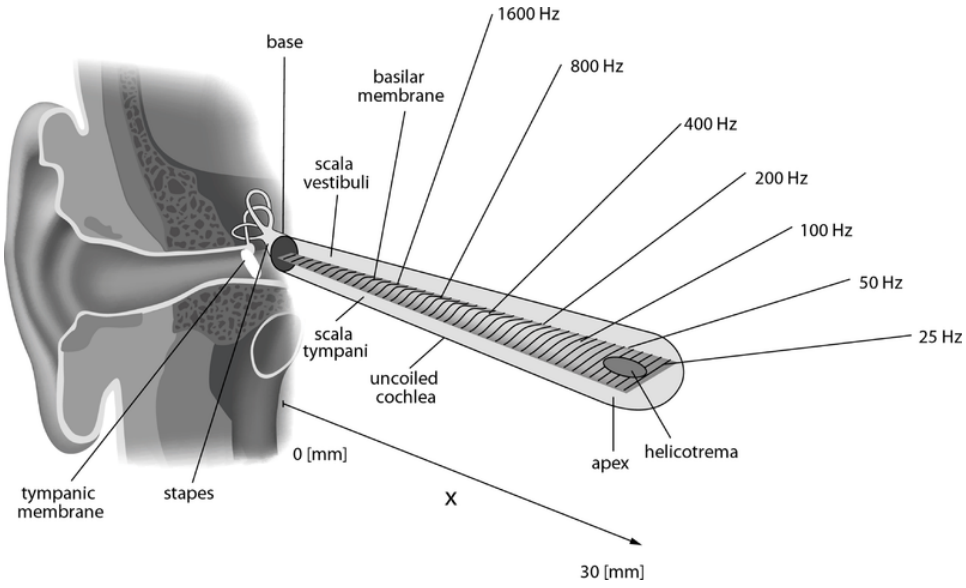

Figure 1.3: The uncoiled basilar membrane within the cochlea. Note that the basilar membrane widens from its base to its apex; this enables different portions of the membrane to be displaced maximally for vibrations of specific frequencies. Namely, the stiffer base has a higher natural frequency of vibration than the more flexible base. This figure was adapted from Kern et al. (2008) and is used in accordance with the PLoS Creative Commons Attribution License.

Frequency tuning throughout the auditory system (e.g. in auditory nerve fibers or a neuron in the central auditory system) can be represented with a tuning curve. This curve illustrates the characteristic frequency (the frequency at which the neuron is most easily excited) and threshold (the sound level required to excite the neuron at each frequency) of the cell or nerve fiber. Figure 4 illustrates a representative tuning curve for an auditory fiber with a characteristic frequency of 15 kHz. Sounds with frequency content further away from the characteristic frequency require increasing sounds levels to

cause the fiber to fire; for auditory nerve fibers the shape of the tuning curve is mainly determined by properties of the cochlear traveling wave discussed above.

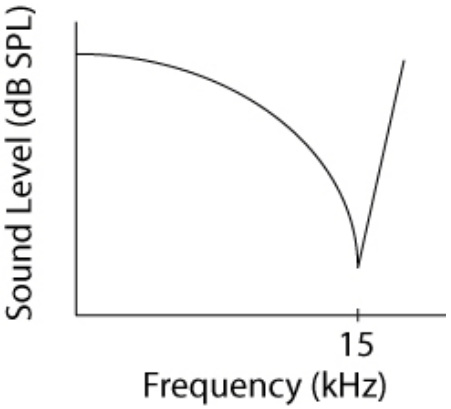

Figure 1.4: A representative tuning curve for an auditory nerve fiber.

As a final note, the type of hearing loss (referred to as sensorineural hearing loss) discussed in this and subsequent chapters is typically caused by damage to hair cells. Namely, when hair cells or stereocilia within a portion of the cochlea are damaged, hearing loss (i.e. elevated hearing thresholds) will be present at frequencies corresponding to that region of the cochlear tonotopy.

1.1.2 Dorsal Cochlear Nucleus

The auditory nerve fibers that enter the cochlear nucleus branch off into its three subdivisions, one of which is the dorsal cochlear nucleus (DCN) (Yost, 2007). While there are many different types of cells in the (dorsal) cochlear nucleus, in this overview it is most important to note that both excitatory and inhibitory neurons and connections are

present. The mixture of interconnected excitatory and inhibitory neurons leads to a wide range of neural response properties in this nucleus. For example, while neurons in the DCN are arranged tonotopically (this tonotopy is inherited from the auditory nerve projections from the periphery), the tuning curves observed in the DCN are not necessarily the same as that seen in Figure 4. Namely, both excitatory and inhibitory regions can be present within a tuning curve for a neuron in the DCN (Pickles, 2008); the functional implication of the presence of inhibition can be sharper tuning even at higher sound intensities. Much work remains to be done on characterizing the function of the DCN, however the multitude of cell types and connections in the DCN imply the ability to process complex sounds (Pickles, 2008).

1.1.3 Inferior Colliculus

The inferior colliculus (IC) is an integration point in the auditory system as it receives the vast majority of ascending auditory inputs, including those from the cochlear nucleus (see Figure 1). The tonotopy of the IC is not directly inherited from the auditory nerve as in the DCN; rather it is derived from the inputs of lower auditory nuclei (Pickels, 2008). Furthermore, unlike the DCN, the IC receives binaural inputs (i.e. from both ears) through various nuclei that are involved in sound localization and identification. These inputs are thought to enable the IC to perform more complex sound localization processing than nuclei lower in the auditory brainstem (Pickles, 2008). Thus, as neural activity moves up the auditory pathway and the outputs of various functional units are integrated the amount of information about the acoustic environment increases.

1.1.4 Primary Auditory Cortex

The final stage in the auditory system that is reviewed here is the primary auditory cortex (AI), which receives auditory information through the medial geniculate body (see Figure 1) and is the first stage of the overall auditory cortical circuit. While AI also contains a tonotopic map, tuning curves observed in awake animals are quite variable and complex (Pickles, 2008); this variability results from interactions between excitatory and inhibitory neurons. Processing in AI occurs within its six layers of distinct cell populations: layers III and IV receive the majority of ascending auditory projections (Pickles, 2008), superficial layers (I and II) contain lateral connections that allow for intracortical processing and are thought to play a role in spectral integration (Stolzberg et al., 2012), and deep layers (V and VI) are output layers that project to subcortical nuclei, higher auditory cortical structures, and other cortical regions. AI forms a complex circuit that may be the earliest auditory region involved in the perception of sound (Meyer, 2011) and sections of which are thought to encode pitch (Bendor and Wang, 2005). Finally, many forms of neural plasticity are observed in AI (Feldman, 2009) and may affect the processing within this network.

1.2 Background: Neural Plasticity

The term neural plasticity refers to the ability of the brain to change over time. More precisely, plasticity encapsulates processes by which the neurons and connections between them are altered (Nelson and Turrigiano, 2008). Neural plasticity is present

throughout the brain and permits learning, the refinement of neural circuits during development and recovery from injury (Feldman, 2009). This background section will provide an overview of two forms of neural plasticity that have been observed and characterized within the cortex and that are investigated with respect to tinnitus in Chapters 2-4: homeostatic plasticity (Chapters 2-4) and Hebbian plasticity (Chapter 4).

1.2.1 Hebbian Plasticity

The idea behind Hebbian-type plasticity (commonly referred to as Hebb's postulate) was put forward by Donald Hebb (Hebb, 1949). The concept can be summarized as follows: if spiking in neuron *A* occurs prior to (typically within milliseconds) spiking in a connected neuron *B*, then the input from neuron *A* to neuron *B* is strengthened; in this scheme, neurons with correlated firing become more strongly interconnected. This plasticity rule describes changes in individual synaptic connections, but on a network level, it captures neural circuit refinement and reorganization, which has implications in sensory processing as well as learning and memory (Bi and Poo, 2001; Caporale and Dan, 2008). However, there is a major issue with the plasticity rule defined above: neurons that fire together will become more strongly interconnected, leading to more correlated firing and potentiation until connections between all correlated neurons are saturated.

While Hebbian plasticity can also describe the weakening of synapses between neurons that do not exhibit correlated activity, the problem stated above remains. Namely, connections between neurons with correlated activity would still saturate, while

connections between neurons with uncorrelated activity would become insignificant. A neural circuit with only these two extremes is not biologically plausible or useful. However, a model of Hebbian-plasticity that can prevent this outcome has been put forward in recent years. Spike-timing-dependent plasticity (for a review see Caporale and Dan, 2008) more precisely defines the way in which synapses are modified by spiking in the pre- and postsynaptic neurons. While a diverse set of temporarily dependent synaptic changes has been categorized as spike-timing-dependent plasticity (Caporale and Dan, 2008), the general rule described here is considered to be a good model for Hebbian-type plasticity in cortical circuits of excitatory neurons. Namely, if neuron *A* fires prior to neuron *B*, the amount by which the input from neuron *A* to neuron *B* is strengthened is inversely proportional to the time elapsed between the spikes. Furthermore, if neuron *A* fires after neuron *B*, the amount by which the input from neuron *A* to neuron *B* is weakened is also inversely proportional to the time elapsed between spikes. The temporal gaps governing these changes are typically on the order of tens of milliseconds. Figure 5 illustrates how the strength of an excitatory synaptic connection is affected by the relative timing of neural spikes. Theoretical models indicate that this form of Hebbian plasticity is stable (i.e. synaptic connections and neural activity will not increase or decrease to the extreme levels discussed above) (for a review see Abbott and Nelson, 2000).

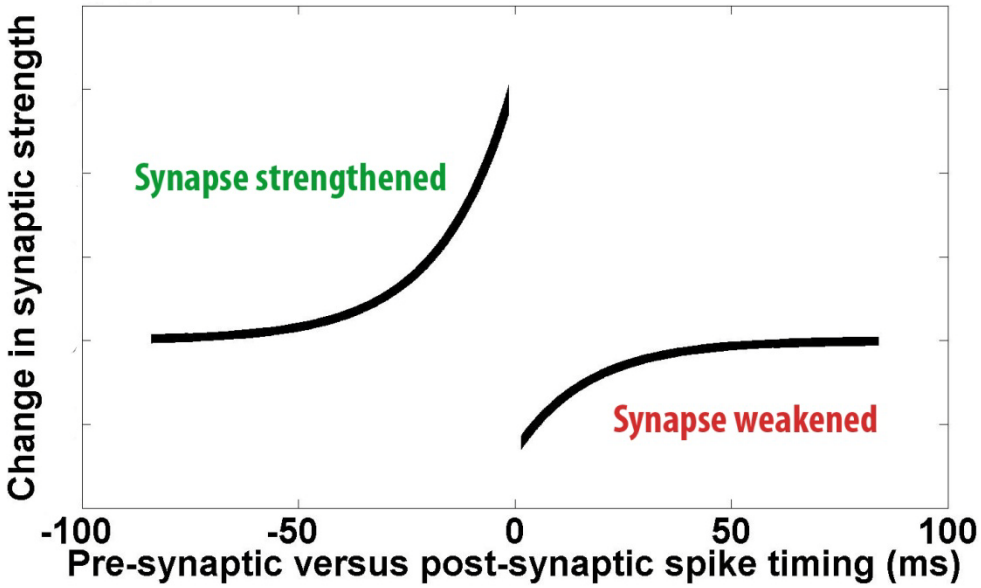

Figure 1.5: Spike-timing-dependent plasticity between excitatory neural units. The amount by which a connection from a pre-synaptic neuron to a post-synaptic neuron is strengthened or weakened falls off exponentially as a function of the relative spike times in the pre- and post-synaptic neurons.

There are other plasticity mechanisms that can ensure stability within a neural network. In particular, homeostatic plasticity is likely to be the most important means by which activity in the brain can remain stable during changes in neural inputs and the action of Hebbian-type plasticity. This form of plasticity is described in the next section.

1.2.2 Homeostatic Plasticity

Neural activity is dynamic and changes depending on what happens to a neuron's synaptic inputs and intrinsic excitability. If information encoded by neurons is to remain

meaningful and neurons are to act as functional components within a neural circuit, neural firing should stay within certain bounds. Homeostatic plasticity acts to maintain activity in a neuron within certain bounds by altering the strength of synaptic inputs or intrinsic properties of that neuron (Turrigiano, 1999). In the context of ongoing brain plasticity, such a mechanism has an important role: as other forms of neural plasticity shape and re-shape neural networks, homeostatic plasticity mitigates the impact on activity in the neural units that comprise these networks (for a review of homeostatic plasticity within this framework see Nelson and Turrigiano, 2008). The timescale at which homeostatic mechanisms operate can vary from hours (Ibata et al., 2008; Chapter 3) to days (Turrigiano et al., 1998; Maffei and Turrigiano, 2008). Thus, the ongoing operation of homeostatic plasticity does not prevent synapse-specific plasticity from changing neural networks. Instead, homeostatic plasticity reduces the possibility of neurons becoming quiescent or hyperactive (Turrigiano, 1999; Turrigiano, 2008).

As mentioned above, homeostatic plasticity can respond to changes in neural activity via changes in intrinsic membrane properties or through changes in synaptic connections. Surprisingly little is known about the underlying mechanisms of homeostatic changes in intrinsic excitability (Nelson and Turrigiano, 2008), although theoretical work indicates that increases or decreases in intrinsic excitability may be triggered by changes in intracellular calcium concentration (Turrigiano, 1999). One way that this trigger can then change excitability is by altering the number and distribution of channels in the membrane such that inward or outward ionic flow is increased or decreased accordingly. While hearing loss can lead to increased intrinsic excitability in

the auditory cortex of developing animals (Kotak et al., 2005), theoretical (Chapter 3) and empirical (Yang et al., 2011) work indicates that this form of plasticity does not play a prominent role in the adult auditory cortex after hearing loss or in the generation of tinnitus.

A better understood form of homeostatic plasticity is synaptic scaling, which is typically defined as a change in the strength of excitatory and/or inhibitory synaptic inputs to a neuron in response to a deviation in that neuron's firing rate from a target range (Turrigiano and Neslon, 2004; Turrigiano, 2008). Namely, if neural firing drops below a target firing rate a homeostatic response can consist of scaling up excitatory synaptic strength and scaling down inhibitory synaptic strength. Furthermore, scaling down excitatory inputs and scaling up inhibitory inputs can reduce neural firing if it exceeds some threshold. Whether synaptic scaling is activated by increased or decreased neural activity, a key aspect of synaptic scaling is that it is multiplicative (Turrigiano, 1999; Turrigiano and Nelson, 2004). This characteristic is important because it preserves the relative strength of synaptic inputs to a neuron (Turrigiano et al., 1999). Thus, this homeostatic mechanism does not interfere with neural connectivity that is crafted by changes in individual synapses via Hebbian plasticity. Figure 6 illustrates how multiplicative synaptic scaling can alter synapses in response to changes in activity without altering the relative strength of synaptic inputs. The role of multiplicative synaptic scaling in the auditory cortex after hearing loss is characterized in Chapters 2-4.

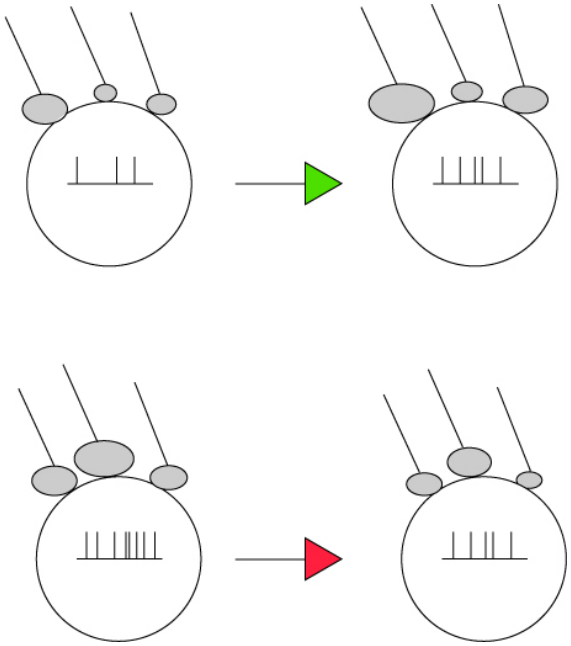

Figure 1.6: A simple schematic of synaptic scaling. The top panel illustrates how neural firing can be increased by scaling up the strength of excitatory synapses (grey ovals). The bottom panel illustrates a reduction in activity through scaling down the strength of excitatory synapses. The efficacy of each synaptic connection is indicated by the size of the oval representing that synapse; the relative strength of synapses remains the same after homeostatic synaptic scaling.

There are several potential mechanisms underlying activation and execution of homeostatic synaptic scaling. When neural activity deviates from a homeostatic target firing rate (possibly indicated by changes in internal calcium concentration), a cascade of signals may initiate changes at synapses across the neuron (Turrigiano, 2008). These changes may include the insertion of additional receptors (AMPA or NMDA) at the postsynaptic site (i.e. in the neuron in which activity has deviated) or presynaptic

alterations (Turrigiano, 2008). The proceeding chapters do not explicitly characterize these underlying mechanisms, and instead focus on how scaling up excitatory connections and scaling down inhibitory connections after hearing loss may contribute to the development of aberrant cortical activity and function at a network level.

Synaptic scaling has been observed in adult auditory cortex (Yang et al., 2011) as well as other adult sensory cortices (Goel and Lee, 2007; Pozo and Goda, 2010). This motivates our theoretical investigation of the potential role of homeostatic plasticity in the development of tinnitus correlates in the primary auditory cortex after hearing loss.

1.3 Tinnitus

1.3.1 Tinnitus and Associated Brain Regions

Tinnitus, a phantom auditory percept commonly described as a ringing, hissing or buzzing sound, has many different origins, and can be transient, intermittent or permanent. Chronic tinnitus, the focus of this thesis (hereafter just referred to as tinnitus), is a complex neurological disorder strongly associated with sensorineural hearing loss, and has no cure. Estimates of the prevalence of tinnitus vary (Heller, 2003; Sanchez, 2004), but it is likely that as much as 10-15% of the population deals with chronic tinnitus every day. Furthermore, at least 1-3% of the population suffers from tinnitus that severe enough to affect their ability to work, sleep and their overall quality of life (Cooper, 1994; Dobie, 2003). This neurological disorder is not limited to particular

segments of the population: while tinnitus is more prevalent in older age groups, a significant percentage (4.7%) of those between the ages of 20 and 29 reports having tinnitus (Heller, 2003). Tinnitus is strongly associated with hearing loss (Eggermont and Roberts, 2004), although there are also cases where tinnitus is present in spite of clinically normal hearing. However, if the hearing loss region begins at frequencies above 8 kHz, it would not be detected clinically (Roberts et al., 2006). Furthermore, even mild noise exposure may permanently reduce activity arising from the auditory periphery without leaving evidence of clinical hearing loss (Schaette and McAlpine, 2011). Therefore, in spite of the existence of different potential causes of tinnitus, it is critical that we elucidate how reduced peripheral activity with or without clinical hearing loss can lead to aberrant plasticity in the brain. This is especially true because tinnitus is likely to become more common in our ageing and noise exposed society.

Studies of damage to the auditory periphery have allowed researchers to shed light on underlying neural mechanisms of this disorder. Important insights into the neuroscience of tinnitus have been gained through salicylate-induced tinnitus (for review see Stolzberg et al., 2012). High doses of salicylate (an active ingredient in aspirin) cause threshold shifts at the auditory periphery as well as tinnitus in humans (Day et al., 1989). Such observations led to the development of reliable animal models (Stolzberg et al., 2012) in which tinnitus could be induced through systemic injection of salicylate. Resulting insights from these models combined with noise trauma models have implicated changes at the auditory brainstem (for review see Kaltenbach, 2007), auditory midbrain (Jastreboff and Sasaki, 1986; Chen and Jastreboff, 1995; Longenecker and

Galazyuk, 2011), and the auditory cortex (Mühlnickel et al., 1998; Seki and Eggermont, 2003; Stolzberg et al., 2012) in tinnitus generation; there is also evidence linking changes in limbic structures to tinnitus (Kraus and Canlon, 2012; Chen et al., in press). Determining which neural correlates of tinnitus in the auditory system are common to salicylate models and noise trauma models may be critical to unraveling the mechanisms underlying tinnitus.

The potential complexity of tinnitus is increased by evidence that the auditory pathway may not be the only part of the brain that is involved in tinnitus generation. Reports of tinnitus modulation through eye, jaw or neck movements (Pinchoff et al., 1998) lead to empirical work implicating somatosensory inputs in the modulation of the phantom auditory percept (Shore et al., 2007; Dehmel et al., 2012). In addition, as mentioned above, a dysregulation in limbic structures has also been implicated in tinnitus (Kraus and Canlon, 2012), likely due to the psychological stress associated with the presence of an unremitting loud phantom noise percept. While the auditory system still plays a key role in such a framework, the implication is that tinnitus is a disorder that involves several pathways. Knowledge of how non-auditory brain structures can contribute to tinnitus has allowed researchers to develop a more complete picture of the tinnitus brain state. That being said, there is convincing evidence that tinnitus is a phenomenon rooted in the central auditory system (for review see Eggermont, 2003; Eggermont and Roberts, 2004; Roberts et al., 2010), which is the focus of the research described in this thesis.

Much of our insights into tinnitus have been gleaned through studies of damage to the auditory periphery. While salicylate is one means of inducing such damage (Stolzberg et al., 2012), studying tinnitus correlates in the context of hearing loss during ageing or through noise trauma is essential because tinnitus is most commonly caused by these factors (Roberts et al., 2010). It is widely agreed that tinnitus is a central phenomenon that may be initiated by peripheral damage, but persists as a result of changes in central auditory structures (Roberts et al., 2010). While objective tinnitus (Møller, 2007) can be heard by an examiner, tinnitus most commonly refers to a subjective percept that is not driven by any detectable acoustic stimulus. Indeed, reports of tinnitus persisting even after sectioning of the auditory nerve (Anari, 1999) indicate that aberrant activity associated with tinnitus is not coming directly from the auditory nerve and that central changes after hearing loss are necessary for the persistence of chronic tinnitus.

The dorsal cochlear nucleus (DCN) is the earliest nucleus in the central auditory system that has been implicated in the development of tinnitus (for review see Kaltenbach, 2007). Early observations suggested that noise trauma elicited spontaneous hyperactivity in the DCN (Kaltenbach et al., 1998). Further empirical work characterized hyperactivity in fusiform cells in the DCN of chinchillas after animals were exposed to acoustic trauma and linked this altered activity to tinnitus (Brozoski et al., 2002). Namely, these animals had significantly improved discrimination (signal not present versus signal present) of 1-kHz tones, which was hypothesized to mean that subjective ringing tinnitus with a 1-kHz frequency increased the likelihood of detecting stimuli at 1-kHz. While it cannot be said with certainty that this psychophysical measure is an

indicator of tinnitus, the fact that noise trauma can evoke tinnitus in humans suggests that increased spontaneous activity in the DCN may be a tinnitus correlate. Furthermore, other behavioural tasks that are thought to determine whether an animal is experiencing tinnitus have also been linked to hyperactivity in the DCN (Dehmel et al., 2012). Importantly, subsequent work has implicated plasticity-mediated reduction in glycinergic inhibition (for review see Wang et al., 2011) and strengthening of somatosensory inputs to DCN (Dehmel et al., 2012) as potential mechanisms underlying noise-induced hyperactivity.

Further up the auditory pathway, the inferior colliculus (IC) has also been implicated in tinnitus in animal models (Jastreboff and Sasaki, 1986; Chen and Jastreboff, 1995; Melcher et al., 2009), in humans (Melcher et al., 2009) and in computational models (Gerken, 1996). While much of the early work implicating elevated spontaneous and driven activity in the IC in tinnitus was done using an animal model of salicylate-induced tinnitus (Jastreboff and Sasaki, 1994), there is also evidence linking IC hyperactivity with tinnitus induced by noise trauma (Ma et al., 2006; Longenecker and Galazyuk, 2011). Interestingly, there seemed to be a gradual reduction in the frequency range representing the tinnitus percept over a period of two to three months after acoustic trauma (Longennecker and Galazyuk, 2011). This change in the purported tinnitus percept may have resulted from threshold recovery at the periphery or plasticity-driven changes in the central auditory system (Milbrandt et al., 2000; Browne et al., 2012). Connecting behavioural evidence of tinnitus with aberrant activity in the IC at different time points has allowed researchers to shed light on how tinnitus correlates develop over time. However, there is still much work to be done in characterizing a process in the

auditory pathway that can gradually lead to chronic tinnitus. More importantly, it is unclear if changes that develop over time occur primarily in subcortical auditory structures.

With evidence of several auditory and non-auditory structures playing a role in tinnitus, there is no doubt that tinnitus has various potential causes. However, as we discuss in greater detail shortly, the auditory cortex is the most likely origin for several correlates of tinnitus, and is therefore likely to be the locus of the tinnitus percept (Eggermont, 2008). Therefore, shedding light on cortical changes that are related to tinnitus is critical in order to understand the phantom auditory percept. Furthermore, since there is a large gap in our knowledge of the neural mechanisms that underlie the emergence of cortical correlates of tinnitus, elucidating these mechanisms is a likely requirement for effective tinnitus treatments. Fortunately, over the last two decades, several key insights have been put forward as to how peripheral damage can result in changes in activity and processing at the level of the auditory cortex. These insights resulted from empirical and computational studies, and have brought us closer to understanding and treating chronic tinnitus.

There are several correlates of tinnitus that have been described in the primary auditory cortex. It is clear that after peripheral damage, tonotopic reorganization can occur at the level of the primary auditory cortex (Robertson and Irvine, 1989; Calford et al., 1993; Seki and Eggermont, 2003; Noreña et al., 2003). Magnetoencephalographic recordings have indicated that cortical reorganization may be correlated with the perception of tinnitus (Mühlnickel et al., 1998), though it is as yet unclear if the tinnitus

percept is represented in the reorganized region of the cortex (Yang et al., 2011) or if reorganization is necessary for tinnitus perception (Langers et al., 2012). Other potential correlates of tinnitus, including increased spontaneous firing and synchrony, have been observed within the reorganized primary auditory cortex (Komiya and Eggermont, 2000; Seki and Eggermont, 2003), indicating that tonotopic reorganization may play a role in tinnitus. At the very least, a correlation between cortical reorganization and tinnitus in the presence of hearing loss indicates that similar neural mechanisms may bring about both. There is evidence that treating tinnitus may require addressing cortical reorganization (Engineer et al., 2011). While this does not necessarily imply that tinnitus is represented in the reorganized region, it does suggest that harnessing the same neural mechanism which brought about cortical reorganization to undo the shifts in tonotopy may also reduce tinnitus. However, changes in cortical receptive fields are not the only potential correlates for tinnitus, and focusing on reorganization alone may hinder tinnitus treatment avenues.

As is the case for subcortical auditory regions, much work has been done to investigate a link between changes in spontaneous activity and tinnitus at the cortical level. Evidence from both noise trauma (Kimura and Eggermont, 1999; Seki and Eggermont, 2003; Noreña and Eggermont, 2003) and salicylate (Stolzberg et al., 2012; Stolzberg et al., 2012) animal models of tinnitus indicate that spontaneous activity in the auditory cortex becomes abnormal after peripheral damage. Elevated spontaneous activity (Kimura and Eggermont, 1999; Seki and Eggermont, 2003) and spontaneous synchrony (Seki and Eggermont, 2003; Noreña and Eggermont, 2003) have been

observed in acute studies of noise trauma, and may underlie tinnitus that occurs soon after exposure to loud sounds. On the other hand, long-term changes in spontaneous cortical activity can be evoked by the action of plasticity mechanisms (Chapter 2) and may contribute more to chronic tinnitus. Characterizing the potential role of neural plasticity in tinnitus generation would benefit from a more complete picture of spontaneous correlates of tinnitus. Recent studies of cortical correlates of tinnitus in humans may provide an important piece of the tinnitus puzzle.

Further evidence linking tinnitus to abnormal spontaneous activity in the cortex has come from studies of oscillatory activity and how it is linked to tinnitus. Increased amplitude in delta- and gamma-band oscillations along with reductions in alpha-band oscillations have been correlated with tinnitus (Weisz et al., 2005; Weisz et al., 2007). In fact, empirical studies suggest a causal link between altered oscillatory activity and tinnitus. Significant tinnitus relief was achieved by tinnitus subjects that were able to normalize delta-band and alpha-band oscillations using a neuro-feedback approach (Dohrmann et al., 2007). Furthermore, delta-band activity was reduced during periods of residual inhibition (a 50% or greater reduction in tinnitus loudness) induced in tinnitus subjects by using a tonal masker (Kahlbrock and Weisz, 2008). These observations along with a link between cortical reorganization and tinnitus (Mühlnickel et al., 1998) highlight the potential importance of plasticity-mediated auditory cortical changes and the phantom auditory percept. A greater understanding of how neural plasticity can contribute to cortical correlates of tinnitus, specifically after hearing loss, will shed light

on the underlying neural mechanisms of tinnitus as well as providing new insights into tinnitus treatments.

1.3.2 Neural Plasticity and Tinnitus

A common theme in the discussion of tinnitus correlates in all auditory structures implicated in tinnitus is the potential role of plasticity. Namely, it appears that neural plasticity can have negative effects if it is activated within an auditory structure after hearing loss (Rajan 2001; Wang et al., 2011; Chapter 3). The primary auditory cortex is no exception; the actions of aberrant cortical plasticity may lead to tinnitus, a neurological disorder that can be very disruptive. However, the questions of which plasticity mechanisms in the auditory cortex contribute to tinnitus and characterizing the way in which they lead to tinnitus correlates are largely unanswered.

Hints as to which aspects of cortical plasticity contribute to tinnitus are found in studies investigating damage to the auditory periphery. An over-representation of frequencies adjacent to the lesioned frequency region develops within months of mechanical lesions in the cochlea (Robertson and Irvine, 1989; Rajan et al., 1993). Changes in the tonotopic organization of the auditory cortex have also been observed after milder forms of hearing loss after acoustic trauma (Eggermont and Komiya, 2000; Seki and Eggermont, 2003). Interestingly, cortical reorganization was not evident immediately after damage (Robertson and Irvine, 1989), suggesting that gradual synaptic changes may be occurring in the auditory cortical circuit over a timescale of days to weeks. Furthermore, soon after acoustic trauma, activity in cortical neurons representing

frequencies below the hearing loss region becomes more correlated with activity of neurons within the affected region (Noreña and Eggermont, 2003). This increase in synchrony could lead to aberrant levels of plasticity, as Hebbian plasticity is driven by synchronous neural activity (for review see Bi and Poo, 2001). Thus, gradual changes in the auditory cortex after damage to the auditory periphery may be mediated by Hebbian-type plasticity. If this were the case, it would implicate one particular form of neural plasticity in tinnitus.

Homeostatic plasticity (HSP) is another neural mechanism that may be involved in changes in a sensory cortex after damage to the periphery (Maffei et al., 2004; Maffei and Turrigiano, 2008). A handful of empirical studies provide evidence of the actions of HSP within the auditory cortex. In particular, animal models of hearing loss models have implicated homeostatic plasticity in increases in the strength of excitatory synaptic inputs (Kotak et al., 2005) as well as in decreases in inhibitory synaptic transmission (Kotak et al,. 2005; Yang et al., 2011) at the level of the primary auditory cortex after damage to the auditory periphery. A study that combined whole-cell recordings with a behavioural measure of tinnitus suggested that the region of the auditory cortex where homeostatic plasticity responded to hearing loss is responsible for the pitch of the tinnitus percept (Yang et al., 2011). However, there is a dearth of knowledge as to the way in which homeostatic plasticity can lead to tinnitus generation at the level of the auditory cortex. Unfortunately, homeostatic plasticity is a complex process, with many potential pathways through which to maintain a desired level of neural activity (for review see Turrigiano, 1999; 2008).

The presence of Hebbian plasticity can theoretically destabilize a cortical network (Turrigiano, 1999; Abbott and Nelson, 2000). Homeostatic plasticity (HSP) aims to prevent this by scaling synaptic weights (Rutherford et al., 1998; Turrigiano et al., 1998; Burrone et al., 2002; Turrigiano, 2008) or neural excitability (Desai et al., 1999) in order to keep neural firing close to a homeostatic set-point. The way in which a synapse is scaled by HSP is also dependent on whether the post-synaptic neuron is excitatory or inhibitory (Rutherford et al., 1998). Early studies of homeostatic plasticity in cortical cultures indicated that activity blockade would, after days to weeks, lead to increases in excitatory synaptic transmission (Turrigiano et al., 1998) and decreases in inhibitory synaptic transmission (Rutherford et al., 1998). Later work provided evidence of HSP as a response to visual deprivation *in vivo* (Maffei et al., 2004; Maffei and Turrigiano, 2008). In addition, computational (LeMasson et al., 1993) and empirical (Desai et al., 1999) studies suggest that altering neural excitability in response to perturbed input activity may be another means of responding to changes mean neural activity. Therefore, a neuron can attempt to retain a certain level of activity in the face of deafferentation or over-stimulation through a wide range of pathways. Furthermore, in spite of early evidence indicating a slow (i.e. days to weeks) timescale of operation for homeostatic plasticity, there is also evidence of rapid homeostatic responses after a drop in neural firing *in vitro* (Ibata et al., 2008) and in intact adult CNS (Riegle and Meyer, 2007). While there is evidence for both synaptic scaling (Kotak et al., 2005; Yang et al., 2011) and changes in neural excitability (Kotak et al., 2005) in the primary auditory cortex after hearing loss, untangling which homeostatic mechanisms may be active for different types

of hearing loss or even the timescales at which these mechanisms operate, are unanswered questions. Furthermore, since homeostatic plasticity has been implicated in tinnitus perception (Yang et al., 2011), it is important to elucidate which mechanisms may be involved in the emergence of the many cortical tinnitus correlates that have been discussed.

Another way in which activity can remain relatively stable in a network is if Hebbian-type plasticity is present in a more restricted form referred to as spike-timing-dependent plasticity (STDP) (for review see Abbott and Nelson, 2000; Caporale and Dan, 2008). In this case, it is not simply correlated neural firing that strengthens connections, but rather, the relative spike timing of two neurons will determine whether and to what extent a connection is strengthened or weakened. Computational modelling work suggests that spike-timing-dependent plasticity can induce competition in a network without creating instabilities as long as individual synapses are restricted to some maximum value (Song et al., 2000). While this makes STDP a plausible neural plasticity mechanism, the presence of STDP along with HSP may allow for a biologically plausible cortical circuit while eliminating the need for artificial constraints or restrictions. Although there is some evidence of both HSP (Kotak et al., 2005; Yang et al., 2011) and STDP (Dahmen et al., 2008) in primary auditory cortex, our understanding of how the two forms of plasticity co-exist and respond to hearing loss are minimal at best. These are important questions on their own, but predicting potential answers to such questions may also be required if we are to understand how cortical mechanisms can contribute to the development of tinnitus.

1.3.3 Computational Models and Tinnitus

Studying the underpinnings of homeostatic or activity-dependent plasticity after hearing loss over a long period using an empirical model may not be technically feasible. However, a computational model could predict how the actions of Hebbian-type plasticity or homeostatic synaptic scaling could lead to cortical reorganization as well as generally agreed upon correlates of tinnitus. This theoretical framework could elucidate how cortical plasticity may respond to hearing loss and which resultant changes in the cortex may have the unintended effect of generating tinnitus. Computational models have been used in the past to shed light on tinnitus correlates at several levels of the auditory system (for a detailed review see Schaette et al., 2012) as well as providing insight into other neurological disorders (Fröhlich et al., 2008) that, like tinnitus, may emerge after plasticity mechanism create hyperexcitability within a neural circuit.

An early computational model suggested that hearing loss could lead to elevated spontaneous activity in the inferior colliculus (Gerken et al., 1996). The conclusion of this model was that a drop in peripheral activity would reduce lateral inhibition in the hearing loss region at the level of the IC and lead to neural hyperexcitability. However, this rate-based model did not capture the changes in spontaneous neural synchrony or any changes in tuning. Furthermore, the potential role of neural plasticity after hearing loss could not be investigated with this model. Finally, while the tinnitus pitch may span the hearing loss region (Roberts et al., 2006), this model only accounted for abnormal activity near the edge of hearing loss. That being said, model predictions that lateral

inhibition could lead to the development of tinnitus correlates was an important theoretical contribution towards our understanding of this auditory disorder.

Further theoretical work suggested that reductions in inhibition, as well as increases in excitation could be mediated by homeostatic plasticity (Dominguez et al., 2006; Schaette et al., 2006). These changes in synaptic efficacy were simulated as a response to reduced peripheral activity after hearing loss (Liberman and Dodds,1984). The models that produced these simulations predicted that abnormal spontaneous activity in the cochlear nucleus (Schaette et al., 2006) and the primary auditory cortex (Dominguez et al., 2006) would emerge as a result of HSP. Thus, a HSP-mediated drive to maintain target levels of mean activity could have undesired effects on spontaneous activity; the resultant elevations in spontaneous firing and synchrony may underlie tinnitus (Eggermont and Roberts, 2004). These models shed light on how homeostatic plasticity may play a role in tinnitus because of its ability to shift the balance between excitation and inhibition in order to maintain a target neural firing rate. While reduced inhibition may arise soon after peripheral damage (Gerken et al., 1996; Scholl and Wehr, 2008), theoretical work suggests that a long-term reduction in inhibition can also be mediated by neural plasticity.

The models described above captured some but not all correlates of tinnitus. Specifically, they show that reduced inhibition along with increased excitation can increase spontaneous or driven firing rates, as well as spontaneous synchrony. These changes in activity are considered to be neural correlates of tinnitus (Eggermont and Roberts, 2004). However, there are other important neural correlates of tinnitus

(Mühlnickel et al., 1998, Weisz et al., 2007) that are not explained by the models described above. In particular, changes in delta and gamma oscillations and changes in tuning and tonotopic map organization necessitate the incorporation of greater biological detail into the models. Extending existing models to exhibit oscillatory behaviour would permit a theoretical study of changes in oscillatory activity after hearing loss.

Furthermore, at the level of the auditory cortex, a more complete model of tinnitus necessitates investigating the way in which neural plasticity can affect receptive fields and tuning in after hearing loss. It is important to note that while cortical reorganization may play a role in tinnitus (Mühlnickel et al., 1998; Engineer et al., 2011), there is debate as to whether reorganization is necessary (Langers et al., 2012) or if tinnitus is represented by regions in the auditory cortex where inhibition has been reduced by HSP (Yang et al., 2011). A computational model that can capture cortical reorganization as well as other tinnitus correlates can shed light on which tinnitus correlates co-exist, and how neural plasticity may cause them to emerge. Indeed, a better understanding of the behaviour of auditory cortical plasticity may help us understand why tinnitus can be correlated with hearing loss regions (Roberts et al., 2006) but also why it may be present without clinically evident peripheral threshold shifts (Weisz et al., 2006).

In spite of the clear need for effective tinnitus treatment or elimination, there is as yet no cure and treatment results have been mixed at best. Since computational models have already characterized how hearing loss can result in some tinnitus correlates, there may be a role for computational models in the development of more effective tinnitus treatments. However, it is likely that a more complete theoretical model of tinnitus, that

can also capture cortical reorganization and changes in oscillatory activity (Weisz et al., 2007), must be developed in order to meaningfully direct future tinnitus therapies.

1.3.4 Summary of Studies

The computational and empirical studies described in this dissertation are important and novel contributions to our understanding of tinnitus correlates at the level of the primary auditory cortex. In addition, these studies have also provided new insights into the function of homeostatic and Hebbian-type plasticity in adult auditory cortex in the context of hearing loss. While this work addresses important unanswered questions about plasticity in adult auditory cortex, ultimately, the significance of these findings is that they can better characterize how tinnitus may develop and how it can be more effectively mitigated.

The first study introduces the role of homeostatic plasticity in the primary auditory cortex and its response to damage at the auditory periphery. The model builds on earlier work where connection weights were changed manually (Dominguez et al., 2006) by describing the computational underpinnings of synaptic scaling. Similar to the previous model and empirical work, the model predicts the development of elevated spontaneous firing and synchrony. In addition, the model predicts changes in cortical receptive fields and the development of short-range travelling waves of spontaneous activity.

The study outlined in Chapter 3 coupled a refined computational model with an empirical study. The purpose of this work was to validate a biologically plausible

computational model of rapid homeostatic plasticity. This was done through an electrophysiological study of the effect of acoustic trauma on receptive fields in adult Sprague-Dawley rat auditory cortex. The empirical work predicted a gradual broadening in receptive fields just below or near the region affected by a tonal trauma. This was in agreement with the computational model, which was used to characterize how such changes can develop gradually while rapid HSP responds to peripheral damage. Furthermore, simulations of the computational model were used to compare different variants of HSP in order to determine which connections and layers of the adult auditory cortical circuit are most likely to explain observations from the multi-unit recordings in the empirical study. Because there is very little existing knowledge of how HSP operates in adult auditory cortex, combining empirical and theoretical work led to important insights in this field. Briefly, it appears that in adult auditory cortex, rapid HSP may most readily act on intracortical synapses in superficial cortical layers. However, like the model described in Chapter 2, this model did not predict tonotopic reorganization. Cortical tonotopic reorganization is observed in studies of damage to the auditory periphery and is a debated correlate of tinnitus.

The final computational study builds on earlier work to capture most of the generally agreed upon tinnitus correlates, including changes in oscillatory activity within the delta and gamma bands, as well as tonotopic reorganization. This required the addition of gap junctions between inhibitory inter-neurons to generate fast synchrony within the gamma band, and spike-timing-dependent plasticity (STDP) at excitatory synapses, building on the previous empirically validated model. Importantly, simulations

with and without the presence of the Hebbian-type plasticity were compared to determine whether including STDP altered predicted changes in spontaneous firing and synchrony from the empirically validated model and the first HSP model. Since predictions were not qualitatively different, the updated model was also used to describe how different hearing loss profiles affect tonotopic organization and increases in delta-band and gamma-band oscillatory activity in the auditory cortex.

Simulations of tinnitus correlates after hearing loss were in agreement with empirical observations and permitted a theoretical investigation of tinnitus treatment strategies. This final step presents an important clinical contribution of this study and of the dissertation as a whole. Namely, it appears that by taking into account cortical plasticity after hearing loss, we may be able to devise more effective measures for reducing tinnitus correlates.

1.3.5 Overview of Methods

Computational modelling development

The computational models described here are network-level models of the primary auditory cortex. The models are described in detail in subsequent chapters, but essentially consist of excitatory and inhibitory neural units that are driven by thalamic input units; the first two models use mutually independent Poisson processes to generate thalamic inputs, while the final model simulates an auditory nerve fibre response that is processed before being input the cortical model. The first model consists of neural units whose behaviour is described by a leaky integrate-and-fire (LIF) neural model.

Furthermore, thalamic inputs in the first model only drive excitatory neural units. Excitatory and inhibitory cortical units are interconnected, but connections from the inhibitory neural units span larger sections of the network. Thus, there is a lack of feed-forward inhibition and the presence of lateral inhibition.

The model described in Chapter 3, utilizes a more biophysically realistic neural model (Izhikevich, 2003) to capture the behaviour of neural units in the network. Furthermore, the network model utilizes balanced inhibition rather than lateral inhibition, in accordance with empirical evidence (Wehr and Zador, 2003; Wu et al., 2008) that balanced inhibitory inputs with the same spatial or frequency range as that of the excitatory inputs are more likely in primary auditory cortex. In addition, this model also took into account feed-forward inhibition (Cruikshank et al., 2007). Finally, activity levels in the model were lowered so as to be more similar to empirical observations.

The model discussed in Chapter 4 builds on the computational model described in Chapter 3, with two main additions to the architecture and one new plasticity mechanism. Firstly, the cortical model is now driven by a model of the auditory periphery (Zilany et al., 2009), which enabled realistic simulations of driven input activity as well as hearing loss. Secondly, the model includes gap junctions between inhibitory neural units, which permitted simulation of certain oscillatory behaviours. Finally, simulation of Hebbian-type plasticity was included in this model by adapting a model of spike-timing-dependent plasticity (Masquelier et al., 2008) to our model.

Empirical methods

The empirical component of this dissertation consists of an electrophysiology study that is described in detail in Chapter 3. Briefly, multi-channel, multi-unit recordings from the primary auditory cortex of adult Sprague-Dawley rats were used to investigate the effect of a tonal noise trauma on excitatory receptive fields over a span of 8 hours.

References

Abbott LF, Nelson SB (2000). Synaptic plasticity: taming the beast. *Nat Neurosci* 3 Suppl:1178-83.

Anari M, Axelsson A, Eliasson A, Magnusson L (1999). Hypersensitivity to sound–questionnaire data, audiometry and classification. *Scand Audiol* 28:219–230.

Bendor D, Wang X (2005). The neuronal representation of pitch in primate auditory cortex. *Nature* 25;436(7054):1161-5.

Bi G, Poo M (2001). Synaptic modification by correlated activity: Hebb's postulate revisited. *Annu Rev Neurosci* 24:139-66.

Browne CJ, Morley JW, Parsons CH (2012). Tracking the expression of excitatory and inhibitory neurotransmission-related proteins and neuroplasticity markers after noise induced hearing loss. *PLoS One* 7(3):e33272.

Brozoski TJ, Bauer CA, Caspary DM. (2002). Elevated fusiform cell activity in the dorsal cochlear nucleus of chinchillas with psychophysical evidence of tinnitus. *J Neurosci* 22(6):2383-90.

Burrone J, Byrne MO, Murthy VN (2002). Multiple forms of synaptic plasticity triggered by selective suppression of activity in individual neurons. *Nature* 420:414-418.

Calford MB, Rajan R, Irvine DR (1993). Rapid changes in the frequency tuning of neurons in cat auditory cortex resulting from pure-tone-induced temporary threshold shift. *Neuroscience* 55:953-964.

Caporale N, Dan Y (2008). Spike timing-dependent plasticity: a Hebbian learning rule. *Annu Rev Neurosci* 31:25-46.

Chen, GD and Jastreboff, PJ (1995). Salicylate-induced abnormal activity in the inferior colliculus of rats. *Hear Res* 82, 158–178.

Chen GD, Manohar S, Salvi R (in press). Amygdala hyperactivity and tonotopic shift after salicylate exposure. *Brain Res* 2012 Mar 13.

Chittka L, Brockmann A (2005). Perception space—the final frontier. *PLoS Biol* 3(4): e137.

Chrostowski M, Yang L, Wilson HR, Bruce IC, Becker S (2011). Can Homeostatic Plasticity in Deafferented Primary Auditory Cortex Lead to Traveling Waves of Excitation? *J Comput Neurosci* 30:279-299.

Chrostowski M, Stolzberg D, Becker S, Bruce IC, Salvi RJ (in revision). A potential role for homeostatic plasticity in adult primary auditory cortex. *J Neurophys* JN-00205-2012.

Cooper JC Jr. (1994). Health and Nutrition Examination Survey of 1971–75: Part II. Tinnitus, subjective hearing loss, and well-being. *J Am Acad Audiol* 5:37–43.

Cruikshank SJ, Lewis TJ, Connors BW (2007). Synaptic basis for intense thalamocortical activation of feedforward inhibitory cells in neocortex. *Nat Neurosci* 10:462-468.

Dahmen JC, Hartley DE, King AJ (2008). Stimulus-timing-dependent plasticity of cortical frequency representation. *J Neurosci* 28(50):13629-39.

Day RO, Graham GG, Bieri D, Brown M, Cairns D, Harris G, Hounsell J, Platt-Hepworth S, Reeve R, Sambrook PN, et al. (1989). Concentration-response

relationships for salicylate-induced ototoxicity in normal volunteers. *Br J Clin Pharmacol* 28(6):695-702.

Dehmel S, Pradhan S, Koehler S, Bledsoe S, Shore S (2012). Noise overexposure alters long-term somatosensory-auditory processing in the dorsal cochlear nucleus--possible basis for tinnitus-related hyperactivity? *J Neurosci* 32(5):1660-71.

Desai NS, Rutherford LC, Turrigiano GG (1999). Plasticity in the intrinsic excitability of cortical pyramidal neurons. *Nature* 2:515-520.

Desai NS, Cudmore RH, Nelson SB, Turrigiano GG (2002). Critical periods for experience-dependent synaptic scaling in visual cortex. *Nat Neurosci* 5:783-789.

Dobie, RA (2003). Depression and tinnitus. *Otolaryngol Clin North Am* 36, 383–388.

Dohrmann K, Weisz N, Schlee W, Hartmann T, Elbert T (2007). Neurofeedback for treating tinnitus. *Prog Brain Res* 166:473-85.

Dominguez M, Becker S, Bruce I, Read H (2006). A spiking neuron model of cortical correlates of sensorineural hearing loss: Spontaneous firing, synchrony, and tinnitus. *Neural Comput.* 18(12):2942-58.

Eggermont JJ, Komiya H (2000). Moderate noise trauma in juvenile cats results in profound cortical topographic map changes in adulthood. *Hear Res* 142:89 –101.

Eggermont JJ, Roberts LE (2004). The neuroscience of tinnitus. *Trends Neurosci* 27:676-682.

Eggermont JJ (2008). Role of auditory cortex in noise- and drug-induced tinnitus. *Am J Audiol* 17(2):S162-9.

Engineer ND, Riley JR, Seale JD, Vrana WA, Shetake JA, Sudanagunta SP, Borland MS, and Kilgard MP (2011). Reversing pathological neural activity using targeted plasticity. *Nature* 470: 101-104.

Fröhlich F, Bazhenov M, Sejnowski TJ. (2008). Pathological effect of homeostatic synaptic scaling on network dynamics in diseases of the cortex. *J Neurosci* 28(7):1709-20.

Gerken GM (1996). Central tinnitus and lateral inhibition: an auditory brainstem model. *Hear Res.*97(1-2):75-83.

Hebb, D (1949). *Organization of behaviour: a neuropsychological theory*. New York: Wiley.

Heller, AJ (2003). Classification and epidemiology of tinnitus. *Otolaryngol Clin North Am* 36, 239–248.

Ibata K, Sun Q, Turrigiano GG (2008). Report Rapid Synaptic Scaling Induced by Changes in Postsynaptic Firing. *Neuron* 819-826.

Izhikevich EM (2003). Simple Model of Spiking Neurons. *IEEE Transactions on Neural Networks* 14:1569-1572.

Jastreboff PJ, Sasaki CT (1994). An animal model of tinnitus: a decade of development. *Am J Otol* 15(1):19-27.

Jastreboff PJ and Sasaki, CT (1986). Salicylate-induced changes in spontaneous activity of single units in the inferior colliculus of the guinea pig. *J. Acoust Soc Am* 80, 1384–1391.

Kahlbrock N, Weisz N (2008). Transient reduction of tinnitus intensity is marked by concomitant reductions of delta band power. *BMC Biol* 16;6:4.

Kaltenbach JA (2007). The dorsal cochlear nucleus as a contributor to tinnitus: mechanisms underlying the induction of hyperactivity. *Prog Brain Res* 166:89-106.

Kern A, Heid C, Steeb WH, Stoop N, Stoop R (2008). Biophysical parameters modification could overcome essential hearing gaps. *PLoS Comput Biol* 4(8):e1000161.

Kimura, M, Eggermont JJ (1999). Effects of acute pure tone induced hearing loss on response properties in three auditory cortical fields in cat. *Hear Res* 135:146-162.

Kotak VC, Fujisawa S, Lee FA, Karthikeyan O, Aoki C, Sanes DH (2005). Hearing loss raises excitability in the auditory cortex. *J Neurosci* 25:3908-18.

Kraus KS, Canlon B. (2012). Neuronal connectivity and interactions between the auditory and limbic systems. Effects of noise and tinnitus. *Hear Res* 288(1-2):34-46.

Langers DR, de Kleine E, van Dijk P (2012). Tinnitus does not require macroscopic tonotopic map reorganization. *Front Syst Neurosci* 6:2.

LeMasson G, Marder E, Abbott LF (1993). Activity-dependent regulation of conductances in model neurons. *Science* 259:1915-1917.

Liberman MC, Dodds LW (1984). Single-neuron labeling and chronic cochlear pathology. II. Stereocilia damage and alterations of spontaneous discharge rates. *Hear Res* 16:43-53.

Liberman MC, Kiang NYS (1978). Acoustic trauma in cats. Cochlear pathology and auditory-nerve activity. *Acta Otolaryngol suppl* 358:1-63.

Longenecker RJ, Galazyuk AV (2011). Development of tinnitus in CBA/CaJ mice following sound exposure. *J Assoc Res Otolaryngol* 12(5):647-58.

Ma WL, Hidaka H, May BJ (2006). Spontaneous activity in the inferior colliculus of CBA/J mice after manipulations that induce tinnitus. *Hear Res* 212(1-2):9-21.

Maffei A, Nelson SB, Turrigiano GG (2004). Selective reconfiguration of layer 4 visual cortical circuitry by visual deprivation. *Nat Neurosci* 7:1353-1359.

Maffei A, Turrigiano GG (2008). Multiple modes of network homeostasis in visual cortical layer 2/3. *J Neurosci* 28:4377-4384.

Masquelier T, Guyonneau R, Thorpe SJ (2008). Spike timing dependent plasticity finds the start of repeating patterns in continuous spike trains. *PLoS One*, 2;3(1):e1377.

Melcher JR, Levine RA, Bergevin C, Norris B (2009). The auditory midbrain of people with tinnitus: abnormal sound-evoked activity revisited. *Hear Res* 257(1-2):63-74.

Meyer K (2011). Primary sensory cortices, top-down projections and conscious experience. *Prog Neurobiol* 94(4):408-17.

Milbrandt JC, Holder TM, Wilson MC, Salvi RJ, Caspary DM, (2000). GAD levels and muscimol binding in rat inferior colliculus following acoustic trauma. *Hear Res* 147, 251-260.

Møller AR (2007). Tinnitus: presence and future. *Prog Brain Res* 166:3-16.

Nelson SB, Turrigiano GG (2008). Strength through diversity. *Neuron* 60(3): 477-482.

Noreña AJ, Tomita M, Eggermont JJ (2003). Neural changes in cat auditory cortex after a transient pure-tone trauma. *J Neurophysiol* 90:2387-401.

Noreña AJ, Eggermont JJ (2003). Changes in spontaneous neural activity immediately after an acoustic trauma: implications for neural correlates of tinnitus. *Hear Res* 183:137-153.

Pickles JO (2008). *An introduction to the physiology of hearing*. Bingley: Emerald Group Publishing Limited.

Pinchoff RJ, Burkard RF, Salvi RJ, Coad ML, Lockwood AH (1998). Modulation of tinnitus by voluntary jaw movements. *Am J Otol* 19(6):785-9.

Rajan R, Irvine DR, Wise LZ, Heil P (1993). Effect of unilateral partial cochlear lesions in adult cats on the representation of lesioned and unlesioned cochleas in primary auditory cortex. *J Comp Neurol* 338:17– 49.

Rajan R (2001) Plasticity of excitation and inhibition in the receptive field of primary auditory cortical neurons after limited receptor organ damage. *Cereb Cortex* 11(2):171-82.

Riegle KC, Meyer RL (2007). Rapid Homeostatic Plasticity in the Intact Adult Visual System. *J Neurosci* 27:10556 -10567.

Roberts LE, Moffat G, Bosnyak DJ (2006). Residual inhibition functions in relation to tinnitus spectra and auditory threshold shift. *Acta Oto-Laryngologica Supplementum* (556), 27–33.

Roberts LE, Eggermont JJ, Caspary DM, Shore SE, Melcher JR, Kaltenbach JA (2010). Ringing ears: the neuroscience of tinnitus. *J Neurosci* 30(45):14972-9.

Robertson D, Irvine DRF (1989). Plasticity of frequency organization in auditory cortex of guinea pigs with partial unilateral deafness. *J Comp Neurol* 282:456–471.

Rutherford LC, Nelson SB, Turrigiano GG (1998). BDNF Has Opposite Effects on the Quantal Amplitude of Pyramidal Neuron and Interneuron Excitatory Synapses. *Neuron* 21:521-530.

Sanchez L (2004). The epidemiology of tinnitus. *Audiol Med* 2(1):8-17.

Schaette R, Kempter R (2006). Development of tinnitus-related neuronal hyperactivity through homeostatic plasticity after hearing loss: a computational model. *Eur J Neurosci* 23(11):3124-38.

Schaette R, McAlpine D (2011). Tinnitus with a normal audiogram: physiological evidence for hidden hearing loss and computational model. *J Neurosci* 31(38):13452-7.

Schaette R, Kempter R. (2012). Computational models of neurophysiological correlates of tinnitus. *Front Syst Neurosci.* 2012;6:34.

Scholl B, Wehr M (2008). Disruption of balanced cortical excitation and inhibition by acoustic trauma. *J Neurophysiol* 100:646-656.

Seki S, Eggermont JJ (2002). Changes in cat primary auditory cortex after minor-to-moderate pure-tone induced hearing loss. *Hear Res* 173(1-2):172-86.

Seki S, Eggermont JJ (2003). Changes in spontaneous firing rate and neural synchrony in cat primary auditory cortex after localized tone-induced hearing loss. *Hear Res* 180:28-38.

Shore S, Zhou J, Koehler S (2007). Neural mechanisms underlying somatic tinnitus. *Prog Brain Res* 166:107-23.

Song, S., Miller, K. D. & Abbott, L. F. Competitive Hebbian learning through spike-timing-dependent synaptic plasticity. *Nature Neurosci* 3, 919–926 (2000).

Stolzberg D, Salvi RJ, Allman BL (2012). Salicylate toxicity model of tinnitus. *Front Syst Neurosci* 2012;6:28.

Stolzberg D, Chrostowski M, Salvi R, Allman B (2012). Intracortical circuits amplify sound-evoked activity in primary auditory cortex following systemic injection of salicylate in the rat. *J Neurophys* 108(1):200-14.

Turrigiano GG (1999). Homeostatic plasticity in neuronal networks : the more things change, the more they stay the same. *Trends Neurosci* 22:221-227.

Turrigiano GG (2008). The self-tuning neuron: synaptic scaling of excitatory synapses. *Cell* 135:422-35.

Turrigiano GG, Nelson SB (2004). Homeostatic plasticity in the developing nervous system. *Nat Rev Neurosci* 5(2):97-107.

Wang H, Brozoski TJ, Caspary DM (2011). Inhibitory neurotransmission in animal models of tinnitus: maladaptive plasticity. *Hear Res* 279(1-2):111-7.

Wehr M, Zador AM (2003). Balanced inhibition underlies tuning and sharpens spike timing in auditory cortex. *Nature* 426:442-446.

Weisz N, Moratti S, Meinzer M, Dohrmann K, Elbert T (2005). Tinnitus perception and distress is related to abnormal spontaneous brain activity as measured by magnetoencephalography. *PLoS Med* 2(6):e153.

Weisz N, Müller S, Schlee W, Dohrmann K, Hartmann T, Elbert T (2007). The neural code of auditory phantom perception. *J Neurosci* 27(6):1479-84.

Wu GK, Arbuckle R, Liu BH, Tao HW, Zhang LI (2008). Lateral sharpening of cortical frequency tuning by approximately balanced inhibition. *Neuron* 58:132-143.

Yang S, Weiner BD, Zhang LS, Cho S-J, Bao S (2011). Homeotatic plasticity drives tinnitus perception in an animal model. *Proc Natl Acad Sci* 108:14974-14978.

Zilany MSA, Bruce IC, Nelson PC, Carney LH (2009). A phenomenological model of the synapse between the inner hair cell and auditory nerve: Long-term adaptation with power-law dynamics. *J Acoust Soc Am* 126(5):2390–2412.

Chapter Two

Preamble

In this chapter I outline a computational model of the primary auditory cortex that also captures the computational underpinnings of homeostatic plasticity (HSP) acting on cortical synapses. This model predicts that after hearing loss, homeostatic mechanisms compensate for a reduction in sound driven activity by reducing inhibitory synaptic strength and increasing the strengths of excitatory inputs in the hearing loss region; the result is increased spontaneous firing and synchrony. Thus, the simulation results suggest that HSP may contribute to the emergence of tinnitus correlates. The novelty of this computational model is that it sheds light on the dynamic process through which synaptic scaling responds to hearing loss whereas past models required manual resetting of input weights to simulate synaptic scaling.

Furthermore, this model contributed a novel prediction about the development of traveling waves of activity in cortex after deafferentation. Namely, while a network model with increased excitatory connections is expected to produce large travelling waves of activity across the network, this biologically plausible model predicted that such waves do not develop in the presence of spontaneous activity. Instead, short-range and short-duration waves of spontaneous activity are more likely to occur after severe

deafferentation. This is the case because the same HSP mechanisms that create a hyper-excitable network also elevate spontaneous activity, which prevents large scale travelling waves of activity from developing because of refractory periods that interrupt the wave of excitation.

Permissions and Contributions

Chapter 2 has been published in the *Journal of Computational Neuroscience*[1]. Material from Chapter 2 is used with permission from Springer Science and Business Media through a License Agreement for use of material in a thesis/dissertation.

For Chapter 2, the idea behind the original computational model was conceived by Dr. Suzanna Becker, Dr. Ian Bruce and Le Yang, a former doctoral student working with Dr. Becker. I was responsible for implementing the final (published) version of the model, developing the novel results on travelling waves, analyzing and interpreting simulations, and writing the manuscript.

[1] Chrostowski M, Yang L, Wilson HR, Bruce IC, Becker S (2011). Can homeostatic plasticity in deafferented primary auditory cortex lead to traveling waves of excitation? *J Comput Neurosci* 30:279-299.

J Comput Neurosci
DOI 10.1007/s10827-010-0256-1

Can homeostatic plasticity in deafferented primary auditory cortex lead to travelling waves of excitation?

Michael Chrostowski · Le Yang · Hugh R. Wilson · Ian C. Bruce · Suzanna Becker

Received: 6 May 2009 / Revised: 6 June 2010 / Accepted: 18 June 2010

Abstract Travelling waves of activity in neural circuits have been proposed as a mechanism underlying a variety of neurological disorders, including epileptic seizures, migraine auras and brain injury. The highly influential Wilson-Cowan cortical model describes the dynamics of a network of excitatory and inhibitory neurons. The Wilson-Cowan equations predict travelling waves of activity in rate-based models that have sufficiently reduced levels of lateral inhibition. Travelling waves of excitation may play a role in functional changes in the auditory cortex after hearing loss. We propose that down-regulation of lateral inhibition may be induced in deafferented cortex via homeostatic plasticity mechanisms. We use the Wilson-Cowan equations to construct a spiking model of the primary auditory cortex that includes a novel, mathematically formalized description of homeostatic plasticity. In our model, the homeostatic mechanisms respond to hearing loss by reducing inhibition and increasing excitation, producing conditions under which travelling waves of excitation can emerge. However, our model predicts that the presence of spontaneous activity prevents the development of long-range travelling waves of excitation. Rather, our simulations show short-duration excitatory waves that cancel each other out. We also describe changes in spontaneous firing, synchrony and tuning after simulated hearing loss. With the exception of shifts in characteristic frequency, changes after hearing loss were qualitatively the same as empirical findings. Finally, we discuss possible applications to tinnitus, the perception of sound without an external stimulus.

Keywords Primary auditory cortex · Peripheral hearing loss · Travelling wave · Homeostatic plasticity · Spiking neural model

Action Editor: S. A. Shamma

This research was supported by a New Emerging Teams Grant from the Canadian Institutes of Health Research to S.B. and I.B. and Discovery grants from the Natural Sciences and Engineering Research Council of Canada to S.B and I.B.

M. Chrostowski (✉)
McMaster Integrative Neuroscience Discovery & Study, McMaster University, 1280 Main Street West, Hamilton, ON, Canada, L8S 4K1
e-mail: chrostm@mcmaster.ca

L. Yang · I. C. Bruce
Department of Electrical and Computer Engineering, McMaster University, 1280 Main Street West, Hamilton, ON, Canada, L8S 4K1

H. R. Wilson
Center for Vision Research, York University, 4700 Keele Street, Toronto, ON, Canada, M3J 1P3

S. Becker
Department of Psychology, Neuroscience and Behaviour, McMaster University, 1280 Main Street West, Hamilton, ON, Canada, L8S 4K1

1 Introduction

Travelling waves of neuronal activity have been implicated in various various pathological conditions including brain injury (for a review, see Charles and Brennan 2009), migraine aura (Milner 1958) and epilepsy (Houweling et al. 2005). Potential mechanisms include transient hypoxia-induced changes in ion

Published online: 10 July 2010

balances (Takano et al. 2007) and long-term changes in the balance of excitation and inhibition. It has been proposed that such adaptations and the ensuing travelling waves may be a general feature of the brain's response to deafferentation (Houweling et al. 2005). In this paper we use a computational model of auditory cortex to explore the conditions under which travelling waves occur after sensory deafferentation, and the possibility that travelling waves may underlie some aspects of hearing loss including tinnitus.

The Wilson-Cowan equations (Wilson and Cowan 1972, 1973) describe the dynamics of a network of interconnected excitatory and inhibitory neurons. These equations predict the emergence of travelling waves of neural activity in the network when lateral inhibitory connections are sufficiently reduced. Travelling waves of activity have been implicated in cortical pathologies that involve deafferentation, such as epileptic seizures (Houweling et al. 2005). Cortical deafferentation also occurs with hearing loss and affects neural activity in the primary auditory cortex (Noreña and Eggermont 2003). However, no evidence of travelling waves has been found in the primary auditory cortex in animals with induced sensorineural hearing loss. We have developed a spiking model of the primary auditory cortex (A1), with excitatory and inhibitory neural units, in order to investigate the conditions required to induce travelling waves of neural activity after deafferentation. We propose a novel, well specified computational formalism for modeling homeostatic plasticity (HSP) within our detailed spiking cortical model as a mechanism to induce synaptic weight changes after deafferentation. The model allows us to shed light on the potential for travelling waves and other abnormal neural activity in A1 after sensorineural hearing loss.

Sensorineural hearing loss induced by aging and/or noise exposure is characterized by hair cell loss and some auditory nerve (AN) fiber damage (Bhattacharyya and Dayal 1989; Liberman 1987). The resulting distorted cochleotopic representation of the sound environment can cause profound changes in auditory brainstem (Brozoski et al. 2002; Kaltenbach et al. 2004), midbrain (Salvi et al. 2000; Wang et al. 2002) and cortex. At the level of primary auditory cortex, pyramidal neurons in the impaired region show increased neural synchrony and enhanced spontaneous activity within 2 hours after noise trauma (Noreña and Eggermont 2003). These cortical abnormalities persist in the weeks following noise exposure (Seki and Eggermont 2002, 2003). Moreover, after moderate to substantial cochlear damage, the tonotopic map is reorganized so that the neurons in the impaired region are re-tuned to respond maximally to frequencies near the edge of the hearing loss spectrum (Robertson and Irvine 1989; Rajan et al. 1993; Dietrich et al. 2001; Noreña et al. 2003). The mechanisms and timescale of the reorganization may depend on the severity of the peripheral damage (Noreña et al. 2003). An intriguing possibility is that the altered responsiveness of the cortex may set up the optimal conditions for travelling waves, which might in turn contribute to phenomena such as map reorganization and/or the phantom percept of tinnitus. We investigated whether travelling waves can propagate from regions representing edge frequencies of hearing loss into the deafferented region.

The underlying mechanisms for hearing loss-induced abnormal activities in A1 are still under investigation. An overall degradation of inhibition, possibly accompanied by the unmasking of excitatory synapses, may contribute to the observed cortical changes (Rajan 1998, 2001; Calford 2002; Noreña and Eggermont 2003). More recently, the compensatory effects of the reduced afferent drive in both auditory midbrain and A1 were discovered in animal experiments. In particular, the intrinsic excitability of the pyramidal neurons in the deafferented region of A1 is shown to be enhanced (Kotak et al. 2005). Moreover, the excitatory synapses targeted on the deafferented neurons are strengthened (Vale et al. 2002; Muly et al. 2004; Kotak et al. 2005) while the inhibitory synapses are weakened (Suneja et al. 1998a, b; Vale et al. 2002; Kotak et al. 2005). These synaptic regulations are consistent with homeostatic plasticity, previously observed in the hippocampus (Turrigiano et al. 1998) and the visual cortex (Desai et al. 2002).

We make the assumption that homeostatic mechanisms are at work in A1 after hearing loss and implement them in our model to scale both excitatory and inhibitory synapses on deafferented neurons. Homeostatic plasticity can ensure that, over a long timescale, the average neural firing rate can be maintained within a proper range, despite chronic changes in driving forces. Interestingly, the effects of homeostasis become detectable 1.5 hours after inducing persistent changes in neural activity and get stronger over a time-course of several days (Gina Turrigiano, personal communication). This timescale is similar to the temporal development of many of the cortical changes after noise trauma (Noreña and Eggermont 2003; Seki and Eggermont 2002, 2003). We propose that homeostatic mechanisms at work in the primary auditory cortex are at least partially responsible for abnormal activity that develops after hearing loss. Furthermore, by reducing lateral inhibitory weights and increasing lateral excitatory

weights, HSP is expected to produce conditions that increase the potential for travelling waves.

Recent theoretical models of hearing loss in the auditory brainstem (Schaette and Kempter 2006) and A1 (Dominguez et al. 2006) provide insights into the possible contributions of HSP to tinnitus, but have not included a sufficient level of biological detail to implement realistic temporal dynamics in neural circuits so as to be able to investigate travelling waves.

Using a comprehensive description of HSP, we can make predictions about conditions required for travelling waves of neural activity. We look at changes in sound-driven and spontaneous activity, along with tuning properties in the auditory cortex, in the hours after hearing loss to determine if our model can reproduce findings in animal models of sensorineural hearing loss. We then investigate the potential for travelling waves. We assume that, during this period of time, changes in cortical activity are dominated by altered thalamic input rates and homeostatic mechanisms within the auditory cortex responding to the altered input. Compared to the previous work by Dominguez et al. (2006), this A1 model is able to better capture the altered cortical activity and changes in neural tuning. Changes in neural activity and tuning sharpness are qualitatively similar to empirical findings. We do not see meaningful shifts in characteristic frequencies after simulated hearing loss. Homeostatic plasticity in our model (and perhaps *in vivo*) may not be a sufficient mechanism for tonotopic reorganization. Furthermore, we do not include peripheral or subcortical changes that would contribute to these shifts. Rather, we focus on alterations in cortical connections and activity.

Surprisingly, our simulations show that travelling waves of excitation with large temporal extent do not manifest as predicted in a spiking model with spontaneous firing. The waves of excitation are prevented from traversing the network by refractory periods produced by spontaneous firing. In the biologically unlikely scenario where there is no spontaneous firing, travelling waves emerge as predicted. While the effect of decreased inhibition is to increase the likelihood of travelling waves, this is offset by the HSP-induced increase in spontaneous firing. However, our model demonstrates that shorter-duration spontaneous travelling waves of excitation become more frequent and span large portions of the hearing loss region. This prediction may be important in explaining the lack of empirical evidence for travelling waves of activity in A1 after sensorineural hearing loss.

2 Spiking A1 model

In this section, the development of our spiking A1 model is presented in detail. In particular, we first describe the network architecture. Then, the model neuron and the input to the A1 model are illustrated. Finally, a novel formulation for the computational principles underlying HSP in different types of synapses is presented.

2.1 Network model

The network is designed based on several key features of A1 observed in animal experiments and neuroimaging studies in humans. First, when stimulated with pure-tone stimuli with varying sound pressure levels (SPL), many A1 pyramidal neurons exhibit a V/U-shaped tuning curve with a single best frequency or characteristic frequency (CF) (Phillips and Irvine 1981; Schreiner et al. 2000; Turner et al. 2005). The CF is usually defined as the frequency with the lowest response threshold. Second, in normal hearing animals and humans, the CFs of the pyramidal neurons show a roughly one-dimensional gradient along the latero-medial axis, and they display a logarithmic relation to the corresponding cortical locations. This property is known as the tonotopic organization of A1 or simply referred to as the tonotopic map (Merzenich et al. 1975; Cheung et al. 2001; Ottaviani et al. 1997). Third, the interneuron population in A1 provides inhibitory inputs that are thought to sharpen the receptive fields of the pyramidal neurons (Chen and Jen 2000; Foeller et al. 2001), a mechanism also observed in subcortical auditory structures such as IC (Gerken 1996; Lu and Jen 2001). Finally, the excitatory connections between pyramidal neurons in the direction of the lateral-medial axis are generally short-range, while lateral connections between pyramidal neurons and inhibitory interneurons span a broader region (Douglas and Martin 1998). For a more comprehensive description of A1 anatomy and functional organization, see Read et al. (2002) and references therein.

With the above observations in mind, we construct the A1 model by modifying the well-known Wilson-Cowan cortical model (Wilson and Cowan 1972, 1973). A schematic diagram of the network structure is given in Fig. 1. Our A1 model is driven by a set of model neurons representing the afferent inputs from the auditory thalamus. In the cortical layer, pyramidal neurons are uniformly distributed along the latero-medial axis connecting the posterior ectosylvian suclus and anterior ectosylvian suclus. There are 201 pyramidal neurons and 67 interneurons, which is consistent with

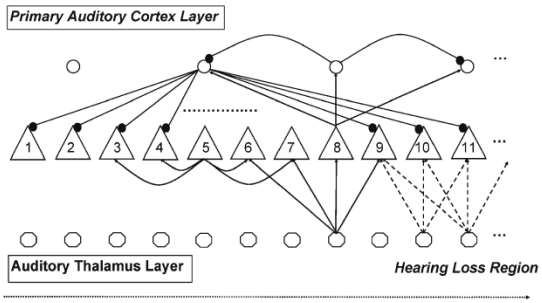

Fig. 1 The schematic structure of the spiking A1 model. The numbered triangles represent pyramidal neurons. The associated digit denotes the spatial coordinate of the given neuron. Inhibitory interneurons and thalamic neurons are represented by open circles and regular octagons, respectively. Arrowed lines are excitatory synapses, while lines ending with full black circles denote inhibitory synapses. Hearing loss is illustrated by using dashed lines for afferent synapses to show the reduction in inputs

the finding that typically around 75% of cortical cells are glutamatergic neurons while the rest are inhibitory neurons (Jones 1995). The number of neurons and connections in our computational model is a subset of what one would find in the auditory cortex, however, it was necessary to make the simulations computationally viable while maintaining the validity of the model and results. We associate each pyramidal neuron with a one-dimensional coordinate x_i such that $x_i = i$, $i = 1, 2, 3, ..., 201$. Note that in contrast to many existing spiking models for auditory midbrain (e.g., Bruce et al. 2003) and A1 (e.g., Dominguez et al. 2006), inhibitory interneurons are separately incorporated in the present model. To facilitate the initialization of the synaptic weight matrices, we organize the interneurons on a straight line parallel to the latero-medial axis. It is assumed that the interneurons are equally spaced with a distance three times larger than that between two pyramidal neurons, as shown in Fig. 1. Therefore, the spatial coordinates for the interneurons y_j are given by $y_j = 3(j-1)+2$, $j = 1, 2, 3, ..., 67$. There are 201 neurons in the auditory thalamus layer. Their spatial coordinates are denoted by z_k, where $z_k = k$, $k = 1, 2, 3, ..., 201$. The CFs of thalamic neurons range from 20 Hz to 20 kHz and correspond to the approximately logarithmic dependence between CF and position on the basilar membrane (Greenwood 1990).

The synapses in the A1 model are initialized under simulated normal hearing conditions, where a pyramidal neuron has the same characteristic frequency as a thalamic neuron when they share the same spatial coordinate. We then simulate hearing loss and a subsequent period of adaptation of the network response to acoustic inputs, during which time the synaptic weights are modified by a set of HSP rules (derived in Section 2.4). The resultant changes in synaptic efficacy can potentially cause shifts in the CFs of pyramidal neurons, i.e., cortical reorganization, while the CFs of thalamic neurons remain fixed.

Based on experimental data (Miller et al. 2001), we require that for normal hearing, a pyramidal neuron is driven by thalamic neurons whose CFs lie in the range of $\pm 1/3$ octaves of the pyramidal neuron's characteristic frequency, through excitatory thalamocortical synapses. When simulating synaptic modifications by HSP in hearing loss scenarios, we assume that pyramidal neurons continue to receive afferent inputs solely from those thalamocortical synapses, i.e., we do not consider any unmasked thalamocortical synapses in this model. In this way, we can investigate the contribution of HSP to the observed cortical changes separately (see more in *Discussion*). The synaptic strength of the afferent connection from the kth thalamic neuron to the ith pyramidal neuron, denoted by $\mathbf{W_a}(i,k)$, is determined by the following Gaussian function[1]:

$$\mathbf{W_a}(i,k) = \begin{cases} 0.3 \cdot \exp\left(-\dfrac{|z_k - x_i|^2}{3.684}\right), & |z_k - x_i| \le 9 \\ 0, & |z_k - x_i| > 9 \end{cases} \tag{1}$$

Pyramidal neurons are also depolarized through lateral excitatory synapses. These connections are assumed to span a range of $\pm 1/6$ octaves with the efficacy of the synapse from the lth pyramidal neuron to the ith one $\mathbf{W_{E,E}}(i,l)$ also falling off as a Gaussian function of distance:

$$\mathbf{W_{E,E}}(i,l) = \begin{cases} 0.21 \cdot \exp\left(-\dfrac{|x_i - x_l|^2}{6.72}\right), \\ |x_i - x_l| \le 5 \text{ and } x_i \ne x_l \\ 0, \\ |x_i - x_l| > 5 \text{ or } x_i = x_l \end{cases} \tag{2}$$

where $l = 1, 2, 3, .., 201$. From the above equation, it can be seen that we do not assume direct self-excitation in our model.

The interneurons in the A1 layer are driven by the output spikes of pyramidal neurons and then feed inhibition back to sharpen frequency tuning. The synaptic weight of the lateral connection from the ith pyramidal

[1]The peak values and variances of the Gaussian functions defined in this subsection are chosen so that a tonal stimulus would only excite a small portion of the pyramidal neurons. See the model response to a 723-Hz pure tone in Fig. 8 for an example.

neuron to the jth interneuron, denoted by $\mathbf{W}_{\mathbf{I,E}}(j,i)$, is expressed as

$$\mathbf{W}_{\mathbf{I,E}}(j,i) = \begin{cases} 0.11 \cdot \exp\left(-\dfrac{|x_i - y_j|^2}{41.5}\right), & |x_i - y_j| \le 20 \\ 0, & |x_i - y_j| > 20 \end{cases} \tag{3}$$

The efficacy of the feedback inhibitory synapse from the jth interneuron to the ith pyramidal neuron $\mathbf{W}_{\mathbf{E,I}}(i,j)$ is determined by

$$\mathbf{W}_{\mathbf{E,I}}(i,j) = \begin{cases} 0.4 \cdot \exp\left(-\dfrac{|x_i - y_j|^2}{41.5}\right), & |x_i - y_j| \le 20 \\ 0, & |x_i - y_j| > 20 \end{cases} \tag{4}$$

In comparison to the pyramidal neurons, the inhibitory interneurons receive lateral excitatory inputs from a wider range of pyramidal neurons, spanning about ±3/4 octaves. Moreover, as shown in (4), feedback inhibition from an interneuron imposes mutual competition between those pyramidal neurons that drive the interneuron to form a lateral inhibitory network.

We also include lateral inhibitory synapses among interneurons. Their synaptic weights are given by

$$\mathbf{W}_{\mathbf{I,I}}(j,m) = \begin{cases} 0.048 \cdot \exp\left(-\dfrac{|y_j - y_m|^2}{220}\right), \\ |y_j - y_m| \le 9 \text{ and} y_j \ne y_m \\ 0, \\ |y_j - y_m| > 9 \text{ or } y_j = y_m \end{cases} \tag{5}$$

where $m = 1, 2, 3, \ldots, 67$. We set the lateral inhibition between interneurons to be small in order to avoid broadening the tuning curves of the pyramidal neurons. And again, there is no self-inhibition. It is worthwhile to point out that as in the previous modeling work (Dominguez et al. 2006), we do not incorporate either corticofugal projections from A1 onto the auditory thalamus or the feed-forward inhibition from thalamic neurons to pyramidal cells via cortical interneurons. Corticothalamic feedback projections may play a role in enhancing tuning curves, but they have not been characterized sufficiently to be included in our model. Feed-forward inhibition may likely be an important mechanism for improving temporal precision of auditory responses. Furthermore, co-tuned inhibition may sharpen tuning curves of cortical neurons while convergence of thalamocortical inputs may be the main contributor to the shape of these tuning curves as has been proposed by Wehr and Zador (2003). However, homeostatic plasticity may alter both the thalamocortical and intracortical connections described above, affecting tuning in A1. Therefore, our model's architecture can provide insights into potential effects of a homeostatic plasticity mechanism on activity in A1.

To reduce network edge effects, appropriate weight adjustments of the synapses targeted on cortical neurons near/at the edge of the A1 layer are performed to match the total excitation/inhibition for neurons in the middle sections. As neurons at or near the array edge can be considered to be missing lateral inputs from one side (tonotopically), this is adjusted for by increasing their existing excitatory and inhibitory connection weights until their total excitation and inhibition are equal to that of a neuron with all of its inputs (as in Bruce et al. 2003). As the start of the hearing loss region is modeled at a sufficient distance from the end of the array of neural units, this compensatory measure will not have an impact on the findings discussed in this paper.

2.2 Model neuron

In this work, both pyramidal neurons and interneurons are modeled as leaky integrate-and-fire neurons (e.g., Gerstner and Kistler 2002). Specifically, when the membrane potential of a cortical neuron reaches a certain threshold, the neuron fires a spike and enters an absolute refractory period of 2 milliseconds (ms). During that period, the membrane potential is fixed at the resting potential and allowed to vary again thereafter. Note that we do not include the relative refractory period in the neuron model for simplicity. The sub-threshold behaviors of the pyramidal neurons and interneurons are governed by

$$\tau \frac{d\mathbf{V}_{\mathbf{E}}(t)}{dt} = -\mathbf{V}_{\mathbf{E}}(t) + \mathbf{W}_{\mathbf{E,E}} \cdot \mathbf{i}_{\mathbf{E}}(t) - \mathbf{W}_{\mathbf{E,I}} \cdot \mathbf{i}_{\mathbf{I}}(t) + \mathbf{W}_{\mathbf{a}} \cdot \mathbf{i}_{\mathbf{a}}(t), \tag{6}$$

and

$$\tau \frac{d\mathbf{V}_{\mathbf{I}}(t)}{dt} = -\mathbf{V}_{\mathbf{I}}(t) + \mathbf{W}_{\mathbf{I,E}} \cdot \mathbf{i}_{\mathbf{E}}(t) - \mathbf{W}_{\mathbf{I,I}} \cdot \mathbf{i}_{\mathbf{I}}(t), \tag{7}$$

respectively. The connection weight matrices $\mathbf{W}_{\mathbf{a}}$, $\mathbf{W}_{\mathbf{E,E}}$, $\mathbf{W}_{\mathbf{I,E}}$, $\mathbf{W}_{\mathbf{E,I}}$ and $\mathbf{W}_{\mathbf{I,I}}$ have been defined in the last subsection. $\mathbf{V}_{\mathbf{E}}(t)$ is a column vector of length 201 containing the membrane potentials of the pyramidal

neurons. $\mathbf{V_I}(t)$ denotes a column vector representing the membrane potentials of the interneurons. τ (=2.75 ms) is the membrane time constant. $\mathbf{i_a}(t)$ and $\mathbf{i_E}(t)$ are column vectors of length 201 describing the afferent and lateral excitatory synaptic currents from the thalamic neurons and pyramidal neurons, respectively. $\mathbf{i_I}(t)$ is the column vector of length 67 describing the inhibitory synaptic currents from the interneurons at time t. Each synaptic current is obtained by convolving the corresponding spike train with a unitary postsynaptic current waveform

$$i(t) = \left(\frac{a}{10\tau}\right)^2 \cdot \exp(-at/\tau) \cdot t, \tag{8}$$

which is commonly referred to as the alpha function (see Dayan and Abbott 2005). Excitatory synaptic currents are generated using an alpha function with $a = 10$, while inhibitory synaptic currents are calculated with $a = 0.5$.

2.3 Model input

We simulate three different input scenarios: one in which the model is stimulated by a simplified acoustic environment, one in which the model is situated in a quiet background, and a simulated pure tone input, which we use to demonstrate changes in network dynamics after hearing loss. For the first scenario, the input consists of the response of the subcortical auditory pathway to sound stimuli, while in the second scenario, the input consists of the afferent spontaneous activity from the auditory midbrain. A real-life acoustically rich environment is a constantly changing mixture of sounds of all frequencies. We approximate this situation using a simplified acoustic environment where the power spectrum of the sound stimuli over the range 20 Hz to 20 kHz is flat and there is no correlation between different frequency components. Accordingly, the spike trains generated by thalamic neurons in response to acoustic inputs are modeled as mutually independent Poisson processes. The sound-driven mean rates of the thalamic neurons' spike trains across the tonotopic map are set to be 150 spikes per second in the case of normal hearing. This input rate is high enough to be delineated from the silent condition and for sufficiently separable simulation results for the three hearing loss conditions we describe below. Furthermore, because the model has a lower density of neurons than real A1 due to computational limitations, having a higher input rate approximates the case of having a larger number of inputs with lower discharge rates. Using input rates that are this high does not qualitatively affect our results, but does lead to mean firing rate in the pyramidal neurons that are higher than what would be found in electrophysiological recordings. Using a uniform input rate for the simplified acoustic environment does not capture the various driving rates that would result from a dynamic acoustically rich-environment, however it does make the simulation of hearing loss curves and effects of the homeostatic mechanism clearer. A benefit of the mutually independent thalamocortical inputs is that it allows us to isolate the effect of hearing loss on cortical synchrony. However, in future work, it will be worthwhile to simulate more dynamic and complex acoustic environments in order to determine how inputs with a more natural spectro-temporal structure affect network activity.

After cochlear damage, it has been observed experimentally that the auditory brainstem response threshold increases and the auditory nerve output decreases (Salvi et al. 1980). Thus, we model the effects of peripheral hearing loss by reducing the sound-driven average rates of the spike trains of thalamic neurons at the impaired frequencies. We simulate a large normal hearing region, a transition region, and a large impaired region to facilitate the analysis and presentation of our results. Auditory peripheral damage mainly affects the processing of high-frequency components of the sound stimuli, because the hair cells tuned to those frequencies are especially vulnerable to noise trauma as well as age-related degeneration. Therefore, we constrain the mean spike rate decrease to the output spike trains of thalamic neurons with relatively high CFs. We define the hearing loss severity as the ratio of the maximum rate reduction to the normal sound-driven thalamic spike rate (=150 spikes/s). In this study, we consider three different hearing loss levels, specifically, 40%, 60% and 80%. Due to the existence of inputs from horizontal fibers and other cortico-cortical synapses, an 80% loss in driving spikes to A1 neurons is less likely to occur in standard animal models of noise-induced hearing impairment. However, we include the simulation results for 80% hearing loss in order to better illustrate the effects of HSP on synaptic weights and cortical activity across a broad range of deafferentation levels. Furthermore, the 80% hearing loss case allows us to more strongly demonstrate our findings related to travelling waves of excitation in the presence of spontaneous firing. For all three hearing-loss scenarios, hearing loss starts at 2.5 kHz, and its severity increases as a linear function of the spatial coordinates of the thalamic neurons until it reaches the maximum at 5 kHz. For the frequency range from 5 kHz to 20 kHz, the amount of hearing loss is the same as that at 5 kHz. As an example,

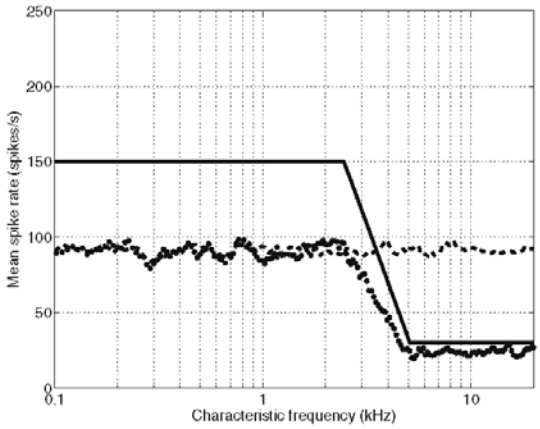

Fig. 2 Mean firing rates of the pyramidal neurons after 80% hearing loss (mean spike rate vs. characteristic frequency). Solid line: hearing loss curve; dotted line: the A1 model without HSP; dashed line: the A1 model with HSP. Note that in this figure and the following Figs. 4 and 6, the values on the x-axis denote the characteristic frequencies that the pyramidal neurons are tuned to under the condition of normal hearing. In other words, they indeed represent the spatial coordinates of the pyramidal neurons

Fig. 2 shows the mean firing rate curve for the 80% hearing loss case, which has a maximum rate reduction of 120 spikes/s. Qualitatively similar hearing loss curves illustrated by the auditory brainstem response (ABR) shift have been induced in cats (Noreña and Eggermont 2003) via excessive noise exposure. More recent audiogram data from humans with noise-induced hearing loss also exhibit similar hearing loss curves (Konig et al. 2006).

When the A1 model is situated in a quiet background, the driving force is the afferent spontaneous activity again modeled as mutually independent Possion spike trains. But in this case, we assume that the mean spike rate is 5 spikes/s across the whole frequency range, regardless of the hearing loss level. This setting is mainly motivated by *in vivo* experiments showing that most neurons in the auditory midbrain have similar spontaneous rates and their spontaneous activities remain largely unchanged after cochlear damage (Wang et al. 1996).

We test the A1 model initialized in the last subsection under two different input scenarios described above: the simplified acoustic environment and the silent condition. For both input scenarios, we simulate the condition of normal hearing in order to estimate mean firing rates of pyramidal neurons in the normal model. We use the pure-tone input condition to test for travelling waves of activity in the hearing loss conditions. The induced thalamic response resulting from a pure tone, $\mathbf{y_{pt}}(i, k)$ centered at neural unit z_k, and with peak amplitude A, is modeled as an increase in spike rate falling off spatially as a Gaussian:

$$\mathbf{y_{pt}}(k) = \begin{cases} A \cdot \exp\left(-\dfrac{|z_k - x_i|^2}{12.5}\right), & |z_k - x_i| \le 9 \\ 0, & |z_k - x_i| > 9 \end{cases} \quad (9)$$

The model operation is simulated using a 4^{th}-order Runge-Kutta algorithm with a fixed time-step of 0.1 milliseconds.

2.4 Homeostatic plasticity

Homeostatic plasticity (HSP) is triggered in response to the deviation of neural activity from a prefixed target rate (r_{target}) and its compensatory effects can bring the average firing rate back to normal (Burrone and Murthy 2003). As shown in animal experiments (Turrigiano et al. 1998; Kilman et al. 2002), HSP operates in a multiplicative fashion, i.e., all synaptic weights are enhanced or suppressed by the same scaling factor. In this way, HSP can stabilize neural activity without distorting the original synaptic distribution. Moreover, it has been observed that HSP regulates the synaptic efficacy slowly but accumulatively (Turrigiano et al. 1998; Desai et al. 2002). van Rossum et al. (2000) proposed a framework for implementing the homeostatic regulation of excitatory synapses targeted on spiking neurons that captures the key features of HSP mentioned above. Based on recent experimental studies on HSP, we extend the modeling work by van Rossum et al. to formulate a set of computational principles of HSP for synapses of different types in our A1 model.

Deafferentation can lead to the scaling-up of the synaptic efficacy of the thalamocortical synapses (Kotak et al. 2005) and the lateral excitatory synapses (Turrigiano et al. 1998; Rutherford et al. 1998; Kotak et al. 2005), while hyperactivity of the pyramidal neurons could lead to multiplicative depression (Turrigiano et al. 1998; Leslie et al. 2001). As such, similar to the realization of HSP for excitatory synapses developed by van Rossum et al. (2000), we use the following equations to update the matrices $\mathbf{W_a}$ and $\mathbf{W_{E,E}}$:

$$\tau_{\mathrm{HSP}} \frac{\mathrm{d}\mathbf{W_a}(i,k)}{\mathrm{d}t} = \left(r_{target} - r_i(t)\right) \cdot \mathbf{W_a}(i,k), \quad (10)$$

and

$$\tau_{\mathrm{HSP}} \frac{\mathrm{d}\mathbf{W_{E,E}}(i,l)}{\mathrm{d}t} = \left(r_{target} - r_i(t)\right) \cdot \mathbf{W_{E,E}}(i,l), \quad (11)$$

where $i = 1, 2, 3, ..., 201$, $k = 1, 2, 3, ..., 201$ and $l = 1, 2, 3, ...201$. The time constant τ_{HSP} is set to be 10^4 s (approximately 2.8 hours). The mechanism underlying the time constant of homeostatic plasticity is not clear, so we assume all cortical neurons have the same HSP time constant. The instantaneous firing rate of the ith pyramidal neuron $r_i(t)$, where $i = 1, 2, 3, ..., 201$, is defined as (van Rossum et al. 2000)

$$\tau_r \frac{dr_i(t)}{dt} = -r_i(t) + \sum_n \delta(t - t_{n,i}) \tag{12}$$

where τ_r is set to be $1s$, $t_{n,i}$ is the time point of the nth spike generated by the ith neuron, and $\delta(x)$ denotes the Dirac delta function. It can be seen from the above equation that $r_i(t)$ increases whenever the neuron fires a spike, and it decreases exponentially between spikes. The value of r_{target} is selected in order to represent the mean firing rate of pyramidal neurons in response to acoustic stimuli under the condition of normal hearing. In our simplified acoustic environment, pyramidal neurons in the cortical layer have mean firing rates around 90 spikes/s, therefore, we use this value for r_{target}. We used a target rate that is higher than the normal spontaneous firing rate of the A1 model in a completely quiet background (=2.5 spikes/s) because humans are generally exposed to acoustic environments that may induce a higher average rate of cortical firing. Furthermore, sensorineural hearing loss has been shown to induce a persistent increase in spontaneous firing of cortical neurons (Seki and Eggermont 2003). This may be partly due to a homeostatic set point for pyramidal neurons in the primary auditory cortex that is above the normal spontaneous firing rate. The purpose of a target firing rate and a homeostatic drive towards it could be to optimize information processing of relevant auditory stimuli (see Parra and Pearlmutter (2007) for a discussion of the optimality of gain adaptation mechanisms).

Compared with the excitatory synapses targeted on pyramidal neurons, our proposed mechanism for HSP adjusts the feedback inhibitory synapses in an opposite direction, consistent with empirical findings by Turrigiano and colleagues (Rutherford et al. 1997; Kilman et al. 2002; Kotak et al. 2005). In other words, hyperactivity of pyramidal neurons would enhance inhibitory neurotransmission while deafferentation induced by hearing loss would reduce the efficacy of the inhibitory synapses. Therefore, building on Eqs. (10) and (11), we develop the following equation to modify the entries in $\mathbf{W}_{E,I}$:

$$\tau_{HSP} \frac{d\mathbf{W}_{E,I}(i, j)}{dt} = -\left(r_{target} - r_i(t)\right) \cdot \mathbf{W}_{E,I}(i, j), \tag{13}$$

where $j = 1, 2, 3, ..., 67$. The homeostatic regulation of the matrix $\mathbf{W}_{I,E}$ is a bit more complex. Experiments show that activity blockade does not influence the lateral connections from pyramidal neurons onto interneurons (Turrigiano et al. 1998; Rutherford et al. 1998), while hyperactivity does increase their efficacy (Rutherford et al. 1998). A hyperactivity threshold for regulating pyramidal projections onto interneurons takes these findings into account and prevents the HSP mechanism from acting on the connections unless the threshold is exceeded. Thus, we formulate the updating equation for $\mathbf{W}_{I,E}$ as follows

$$\tau_{HSP} \frac{d\mathbf{W}_{I,E}(j, i)}{dt} = -\left(r_{target} - r_i(t)\right) \cdot u(-\left(r_{target} - r_i(t)\right) - h) \cdot \mathbf{W}_{I,E}(j, i), \tag{14}$$

where $u(x)$ is the unit-step function, that is, $u(x) = 1$ if $x \geq 0$; otherwise, $u(x) = 0$. h is the prefixed threshold for gating the hyperactivity, which is set to be 10 spikes/s. To our knowledge, there is no evidence on the homeostatic regulation for lateral inhibitory connections between interneurons. As such, we simply fix them during computer simulations.

For our model we have set τ_{HSP} so that HSP acts on a timescale of hours, consistent with some empirical findings (Gina Turrigiano, personal communication). However, homeostatic plasticity in the adult visual system of a goldfish with an intact CNS was found to operate on a timescale of 90 minutes (Riegle and Meyer 2007). HSP mechanisms acting on a shorter timescale than what is implemented in our model may be feasible but require further investigation.

At this point, the specification of the spiking A1 model with homeostatic plasticity is complete and the operations of the homeostatic mechanisms and model behavior after hearing loss are simulated.

3 Results

In this section, we investigate the performance of the model through computer simulations. Specifically, the model is first trained under different hearing loss scenarios for a sufficiently long time period so that the sound-driven firing activity of the pyramidal neurons can reach equilibrium under the control of HSP. For all three hearing loss scenarios, we observe that homeostatic plasticity is able to compensate for the deafferentation and maintain the mean sound-driven neural firing rate of the pyramidal neurons in

a small region around the pre-fixed target value r_{target} (=90 spikes/s). Figure 2 shows comparative curves representing the average firing rates of the pyramidal neurons with and without HSP in the case of 80% hearing loss. It can be seen that with HSP, the average firing rate curve is relatively flat around 90 spikes/s, while the average firing rate curve generated by the A1 model without HSP exhibits a negative slope similar to the hearing loss curve. In Fig. 3, we plot the connection weights of synapses targeting on two pyramidal neurons, one in the normal hearing region and the other in the mid-section of the most substantially deafferentated region. With HSP, the shape of the weight distribution for synapses targeted on the impaired neuron is not changed. This is because the afferent and lateral excitatory connections are strengthened in a multiplicative fashion, and the feedback inhibitory synapses are weakened by the same factor. The excitatory connections on the interneurons are not affected by our HSP mechanism, as explained above. More importantly, the weight envelopes in Fig. 3 describing the peak synaptic weight for neurons across the tonotopic axis, show that the amount of synaptic adjustment induced by HSP is a function of the hearing loss level; a sufficient level of hearing loss in our model should therefore lead to conditions that are favourable to travelling waves. The more severe the hearing loss, the greater compensatory effects and the higher the excitability of the pyramidal neurons would be, which is consistent with experimental results on homeostatic plasticity (Turrigiano et al. 1998; Rutherford et al. 1998; Kilman et al. 2002). This also holds for inhibitory connection weights, which are reduced in proportion to the level of deafferentation. Because our HSP mechanism scales synapses multiplicatively, the ratio of afferent to lateral excitation remains fairly constant. On the other hand, the ratio of lateral inhibition to lateral excitation on pyramidal cells drops as the level of hearing loss increases; this may

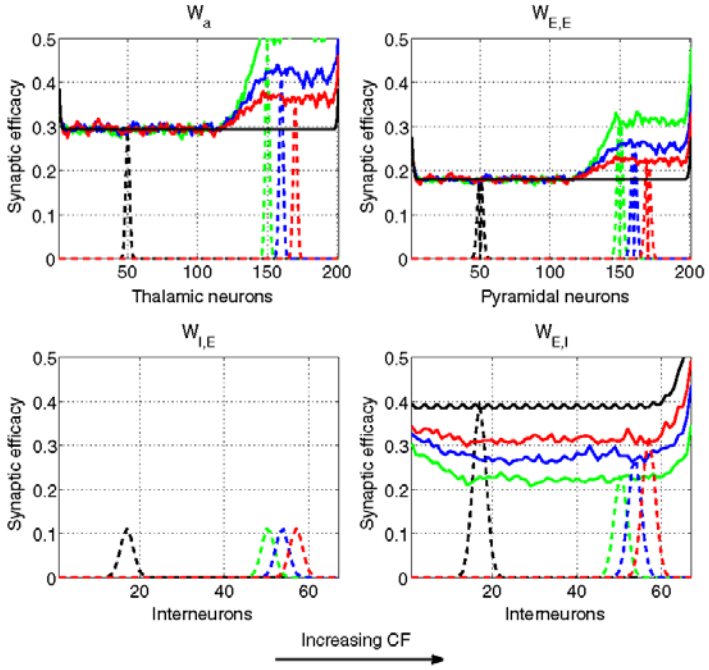

Fig. 3 Connection weight distribution comparison after HSP. Dashed lines show example weight distributions for synapses targeted on the 50th pyramidal neuron (CF=0.37 kHz) and a pyramidal neuron in the deepest hearing loss region for each hearing loss level. Solid curves represent peak synaptic efficacy in weight distributions for each neuron (shown only for synapses projecting onto excitatory neurons). Black curve: Unimpaired neurons with synapses unaffected by HSP (initial weights are all at this level except for weights at edges). Green curve: synapses targeted on the 150^{th} pyramidal neuron (CF=5.76 kHz) after 80% hearing loss; Blue curve: synapses targeted on the 160^{th} pyramidal neuron (CF=7.34 kHz) after 60% hearing loss; Red curve: synapses targeted on the 170^{th} pyramidal neuron (CF=9.41 kHz) after 40% hearing loss. sub-figure $\mathbf{W_a}$: weight comparison for thalamocortical afferent synapses; sub-figure $\mathbf{W_{E,E}}$: weight comparison for lateral excitatory synapses; sub-figure $\mathbf{W_{I,E}}$: weight comparison for synapses projecting onto interneurons; sub-figure $\mathbf{W_{E,I}}$: weight comparison for feedback inhibitory synapses

have implications for the development of travelling waves, as will be discussed later.

The inputs to the model are independent and do not take into account potential HSP-induced changes in lateral inhibitory connections in lower auditory structures such as the inferior colliculus (Gerken 1996). This allows us to consider changes in the auditory cortex independent of confounding factors in the inputs. However, we acknowledge that future versions of the model should address potential changes at subcortical levels to determine their effect on our simulations.

Next, we fix the synaptic weights and expose the model to afferent spontaneous activity or transient tonal stimuli. We present the obtained model responses in the following subsections. The first two sections are meant to validate the model by comparing its simulations to empirical findings. In the following section, we evaluate the robustness of our model with respect to two key validating results. Finally, we outline simulations related to our novel prediction on the existence of travelling waves of excitation in A1.

3.1 Spontaneous activity and synchrony

In Fig. 4, we plot the mean firing rates of the pyramidal neurons in the A1 layer in response to the afferent spontaneous activity from the auditory thalamus. The results presented here are calculated on the basis of a simulated 30-second recording. As we can see from the figure, for all three hearing loss scenarios, the impaired region of the A1 model shows a significant increase in its spontaneous activity, which is qualitatively consistent with empirical findings in animals with noise-induced hearing loss (Popelar et al. 1994; Komiya and Eggermont 2000; Seki and Eggermont 2003). Furthermore, the input-output plot in the figure shows that when a deafferented neuron is driven by tonal stimuli of different intensities, the neuron consistently has a greater level of excitability than an unimpaired neuron for a given input spike rate. Spontaneous activity in the impaired region for 60% hearing loss is around two to three times higher than that for 40% hearing loss. Increase in spontaneous firing rate in the case of 80% hearing loss is even more significant (around five times higher than that of 40%). This is due to the fact that more substantial hearing loss results in greater enhancement in the excitability of pyramidal neurons, as observed in the previous section. In animal experiments, the enhanced spontaneous activity in the impaired cortical region is no higher than double the normal value (Komiya and Eggermont 2000; Seki and Eggermont 2003). Our results showing a much higher increase in spontaneous firing rate in the case of 80% hearing loss can be attributed to the substantially reduced afferent driving forces, which is less likely to be observed in standard animal models, as mentioned earlier. However, this qualitatively valid result allows us to gain more insight into why long-range travelling waves of activity may not develop in the impaired A1, regardless of the level of hearing loss.

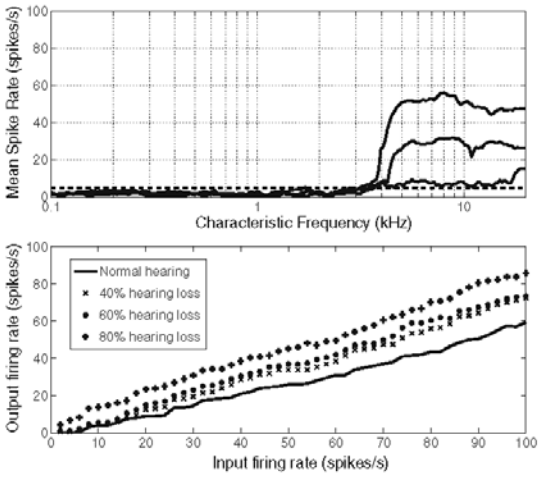

Fig. 4 Top panel: mean firing rates of the pyramidal neurons in response to spontaneous activity in the auditory thalamus (spike rate vs. characteristic frequency). Dashed curve: mean spike rate of the spontaneous input; Upper curve: model response after 80% hearing loss and HSP; Middle curve: model response after 60% hearing loss and HSP; Bottom curve: model response after 40% hearing loss and HSP. Bottom panel: input-output curves following HSP for different levels of hearing loss

Changes in spontaneous firing rates (SFR) induced by acoustic trauma have been studied in the auditory nerve fibers (where a drop in SFR is observed), dorsal cochlear nucleus (where an increase in SFR is observed), the inferior colliculus (where a drop in SFR is observed) and the A1 (where an increase in SFR is observed) (Basta et al. 2004; Eggermont and Roberts 2004). However, spontaneous firing rates in the auditory thalamus have not been sufficiently characterized. We modeled hearing loss in our thalamocortical inputs as an overall decrease in average firing rate based on firing rate changes in the inferior colliculus.

To investigate synchronous firing in the spontaneous activity of the A1 model, we compute the cross-correlation of the spike trains generated by different pyramidal neurons, using the following equation (Seki and Eggermont 2003; Noreña and Eggermont 2003):

$$p_{i,l}(d) = \frac{\left(\sum_t x_i(t)x_l(t-d) - N_i N_l/N\right)}{(N_i \cdot N_l)^{0.5}}, \qquad (15)$$

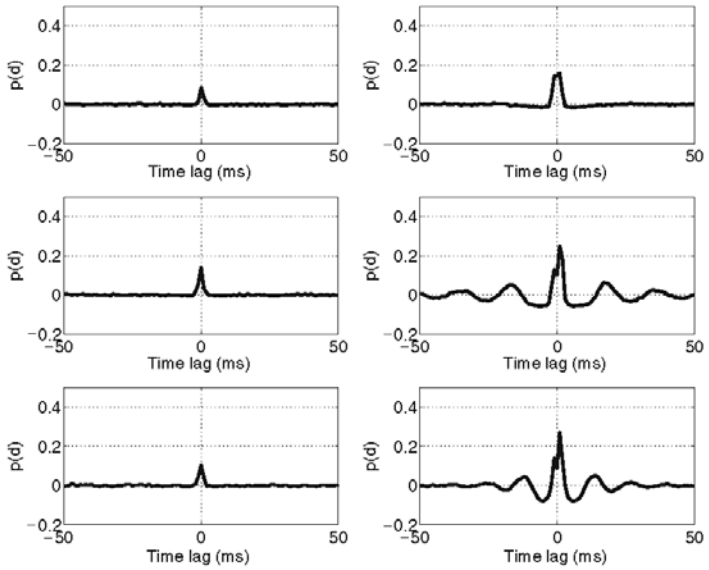

Fig. 5 Cross-correlation of the spontaneous activity of pyramidal neurons. The sub-figures in the first column present synchrony between the 51st pyramidal neuron (CF=380 Hz) and the 56th pyramidal neuron (CF=450 Hz), both of which are within the unimpaired region. The sub-figures in the second column show cross-correlation of firing activities between the 151st pyramidal neuron (CF=5.9 kHz) and the 156th pyramidal neuron (CF=6.6 kHz), both of which are within the impaired region. Results for different hearing loss levels are arranged in rows. The 1^{st} row: 40% hearing loss; the 2^{nd} row: 60% hearing loss; the 3^{rd} row: 80% hearing loss

where $x_i(t)$ and $x_l(t)$ represent the spike trains of the ith and the lth pyramidal neurons, respectively, d denotes the time lag spanning the range from −50ms to 50ms, N_i and N_l are the total number of spikes in $x_i(t)$ and $x_l(t)$, respectively, and N is the number of bins (bin size=2ms). In Fig. 5, we plot the cross-correlation as a function of the time lag d for two pairs of pyramidal neurons, one pair in the normal hearing region and the other pair in the impaired region. The neural synchrony between deafferentated excitatory neurons is significantly increased, compared with two normal neurons with the same spatial distance. Specifically, as shown in the figure, the peak value of the cross-correlation curve increases from approximately 0.1 to 0.17, 0.23, and 0.24 for 40%, 60% and 80% hearing loss levels, respectively. Although qualitatively similar, cross-correlation values obtained from simulations were an order of magnitude higher than those found in the literature (Seki and Eggermont 2002, 2003). This can be explained by the fact that our model of the auditory cortex contains significantly fewer neurons and connections (both lateral and afferent) than would be found in actual cortex. We developed a proof of concept model (not shown) with a variable number of inputs and outputs to demonstrate the effect of network connection complexity on peak cross-correlation values. As the number of input or output units in the network increased, the cross-correlation between any two output neurons decreased. Due to the computational complexity of a much larger network, we could not address this issue by scaling up our network.

In Fig. 6, we study the variations of the cross-correlation peaks as a function of the original characteristic frequencies of the pyramidal neurons. The peak value associated with each CF is determined by the maximum of the cross-correlation between the pyramidal neuron tuned to that CF under the condition of normal hearing (say, the ith neuron) and the other one

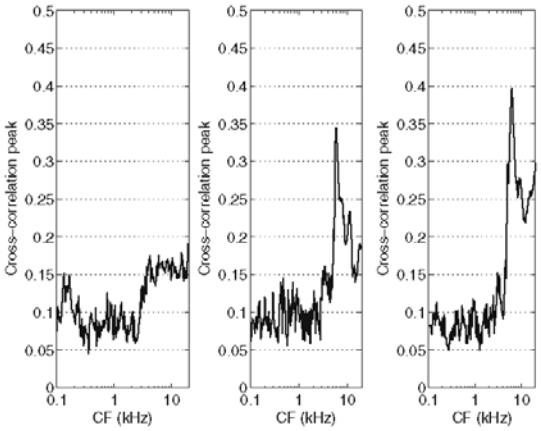

Fig. 6 The variation of cross-correlation peaks as a function of characteristic frequencies (CF). The peak value associated with each CF is the maximum of the cross-correlation between one pyramidal neuron with the same CF and another with spatial distance 6. Left sub-figure: peak variation curve after 40% hearing loss; Middle sub-figure: peak variation curve after 60% hearing loss; Right sub-figure: peak variation curve after 80% hearing loss

with spatial coordinate $i + 6$. From the figure, we can observe a clear elevation of the synchrony starting from the beginning of the hearing loss region at 2.5 kHz. Figure 6 shows that for higher levels of simulated hearing loss (60% and 80%), the greatest increase in synchrony occurs near the hearing-loss edge, where there is a stronger tendency for edge frequencies to drive these neurons. However, peak cross-correlation values are elevated across the hearing loss region. Thus, our model predicts that elevated synchrony in the hearing loss region may result from HSP-induced increased lateral excitation and decreased lateral inhibition; these are the same conditions that would be expected to produce travelling waves of activity.

3.2 Tuning properties after hearing loss

Since we are adjusting connection weights, it is important to look at potential changes in tuning. We do this by simulating a 50-ms input tone, varying its amplitude and center frequency, and observing the response of a neural unit in the hearing loss region. In Table 1, we look at potential changes in characteristic frequency and tuning sharpness for a unit with a normal CF of 5.2 kHz. We represent tuning sharpness using Q-values (Q20 in this case), which is analogous to what would be done for frequency-response-area plots obtained from electrophysiological recordings. Since our inputs are spikes at a certain rate rather than a sound level, Q20 is calculated by dividing the unit's CF by its bandwidth at an input rate 20 spikes/s above the minimum threshold. The minimum threshold is the lowest input tone rate required to elicit firing in the neuron; the center frequency of this tone is the unit's characteristic frequency. To determine the relevant bandwidth, the input tone's level is set to 20 spikes/s above the minimum threshold, and the lowest- and highest-frequency input tones that can elicit firing are determined. Tuning sharpness is reduced as the level of hearing loss increases; this is true for neural units throughout the hearing loss region. At 60% and 80% hearing loss, the Q20 value is substantially lower than in the normal scenario. Our model only shows small shifts in CF; they ranged from 0.05 octaves to 0.2 octaves in the neural units we looked at. In Table 1, we see a shift away from the hearing loss edge. Units closer to, or within, the sloping region of the hearing loss curve are more likely to exhibit CF-shifts to lower frequencies. On the other hand, units deeper in the hearing loss region could show CF-shifts towards higher or lower frequencies. This may be a result of the symmetry in our initial network connection weights. Namely, as the hearing loss curve is flat in these areas, the relative homeostatic adjustments may be stronger on one side of these units. The magnitude of weight adjustment could vary depending on the spontaneous inputs generated (using mutually independent Poisson processes) during homeostatic plasticity in our model. Furthermore, there may be an influence of the network edge at higher frequencies.

Table 1 Tuning properties of a neuron in the hearing loss region

Hearing loss level	Q20	Characteristic frequency (kHz)
No hearing loss	2.87	5.20
40% loss	2.40	5.76
60% loss	0.448	5.48*
80% loss	0.427	5.48*

This neural unit has a CF of 5.2 kHz when there is no hearing loss. At 60% and 80% hearing loss, there was no single frequency with the lowest threshold, so the one which evoked the strongest response is said to be the CF

While our homeostatic mechanism does not lead to significant tonotopic reorganization, it does have a substantial effect on tuning. Figure 7 compares changes in tuning for different levels of hearing loss in our model with tuning observed in a noise trauma experiment. To produce the rate-frequency-intensity contours we simulated 50-ms tones at frequencies from 1 kHz to 16 kHz and at levels from 10 to 65 spikes/s. We ran 5 simulations for each scenario and combined the responses. Noreña et al. (2003) presented each 15-ms tone pip 5 times at frequencies ranging from 625 Hz to 20 kHz. Our simulations show a broadening of the tuning curve with increased hearing loss. Furthermore, the CF becomes difficult to distinguish at 60% and 80% hearing loss levels. As in Table 1, it is evident that tuning becomes very broad for the higher levels of hearing loss in our model. We do not see threshold increases with hearing loss, and for this neural unit, a decrease in threshold is evident after 40% hearing loss. This may be due to too much compensation from our homeostatic mechanism and the lack of a realistic peripheral input model. The multi-unit activity (Noreña et al. 2003) after tonal trauma shows a variety of possible effects including a threshold decrease (see iii versus vii in Fig. 7(E)).

3.3 Sensitivity analysis

A sensitivity analysis demonstrates the impact of modifying key model parameters on two of our results: peak cross-correlation between two neural units and the spontaneous firing rate of a neural unit in the hearing loss region. Specifically, we look at the peak cross-correlation, in the region of simulated hearing loss, between neurons with characteristic frequencies

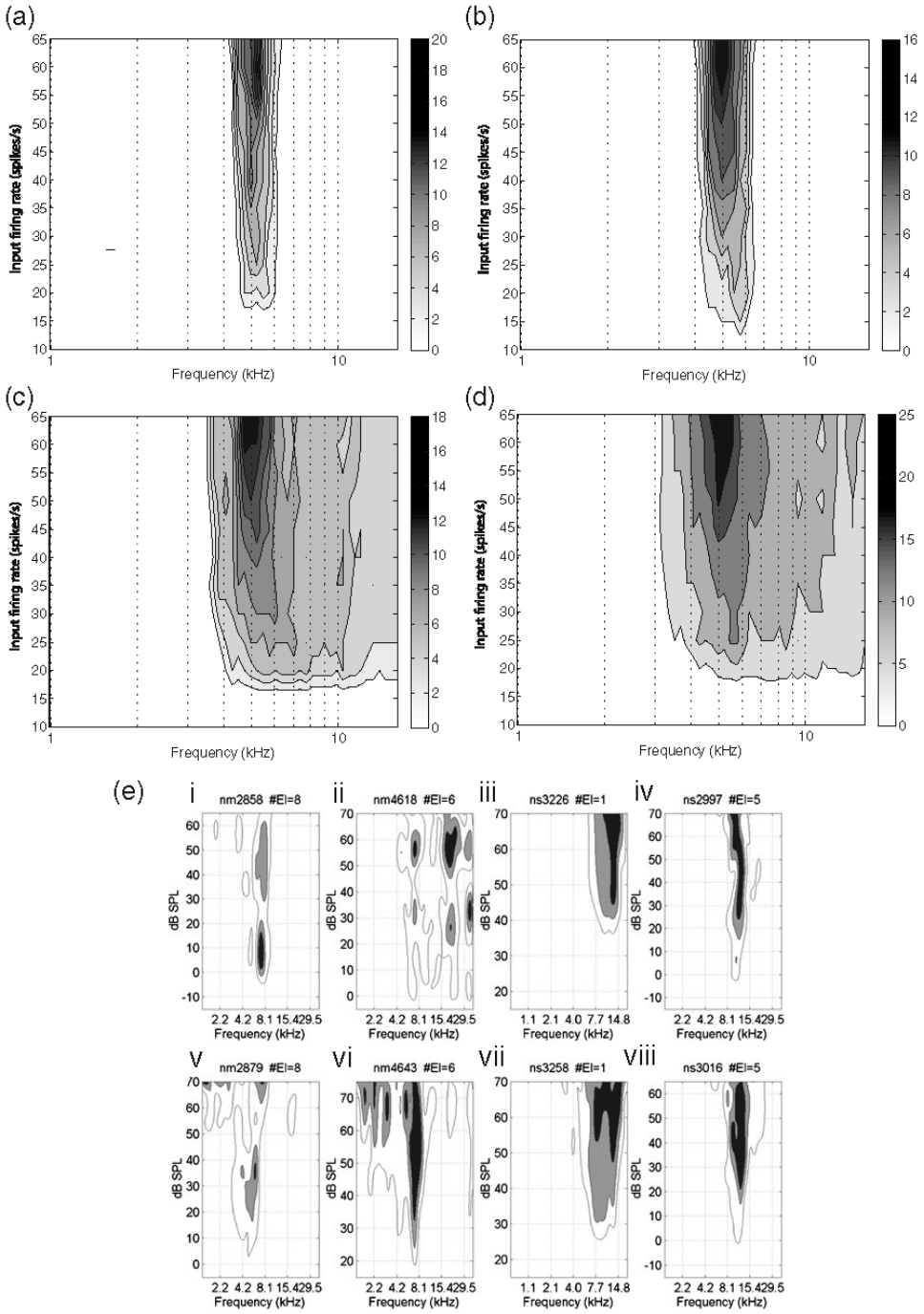

Fig. 7 Rate-frequency-intensity contours from our model and cat primary auditory cortex. The top portion of the figure shows simulated tuning curves from our model with no hearing loss (A), 40% (B), 60% (C) and 80% (D) hearing loss. Below (E), we include tuning curves from anesthetized cats before (top half) and after (bottom half) a 120 dB pure-tone trauma (Fig. 4 from Noreña et al. 2003)

Table 2 Sensitivity analysis

Parameter (*0.5:*2)	Peak cross-correlation	Spontaneous firing rate
Driving input rate	−0.7%:+22%	+34%:−27%
W_a initial	+67%:−37%	+52%:−14%
$W_{E,E}$ initial	−39%:+74%	+36%:−32%
$W_{I,E}$ initial	+12%:+4.3%	+5.3%:+3.9%
$W_{E,I}$ initial	−6.8%:+3.1%	−15%:22%

For each parameter, the value on the left and right side of the colon represents the change in the output metric after halving or doubling that parameter, respectively. The parameters we look at are: the driving rate in the simplified acoustic environment, the afferent connection weights, the connection weights between excitatory neurons, excitatory to inhibitory connection weights, and inhibitory to excitatory connection weights, respectively

5.2 kHz and 5.9 kHz (spatial distance of 6 neural units) and the spontaneous firing rate of the neural unit with a CF of 5.2 kHz. Table 2 lists changes in the output metrics when each parameter is halved or doubled. To reduce the number of required simulations, we choose one hearing loss condition (80% hearing loss) and modify the parameters for that scenario.

Increases in peak cross-correlation or spontaneous firing that result from changing parameters are acceptable since we expect these values to be elevated after hearing loss. The 37% and 39% decreases in peak cross-correlation that occur after doubling the initial afferent synaptic weights or halving the initial lateral excitatory weights, respectively, are still an order of magnitude lower than the increase in synchrony seen for 80% hearing loss (see Fig. 6). The same argument holds for the 27% and 32% reduction in spontaneous firing when the driving input rate during the homeostatic compensation is doubled or the initial connection weights between excitatory neurons are doubled, respectively (see top panel in Fig. 4).

3.4 Model prediction: spontaneous travelling waves

It is well known that travelling waves will appear in the rate-based Wilson-Cowan cortical model (Wilson and Cowan 1972, 1973; Wilson 1999) if the lateral inhibitory connections are weakened and excitatory connections are strengthened sufficiently (Wilson 1999; Wilson et al. 2001). Accordingly, we hypothesized that pyramidal neurons in our spiking A1 model (inspired by the Wilson-Cowan equations), might also generate travelling waves in the impaired region. Given that the amount of synaptic weight regulation is proportional to the hearing loss level, we predicted that travelling waves would be more likely for substantial hearing loss.

To test our hypothesis, we conducted the following simulations. The A1 models trained by HSP under different hearing loss scenarios are stimulated simultaneously by two pure tones with a duration of 15ms and input level of 50 spikes/s. We do not scale these

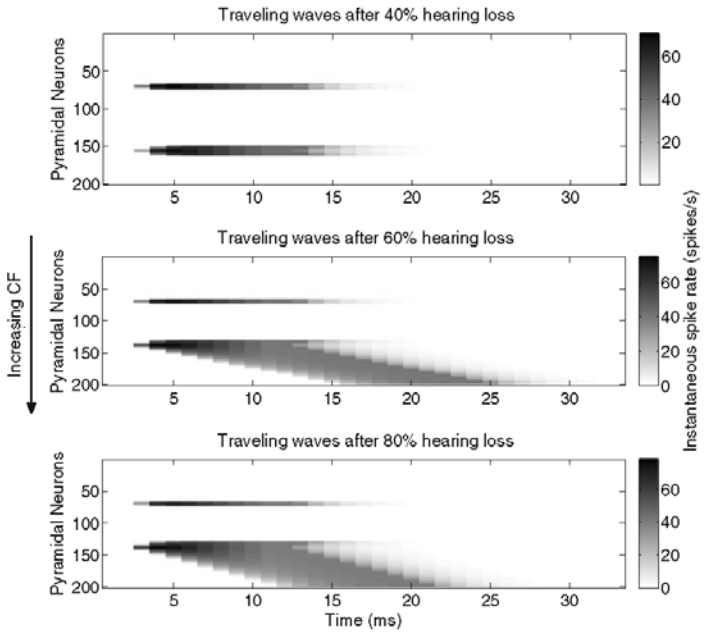

Fig. 8 Model responses to pure tones with no background spontaneous activity. For 40% hearing loss (top), the frequencies of the input pure tones are 723 Hz and 7.2 kHz. For 60% (middle) and 80% (bottom) hearing loss, the tonal stimuli have center frequencies of 723 Hz and 4.27 kHz. The bars beside the figures illustrate the intensity scale, where darker shades indicate higher stimulus-driven firing rates

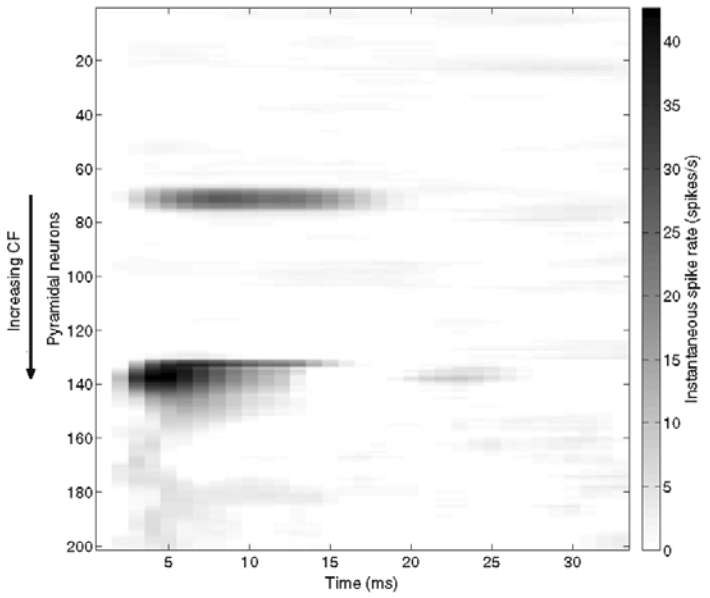

Fig. 9 The figure shows the lack of travelling waves when spontaneous firing is included in the input. The plot was created as follows: 100 trials of the 80% hearing loss scenario with input tones as described in Fig. 8 but with spontaneous firing included were averaged, 100 trials with only spontaneous firing were averaged, and finally, the latter average was subtracted from the former average

tones according to the level of hearing loss, as we have not described them as having the same sound level but rather, as inducing the same thalamic input rate. Scaling the tones according to the level of hearing loss does not qualitatively affect the results or existence of travelling waves discussed below. We first look at a case where there is no spontaneous firing, which is a scenario that is more analogous to the rate-based Wilson-Cowan cortical model.

The frequencies of the test tones are chosen so that one is within the normal region and the other is within the hearing loss region. The model responses to the

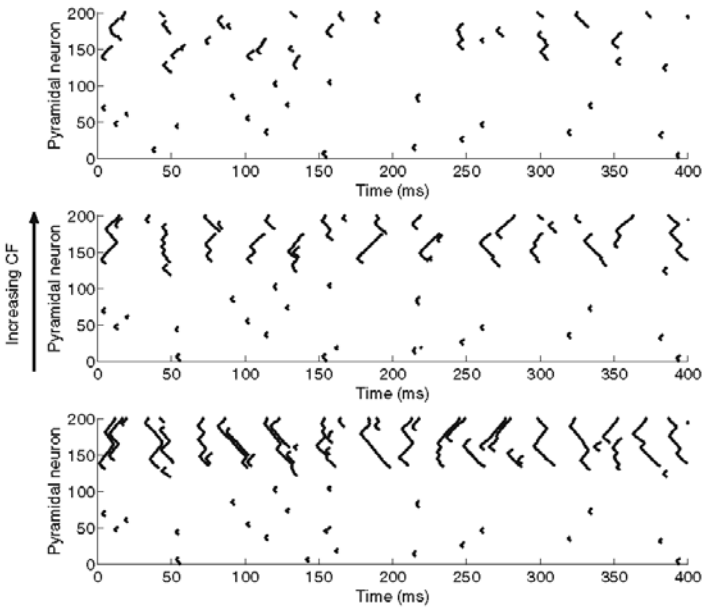

Fig. 10 Raster plots of spontaneous activity across the model A1 for different levels of hearing loss (deafferented region spans neurons 125–201). Top: 40%, middle: 60% and bottom: 80% all show increase in occurence and spatial extent of waves of excitation

tonal stimuli, quantitatively described by the instantaneous firing rates of the pyramidal neurons, were calculated using Eq. (12) with τ_r set to be 5ms. In the case of 60% and 80% hearing loss, pure tones at 723 Hz and 4.27 kHz are used, while for 40% hearing loss, pure tones at 723 Hz and 7.2 kHz are applied. For the 40% hearing loss scenario, the second tone was applied deeper in the impaired region to highlight that for this level of hearing loss, our model will not show tone-induced travelling waves. This is the case even though there is no spontaneous firing and the tone is applied in the region where lateral inhibitory connections are weakest. However, even at this level, spontaneous short-duration waves (shown in Fig. 10) occur. Thus, we establish that in our model, deafferentation above 40% is necessary to produce travelling waves of excitation when no spontaneous firing is present. In Fig. 3 we observe that the ratio of peak lateral inhibition on a pyramidal cell to peak lateral excitation drops to approximately 1 only at 60% hearing loss. This may be a necessary condition for the development of travelling waves when spontaneous firing is not present.

In Fig. 8, we plot the model responses in intensity maps of firing rates across spatial coordinates of the pyramidal neurons and time, in order to illustrate the propagation of the travelling waves in the case of no background spontaneous activity. After 60% and 80% hearing loss, a brief pure tone applied in the sloping region of the hearing loss curve caused sequential firing of the pyramidal neurons previously tuned to frequencies higher than the stimulus. In other words, a travelling wave appears; more importantly, with the travelling wave, all of the pyramidal neurons in the region of maximum hearing loss now become responsive to an edge frequency of the hearing loss spectrum (=4.27 kHz), which indicates the potential for cortical reorganization. This phenomenon can again be explained by the fact that HSP degrades inhibition and strengthens lateral excitation more for severe hearing loss. In contrast, after 40% hearing loss, even a tonal stimulus located within the most deafferentated region does not lead to propagating neural firing. Instead, compared with the model response to the 723-Hz pure tone in the normal hearing range, more neurons in the impaired region are excited by the input at 7.2 kHz. This phenomenon indicates the broadening of the tuning curves of the pyramidal neurons after hearing loss, which is consistent with experimental findings (Calford et al. 1993; Seki and Eggermont 2002; Noreña and Eggermont 2003).

As our model is based on a modified Wilson-Cowan cortical model, and travelling waves are clearly observed in this model for low levels of inhibition, it is expected that with a sufficient reduction in inhibition and increase in excitation, neural activity may propagate into neighboring neurons. Although we found that tonal stimulation in the deafferented region did produce long-range travelling waves with 60% and 80% hearing loss (Fig. 8), interestingly, this did not hold true when the model was also driven by inputs exhibiting spontaneous firing (5 spikes/s) (Fig. 9). This constitutes an unexpected finding by our model, as we are able to show that the types of long-range travelling waves predicted in a rate-based Wilson-Cowan cortical network will not necessarily occur in a spiking model with spontaneous firing inputs. Although we use a spontaneous input rate of 5 spikes/s, our simulations show that long-range travelling waves can be eliminated with spontaneous input rates as low as 1.5 spikes/s. It is also evident that even though travelling waves do not propagate across the hearing loss region, deafferented neurons do have less selective tuning.

A raster plot (Fig. 10) of activity during the silent condition, where the continuous driving rate is low, shows spontaneous waves of excitation with low temporal extent. We argue that with hearing loss, the rate of occurrence of waves of excitation increases, but their temporal extent is relatively unchanged because of interference from other waves of excitation. This lead to the hypothesis that while long-range travelling waves of excitation could be induced after hearing loss, interference by spontaneously evoked waves of excitation would severely limit their temporal extent. This could explain the lack of empirical evidence for long-range travelling waves of excitation in auditory cortex in spite of the presence of an increase in synchrony.

4 Discussion

We have presented a spiking model of primary auditory cortex (A1) and computational rules for the homeostatic regulation of synapses of different types, to address the question of whether travelling waves of neural activity could occur in A1 after hearing loss. The homeostatic plasticity (HSP) mechanisms were assumed to be the main driving force behind necessary changes to inhibition and excitation that would allow for travelling waves according to the Wilson-Cowan cortical equations. In addition, we postulated that homeostatic plasticity may be the neural mechanism underlying persistent abnormal neural activity in A1 observed after peripheral hearing loss. We showed through computer simulations that homeostatic

plasticity can scale synapses multiplicatively to bring the mean sound-driven firing rates of the deafferented cortical neurons back to a pre-specified target rate (i.e., the average firing rate of pyramidal neurons when stimulated by the same sound stimulus under the normal hearing condition). The compensatory effects of HSP lead to increased spontaneous activity and neural synchrony in impaired cortical regions, as has been found empirically (Seki and Eggermont 2003). These neural correlates of hearing loss in the auditory pathway, especially those in A1, are widely considered as potential substrates of tinnitus, the phantom sensation of a sound in the absence of any physical sound stimuli (Muhlnickel et al. 1998; Kaltenbach 2000; Eggermont 2003, 2005). Furthermore, our model shows an expansion of the excitatory response area for neurons in the hearing loss region. Calford et al. (1993) observed similar enlarged response areas in some neurons in A1 after tone-induced hearing loss. Unlike that study, we did not find contraction of any response areas or more complex changes. The reduced selectivity of the neural units in our model results from reduced lateral inhibition, which allows weaker thalamocortical inputs as well as cortico-cortical inputs to depolarize the neural unit above its threshold. Our simulations did not show tonotopic reorganization on the scale that has been described in studies of cochlear lesions (Robertson and Irvine 1989) and acoustic trauma (Seki and Eggermont 2002). The largest shifts we found were 0.2 octave shifts. Aside from peripheral and subcortical changes, there may be other mechanisms that we have not described in our model, which lead to tonotopic reorganization. Furthermore, they may operate on timescales that are greater than those in our analysis (Robertson and Irvine 1989). We observed shifts ranging from 0.05 to 0.2 octaves, with larger shifts occurring closer to the hearing-loss edge. These are certainly lower than shifts described by Robertson and Irvine (1989) (up to 0.625 octaves) after unilateral cochlear lesions and those (0.64–0.76 octaves) observed by Noreña et al. (2003) after pure-tone trauma. Near the edge of hearing loss, there are intact inputs from the normal hearing loss region that can shift the CF to lower frequencies. It should be pointed out that, our model sometimes showed an increase in CF, while most studies demonstrate a shift toward the frequencies of the lesion or noise trauma. We suggest that this may be the result of our network architecture: symmetrical connection weight distributions and perhaps network edge-effects at very high frequencies. Furthermore, this may imply that connections in our model do not span large enough distances, and so neural units that are not deafferented cannot sufficiently drive neurons deeper in the hearing loss region. Further evidence of this is the fact that greater shifts in CF occur closer to, and within, the sloping region of the hearing loss curve.

Hearing loss may also alter the inherent excitability of pyramidal neurons, which we did not include in our model. Kotak et al. (2005) found that sensorineural hearing loss can lead to a slightly depolarized resting membrane potential in pyramidal neurons of the auditory cortex. This may contribute to a higher spontaneous firing rate in these cortical neurons but does not necessarily explain an increase in synchrony of firing between cortical neurons. The elevated synchrony is better predicted by the strengthening of excitatory synapses on deafferented neurons (Vale et al. 2002; Muly et al. 2004; Kotak et al. 2005) and the weakening of inhibitory synapses onto these neurons (Suneja et al. 1998a, b; Vale et al. 2002; Kotak et al. 2005).

If homeostatic mechanisms enhance lateral excitatory and reduce lateral inhibitory connections, the Wilson-Cowan cortical model predicts travelling waves of neural activity. Our model indicates that travelling waves of activity are unlikely to develop in deafferented A1 when spontaneous activity is present. Rather, spontaneous, short-duration waves of excitation occur more frequently. The long-range travelling waves that are predicted by the Wilson-Cowan equations are prevented from spreading by these spontaneous short-duration waves. Specifically, it is the resultant refractory periods that prevent large-scale activity propagation in the network. Furthermore, the increased spontaneous firing that occurs in A1 after hearing loss would counteract network conditions that favor travelling waves because of the increase in spontaneous short-duration waves. Perhaps, as in the interactions of avalanches in models of running sandpiles (Hwa and Kardar 1992), the interactions of these spontaneous waves with each other and with any stimulus-induced wave, impede the observation of a single dominant travelling wave. However, the refractory period that follows the spontaneous short-duration waves, produces destructive interference, which differs from avalanche interaction and seems to be the main factor behind the lack of long-range travelling waves of activity.

While Fig. 8 clearly shows broadened tuning curves after the homeostatic modifications of connection weights, broadening of the tuning curves is also seen when spontaneous activity is introduced. Namely, Fig. 9 indicates that in the hearing loss region, neurons are less selective. Therefore, our model does not require conditions that allow for long-range travelling waves in order to demonstrate the broadening of tuning curves.

A recent model for epileptogenesis in isolated neocortex has produced results similar to the Wilson-Cowan equation predictions (Houweling et al. 2005). Using a network of Hodgkin-Huxley style neurons with both excitatory and inhibitory interactions, it was shown that HSP could lead to neural bursting and to waves travelling at 1.0–3.0 cm/s. A key difference between that model and the one we present here is that we apply HSP to a model of auditory cortex in which there was only partial deafferentation; this is more appropriate for hearing loss. In addition, deafferentation was restricted to the high frequency region of our model. Because of these differences we were able to show that only short-duration waves could span sections of the hearing loss region. As observed waves of excitation could develop throughout the impaired region, they may also play a role in cases of tinnitus where the percept is matched to frequencies spanning the hearing loss region (Eggermont and Roberts 2004). Furthermore, our simulation results (Fig. 10) imply that the short-duration waves may contribute to two changes in neural activity linked to tinnitus: increased spontaneous firing rates in deafferented neurons as well as increased synchrony between them and neurons they are connected to. Since neurons in the hearing loss region are less selective and allow for short-duration activity propagation, the spontaneous firing of each afferent will excite a greater number of cortical neurons, leading to greater spontaneous firing and synchrony. The similarity of our results to the results of Houweling et al. (2005) suggests that HSP may play a role in a range of cortical activity disorders including epilepsy and tinnitus. This has also been suggested in recent work by Fröhlich et al. (2008).

Several simpler computational models of the auditory system have addressed the role of HSP and related adaptation mechanisms to tinnitus. Schaette and Kempter (2006) proposed a single neuron model that qualitatively reproduces the hyperactivity observed in dorsal cochlear nucleus after increasing the synaptic gains of excitatory inputs. However, the choice of rate-based model neurons and lack of lateral connections in their model limits its ability to address the network-level changes in the temporal firing patterns such as neural synchrony. Dominguez et al. (2006) proposed a simple auditory cortical circuit model using spiking neurons, in which loss of auditory input was compensated for by enhancing the excitatory synapses and weakening inhibitory synapses on lateral connections. This model was able to capture enhanced synchrony in the deafferented region but was nonetheless limited in its ability to capture the full range of temporal dynamics, such as relative timing of excitatory and inhibitory responses. Our model builds on this work by 1) incorporating a computationally principled scheme for implementing HSP rather than manually adjusting the synaptic strengths, and 2) incorporating separate layers of excitatory and inhibitory neurons, so that more realistic temporal dynamics including travelling waves can be captured.

Finally, Fröhlich et al. (2008) use a computational network model of the neocortex to shed light on the development of dysfunctional cortical dynamics after deafferentation-induced homeostatic scaling of recurrent excitatory connections. This model predicted aberrant periodic bursting in the network if there was a critical level of deafferentation. We investigate the possibility of travelling waves by providing a more complete description of the changes in network dynamics through homeostatic plasticity. Namely, we propose formal computational mechanisms for HSP in both lateral and afferent connections. This addresses the lack of regulation of afferent connections and lateral connections onto inhibitory interneurons in the Fröhlich et al. (2008) model. In addition, while our homeostatic time constant is supported experimentally (Turrigiano et al. 1998), its update rate operates on the timescale of our simulated neural activity. This is not the case in the Fröhlich et al. (2008) model, where synaptic weights are updated at each 4-second interval.

One aspect of our model that is anatomically oversimplified is the manner by which we connect the input thalamic layer to the cortical layer to obtain relatively realistic tuning curves. It has been shown empirically that the functional convergence of thalamocortical projections spans about $\pm 1/3$ octaves (Miller et al. 2001), and we set the thalamo-cortical connections to match this functional convergence. However, it should be noted that auditory thalamic neurons can project to a much wider cortical region, while under normal hearing conditions, a large proportion of the excitatory synapses are functionally masked by thalamo-cortical input-driven inhibition. This feature is believed to provide the physiological basis for the rapid shifts in tuning curves, presumably due to unmasking of silent synapses, observed shortly after peripheral damage (Rajan 1998, 2001; Calford 2002; Noreña and Eggermont 2003). More specifically, it has been postulated that peripheral damage can reduce the stimulus-driven inhibition so that previously inhibited responsiveness can be unmasked. Our model developed in this paper has limited capability to fully account for the possible contributions of rapid unmasking to cortical changes observed shortly after cochlear impairment. Instead, we set up more constrained thalamo-cortical projections to separately investigate the potential role of HSP in inducing the cortical

abnormalities. It is possible that the acute cortical changes induced by unmasking effects, which might be weak at the beginning, are stabilized and strengthened by HSP so that they become detectable 2 hours after noise trauma (Noreña and Eggermont 2003) and persist in the following weeks (Seki and Eggermont 2003).

In the current version of our model, we did not include any Hebbian-like plasticity mechanism, such as spike timing dependent plasticity (Markram et al. 1997). This is largely because there is insufficient information on the characteristics of the output of the auditory thalamus. In our simulations with HSP, we assumed that the hearing-impaired model was exposed to a simplified acoustic environment where all the audible frequency components are mutually independent and possess the same average power over a large timescale. Under this assumption, correlation-based synaptic plasticity would not learn any pattern-specific features from the incoming acoustic stimuli, while HSP still functions. In future developments of the model, with the help of peripheral models such as the one developed by Zilany and Bruce (2006), we will combine pattern-specific learning with HSP.

Finally, the homeostatic response we simulate in response to hearing loss without including other factors or mechanisms may also compensate too well. If this is the case, it may reconcile the fact that in our model, tonal stimuli sometimes elicit stronger firing rates in the hearing loss region, even after their input rate is reduced according to the hearing loss level. Furthermore, this may help to explain why we do not see an elevated threshold after hearing loss in our model. Inclusion of a peripheral model that can incorporate cochlear hair cell impairment (such as that of Zilany and Bruce 2006) will allow more direct investigation of the effects of threshold elevation and other changes in peripheral tuning and excitability.

However, even with the above limitations, our model was able to produce a novel prediction with respect to travelling waves of neural activity in the deafferented A1. Using our comprehensive homeostatic mechanisms that scale different types of synapses, we were able to reproduce activity changes that are seen in animal models of sensorineural hearing loss. These alterations in spontaneous firing and neural synchrony resulted from homeostatic decreases of inhibition and increases of excitation in response to hearing loss. Furthermore, our model shows the broadening of tuning curves and some potential for slight tonotopic reorganization after hearing loss. While the Wilson-Cowan cortical model predicts long-range travelling waves under such conditions, by incorporating a greater level of biophysical detail including spiking neuronal dynamics and spontaneous activity, we refine this prediction; it is postulated that short-duration travelling waves of a more limited spatial extent could be observed in animal models of hearing impairment and tinnitus. Our findings on spontaneous short-range waves of excitation provide new insight into potential mechanisms underlying tonotopic remapping after deafferentation that will be explored in future work.

Acknowledgements The authors would like to express their gratitude to the reviewers for important feedback and advice, and to Dr. Jos J. Eggermont for his critical comments on earlier versions of this manuscript.

References

Basta, D., & Ernest, A. (2004). Noise-induced changes of neuronal spontaneous activity in mice inferior colliculus brain slices. *Neuroscience Letters, 368*, 297–302.

Bhattacharyya, T., & Dayal, V. (1989). Influence of age on hair cell loss in the rabbit cochlea. *Hearing Research, 40*, 179–183.

Brozoski, T., Bauer, C., & Caspary, D. (2002). Elevated fusiform cell activity in the dorsal cochlear nucleus of chinchillas with psychophysical evidence of tinnitus. *Journal of Neuroscience, 22*, 2383–2390.

Bruce, I., Bajaj, H., & Ko, J. (2003). Lateral-inhibitory-network models of tinnuts. In *Proceedings of the 5th IFAC symposium on modeling and control in biomedical systems* (pp. 359–363). Dordrecht: Elsevier.

Burrone, J., & Murthy, V. (2003). Synaptic gain control and homeostasis. *Current Opinion in Neurobiology, 13*, 560–567.

Calford, M. (2002). Dynamic representational plasticity in sensory cortex. *Neuroscience, 111*, 709-738.

Calford, M., Rajan, R., & Irvine, D. R. F. (1993). Rapid changes in the frequency tuning of neurons in cat aduitory cortex resulting from pure-tone-induced temporary threshold shift. *Neuroscience, 55*(4), 953-964.

Charles, A. & Brennan, K. (2009). Cortical spreading depression-new insights and persistent questions. *Cephalagia, 29*(10), 1115–1124.

Chen, Q., & Jen, P. (2000). Bicuculline application affects discharge patterns, rate-intensity functions, and frequency tuning characteristics of bat auditory cortical neurons. *Hearing Research, 150*, 161–174.

Cheung, S., Bedenbaugh, P., Nagarajan, S., & Schreiner, C. (2001). Functional organization of squirrel monkey primary auditory cortex: Responses to pure tones. *Journal of Neurophysiology, 85*, 1732–1749.

Dayan, P., & Abbott, L. F. (2005). *Theoretical neuroscience: Computational and mathematical modeling of neural systems*. The MIT Press.

Desai, N., Cudmore, R., Nelson, S., & Turrigiano, G. (2002). Critical periods for experience-dependent synaptic scaling in visual cortex. *Nature Neuroscience, 5*, 783–789.

Dietrich, V., Nieschalk, M., Stoll, W., Rajan, R., & Pantev, C. (2001). Cortical reorganization in patients with high frequency cochlear hearing loss. *Hearing Research, 158*, 95–101.

Dominguez, M., Becker, S., Bruce, I., & Read, H. (2006). A spiking neuron model of cortical correlates of sensorineural hearing loss: Spontaneous firing, synchrony and tinnitus. *Neural computation, 18*(12), 2942–2958.

Douglas, R., & Martin, K. (1998). Neocortex. In G. M. Shepherd (Ed.), *The synaptic organization of the brain* (pp. 459–509). New York: Oxford University Press.

Eggermont, J. (2000). Sound induced correlation of neural activity between and within three auditory cortical areas. *Journal of Neurophysiology, 83*, 2708–2722.

Eggermont, J. (2003). Central Tinnitus. *Auris Nass Larynx, 30*, 7–12.

Eggermont, J. (2005). Tinnitus: Neurobiological substrates. *Drug Discovery Today 19*, 1283–1290.

Eggermont, J., & Roberts L. E. (2004). The neuroscience of Tinnitus. *Trends in Neurosciences, 27*, 676–682.

Foeller, E., Vater, M., & Kossl, M. (2001). Laminar analysis of inhibition in the gerbil primary auditory cortex. *Journal of the Association for Research in Otolaryngology, 2*(3), 279–296.

Fröhlich, F., Bazhenow, M., & Sejnowski, T. (2008). Pathological effect of homeostatic synaptic scaling on network dynamics in diseases of the cortex. *Journal of Neuroscience, 28*(7), 1709–1720.

Gerken, G. (1996). Central tinnitus and lateral inhibition: An auditory brainstem model. *Hearing Research, 97*, 75–83.

Gestner, W., & Kistler, W. (2002). *Spiking neuron models: Single neurons, populations, plasticity*. Cambridge University Press.

Greenwood, D. (1990). A cochlear frequency-position function for several species-29 years later. *Journal of the Acoustical Society of America, 87*, 2592–2605.

Houweling, A., Bazhenov, M., Timofeev, I., Steriade, M., & Sejnowski, T. (2005). Homeostatic synaptic plasticity can explain post-traumatic epileptogenesis in chronically isolated neocortex. *Cerebral Cortex, 15*, 834–845.

Hwa, T., & Kardar, M. (1992). Avalanches, hydrodynamics, and discharge events in models of sandpiles. *Physical Review A, 45*, 7002–7023.

Jones, E. (1995). Overview: Basic elements of the cortical network. In M. J. Gutnick & I. Moody (Ed.), *The Cortical Neuron* (pp. 111–122). New York: Oxford University Press.

Kaltenbach, J. (2000). Neurophysiologic mechanisms of Tinnitus. *Journal of the American Academy of Audiology, 11*, 125–137.

Kaltenbach, J., Zacharek, M., Zhang, J., & Frederick, S. (2004). Activity in the dorsal cochlear nucleus of hamsters previously tested for tinnitus following intense tone exposure. *Neuroscience Letters, 355*, 121–125.

Kilman, V., van Rossum, M., & Turrigiano, G. (2002). Activity deprivation reduces miniature IPSC amplitude by decreasing the number of postsynaptic GABA(A) receptors clustered at neocortical synapses. *Journal of Neuroscience, 22*, 1328–1337.

Komiya, H., & Eggermont, J. (2000). Spontaneous firing activity of cortical neurons in adult cats with reorganized tonotopic map following pure-tone trauma. *Acta Otorhinolaryngologica, 120*, 750–756.

Konig, O., Schaette, R., Kempter, R., & Gross, M. (2006). Course of hearing loss and occurrence of tinnitus. *Hearing Research, 221*, 59–64.

Kotak, V., Fujisawa, S., Lee, F., Aoki, C., & Sanes D. (2005). Hearing loss raises excitability in the auditory cortex. *Journal of Neuroscience, 25*, 3908–3918.

Liberman, M. (1987). Chronic ultrastructural changes in acoustic trauma: Serial-section reconstruction of stereocilia and cuticular plates. *Hearing Research, 26*, 65–88.

Leslie, K., Nelson, S., & Turrigiano, G. (2001). Postsynaptic depolarization scales quantal amplitude in cortical pyramidal neurons. *Journal of Neuroscience, 21*, 1–6.

Lu, Y., & Jen, P. (2001). GABAergic and glycinergic neural inhibition in excitatory frequency tuning of bat inferior collicular neurons. *Experimental Brain Research, 141*, 331–339.

Markram, H., Lubke, J., Frotscher, M., & Sakmann, B. (1997). Regulation of synaptic efficacy by coincidence of postsynaptic APs and EPSPs. *Science, 275*, 213–215.

Merzenich, M., Knight, P., & Roth, G. (1975). Representation of cochlea within primary auditory cortex in the cat. *Journal of Neuroscience, 38*, 231–249.

Miller, L., Escabi, M., Read, H., & Schreiner, C. (2001). Functional convergence of response properties in the auditory thalamocortical system. *Neuron, 32*, 151–160.

Milner, P. M. (1958). Note on a possible correspondence between the scotomas of migraine and spreading depression of Leao. *Electroencephalography and Clinical Neurophysiology, 10*, 705.

Muhlnickel, W., Elbert, T., Taub, E., & Flor, H. (1998). Reorganization of auditory cortex in tinnitus. *Proceedings of the National Academy of Sciences, 95*, 10340–10343.

Muly, S., Gross, J., & Potashner, S. (2004). Noise trauma alters D-[3H]aspartate release and AMPA binding in chinchilla cochlear nucleus. *Journal of Neuroscience Research, 75*, 585–596.

Noreña, A. & Eggermont, J. (2003). Changes in spontaneous neural activity immediately after an acoustic trauma: Implications for neural correlates of tinnitus. *Hearing Research, 183*, 137–153.

Noreña, A., Tomita M., & Eggermont, J. (2003). Neural changes in cat auditory cortex after a transient pure-tone trauma. *Journal of Neurophysiology, 90*, 2387–2401.

Ottaviani, F., Di Girolamo, S., Briglia, G., De Rossi, G., Di Giuda, D., & Di Nardo, W. (1997). Tonotopic organization of human auditory cortex analyzed by SPET. *Audiology, 36*, 241–248.

Parra, L. C. & Pearlmutter, B. A. (2007). Illusory percepts from auditory adaptation. *Journal of the Acoustical Society of America, 121*, 1632–1641.

Phillips, D., & Irvine, D. (1981). Responses of single neurons in physiologically defined primary auditory cortex AI of the cat: Frequency tuning and responses to intensity. *Journal of Neurophysiology, 45*, 48–58.

Popelar, J., Erre, J., Aran, J., & Cazals, Y. (1994). Plastic changes in ipsicontralateral differences of auditory cortex and inferior colliculus evoked potentials after injury to one ear in the adult guinea pig. *Hearing Research, 72*, 125–134.

Rajan, R. (1998). Receptor organ damage causes loss of cortical surround inhibition without topographic map plasticity. *Nature Neuroscience, 1*, 138–143.

Rajan, R. (2001). Plasticity of excitation and inhibition in the receptive field of primary auditory cortical neurons after limited receptor organ damage. *Cerebral Cortex, 11*, 171–182.

Rajan, R., Irvine, R., Wise, L., & Heil, P. (1993). Effect of unilateral partial cochlear lesions in adult cats on the representation of lesioned and unlesioned cochleas in primary auditory cortex. *Journal of Comparative Neurology, 338*, 17–49.

Read, H., Winer, J., & Schreiner, C. (2002). Functional architecture of the auditory cortex. *Current Opinion in Neurobiology, 12*, 433–440.

Riegle, K., & Meyer, R. (2007). Rapid homeostatic plasticity in the intact adult visual system. *Journal of Neuroscience, 27*, 10556–10567.

Robertson, D., & Irvine, D. R. F. (1989). Plasticity of frequency organization in auditory cortex of guinea pigs with partial

unilateral deafness. *Journal of Comparative Neurology*, 282, 456–471.

van Rossum, M., Bi, G., & Turrigiano, G. (2000). Stable Hebbian learning from spike-timing dependent plasticity. *Journal of Neuroscience, 20*, 8812–8821.

Rutherford, L., Dewan, A., Lauer, H., & Turrigiano G. (1997). Brain-deprived neutrotrophic factor mediates the activity-dependent regulation of inhibition in neocortical cultures. *Journal of Neuroscience, 17*, 4527–4535.

Rutherford, L., Nelson, S., & Turrigiano, G. (1998). Opposite effects of BDNF on the quantal amplitude of pyramidal and interneuron excitatory synapses. *Neuron, 21*, 521–530.

Salvi, R., Henderson, D., Hamernik, R., & Parkins, C. (1980). VIII nerve response to click stimuli in normal and pathological cochleas. *Hearing Research, 2*, 335–342.

Salvi, R., Wang, J., & Ding, D. (2000). Auditory plasticity and hyperactivity following cochlear damage. *Hearing Research*, 147, 261–274.

Schaette, R., & Kempter, R. (2006). Development of tinnitus-related neuronal hyperactivity through homeostatic plasticity after hearing loss: a computational model. *European Journal of Neuroscience, 23*, 3124–3138.

Schreiner, C., Read, H., & Sutter, M. (2000). Modular organization of frequency integration in primary auditory cortex. *Annual Review of Neuroscience, 23*, 501–529.

Seki, S., & Eggermont, J. (2002). Changes in cat primary auditory cortex after minor-to-moderate pure-tone induced hearing loss. *Hearing Research, 173*, 172–186.

Seki, S., & Eggermont, J. (2003). Changes in spontaneous activity firing rate and neural synchrony in cat primary auditory cortex after localized tone-induced hearing loss. *Hearing Research, 180*, 28–38.

Suneja, S., Benson, C., & Potashner, S. (1998a). Glycine receptors in adult guinea pig brain stem auditory nuclei: Regulation after unilateral cochlear ablation. *Experimental Neurology, 154*, 473–488.

Suneja, S., Potashner, S., & Benson, C. (1998b). Plastic changes in glycine and GABA release and uptake in adult brain stem auditory nuclei after unilateral middle ear ossicle removal and cochlear ablation. *Experimental Neurology, 151*, 273–288.

Takano, T., Tian, G. F., Peng, W., Lou, N., Lovatt, D., Hansen, A. J., et al. (2007). Cortical spreading depression causes and coincides with tissue hypoxia. *Nature Neuroscience, 10*(6), 754–762.

Turner, J., Hughes, L., & Caspary, D. (2005). Divergent response properties of layer-V neurons in rat primary auditory cortex. *Hearing Research, 202*, 129–140.

Turrigiano, G., Leslie, K., Desai, N., Rutherford, L., & Nelson, S. (1998). Activity dependent scaling of quantal amplitude in neocortical pyamidal neurons. *Nature, 391*, 892–895.

Vale, C., & Sanes, D. (2002). The effect of bilateral deafness on excitatory and inhibitory synaptic strength in the inferior colliculus. *European Journal of Neuroscience*, 16, 2394–2404.

Wang, J., Salvi, R., & Powers, N. (1996). Plasticity of response properties of inferior colliculus neurons following acute cochlear damage. *Journal of Neurophysiology, 75*, 171–183.

Wang, J., Ding, D., & Salvi, R. (2002). Functional reorganization in chinchilla inferior colliculus associated with chronic and cochlear damage. *Hearing Research, 168*, 238–249.

Wehr and Zador (2003). Balanced inhibition underlies tuning and sharpens spike timing in auditory cortex. *Nature, 426*, 442–446.

Wilson, H. (1999). *Spikes, decisions and actions: dyanmic foundations of neuroscience*. Oxford University Press.

Wilson, H., & Cowan, J. (1972). Excitatory and inhibitory interactions in localized populations of model neurons. *Biophysical Journal, 12*, 1–24.

Wilson, H., & Cowan, J. (1973). A mathematical theory of the functional dynamics of cortical and thalamic nervous tissue. *Kybernetics, 13*, 55–80.

Wilson, H., Blake, R., & Lee, S. (2001). Dynamics of travelling waves in visual perception. *Nature, 412*, 907–910.

Zilany, M., & Bruce, I. (2006). Modeling auditory-nerve responses for high sound pressure levels in the normal and impaired auditory periphery. *Journal of the Acoustical Society of America, 120*, 1446–1466.

Postscript

The preceding chapter introduced the potential importance of homeostatic plasticity after hearing loss. The model predicted the development of tinnitus correlates in spontaneous activity that emerged as a result of a shift in the balance of excitation and inhibition due to a homeostatic response to deafferentation. However, this model simulated a comprehensive homeostatic response acting on many connections types; it is unclear if such a comprehensive response is present in the primary auditory cortex. Furthermore, the model could be more biologically plausible and would benefit from empirical validation. This would strengthen the hypothesis that homeostatic plasticity reacts to hearing loss in adult primary auditory cortex.

Chapter Three

Preamble

In this chapter, I describe an integration of electrophysiology and computational modelling. The model discussed in Chapter 2 was refined and made more biologically plausible. This was done by using neural units in the model that reproduce behaviours in a vast array of cortical neurons, and by changing the structure of network connections such that they were closer to those observed in the primary auditory cortex (e.g. co-tuned rather than lateral inhibition and the inclusion of feed-forward inhibition). We also took advantage of the detailed HSP dynamics that we described in the preceding model in order to show changes in activity and receptive fields at different time points after deafferentation. The purpose of this was to show that the gradual effects of HSP can induce tinnitus correlates in a fairly rapid fashion; aberrant changes in cortical activity and processing occurred in the model before HSP could bring activity back to a target firing rate.

The model was validated through an electrophysiological study. Multi-channel multi-unit recordings were obtained from adult Sprague-Dawley primary auditory cortex both before and up to 8 hours after a tonal trauma. These experiments indicated that receptive fields could broaden gradually over such a timescale. The empirical results were in agreement with computational simulations, which indicated that several potential homeostatic mechanisms could bring about gradual expansion of receptive fields after localized peripheral damage. Importantly, this presented novel evidence of the rapid

action of homeostatic plasticity in adult auditory cortex. While studies had shown evidence of HSP in other adult cortices, this was the first characterizing rapid HSP in adult auditory cortex, and also the first investigating such a response after tonal trauma. Finally, the computational model was used to elucidate how such changes could occur: the model predicted that synaptic scaling of intracortical excitatory (up-regulation) and inhibitory (down-regulation) synapses was the likely candidate mechanism for rapid changes in receptive fields.

Permissions and Contributions

Chapter 3 has been submitted to and is under review by the *Journal of Neurophysiology*[1]. Material for Chapter 3 is used with consent from the editor of the *Journal of Neurophysiology*.

For Chapter 3, I was responsible for all aspects of research including model conception and implementation, experimental design, data collection and analysis, and writing. Drs. Becker, Bruce and Salvi assisted with revising the manuscript. Daniel Stolzberg assisted with data analysis.

[1] Chrostowski M, Stolzberg D, Becker S, Bruce IC, Salvi RJ (in revision). A potential role for homeostatic plasticity in adult primary auditory cortex. *J Neurophys* JN-00205-2012.

Abstract

Damage at the auditory periphery can alter tuning and activity in the primary auditory cortex (AI) via mechanisms operating on various timescales. Here, we propose that rapid homeostatic plasticity (HSP) contributes to changes observed in adult AI less than one day after acoustic trauma. We used multi-channel electrodes to record multi-unit activity in adult rat AI for 8 hours (a timescale appropriate for putative rapid HSP) after tonal trauma. We did not observe sustained changes in spontaneous firing but did observe a gradual reduction in tuning sharpness over a span of 8 hours after the tonal trauma; this reduction was additional to any immediate post-trauma changes in tuning. To investigate which homeostatic mechanisms could contribute to such post-trauma changes in tuning and spontaneous activity, we developed a biologically-plausible network model of AI and incorporated several rapid-HSP mechanisms. We compared the effects of synaptic scaling, changes in neural excitability and HSP restricted to superficial cortical layers on activity throughout AI. Our simulations indicate that homeostatic scaling of intracortical synapses most readily explains the slight and gradual broadening in tuning we observed even when spontaneous activity had not returned to pre-exposure levels. Furthermore, the model predicts that intracortical synaptic scaling restricted to a superficial layer is sufficient to explain broadened tuning in that layer and in layers where HSP is absent. Our empirical observations and computational simulations provide novel insights into how even limited rapid HSP may affect tuning and activity in AI.

Keywords: hearing loss, synaptic scaling, adult cortical plasticity

Introduction

For many, both workplace and recreational activities can contribute to noise-induced damage to the auditory periphery. It is well established that such damage can have both immediate and long-lasting effects on processing in the auditory cortex, but what happens in the auditory cortex during the transition between immediate changes and eventual structural reorganization is unclear. Delineating how these events unfold during the immediate to long-term post-trauma period could help shed light on mechanisms involved in recovery after damage and the plasticity mechanisms at play in normal auditory cortex, and could have implications for treatment of disorders such as tinnitus.

Peripheral damage appears to cause a variety of changes in receptive fields in central auditory regions in the short term (Calford et al. 1993; Wang et al. 1996) and long term (Robertson and Irvine 1989). Whole-cell recordings in primary auditory cortex (AI) neurons soon after tonal trauma (Scholl and Wehr 2008) suggest that altered levels of inhibition play a predominant role in the immediate changes in receptive fields after acoustic trauma (Kimura and Eggermont 1999; Noreña et al. 2003). These rapid changes in central inhibition after peripheral damage likely result from an immediate reduction in afferent neural input from the cochlea that reduces the input to the auditory cortex (Liberman and Dodds 1984). Subsequent post-trauma changes in AI (Robertson and Irvine 1989; Noreña et al. 2003) provide evidence that central plasticity mechanisms can further disrupt processing. However, which plasticity mechanisms are active and the loci of their activity are as yet undetermined.

Empirical evidence suggests that within hours of peripheral damage, rapid homeostatic plasticity (HSP) may be employed in sensory cortices to compensate for the disrupted inputs (Ibata et al. 2008). While, early *in vitro* work suggested that HSP required days or weeks to significantly affect synaptic strength (Turrigiano et al. 1998, Rutherford et al. 1998; Burrone et al. 2002), recent evidence suggests that HSP acts within 4-24 hours in several brain regions (Riegle and Meyer 2007; Ibata et al. 2008). To date, little work has been done to elucidate whether HSP acting on synaptic transmission (Turrigiano et al. 1998; Saliba et al. 2007) or membrane excitability (Turrigiano et al. 1994; Desai et al. 1999) can operate on this timescale within adult AI. Kotak et al. (2005) suggested that HSP may alter synaptic and intrinsic membrane properties in AI to compensate for deafening in developing animals. Furthermore, one week after acoustic trauma, there is evidence of HSP reducing inhibitory transmission in adult AI (Yang et al. 2011). Key unresolved issues include characterizing the locus and time course of rapid HSP mechanisms that can contribute to cortical changes within hours of peripheral damage. As a first step, we characterized functional changes by investigating receptive fields and spontaneous activity *in vivo* over a span of 8 hours after acoustic trauma. We then employed detailed computational models of AI with HSP to examine the most likely homeostatic mechanisms to have generated the observed functional changes. The work reported here represents the first attempt to rigorously characterize the functional and structural changes associated with HSP within hours of peripheral damage.

Previously, we investigated homeostatic changes following acoustic trauma by proposing a computational model that describes how homeostatic synaptic scaling can respond to AI deafferentation; we showed that the model can explain changes in spontaneous activity and synchrony after hearing loss (Chrostowski et al. 2011). However, this preliminary model did not clarify whether HSP in adult AI necessarily operates on all types of synaptic connections, intrinsic excitability, or even whether HSP is present in the entire AI circuit. Empirical data are required to further constrain the model, and more detailed model refinement can then better characterize the operation of HSP in the early stages after peripheral damage. We therefore investigated the gradual effect of tonal trauma on tuning and spontaneous activity in AI using multi-channel electrode recordings in an adult-rat model of noise trauma. We were particularly interested in how AI receptive fields change during the first 8 hours post-trauma. Using a computational model of HSP in AI, we investigated which homeostatic mechanisms might best explain our experimental observations. Rather than selecting homeostatic mechanisms a priori, we determined likely candidates by simulating their gradual effect on activity. This combined approach provides new insight into how HSP may operate in adult AI.

Materials and Methods

Experimental procedure. Multi-channel recordings were performed in primary auditory cortex (AI) of adult male Sprague-Dawley rats before, immediately after, and 1, 2, 4, and 8 hours after acoustic trauma. All experimental protocols were approved by the

University at Buffalo, the State University of New York, Institutional Animal Care and Use Committee and carried out according with the National Institutes of Health guidelines. More detailed experimental methods for the animal surgery and auditory cortex recordings are described in Stolzberg et al. (2011).

Surgery. Adult male Sprague-Dawley rats (n=9) were anesthetized using ketamine/xylazine (50/6 mg/kg, i.m.). The animal's body temperature was maintained at 37˚C throughout surgery and recordings using a homeothermic heating pad. The head was fixed using a stereotaxic frame with blunted ear bars, the skull was surgically exposed, and a head post was attached using dental cement. A small opening (spanning a region 4.5mm to 6mm caudal to bregma) was made in the exposed temporal bone. At this point the animal was removed from the stereotaxic frame and placed on a platform for free-field sound stimulation of the ear contralateral to the craniotomy. The animal's head was held with a custom head post holder for dura resection as well as throughout sound stimulation and electrophysiological recordings.

Electrophysiology. A 16-channel silicon multi-electrode (NeuroNexus Technologies, Ann Arbor, MI, USA) with four shanks (125-µm separation) and four channels per shank (100-µm separation) was inserted into exposed auditory cortex. An insertion into the primary auditory cortex was confirmed using multi-unit (MU) and local-field potential (LFP) response characteristics as well as initial frequency-response area maps (see Stolzberg et al. 2011). Confirmation of a successful insertion was followed by slow advancement of the electrode until MU responses were observed on all channels. After a second frequency-response area test on all channels ensured sufficient advancement of

the electrode, a drop of mineral oil was placed on the surface of the exposed cortex to prevent drying. A waiting period of 30-45 minutes preceded baseline recordings to reduce the possibility of recovery from potential cortical dimpling during the recording session. During recordings, rats were maintained on a light plane of ketamine-anesthesia (~5mg/kg/h, i.m.); saline was injected to keep the animal hydrated (0.5-1mL/h, subcutaneous).

Each recording block included frequency receptive field maps and spontaneous activity recordings in 10 minutes of silence. Sound stimuli were generated (TDT RX6-2, ~100-kHz sampling rate) and presented with a free-field magnetic speaker (Fostex FT28D) to the ear contralateral to the AC recording site. Frequency receptive field maps for each channel were generated by summing the MU response for 50 ms following the onset of tone bursts (25-ms duration, $\cos^2$ gate, 5-ms rise/fall, presented at 3 Hz). Tone bursts were logarithmically spaced in frequency (40 steps between 1 and 48 kHz), had sound levels between 0 and 90 dB SPL (in 5-dB steps), and were presented in a pseudo-randomized fashion (five repetitions). AC recordings presented here occurred at baseline and 0, 1, 2, 4 and 8 hours after a 1-hour tonal trauma or 1 hour of silence (controls).

Acoustic trauma. In four rats, a tonal trauma (110 dB) was presented for 1 hour at a frequency approximately 0.25 to 1 octave above characteristic frequencies (CFs) observed on the recording channels of the four-shank electrode array; on average the tonal trauma was 0.569 ± 0.091 octaves above CF. Tonal trauma was produced using a free-field magnetic speaker (Fostex FT17H). The CF for a channel was determined from

the corresponding frequency receptive field map and was deemed to be the frequency at which the lowest-intensity tone burst evoked a driven response. The trauma was presented to the ear contralateral to the recording site. The tonal trauma was presented above the CF so that, immediately after the trauma, inputs to the region of interest would be affected, but receptive fields in this region would not be as drastically altered as receptive fields of neurons with CFs above the trauma frequency.

Q-factor and synchrony measures. To determine the change in tuning bandwidth we used the Q20 factor for frequency receptive field maps on each channel (tonal-trauma: n = 49 channels; controls: n = 54 channels). The Q20 value is obtained by dividing the CF observed on a channel by the bandwidth (BW) of the frequency receptive field at 20 dB above the minimum threshold ($\frac{f_{CF}}{BW_{20dB}}$).

To estimate the synchrony between MUs, we determined peak cross-correlation coefficients (see Seki and Eggermont 2003) based on our recordings of spontaneous activity. Before analysis, we removed spikes occurring within 150 μs, since these may have resulted from cross-talk (Noreña and Eggermont 2003; Seki and Eggermont 2003). We determined cross-correlation values using bin sizes of 2 ms and 5 ms.

Statistical analysis. Data are presented as mean ± standard error of the mean (SEM). Single-factor repeated-measures ANOVAs were used to assess changes over time for each group. When results of the ANOVAs were significant, post-hoc comparisons (two-tailed Student's t-tests) with Bonferroni adjustment for multiple comparisons were used

to investigate the significance of pairwise differences relative to baseline. All statistical tests, with the exception of correlation and peak cross-correlation measures (done in MATLAB), were performed using SPSS Statistical Software. In tables and figures showing empirical data, a single, double or triple asterisk indicates statistical significance at $p < 0.05$, $p<0.01$ and $p<0.001$ levels, respectively. Where shown, error bars are SEM.

Computational model design. We modeled AI as a network of spiking neurons with 400 excitatory neural units and 80 inhibitory neural units (Fig. 1). The behavior of the neural units is described by the Izhikevich spiking model (Izhikevich 2003), which is capable of reproducing neural activity seen in a wide variety of cortical neurons. We made one change to this model: we replaced a constant with an excitability parameter *e* in the equation (1) describing the membrane potential (*v*) dynamics. This allowed us to manipulate excitability with a homeostatic response mechanism. We did not change the recovery (*u*) and after-spike response behavior defined in (2) and (3), respectively. The equations describing membrane dynamics in our model are thus:

$$\frac{dv}{dt} = 0.04v^2 + 5v + e - u + I \qquad (1)$$

$$\frac{du}{dt} = a(bv - u) \qquad (2)$$

$$\text{if } v \geq 30 \text{ mV, then } \begin{cases} v \leftarrow c \\ u \leftarrow u + d \end{cases} \qquad (3)$$

We set the dimensionless parameters *a*, *b*, *c*, and *d* to produce regular-spiking excitatory neurons (0.02, 0.2, -65, and 8, respectively) and fast-spiking inhibitory neurons (0.1, 0.2, -65, and 2, respectively) as per Izikevich (2003). Parameter *e* was initially set to 140 (mV/ms), which is the constant used in the original equation (Izhikevich 2003). In equation (1), *I* represents the total synaptic input currents for each neural unit. We simulate neural behavior with 0.2-ms time resolution.

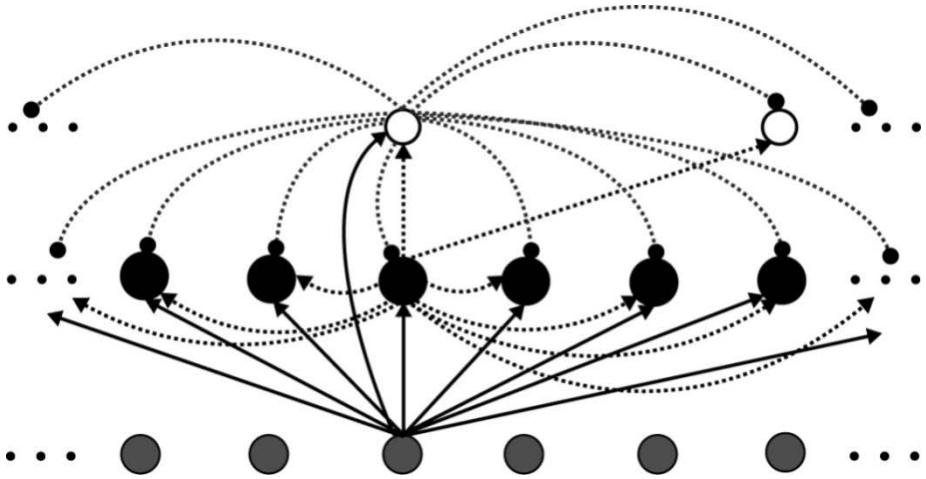

Figure 3.1: A subsection of the AI network model. Grey, black and empty circles represent thalamic input units, regular-spiking excitatory units, and fast-spiking inhibitory units, respectively. Solid lines represent thalamocortical inputs, while dashed lines represent intracortical connections. Dashed lines ending in small filled circles represent inhibitory connections.

The network was set up to have a tonotopy that is based on the relationship between basilar membrane position and characteristic frequency (CF) (Greenwood et al. 1990). Inputs at the low frequency end have CFs starting at 100 Hz and successive inputs have CFs increasing logarithmically to 80 kHz. As in our empirical work, we restricted our analysis to frequencies from 1 kHz to 48 kHz. The weights for excitatory connections were set up such that each neural unit had a CF that drove it most strongly; thalamocortical weights decreased according to a Gaussian function for frequencies further away from the CF. This is similar to the setup in our previous model (Chrostowski et al. 2011), but here we assumed co-tuned inhibitory and excitatory inputs, as supported by empirical data (Wehr and Zador 2003) and we included feedforward as well as feedback inhibition. Since frequencies as much as two octaves away can elicit post-synaptic potentials at neurons in rat AI (Scholl and Wehr 2008; Wu et al. 2008), we set the range of our weight functions to two octaves on either end of the peak input weight.

Weights originating from excitatory neural units drop off faster than those from inhibitory units (Fig. 2A); this type of distribution sharpens the tuning curve (Wu et al. 2008). We also set the peak inhibitory weights so that the total inhibitory input weights are lower (by 50%) than total excitatory inputs. In accord with empirical data, lateral excitatory weights are more sharply tuned than thalamocortical inputs and have a maximum weight such that total lateral excitation onto a unit is lower (by 50%) than total thalamocortical excitation (Liu et al. 2007). Thalamocortical inputs to inhibitory neural

units were also set to be stronger than thalamocortical weights for excitatory units (Cruikshank et al. 2007).

A (i) **(ii)**

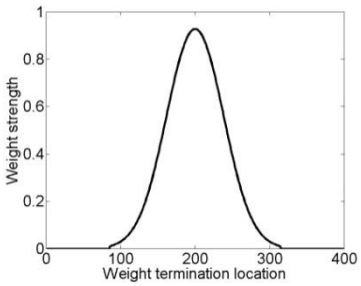

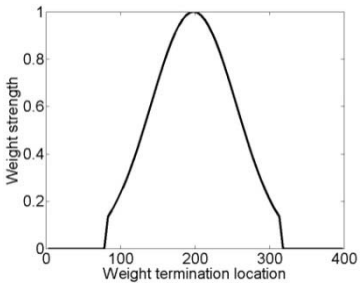

(iii)

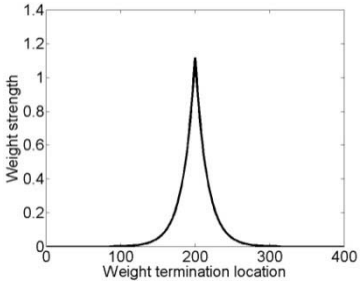

(iv) **(v)**

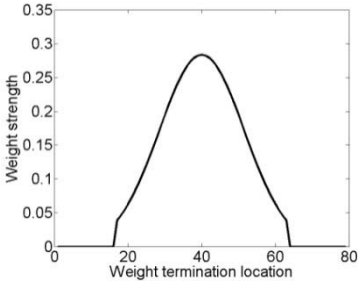

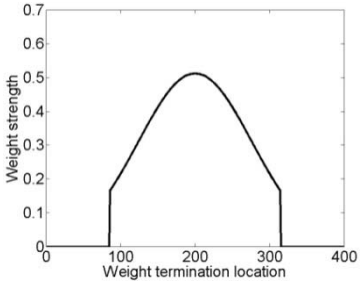

(vi)

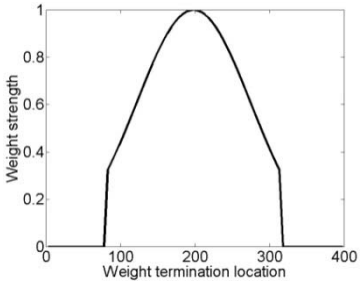

B (i) **(ii)**

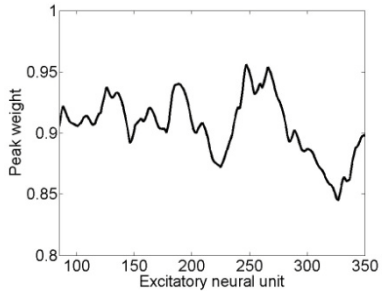

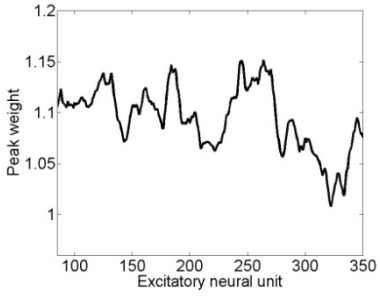

(iii)

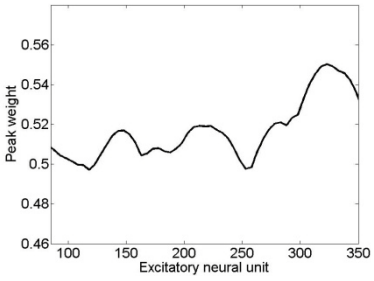

Figure 3.2: Neural network weights. ***A,*** *Weight functions corresponding to (i)* $\boldsymbol{W_{a,e}}$*, (ii)* $\boldsymbol{W_{a,i}}$*, (iii)* $\boldsymbol{W_{e,e}}$*, (iv)* $\boldsymbol{W_{e,i}}$*,(v)* $\boldsymbol{W_{i,e}}$ *and (vi)* $\boldsymbol{W_{i,i}}$*. The x-axis displays the network position that the connection terminates at; excitatory units are present at positions 1, 2, 3, ... 400,*

*while inhibitory units are present at positions 3, 8, 13 ..., 398. Weight functions for those weights that are altered by homeostatic mechanisms (**$W_{a,e}$**, **$W_{e,e}$**, and **$W_{i,e}$**) have different peak values than those set before initialization (coefficients in eqns. 4, 6 and 8, respectively).* ***B,*** *Peak values of weight functions across the network at baseline. Peak values for weights that are modulated during initialization are shown: (i) **$W_{a,e}$**, (ii) **$W_{e,e}$**, and (iii) **$W_{i,e}$**. Weights **$W_{a,i}$**, **$W_{e,i}$** and **$W_{i,i}$** have constant peak values (1.0, 0.3, and 1.0, respectively) across the network; these values are the coefficients from eqns. 5, 7 and 9, respectively. Values are plotted for neural units with CFs spanning frequencies displayed in frequency response area maps from our recordings (1-48 kHz).*

The weights in the model were initialized according to the following equations, where the subscripts- *a* (thalamocortical/ascending), *e* (excitatory regular-spiking unit) and *i* (inhibitory fast-spiking unit) for each weight matrix **W** indicate the type of connection (source and destination):

$$\mathbf{W_{a,e}} = 0.5 \cdot \exp\left(-\frac{|a_j - e_k|^2}{53.74}\right), \text{ for } a_j, e_k \in \{1, 2, 3, \ldots, 400\}, \ |a_j - e_k| \leq 114, \quad (4)$$

$$\mathbf{W_{a,i}} = 1.0 \cdot \exp\left(-\frac{|a_j - i_k|^2}{80.61}\right), \text{ for } a_j \in \{1, 2, 3, \ldots, 400\}, \ i_k \in \{3, 8, 13, \ldots, 398\},$$

$$|a_j - i_k| \leq 114, \quad (5)$$

$$\mathbf{W_{e,e}} = 0.6 \cdot \exp\left(-\frac{|e_j - e_k|}{16}\right), \text{ for } e_j, e_k \in \{1, 2, 3, \ldots, 400\}, \ |e_j - e_k| \leq 114, \quad (6)$$

$$\mathbf{W_{e,i}} = 0.3 \cdot \exp\left(-\frac{|e_j - i_k|^2}{80.61}\right), \text{ for } e_j \epsilon \{1, 2, 3, \dots, 400\},\ i_k \epsilon \{3, 8, 13, \dots, 398\},\ |e_j - i_k| \leq 114, \quad (7)$$

$$\mathbf{W_{i,e}} = 0.9 \cdot \exp\left(-\frac{|i_j - e_k|^2}{107.48}\right), \text{ for } i_j \epsilon \{3, 8, 13, \dots, 398\},\ e_k \epsilon \{1, 2, 3, \dots, 400\},\ |i_j - e_k| \leq 114, \quad (8)$$

$$\mathbf{W_{i,i}} = 1.0 \cdot \exp\left(-\frac{|i_j - i_k|^2}{107.48}\right), \text{ for } i_j \epsilon \{3, 8, 13, \dots, 398\},\ i_k \epsilon \{3, 8, 13, \dots, 398\},\ |i_j - i_k| \leq 114, \quad (9)$$

There were 400 thalamocortical (input) and 400 excitatory regular spiking units spanning the tonotopy. We also included 80 inhibitory units (20% of cortical units), which were spaced apart uniformly with one inhibitory unit for every five excitatory units; using this number of inhibitory units is similar to empirical observations throughout layers of the auditory cortex (Prieto et al. 1994; Yuan et al. 2011). The network weights were initially set to values that, relative to each other, were in line with experimental observations (Cruikshank et al. 2007; Liu et al. 2007; Wu et al. 2008). After initializing with the above values, we used our homeostatic learning rules to re-calibrate weights in the network such that the mean spontaneous firing rate was about 6 spikes/s; this is a reasonable value for spontaneous activity in the auditory cortex (Moshitch et al. 2005). The shape of the weight functions describing the spatial distribution of input weights onto each individual neural unit was preserved (Fig. 2A) because our homeostatic scaling mechanisms work multiplicatively (Turrigiano et al. 1998).

However, this initialization increased variance in weights across the network and created a more biologically plausible cortical model; the variance across the network is indicated in a plot of the peak values of weight functions (Figs. 2B and 7). A noteworthy change evident in Fig. 2 is that excitatory weights increased and inhibitory weights decreased relative to their initial values to produce the desired spontaneous cortical rate. This change partly depended on the value we set for our spontaneous thalamic input rate (20 spikes/s) and magnitudes of weights that were not altered by homeostatic mechanisms ($\mathbf{W_{a,i}}$, $\mathbf{W_{e,i}}$ and $\mathbf{W_{i,i}}$). Importantly, a sensitivity analysis indicated that fixing these parameters did not qualitatively affect model predictions. The input spikes that were used to set up the baseline model and those input spikes used in all subsequent simulations were generated using mutually independent Poisson processes (Chrostowski et al. 2011).

Homeostatic plasticity rules. Homeostatic mechanisms in this model responded to deviations in a neural unit's spontaneous spiking rate from a homeostatic target firing rate. A target firing rate may depend on an equilibrium between signalling pathways that up-regulate and down-regulate a neuron's excitability (Turrigiano 2008); we assumed that for our neural units this equilibrium occurs at 6 spikes/s. We use a 4^{th}-order Runge-Kutta algorithm with 0.2-ms time resolution to simulate the operation of the activity estimation and homeostatic update operations described below (eqns. 10-14).

We estimated activity (r) in each neuron (i) with a metric that increases with each post-synaptic spike (n) and decreases exponentially otherwise (van Rossum et al. 2000):

$$\tau_r \frac{dr_i(t)}{dt} = -r_i(t) + \sum_n \delta(t - t_{i,n}), \text{ for } i \in \{1, 2, 3, \ldots, 400\}, \qquad (10)$$

where the time constant (τ_r) for spontaneous rate estimation is set to 1 second, and $\delta(x)$ is the Dirac delta function. We also used this metric to determine the spontaneous firing rate in the trauma region at time points throughout recovery from a simulated tonal trauma.

The homeostatic mechanism operated on each neural unit based on that unit's activity, whenever spontaneous activity deviated from the homeostatic set-point by more than 1 spike/s. Weights onto the neural unit were scaled multiplicatively, since this type of scaling seems to occur both with complete blockade of a neuron's firing, and with a decrease in spontaneous firing rate (Riegle and Meyer 2007; Ibata et al. 2008). Riegle and Meyer (2007) observed that scaling of excitatory currents was proportional to the level of activity reduction and that excitatory currents were scaled down if there was too much activity. Therefore, we scaled incoming excitatory synaptic weights for each unit *j* = 1, 2, 3, ..., 400 as in our previous model (Chrostowski et al. 2011):

$$\tau_{HSP} \frac{d\mathbf{Wa,e}(\mathrm{j})}{dt} = \left(r_{target} - r_j(t)\right) \cdot \mathbf{W_{a,e}}(\mathrm{j}), \qquad (11)$$

$$\tau_{HSP} \frac{d\mathbf{We,e}(\mathrm{j})}{dt} = \left(r_{target} - r_j(t)\right) \cdot \mathbf{W_{e,e}}(\mathrm{j}), \qquad (12)$$

Inhibitory inputs to excitatory neurons also seem to scale in response activity changes, but in the opposite direction of excitatory inputs to excitatory neurons

(Rutherford et al. 1997; Rutherford et al. 1998; Kilman et al. 2002). Accordingly, our HSP rule for these synapses is as follows:

$$\tau_{HSP}\frac{d\mathbf{W_{i,e}}(\mathrm{j})}{dt} = -\left(r_{target} - r_j(t)\right)\cdot \mathbf{W_{i,e}}(\mathrm{j}), \quad (13)$$

As mentioned above, each neural unit's intrinsic excitability was modulated according to the variable *e* which we introduced into the membrane potential equation (1). This variable models changes in excitability that may result when there is a deviation from a target internal calcium concentration (LeMasson et al. 1993; Turrigiano et al. 1994; Turrigiano 1999). An increase in this variable resulted in a lower firing threshold, in agreement with changes seen after activity reduction *in vitro* and *in vivo* (Desai, et al. 1999; Maffei and Turrigiano 2008). The excitability parameter (*e*) was two orders of magnitude greater than a typical weight value in our network, and even very small changes in this parameter were sufficient to significantly alter the dynamics of a neural unit. Thus, we added a scaling coefficient (0.01) to the homeostatic update rule for excitability so that the effect of the change in excitability did not render negligible the effects of synaptic scaling mechanisms:

$$\tau_{HSP}\frac{d\mathbf{e}(\mathrm{j})}{dt} = 0.01\left(r_{target} - r_j(t)\right)\cdot \boldsymbol{e}(\mathrm{j}), \quad (14)$$

In our single-compartment neural units, we scaled inputs multiplicatively, as suggested by Turrigiano et al. (1998), in response to the respective unit's deviations from a set spiking rate. To simulate the operation of rapid homeostatic plasticity (which may

be detectable in less than four hours), we set $\tau_{HSP} = 1000$s. Because we simulate real-time homeostatic scaling, we were able to determine the gradual effect of the plasticity mechanisms after loss of input and compare the model simulations to our empirical observations.

There is evidence that in adult cortex, homeostatic plasticity is restricted to layer 2/3 (Goel and Lee 2007; Feldman 2009). Thus, a key question was whether our empirical observations in adult models of hearing loss could be explained by putative homeostatic mechanisms operating exclusively in layer 2/3 of auditory cortex. To gain insight into this we also ran simulations where only intracortical connections were scaled and there was no homeostatic scaling of thalamic input weights ($\mathbf{W_{a,e}}$). In addition, we developed a simple two-layer model which consisted of two interconnected instances of the above single-layer network: a thalamorecipient layer and a layer receiving only cortical inputs. We included homeostatic mechanisms in the more superficial layer and simulated hearing loss as above. Thus, we were able to determine if homeostatic scaling of intracortical connections (perhaps in a superficial layer) was sufficient to produce changes in tuning and activity similar to those observed in our recordings.

Simulations. To simulate the effect of acoustic trauma on the auditory nerve, we used a simplified model: reducing the ascending spontaneous input rate, consistent with empirical data (Salvi et al. 1980; Eggermont and Roberts 2004), in a region spanning one octave in our network. While other changes to spontaneous firing distributions have also

been observed (Liberman and Kiang 1978), we did not consider these in our simulations. We simulated mild and moderate levels of impairment as 25% and 50% reductions in the spontaneous firing of thalamic input units within a trauma region. After simulating the tonal trauma, we allowed activity in the cortical network to recover via homeostatic mechanisms described above. In our model, input activity was fixed at these reduced levels during simulation of homeostatic recovery of cortical activity and during all post-recovery simulations. Importantly, HSP in our model responded to changes in a neural unit's spontaneous activity and not driven activity. Because the homeostatic response we model scaled all synapses onto a unit proportionally, the simulation results would have been the same whether the reduction in spontaneous firing in a cortical neuron resulted from an overall reduction in afferent spontaneous activity (as we model it) or from suppression of particular inputs (e.g. inputs driven by higher frequencies that were affected by the trauma).

We plotted pre-trauma, partial recovery, and post-recovery frequency receptive field maps for a neural unit with a CF half an octave below the trauma tone and quantified the effect of the trauma and HSP on tuning. We used a spiking-model version of the Q-factor (Chrostowski et al. 2011) so that we could qualitatively compare tuning sharpness changes in our computational model with those observed in our animal model of tonal trauma. To do this, we directly equated input intensity (dB SPL) to thalamic spiking rate. Thus, Q20 for a neural unit in the model is the unit's CF divided by its bandwidth at an input rate 20 spikes/s above the unit's minimum threshold ($f_{CF}/BW_{20\ spikes/s}$).

The frequency receptive field map was determined by simulating neural responses to 100-ms tones with peak spiking rates of 0 to 100 spikes/s (in 10-spike/s steps) and tone centre locations ranging from 1 kHz to 48 kHz. Final frequency receptive field maps presented herein consist of the sum of 10 frequency-intensity sweeps, with different initial random seeds for the input spike generators for each sweep. Simulated tones always had frequencies that match a CF of one of our neural units. We modeled the thalamic response ($y_{pt}(j)$) to an input tone as an increased firing rate (A) that falls off spatially as a Gaussian on either side of the neural unit (at position j) having a CF that matches the frequency of the tone:

$$y_{pt}(j) = \begin{cases} A \cdot \exp\left(-\frac{|\mathrm{j}-\Delta|^2}{11.88}\right), & \text{for } |\mathrm{j}-\Delta| \leq 10 \\ 0, & \text{for } |\mathrm{j}-\Delta| \geq 10 \end{cases} \quad (15)$$

We also compared spontaneous activity before, during and after the homeostatic response to the simulated tonal trauma. In this way we were able to compare tuning changes that occurred before spontaneous activity returned to the homeostatic set-point, which has important implications for comparisons with our empirical observations.

Results

Electrophysiology

Effects of tonal trauma on tuning

We quantified tuning sharpness observed on each channel using the Q20 value: CF divided by the tuning bandwidth at 20 dB above the minimum threshold. Q20 values for the noise-exposed group (n = 49 channels) dropped significantly over 8 hours ($p = 0.0032$), as shown in Fig. 3A. Q20 values for the control group (n=54 channels) did not change over time ($p = 0.1728$). While tuning sharpness seems to drop immediately after trauma (indicating inhibitory unmasking), post-hoc comparisons indicated that Q20 values were significantly lower (i.e. tuning is broader) than baseline only at 8 hours post-trauma (baseline: 1.102 ± 0.058; 8 hours post-trauma: 0.933 ± 0.024). Thus, it appears that auditory cortical neurons downstream of the traumatized region of the periphery can exhibit a gradual broadening in tuning over a period of 8 hours after trauma. While other studies have observed broader tuning soon after acoustic trauma (Noreña et al. 2003), our longer recording session allowed us to observe additional broadening 8 hours post-trauma. This novel observation indicates that central plasticity mechanisms may operate within this timeframe to induce further changes to receptive fields in AI.

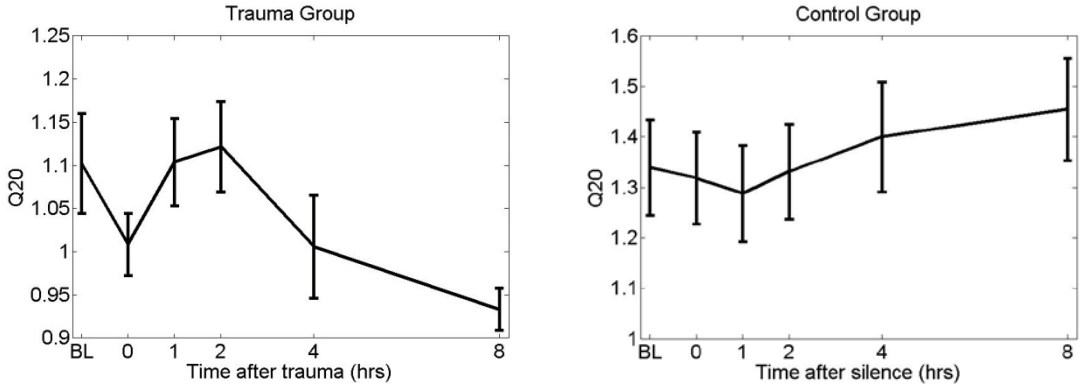

Figure 3.3: Tuning broadness after tonal trauma. Mean Q20 values for units in the region below the tonal trauma at baseline (BL) and at 0, 1, 2, 4 and 8 hours post-trauma. Plots on the left are from tonal-trauma group, while plots on the right are from the control group. Q20 values at 8 hours post-trauma were significantly lower than baseline values. Plots on the left are from tonal-trauma group, while plots on the right are from the control group. Q20 values at 8 hours post-trauma were significantly lower than baseline values.

Since noise trauma can induce tonotopic reorganization in AI in the long-term, we looked at whether tuning curves shifted after our noise exposure. Characteristic frequencies did not change significantly for controls ($p = 0.9379$), however, characteristic frequencies did decrease slightly following the tonal trauma ($p = 0.0161$) (Fig. 4). Since the tonal-trauma frequency was above the baseline CF, the lower post-trauma CFs likely resulted from a reduction in higher-frequency inputs, rather than a plasticity-driven shift in tuning that would not be expected to affect CFs until days or weeks after peripheral damage. Importantly, this CF drop does reflect a disruption in inputs to the units from which we recorded. We argue that the central plasticity mechanism that caused gradual

broadening of receptive fields was a homeostatic response initiated by reduced high-frequency inputs.

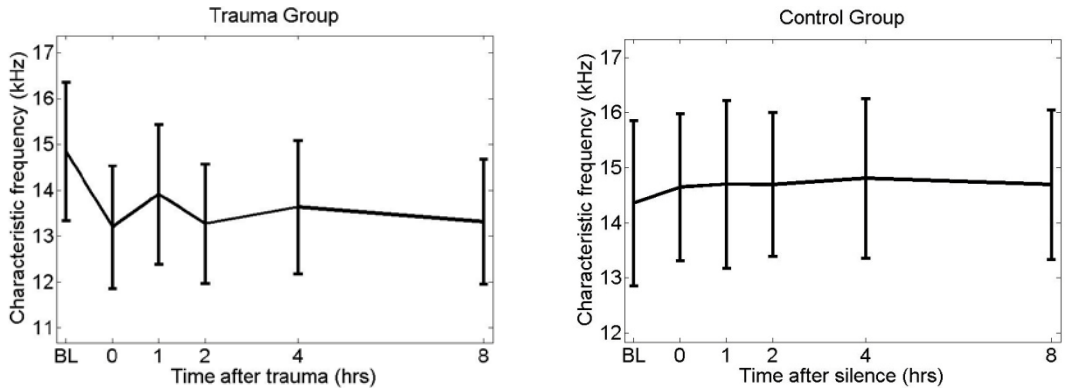

Figure 3.4: Mean characteristic frequency shifts. While controls (right) showed no significant change in CFs, the tonal-trauma group (left) showed a small but significant ($p<0.05$) reduction in CF immediately after trauma. CFs at subsequent time points were not significantly lower than baseline values.

The impact of the trauma did not appear to be sufficient to significantly elevate minimum thresholds in AI; this was similar to observations in the inferior colliculus after a similar acoustic trauma paradigm (Wang et al. 1996). This may be because the trauma tone was generally above the CFs of neurons in the recorded region and so peak damage would occur above these CFs. Furthermore, in spite of large (40 dB) peripheral threshold shifts, small (5.6 dB) cortical threshold shifts have been previously observed for neurons with CFs below the frequency of the tonal trauma (Noreña and Eggermont 2003).

Spontaneous firing and synchrony

Others have noted changes in spontaneous firing and synchrony after acoustic trauma (Kimura and Eggermont 1999; Noreña and Eggermont 2003; Seki and Eggermont 2003). We observed changes in spontaneous activity over time in both noise and control groups (Fig. 5A). A repeated measures ANOVA indicated that there was an increase in spontaneous firing rate (SFR) after a tonal trauma ($p<0.0005$). However, post-hoc comparisons indicated that by 8 hours post-trauma, spontaneous firing had returned to baseline levels. Furthermore, we also observed a temporary increase in SFR for the control group ($p<0.0005$). Since we observed increased spontaneous firing and an eventual return to baseline levels in both groups, it is likely that ketamine build-up and the general health of the animal affected spontaneous activity more so than the tonal trauma or any plasticity-dependant response to the trauma.

A

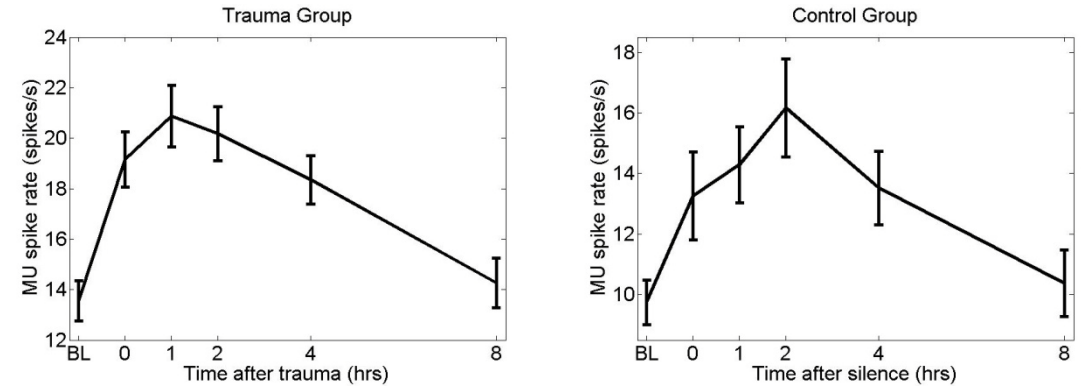

B

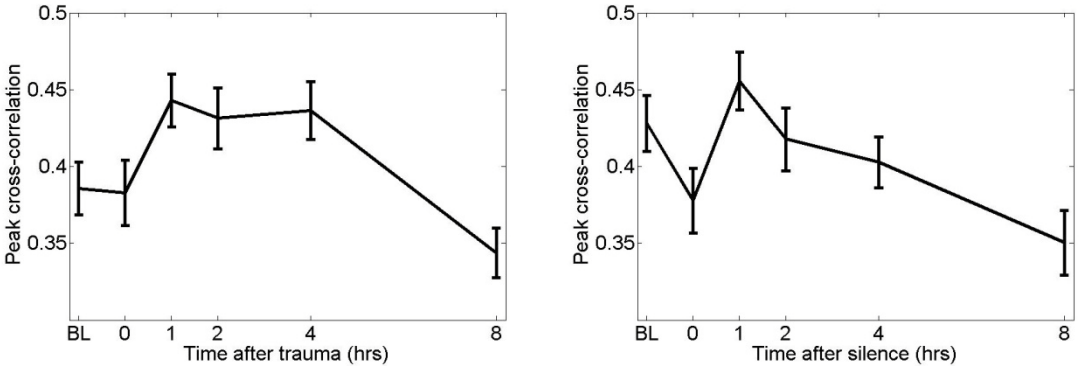

Figure 3.5: Spontaneous activity. ***A,*** *Both groups show a similar trend in spontaneous firing, although activity in the tone-trauma group (left) is generally higher. The number of spikes recorded on each channel was divided by the recording duration to give the MU firing rate in spike/s.* ***B,*** *Mean peak cross-correlation (5-ms bins) values for MUs on electrodes with 125-μm separation. There is a temporary increase observed at 1, 2 and 4 hours post-trauma; at 8 hours post-trauma the value drops back to baseline. Controls (right) show an eventual drop in peak cross-correlation relative to baseline at 8 hours post-trauma.*

To determine if there was a gradual increase in spontaneous synchrony in activity between units on channels spaced 125 μm apart (controls: n=45 pairs; noise-trauma: n=42 pairs), we used a peak cross-correlation measure (as per Seki and Eggermont 2003) with 5-ms time bins. In the tonal-trauma group peak cross-correlation increased transiently after the tonal trauma ($p<0.0005$): a post-hoc analysis indicated that peak cross-correlation values at 1, 2 and 4-hours post-trauma were significantly higher than baseline values (baseline: 0.386 ± 0.017; 1 hour post-trauma: 0.443 ± 0.017; 2 hours post-trauma: 0.431 ± 0.020; 4 hours post-trauma: 0.436 ± 0.019). However, these values were not significantly higher than corresponding control values at any time point. Peak cross-correlation values in controls fluctuated slightly before dropping significantly 8 hours post-silence (baseline: 0.428 ± 0.018; 8 hours post-silence: 0.350 ± 0.021). Similar results were observed if we used 2-ms time bins or looked at synchrony measures between units on channels 250 μm apart. This is consistent with previous findings that neural synchrony between AI neurons with CFs below the trauma frequency may not increase after a tonal trauma (Noreña and Eggermont 2003).

During recording sessions as long as those described here, changes in the level of anesthesia, the health of the animal, the number of units per electrode channel, and levels of spontaneous firing could affect our synchrony measures (Gerstein 2000; Noreña and Eggermont 2003). We looked more closely at the potential influence of spontaneous firing rates on peak cross-correlation values. Tables 1 and 2 indicate how correlated the changes (relative to baseline) in peak cross-correlation values were with changes (relative to baseline) in spontaneous firing rate; we used the SFR recorded on the two channels

used to determine the peak cross-correlation value (as per Noreña and Eggermont 2003). Changes in peak cross-correlation value or spontaneous firing rate are calculated as the ratio between the value at one of the time points and the value at baseline. In controls, changes in our synchrony measure were significantly ($p<0.001$ for all time-points) correlated with changes in spontaneous firing rate; this is true whether spikes are grouped into 2-ms or 5-ms bins. However, there was no significant correlation between changes in synchrony and changes in spontaneous firing rate in our tonal-trauma group at any time-point when spikes were grouped into 2-ms bins. For 5-ms bins, there was a low, but significant ($p<0.05$) correlation between peak cross-correlation and SFR at 2, 4 and 8 hours post-trauma. Thus, unlike changes in peak cross-correlation values in controls, changes in peak cross-correlation in the tonal-trauma group were not mainly determined by changes in spontaneous firing rate. However, the influence of spontaneous firing rates that gradually dropped may still have prevented us from observing a persistent increase in spontaneous synchrony.

Table 3.1:. Correlation between change in spontaneous firing rate and change in peak cross-correlation (2-ms bins)

	0 hours	1 hour	2 hours	4 hours	8 hours
Trauma	0.201	0.070	0.110	0.161	0.155
Controls	0.734***	0.732***	0.567***	0.670***	0.720***

Table 3.2: Correlation between change in spontaneous firing rate and change in peak cross-correlation (5-ms bins)

	0 hours	1 hour	2 hours	4 hours	8 hours
Trauma	0.216	0.116	0.351*	0.384*	0.337*
Controls	0.848***	0.820***	0.728***	0.789***	0.810***

It is not immediately clear how to reconcile a gradual broadening in tuning with a lack of persistently elevated spontaneous firing and synchrony in our experimental observations. Therefore, we used our computational model to investigate the relationship between spontaneous activity and tuning in the auditory cortex during HSP-driven recovery from reduced afferent input. Accordingly, we were able to determine whether a reduction in tuning sharpness could occur in spite of spontaneous firing rates and synchrony levels that were below baseline. Furthermore, we used the model to suggest specific homeostatic mechanisms that could explain our empirical observations.

Model simulations

Effects of HSP on tuning

Our simulations indicated that tuning sharpness would decrease as homeostatic mechanisms compensated for reduced input activity; this was the case for each variant of HSP we simulated. The model predicted that even small changes in synaptic weights can alter frequency response areas. Furthermore, in simulations, tuning sharpness decreased

even when spontaneous firing levels had not returned to normal. Based on model simulations, we propose that the slight changes in tuning we observed *in vivo* are best explained by restricted intracortical scaling that may occur in superficial layers of adult AI.

We used a spiking model analog of the Q20 value (Chrostowski et al. 2011) to quantify tuning changes in a neural unit half an octave below the tonal trauma; this location in the network corresponds to the region of interest in our multi-channel recordings. After the network was initialized, we determined a baseline frequency receptive field map (Fig. 6A) and a baseline Q20 value: 1.279. We then simulated a tonal trauma (50% drop in input firing rate) in a region of the network and allowed the network to recover activity levels via homeostatic mechanisms acting on excitatory and inhibitory weights, as well as intrinsic membrane excitability. We determined the post-recovery frequency receptive field map (Fig. 6B) and a post-recovery Q20 value: 0.780 in a neural unit that was half an octave below the center of the trauma (neighboring neural units had very similar receptive fields at baseline and after recovery). In addition to being more excitable, the neuron in the affected region now responds to inputs that previously elicited only sub-threshold responses.

A

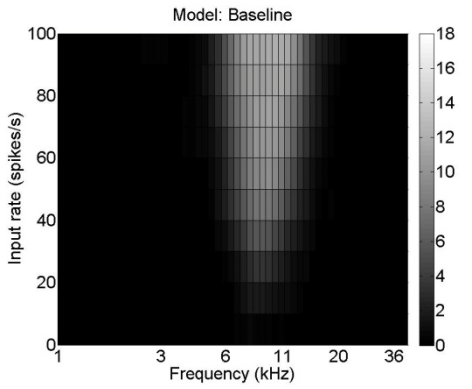
Model: Baseline
Input rate (spikes/s)
Frequency (kHz)

B

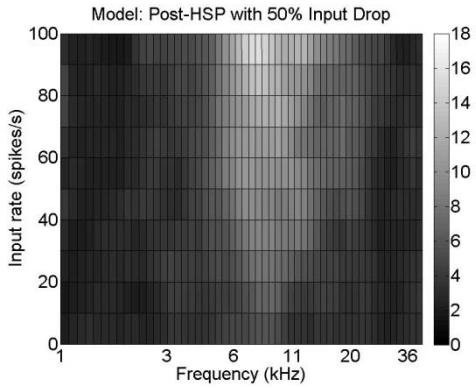
Model: Post-HSP with 50% Input Drop
Input rate (spikes/s)
Frequency (kHz)

C

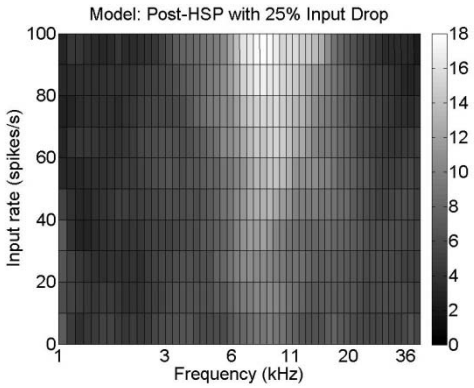
Model: Post-HSP with 25% Input Drop
Input rate (spikes/s)
Frequency (kHz)

D

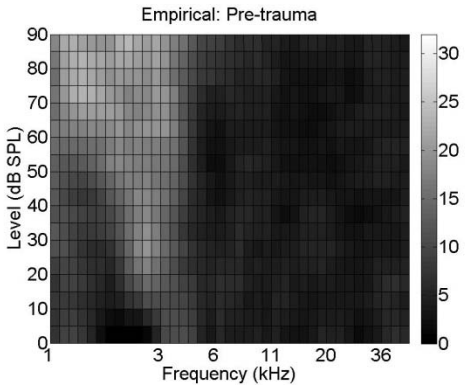
Empirical: Pre-trauma
Level (dB SPL)
Frequency (kHz)

E

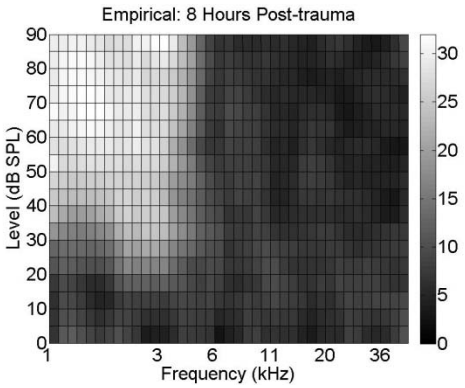
Empirical: 8 Hours Post-trauma
Level (dB SPL)
Frequency (kHz)

Figure 3.6: Simulated and recorded tuning changes. ***A,*** *A frequency receptive field map in the initialized model.* ***B,*** *The same unit's frequency receptive field map after recovery from the 50% reduction in input rate.* ***C,*** *A frequency receptive field map in the same neural unit after recovery from a 25% reduction in input rate.* ***D,*** *A sample frequency receptive field map from a baseline recording.* ***E,*** *The frequency receptive field map from the same channel, but 8 hours post-trauma. Color bars indicate the number of spikes (from the model neural unit or recording channel).*

Importantly, widening also occurred below the trauma when we modeled a less severe tonal-trauma (25% drop in input firing rate), as can be seen in the excitatory receptive field plots (Fig. 6C) and in the post-recovery Q20 value of 0.608. The Q20 value after HSP-mediated recovery of cortical activity from a 25% drop in input firing rate is lower than after recovery from a 50% drop in input rate. This may be because the persistent 50% drop in driven activity was so drastic that fewer subthreshold inputs were unmasked even after HSP brought spontaneous activity back to baseline. On the other hand, tonal trauma does produce variable changes in tuning in AI (Noreña et al. 2003); changes in cortical tuning do not necessarily have a linear relationship with the amount of peripheral damage. An additional concern is that the decrease in Q20 after the reduced drop in input firing rate is more substantial than what we typically observed empirically (baseline: 1.102 ± 0.058; 8 hours post-trauma: 0.933 ± 0.024), even though we did observe substantial widening in tuning in some recordings (Fig. 6D-E). One reason the tuning curves in the empirical data were more variable could be that spontaneous firing

rates had not yet stabilized, whereas in our simulations we allowed spontaneous activity to recover fully before calculating tuning curves and Q20 values. To investigate this further, we determined receptive fields in the model before HSP brought spontaneous activity back to baseline (see below). That being said, the simulation results discussed above support the assertion that a comprehensive form of HSP can contribute to the type of receptive field broadening we observed experimentally.

The changes in synaptic weights and excitability required to bring about noticeable reductions in tuning sharpness were relatively small (Fig. 7A-B). After an HSP-mediated recovery from a 50% reduction in input activity, the mean increases in both peak thalamic and lateral excitatory weights onto excitatory neurons in the trauma region were 13.0% and 13.2%, respectively. The mean reduction in peak inhibitory inputs to excitatory neurons was 9.7%. The mean change in the excitability parameter in this region was always very small because even a small change has a notable effect on activity generated by a neural unit described by eqns. 1-3. In this case, the mean excitability parameter in the trauma region increased from 140.70 to 140.88. After recovery from a 25% reduction in input activity in the trauma region, the mean increases in thalamic and lateral excitatory weights onto excitatory neurons were 5.9% and 6.3%, respectively. The mean reduction in inhibitory inputs to excitatory neurons was 5.7%. The mean excitability parameter in this region increased from 140.70 to 140.80. These simulation results imply that even if HSP only had small effects on synaptic strength and intrinsic excitability at 8 hours post-trauma, it may be sufficient to explain our empirically observed reduction in tuning sharpness.

A(i) **(ii)**

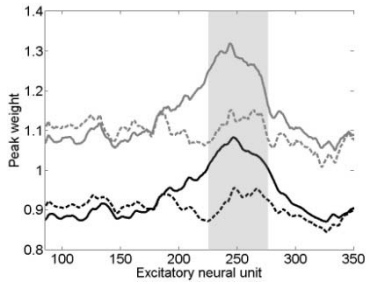

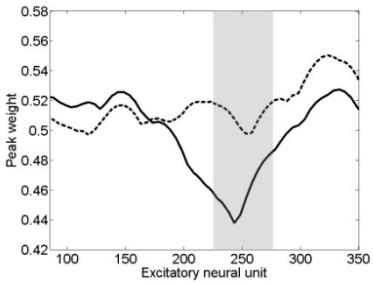

(iii)

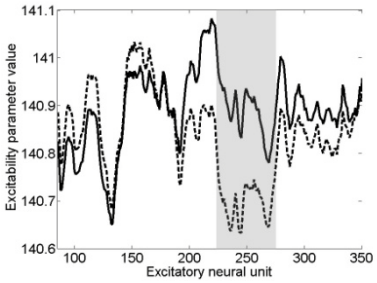

B(i) **(ii)**

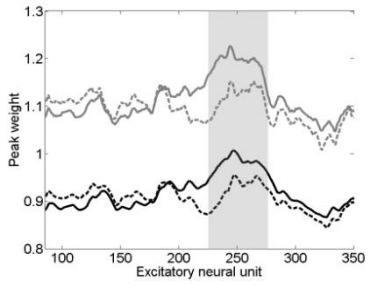

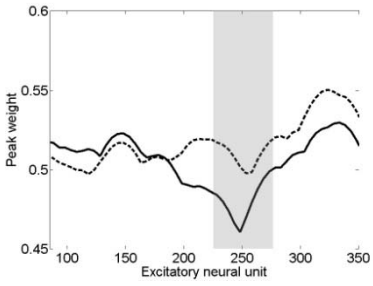

(iii)

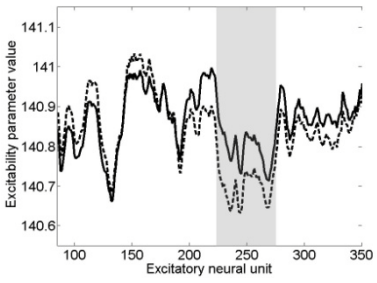

Figure 3.7: Peak excitatory and inhibitory weights and the excitability parameter for excitatory neural units in the region of interest. ***A,*** *(i) Peak thalamic (black line) and lateral-excitatory (grey line) input weights, (ii) peak inhibitory input weights, and (iii) excitability parameter values after recovery from a 50% input-rate drop. Dashed lines indicate corresponding baseline values (before trauma); the grey highlight indicates the deafferented region of the network.* ***B,*** *Corresponding plots (i-iii) after recovery from a 25% input-rate drop. The region of interest in the network is the similar to the range of frequencies analyzed in frequency response area maps in our recordings (1-48 kHz).*

We also wanted to determine if a comprehensive homeostatic response in all synaptic connections types was necessary to explain our empirical results, or if a more restricted response was sufficient. With this in mind, we investigated the effect of tonal trauma (50% drop in input rate) on tuning in the absence of two forms of homeostatic regulation that may not contribute to rapid HSP in adult AI: HSP-driven mediation of thalamic inputs to excitatory neurons ($\mathbf{W_{a,e}}$), and intrinsic excitability ($\mathbf{e}$). Removing either or both of these HSP mechanisms increased changes brought about by the remaining HSP mechanisms; reductions in tuning sharpness relative to the baseline value (1.279) still occurred (Fig. 8). Removing the homeostatic mechanism acting on thalamic inputs forced greater changes in lateral connections and led to even broader tuning (Q20 of 0.647) than when this mechanism was present (Q20 of 0.780). Removing the homeostatic modulation of intrinsic excitability also resulted in a severe drop in tuning sharpness (Q20 value is 0.667). When only intracortical synapses were scaled, the Q20

value dropped to 0.696. These reductions in tuning sharpness developed during a complete recovery of spontaneous activity and were greater than what we observed *in vivo* after 8 hours post-trauma: Q20 dropped from 1.102 to 0.933 over 8 hours. However, when we simulated 8 hours of intracortical synaptic scaling (Fig. 8D), the resulting Q20 value (0.882) was closer to our empirical observations. This similarity indicates that intracortical synaptic scaling may have been sufficient to explain our empirical observations. Furthermore, the increase in lateral excitatory weights and decrease in lateral inhibitory weights required to bring about the change seen in Fig. 8D were both small (5.5% and 4.6%, respectively), and may be in line with 8 hours of homeostatic regulation. HSP acting on thalamocortical synapses, and on overall excitability, are not necessary to explain our empirical data.

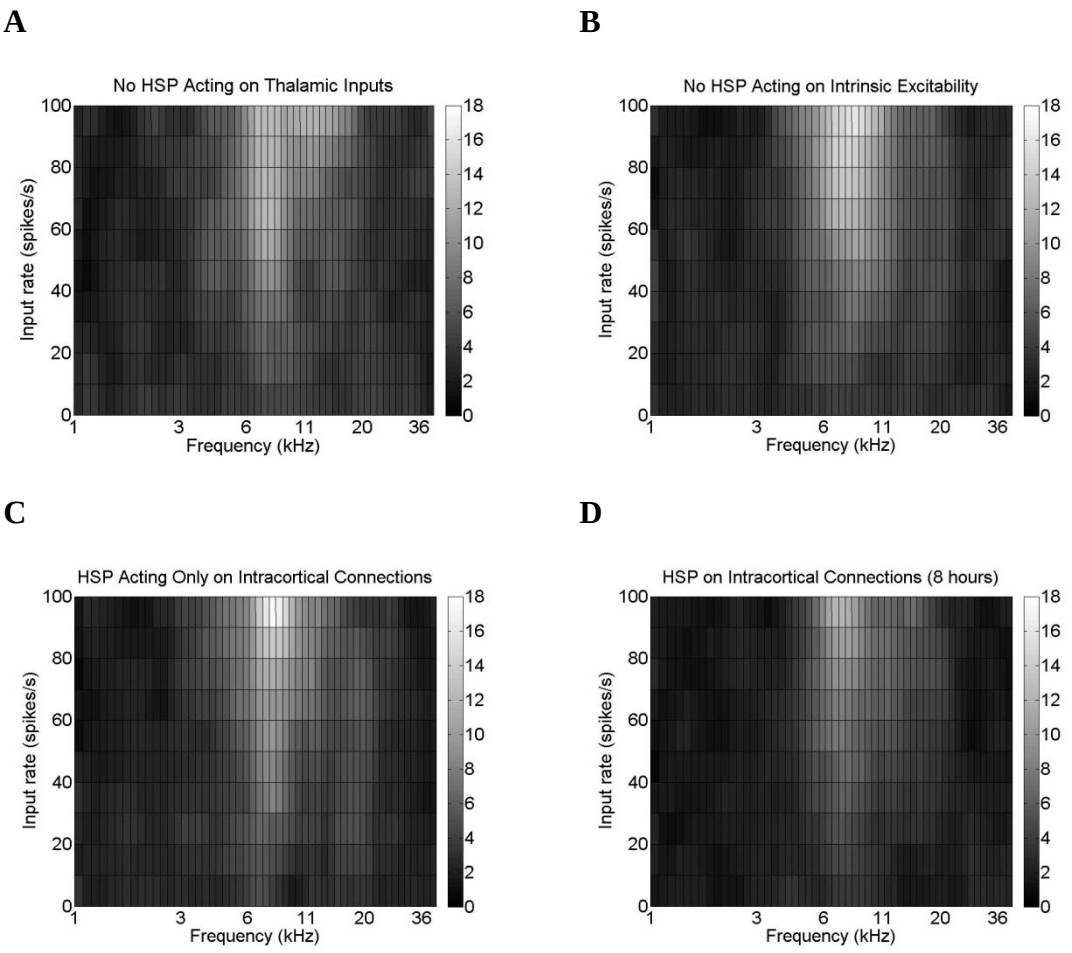

Figure 3.8: Simulated frequency response areas for special cases. ***A,*** *After recovery without homeostatic scaling of thalamic inputs onto excitatory units.* ***B,*** *After recovery without homeostatic modifications of excitability.* ***C,*** *After recovery with only intracortical synaptic scaling.* ***D,*** *Receptive field after 8 hours of simulated recovery with only intracortical synaptic scaling. Input activity in the trauma region was reduced by 50%.*

We next considered whether HSP restricted to superficial layers was sufficient to explain our empirical data. Motivated by some empirical findings (Goel and Lee 2007)

suggesting that in adult cortex HSP is only present in layer 2/3, we used a simplified two-layer model to determine whether synaptic HSP in a superficial layer would induce tuning changes in other layers. The model consisted of two interconnected instances of our one-layer model: a thalamorecipient layer and a superficial layer which received only intracortical inputs. Lateral and feed-forward connections in both layers were defined as in equations 4-9, with the exception that ascending inputs to the superficial layer originated from the thalamorecipient layer. Additionally, we included excitatory feedback projections from the superficial layer to excitatory and inhibitory units in the thalamorecipient layer; these were defined according to equations 5 and 7, respectively. The network was calibrated by modifying all input connections to excitatory neurons according to the same learning rules as those for the single-layer model; the homeostatic set-points for activity in the thalamorecipient and superficial layers were 6 and 3 spikes/s, respectively. This was a simplified implementation of a cortical circuit in AI, but it allowed us to determine the effect of HSP restricted to the superficial layer on tuning in both layers. In this case, the baseline Q20 values in the thalamorecipient and superficial layers were 1.224 and 1.172, respectively. After recovery from trauma via synaptic HSP in only the superficial layer, Q20 values for the thalamorecipient and superficial layers were 0.755 and 0.672, respectively. A result similar to our empirical observations held when we simulated 8 hours of recovery in the two-layer model: the Q20 values in the thalamorecipient and superficial layers dropped to 0.777 and 0.884, respectively. Thus, homeostatic mechanisms restricted to the superficial layers of adult cortex are sufficient to explain our empirical observations.

Spontaneous firing and synchrony during HSP-mediated recovery

As further validation of our model and to better predict which homeostatic mechanisms may be active in the early post-trauma stage, we examined how well the model accounted for the time course of the empirical data. In our model, a neuron's spontaneous firing rate (SFR) activates HSP mechanisms when the SFR deviates from its homeostatic set-point (6 spikes/s) by more than 1 spike/s. This means that spontaneous firing in the model should eventually settle in the 5-7 spikes/s range. This differed from the higher set-point we used in our previous model (Chrostowski et al. 2011), which assumed an acoustically rich environment. Here we focused on spontaneous activity while the animal was present in a sound attenuating booth during purported homeostatic recovery. Furthermore, interpreting the spontaneous firing rate in the model after HSP-mediated recovery is complete would not be analogous to the incomplete process we observed with only 8 hours of recordings. Instead, we focused on how different forms of HSP in the model affected the time course of recovery. We were also able to compare changes in tuning and spontaneous synchrony at selected time points during simulated recovery of spontaneous firing rates.

Figure 9 indicates the recovery (after a 50% or 25% drop in input firing) of spontaneous firing for each of the HSP variants we simulated; plots were smoothed with a 5-point moving average. The firing rates eventually settled near 6 spikes/s for each scenario. A less severe drop in input firing rate led to a quicker recovery in spontaneous firing (Fig. 9A versus Fig. 9E and Fig. 9D versus Fig. 9F). On the other hand, removing

HSP mechanisms acting on thalamic inputs or intrinsic excitability, or leaving only intracortical synaptic scaling (Fig. 9B-D, respectively) slowed the recovery process to varying degrees; Fig. 9D indicates that cortical recovery from deafferentation was slowest if only intracortical synapses were scaled. Since our experimental observations indicated that there was little sustained change in spontaneous firing even if tuning becomes broader, it is possible that any homeostatic response that did occur within 8 hours was restricted to a slight change in intracortical synaptic efficacy. Fig 8D indicates that after 8 hours of intracortical synaptic scaling in response to a drop in activity tuning sharpness dropped (Q20 of 0.882 versus 1.279 at baseline) to an extent similar to our experimental observations (baseline: 1.102 ± 0.058; 8 hours post-trauma: 0.933 ± 0.024). As is evident in Fig. 9, spontaneous activity was not at baseline levels 8 hours post-trauma for any of our simulated scenarios (and particularly not when only intracortical weights were scaled). We argue that homeostatic scaling restricted to intracortical synapses contributed to the relatively slight broadening in tuning we observed even when spontaneous firing was below baseline.

A **B**

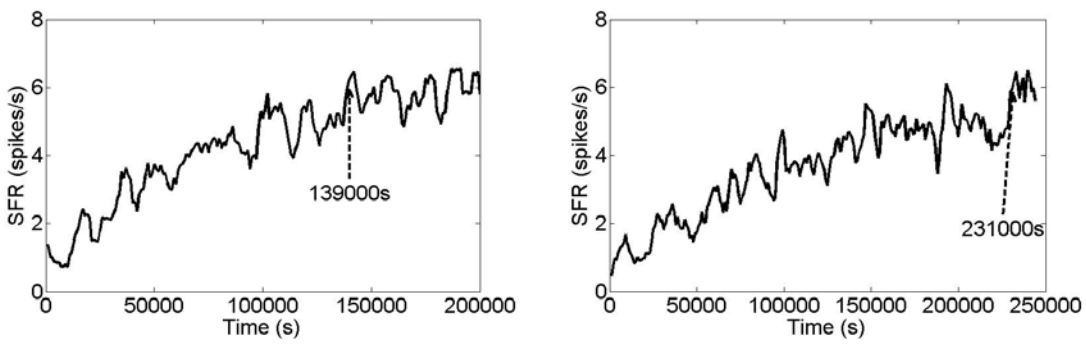

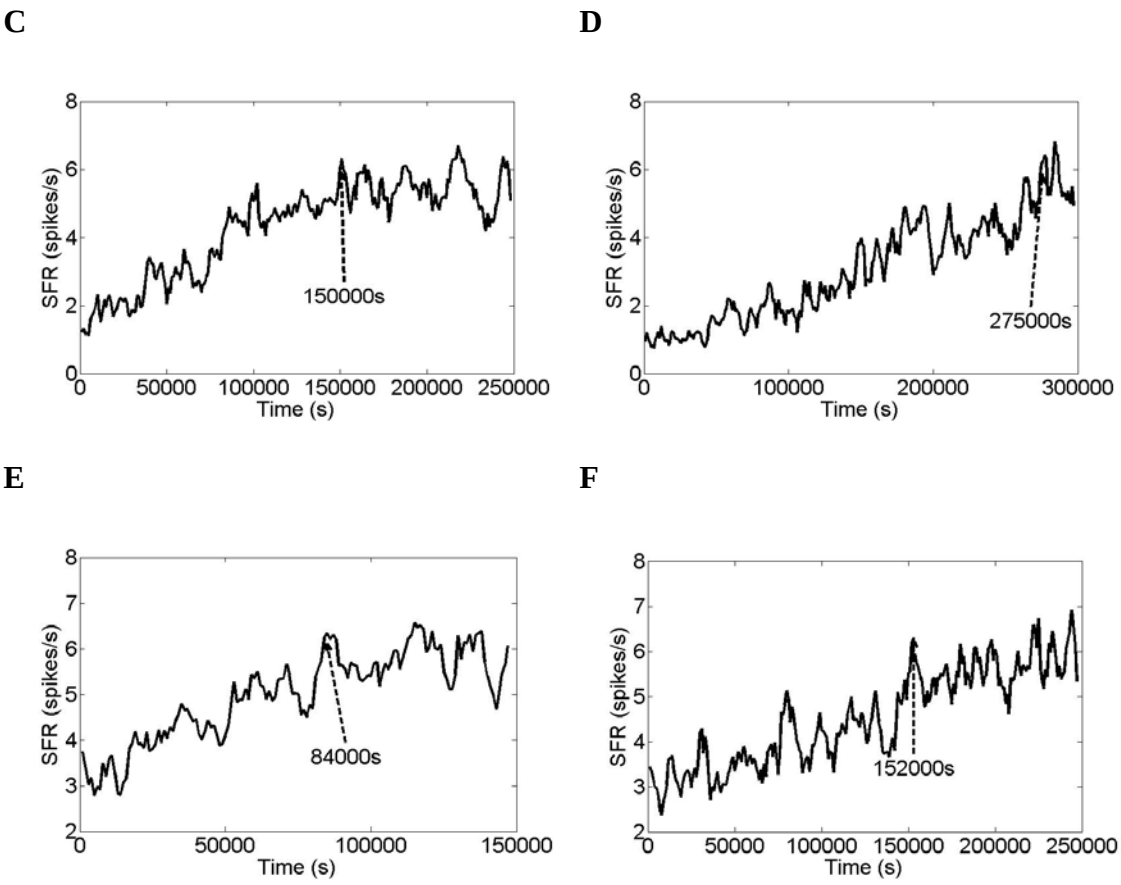

Figure 3.9: Recovery of spontaneous firing under different homeostatic conditions. ***A,*** *Recovery using a comprehensive (i.e. all scaling mechanisms active) HSP response.* ***B,*** *Recovery without scaling thalamic inputs.* ***C,*** *Recovery with no homeostatic modifications to intrinsic membrane excitability.* ***D,*** *Recovery with synaptic scaling acting only on intracortical synapses.* ***E,*** *Recovery using comprehensive HSP response after a 25% reduction in input firing rate.* ***F,*** *Recovery from a 25% drop in input rate with only intracortical synaptic scaling. The dashed arrows provide a comparison for the different scenarios by indicating the point in time at which spontaneous activity reaches 6 spikes/s.*

We also compared simulated data with peak cross-correlation values on electrodes spaced 125 μm apart. To do this, we looked at the mean peak-cross correlation value (2-ms bins) between neurons in the network that were 15 units apart within a region spanning 1 octave below the tonal trauma. For this measure, we focused on the post-recovery time point for all scenarios, as well as an 8-hour time point for a comprehensive and intracortical homeostatic response. Simulations generally showed a slight drop in peak cross-correlation after recovery, which was in agreement with our empirical observations (Fig. 5B) at 8 hours post-trauma. Mean peak cross-correlation in a baseline 1-layer network was 0.191. After homeostatic recovery from 50% and 25% input rate reductions, the mean peak cross-correlation values were 0.185 and 0.170, respectively. Furthermore, when we excluded homeostatic regulation of thalamic inputs to excitatory neurons or additionally removed homeostatic changes to intrinsic neural excitability, recovery from a 50% drop in input firing rate also resulted in drops in peak cross-correlation: 0.189 and 0.174, respectively. Mean peak cross-correlation values also dropped after only 8 hours of recovery were simulated: 0.165 for intracortical HSP and 0.186 for comprehensive HSP. Thus, our model predicts that unlike the effects of widespread and substantial deafferentation triggering HSP to restore activity levels to those present in an acoustically rich environment (as simulated by Chrostowski et al. 2011), a narrower trauma does not necessarily lead to a persistent increase in synchronous activity in affected neural units (but see results below).

Our model did however predict a transient increase in synchrony immediately after a simulated tonal trauma: mean peak cross-correlation values were 0.2084 for a 25%

drop in input firing and 0.2362 for a 50% drop in input firing. An increase in synchrony within a few hours of acoustic trauma is in agreement with our empirical observations and those of others (Seki and Eggermont 2003, Noreña and Eggermont 2003). This increase is likely to be mediated by inhibitory unmasking that occurs when the drive to feed forward inhibition drops. For synchrony increases to persist after HSP-mediated recovery in our model, we had to either simulate greater deafferentation or fix the excitability parameter at 140 during the initial training of the network. Originally, we chose to modulate the excitability parameter during network initialization regardless of whether we excluded homeostatic modulation of excitability after trauma; this resulted in a baseline value of 140.70. To investigate the effect of lower baseline intrinsic excitability, we fixed the excitability parameter at 140 and simulated recovery from a tonal trauma (50% drop in input firing rate). In this case the mean peak cross-correlation value was 0.232, and thalamic, lateral excitatory, and lateral inhibitory weights onto excitatory units changed by 35.5%, 33.2% and -22.8%, respectively. If a more severe and widespread trauma was simulated, synaptic HSP would cause connection weight increases about twice as large as those in the current model, also resulting in increased synchrony (Chrostowski et al. 2011).

To gain insight into what may happen to spontaneous activity in adult AI, where HSP may only be present in superficial layers, we looked at changes in spontaneous synchrony in our two-layer model. The baseline peak cross-correlation value in the thalamorecipient layer (0.139) was very similar to the corresponding value after recovery with HSP in both layers (0.133). However, our model predicted elevated peak cross-

correlation values (0.190) in the thalamorecipient layer if homeostatic mechanisms were only active in the superficial layer. This may have occurred because a lack of homeostatic scaling in the thalamorecipient layer allowed unmasking of feed-forward inhibition to persist even after recovery of activity levels. Thus, our model suggests that when HSP was restricted to one layer, lateral excitatory connections must increase and inhibition must decrease to a greater extent; the resulting state of the affected region may contribute to increased spontaneous synchrony in thalamorecipient layers. This is a somewhat unexpected finding, and predicts that homeostatic scaling of intracortical synapses in superficial layers may exacerbate rather than normalize the elevated spontaneous synchrony that others have observed after acoustic trauma (Noreña and Eggermont 2003; Seki and Eggermont 2003). Furthermore, because the increase in synchrony in the model was present after HSP brought spontaneous firing rates back to target levels, this may help explain our *in vivo* observation that changes in spontaneous synchrony do not necessarily correlate well with changes in spontaneous firing rates.

Discussion

Previous studies have observed broader cortical tuning curves soon after acoustic trauma (Norena 2003). Importantly, we observed further changes in tuning during the 8 hours following tonal trauma. By continuously recording activity in AI for a longer period than in previous studies, we found evidence that receptive fields continue to broaden throughout this time interval. We propose that a persistent reduction in high-frequency inputs activated homeostatic mechanisms in AI and contributed to the gradual

broadening in tuning that we observed. Our computational model predicted that a homeostatic response to moderate reductions in input activity can increase tuning bandwidth in AI even when this response induces slight (4-6%) changes in synaptic weights. Since homeostatic scaling may alter synaptic efficacy by 15-30% over two days (Desai et al. 2002), HSP acting for 8 hours post-trauma may have been sufficient to contribute to the changes in tuning we observed. While a few studies have provided evidence of HSP in AI (Kotak et al. 2005; Yang et al. 2011), these have focused on the end result of a putatively plasticity-driven response to reduced peripheral inputs. Supported by our empirical data, our simulations provide novel insights into the manner in which HSP can quite rapidly affect AI function.

We argue that the receptive field changes we observed are mediated by rapid multiplicative synaptic scaling similar to that observed in cortical circuits within 4 hours of reduced or enhanced activity (Riegle and Meyer 2007; Ibata et al. 2008). Our model predicts that intracortical synaptic scaling can broaden tuning in deafferented neurons even if spontaneous activity does not increase; in our empirical observations we observed gradual expansion in receptive fields without persistently elevated spontaneous activity. This addresses an important unresolved question in the literature: does the wide range of changes after acoustic trauma (in receptive fields and spontaneous activity) reflect immediate unmasking, rapid HSP or longer-term plastic re-organization? Our combined experimental and computational approach supports our argument that, regardless of its effect on spontaneous activity, homeostatic synaptic scaling may be sufficient to explain

the early changes seen in cortical tuning associated with above CF trauma. Thus, HSP may play an important role in managing processing in normal adult auditory cortex.

In order for HSP mechanisms to be activated, there must be a disruption in neural activity; we assumed that a sufficient disruption in inputs and activity occurred after our tonal trauma. However, acoustic trauma can affect AI neurons non-uniformly across the tonotopic map (Noreña et al. 2003; Scholl and Wehr 2008). Previous experiments utilizing similar tonal trauma exposures (albeit in cats) demonstrated broadband hearing loss with average threshold shifts of 40 dB (Noreña et al. 2003). While there may have been a similar loss profile in our animals, a limitation of our study was that we did not record auditory brainstem responses to delineate frequency specific peripheral threshold shifts. These recordings are valuable in characterizing how different frequency inputs are affected post-trauma and will be utilized in future experiments. Regardless, we did consistently note an immediate and persistent reduction in higher frequency inputs (Fig. 4) post-trauma; we assume this reduction in afferent drive was sufficient to induce a homeostatic response.

We observed significantly broader tuning in AI at 8 hours post-trauma but not at 4 hours post-trauma, supporting the hypothesis that there were cumulative synaptic changes in AI after the acoustic trauma. While the immediate drop in Q20 values in AI after noise trauma was not significant in our experiment (after Bonferroni correction for multiple comparisons), this does not imply that no inhibitory unmasking occurred. In fact, the temporary increase in spontaneous synchrony we observed *in vivo* and in simulations indicates that a tonal trauma can, at least temporarily, reduce the drive to inhibitory

neurons. Importantly, while others have shown that tuning is altered soon after an acoustic trauma (Noreña et al. 2003), our observations indicate that by 8 hours post-trauma, additional changes in tuning can occur. Although various plasticity mechanisms may operate in AI, our model predicts that synaptic scaling can explain the gradual receptive field broadening we observed.

To gain further insight into the effects of putative HSP mechanisms we investigated whether gradual changes in spontaneous activity could be observed after acoustic trauma. The spontaneous firing rate (SFR) decreased significantly after the end of our 8-hour recording session in both the control and tonal-trauma groups; this likely resulted from prolonged anesthesia. Since our synchrony measure (peak cross-correlation between neighbouring channels) is affected by the SFR, it also dropped at 8-hours post-trauma in both groups. Thus, we only observed increases in peak cross-correlation for limited periods (1-hour for 2-ms bins, and 1, 2, and 4-hours for 5-ms bins) post-trauma. Additionally, the peak cross-correlation values were not significantly higher than those observed in controls. However, the tonal trauma did seem to affect spontaneous synchrony, since changes in peak cross-correlation values in the tonal-trauma group were not generally correlated with changes in the SFR. Importantly, the absence of a sustained increase in spontaneous synchrony or firing after tonal trauma does not preclude the presence of HSP. Our model predicted receptive field expansion as the network recovered from a drop in input rate, even if the mean SFR and peak cross-correlation in the network were below baseline. Thus, the tonal trauma may have initiated a homeostatic response

sufficient to broaden tuning but not sufficient to overcome a drop in spontaneous activity that was exacerbated by prolonged ketamine anesthesia.

Do the homeostatic responses we propose necessarily occur in adult AI, or could the changes in neural activity be caused by changes in subcortical auditory structures? There is evidence for reduced inhibition and increased excitation in developing and adult inferior colliculus after severe peripheral damage (Suneja et al. 1998; Mossop et al. 2000; Vale and Sanes 2002). While we do not dismiss inherited subcortical changes, we do argue that HSP in AI is initiated once peripheral damage occurs. Kotak et al. (2005) observed increased membrane excitability and excitatory synaptic strength along with reduced inhibitory inputs in AI of deafened developing animals. In addition, Yang et al. (2011) observed a putatively homeostatic reduction in inhibitory synaptic transmission in rat AI one to two weeks after a severe acoustic trauma. Synaptic scaling has been observed in layer 2/3 of adult V1 (Goel and Lee 2007) as well as in adult barrel cortex (reviewed by Pozo and Goda 2010), suggesting that homeostatic responses to persistent input changes might be a general feature of adult sensory cortices. Our model predicts that a range of potential homeostatic mechanisms would be capable of altering processing in AI. However, our experimental observations are well matched by simulations of synaptic scaling restricted to intracortical connections. Furthermore, our two-layer model predicted that, even after 8 hours, intracortical scaling in a superficial layer would decrease tuning sharpness in that layer and in the thalamorecipient layer to a similar extent as in our experimental observations. Thus HSP in the adult cortex restricted to

synapses in superficial layers is sufficient to explain functional changes across multiple cortical laminae.

In addition to homeostatic synaptic scaling, homeostatic modifications of intrinsic neural membrane excitability may also mitigate deafferentation (Desai et al. 1999; Davis and Bezprozvanny 2001; Maffei and Turrigiano 2008). However, our simulations suggest that intrinsic excitability is not the main cause of altered receptive fields, as fixing intrinsic excitability in our model did not prevent tuning broadening. Furthermore, changes in membrane excitability in the primary visual cortex are only observed after two to four days of visual deprivation (Maffei et al. 2004; Maffei and Turrigiano 2008), whereas we observed shifts in tuning curves within the first 8 hours after tonal trauma. Since both synaptic and intrinsic changes are observed in AI of deafened animals (Kotak et al. 2005), it is possible that damage to the auditory periphery activates homeostatic mechanisms acting on synaptic connections and intrinsic excitability, but on different timescales. Our model predicts that the changes in tuning sharpness we see at 8 hours post-trauma can be explained by synaptic scaling alone, but does not rule out additional contributions via slower changes in excitability.

If synaptic scaling is present in AI, perhaps it only plays a partial role in altering activity and tuning during the first hours after peripheral damage. In the present study we looked at changes up to 8 hours post-trauma, but previous work in adult mouse visual cortex indicates that significant homeostatic modulation of AMPA receptors require 2 days of light deprivation (Goel and Lee 2007). Furthermore, early *in vitro* findings support the idea that large increases in miniature excitatory postsynaptic currents require

about 48 hours of activity blockade (Turrigiano et al. 1998). That being said, a range of homeostatic mechanisms seem to be at work concurrently, and some may be more rapid than others. There is evidence of synaptic scaling in the cortex occurring within 4 hours of activity reduction (Ibata et al. 2008) and even sooner for inhibitory synapses (Hartmann et al. 2008). Even in an adult brain, where the need for HSP may not be as great as during development, there is evidence of synaptic scaling responding to reduced activity within 90 minutes (Riegle and Meyer 2007). Slower forms of plasticity such as structural plasticity in dendritic spines (Feldman 2009) are unlikely to contribute to changes in AI tonotopy within the timeframe we investigated; the drop in characteristic frequency we observed immediately after tonal trauma most likely resulted from peripheral changes and not cortical reorganization. We argue that homeostatic mechanisms that are not too rapid to interfere with Hebbian plasticity but that can respond to reduced input within a few hours contributed to the tuning changes we observed and may be active in normal AI.

To what extent HSP plays a role in human adult AI remains to be seen. Since plasticity seems to be less potent in adult primates than in rodents (Feldman 2009), it is difficult to say whether changes observed in this study would occur on the same timescale in humans. However, it seems likely that aberrant plasticity plays a role in the development of hearing loss related disorders such as tinnitus. Furthermore, since homeostatic plasticity may be present in layer 2/3 of adult cortex (Goel and Lee 2007), it may well induce functional changes after hearing loss. Since most experimental work on homeostatic plasticity involves drastic reductions or increases in activity, the question of

whether HSP acts during less dramatic changes arises. If synaptic scaling or changes in intrinsic excitability depend on some homeostatic set-point, it stands to reason that HSP can respond during a slight but persistent disturbance caused by acoustic trauma. We propose that rapid HSP – perhaps mainly acting on synapses in superficial layers – can affect the function of adult AI after acoustic trauma.

References

Burrone J, Byrne MO, Murthy VN (2002). Multiple forms of synaptic plasticity triggered by selective suppression of activity in individual neurons. *Nature* 420:414-418.

Calford MB, Rajan R, Irvine DR (1993). Rapid changes in the frequency tuning of neurons in cat auditory cortex resulting from pure-tone-induced temporary threshold shift. *Neuroscience* 55:953-964.

Chrostowski M, Yang L, Wilson HR, Bruce IC, Becker S (2011). Can homeostatic plasticity in deafferented primary auditory cortex lead to traveling waves of excitation? *J Comput Neurosci* 30:279-299.

Cruikshank SJ, Lewis TJ, Connors BW (2007). Synaptic basis for intense thalamocortical activation of feedforward inhibitory cells in neocortex. *Nat Neurosci* 10:462-468.

Davis GW, Bezprozvanny I (2001). Maintaining the stability of neural function: a homeostatic hypothesis. *Annu Rev Physiol* 63:847-869.

Desai NS, Rutherford LC, Turrigiano GG (1999). Plasticity in the intrinsic excitability of cortical pyramidal neurons. *Nature* 2:515-520.

Desai NS, Cudmore RH, Nelson SB, Turrigiano GG (2002). Critical periods for experience-dependent synaptic scaling in visual cortex. *Nat Neurosci* 5:783-789.

Eggermont JJ, Roberts LE (2004). The neuroscience of tinnitus. *Trends Neurosci* 27:676-682, 2004.

Feldman DE (2009). Synaptic mechanisms for plasticity in neocortex. *Annu Rev Neurosci* 32:33-55, 2009.

Frank CA, Kennedy MJ, Goold CP, Marek KW, Davis GW (2006). Mechanisms underlying the rapid induction and sustained expression of synaptic homeostasis. *Neuron* 52:663-677.

Gerstein GL (2000). Cross-correlation measures of unresolved multi-neuron recordings. *J Neurosci Methods* 100:41-51.

Goel A, Lee H-kyoung (2007). Persistence of experience-induced homeostatic synaptic plasticity through adulthood in superficial layers of mouse visual cortex. *J Neurosci* 27:6692- 6700.

Hartmann K, Bruehl C, Golovko T, Draguhn A (2008). Fast homeostatic plasticity of inhibition via activity-dependent vesicular filling. *PLoS ONE* 3:e2979.

Ibata K, Sun Q, Turrigiano GG (2008). Rapid synaptic scaling induced by changes in postsynaptic firing. *Neuron*:819-826.

Izhikevich EM (2003). Simple model of spiking neurons. *IEEE Transactions on Neural Networks* 14:1569-1572.

Kilman V, Rossum MCW van, Turrigiano GG (2002). Activity deprivation reduces miniature IPSC amplitude by decreasing the number of postsynaptic GABA A receptors clustered at neocortical synapses. *J Neurosci* 22:1328-1337.

Kimura, M; Eggermont JJ (1999). Effects of acute pure tone induced hearing loss on response properties in three auditory cortical fields in cat. *Hear Res* 135:146-162.

Kotak VC, Fujisawa S, Lee FA, Karthikeyan O, Aoki C, Sanes DH (2005). Hearing loss raises excitability in the auditory cortex. *J Neurosci* 25:3908-18.

LeMasson G, Marder E, Abbott LF (1993). Activity-dependent regulation of conductances in model neurons. *Science* 259:1915-1917.

Liberman MC, Kiang NYS (1978). Acoustic trauma in cats. Cochlear pathology and auditory-nerve activity. *Acta Otolaryngol suppl* 358:1-63.

Liberman MC, Dodds LW (1984). Single-neuron labeling and chronic cochlear pathology. II. Stereocilia damage and alterations of spontaneous discharge rates. *Hear Res* 16:43-53.

Liu BH, Wu GK, Arbuckle R, Tao HW, Zhang LI (2007). Defining cortical frequency tuning with recurrent excitatory circuitry. *Nat Neurosci* 10:1594-1600.

Maffei A, Nataraj K, Nelson SB, Turrigiano GG (2006). Potentiation of cortical inhibition by visual deprivation. *Nature* 443:81-84.

Maffei A, Nelson SB, Turrigiano GG (2004). Selective reconfiguration of layer 4 visual cortical circuitry by visual deprivation. *Nat Neurosci* 7:1353-1359.

Maffei A, Turrigiano GG (2008). Multiple modes of network homeostasis in visual cortical layer 2/3. *J Neurosci* 28:4377-4384.

Moshitch D, Las L, Ulanovski N, Bar-Yosef O, Nelken I (2006). Responses of neurons in primary auditory cortex (A1) to pure tones in the halothane-anesthetized cat. *J Neurophysiol* 95:3756-3769.

Mossop JE, Wilson MJ, Caspary DM, Moore DR (2000). Down-regulation of inhibition following unilateral deafening. *Hear Res* 147:183-187.

Noreña AJ, Eggermont JJ (2003). Changes in spontaneous neural activity immediately after an acoustic trauma: implications for neural correlates of tinnitus. *Hear Res* 183:137-153.

Noreña AJ, Tomita M, Eggermont JJ (2003). Neural changes in cat auditory cortex after a transient pure-tone trauma. *J Neurophysiol* 90:2387-401.

Pozo K, Goda Y. (2010) Unraveling mechanisms of homeostatic synaptic plasticity. *Neuron* 66:337-351.

Prieto JP, Peterson BA, Winer JA (1994). Morphology and spatial distribution of GABAergic neurons in cat primary auditory cortex (AI). *J Comp Neurol* 344:349-382.

Rajan R. Plasticity of excitation and inhibition in the receptive field of primary auditory cortical neurons after limited receptor organ damage (2001). *Cereb Cortex* 11:171-82.

Riegle KC, Meyer RL (2007). Rapid homeostatic plasticity in the intact adult visual system. *J Neurosci* 27:10556 -10567, 2007.

Robertson D, Irvine DRF (1989). Plasticity of frequency organization in auditory cortex of guinea pigs with partial unilateral deafness. *J Comp Neurol* 282:456-471.

Rossum MCW van, Bi GQ, Turrigiano GG (2000). Stable Hebbian learning from spike timing-dependent plasticity. *J Neurosci* 20:8812-8821.

Rutherford LC, DeWan A, Lauer HM, Turrigiano GG (1997). Brain-derived neurotrophic factor mediates the activity-dependent regulation of inhibition in neocortical cultures. *J Neurosci* 17:4527- 4535.

Rutherford LC, Nelson SB, Turrigiano GG (1998). BDNF has opposite effects on the quantal amplitude of pyramidal neuron and interneuron excitatory synapses. *Neuron* 21:521-530.

Saliba RS, Michels G, Jacob TC, Pangalos MN, Moss SJ (2007). Activity-dependent ubiquitination of GABA A receptors regulates their accumulation at synaptic sites. *J Neurosci* 27:13341-13351.

Salvi R, Henderson D, Hamernik RP, Parkins C (1980). VIII Nerve response to click stimuli in normal and pathological cochleas. *Hear Res* 2:335-342.

Scholl B, Wehr M (2008). Disruption of balanced cortical excitation and inhibition by acoustic trauma. *J Neurophysiol* 100:646-656.

Seki S, Eggermont JJ (2003). Changes in spontaneous firing rate and neural synchrony in cat primary auditory cortex after localized tone-induced hearing loss. *Hear Res* 180:28-38.

Stellwagen D, Malenka RC (2006). Synaptic scaling mediated by glial TNF-a. *Nature* 440:1054-1058.

Stolzberg D, Chen G-D, Allman BL, Salvi RJ (2011). Salicylate-induced peripheral auditory changes and tonotopic reorganization of auditory cortex. *Neuroscience*: 1-8.

Suneja SK, Potashner SJ, Benson CG (1998). Plastic changes in glycine and GABA release and uptake in adult brain stem auditory nuclei after unilateral middle ear ossicle removal and cochlear ablation. *Exp Neurol* 151:273-288.

Turrigiano GG (1999). Homeostatic plasticity in neuronal networks : the more things change, the more they stay the same. *Trends Neurosci* 22:221-227.

Turrigiano GG (2008). The self-tuning neuron: synaptic scaling of excitatory synapses. *Cell* 135:422-35.

Turrigiano GG, Abbott LF, Marder E (1994). Changes in the Intrinsic Activity-Dependent Properties of Cultured Neurons. *Science* 264:974-977.

Turrigiano GG, Leslie KR, Desai NS, Rutherford LC, Nelson SB (1998). Activity-dependent scaling of quantal amplitude in neocortical neurons. *Nature* 391:892-895.

Vale C, Sanes DH (2002). The effect of bilateral deafness on excitatory and inhibitory synaptic strength in the inferior colliculus. *Eur J Neurosci* 16:2394-2404.

Wang J, Salvi RJ, Powers N (1996). Plasticity of response properties of inferior colliculus neurons following acute cochlear damage. *J Neurophysiol* 75:171-183.

Wehr M, Zador AM (2003). Balanced inhibition underlies tuning and sharpens spike timing in auditory cortex. *Nature* 426:442-446.

Wu GK, Arbuckle R, Liu BH, Tao HW, Zhang LI (2008). Lateral sharpening of cortical frequency tuning by approximately balanced inhibition. *Neuron* 58:132-143.

Yang S, Weiner BD, Zhang LS, Cho S-J, Bao S (2011). Homeotatic plasticity drives tinnitus perception in an animal model. *Proc Natl Acad Sci* 108:14974-14978.

Yuan K, Shih JY, Winer JA, Schreiner CE (2011). Functional networks of parvalbumin-immunoreactive neurons in cat auditory cortex. *J Neurosci* 31:13333-13342.

Postscript

The preceding chapter provided further evidence of the potential role of homeostatic plasticity in the development of tinnitus correlates. While it elucidated the general operation of HSP in the adult primary auditory cortex, it also shed light on how such activity can contribute to tinnitus within hours of peripheral damage. This is an important contribution as it may have implications for developing effective tinnitus treatments. While the models described in the first two chapters have been validated empirically and provide insights into the development of two tinnitus correlates (elevated spontaneous firing and synchrony), other tinnitus correlates were not investigated or were not evident in this model. This indicated that further additions to the model were necessary to capture the role of cortical plasticity after hearing loss. Such additions could produce a more complete model of central tinnitus and would have implications for treatment testing and development.

Chapter Four

Preamble

The preceding chapters discuss the importance of homeostatic plasticity (HSP) as well as how HSP may behave *in vivo* after acoustic trauma. Here, I build on our previous computational work to elucidate how Hebbian-type plasticity (spike-timing-dependent plasticity or STDP) can lead to tonotopic reorganization. Reorganization is debated potential correlate of tinnitus that was not evident in the previous models, which only simulated the action of homeostatic plasticity. I also discuss other tinnitus correlates to determine whether including STDP in the model leads to simulation results that are in agreement with empirical research on the development of tinnitus correlates after hearing loss. The other tinnitus correlates I focus on are increased spontaneous firing, increased spontaneous synchrony and increased delta-band and gamma-band activity. I then use the model to provide insights into whether tonotopic reorganization is necessary for tinnitus perception.

This chapter describes simulations indicating that STDP working in concert with HSP is sufficient for cortical reorganization and that including STDP does not qualitatively change model predictions of other tinnitus correlates developing after hearing loss. Furthermore, the model indicates that tinnitus correlates in spontaneous activity can develop irrespective of tonotopic reorganization. After describing how the model of HSP and STDP responds to different hearing loss levels and types, I simulate

the use of a hearing aid and sound therapy to determine how these affect the tinnitus correlates captured by the model.

Simulation results indicate that early hearing aid use is more beneficial than late hearing aid use in terms of reducing cortical reorganization and neural synchrony. However, simulations indicate that a hearing loss prescription that does not take into account high frequency hearing loss may not be an effective strategy for tinnitus reduction. On the other hand, simulations of acoustic therapy (an acoustically enriched environment that takes into account the hearing loss profile) indicate that while it cannot undo tonotopic reorganization, it does seem to reduce other tinnitus correlates.

Introduction

In the last three decades substantial progress has been made toward understanding the mechanisms underlying the phantom auditory percept known as tinnitus. Along with breakthroughs in basic research, various tinnitus treatment strategies have been proposed (e.g. Londero et al., 1999; Dohrmann et al., 2007; Schaette et al., 2010; Engineer et al., 2011) to assist the 5-15% of the population that is affected by chronic tinnitus to various degrees (Eggermont and Roberts, 2004). Unfortunately, these treatments have had mixed results and no generally accepted treatments exist at this point. This is partly due to an insufficient understanding of how treatments interact with the underlying neural mechanisms of tinnitus. Even in the auditory cortex, a potentially critical circuit for tinnitus perception (Eggermont, 2008; Stolzberg et al., 2012), plasticity mechanisms that may contribute to sufficient conditions for tinnitus generation have not been fully characterized. The response of these mechanisms to tinnitus treatment strategies is even less well understood.

Here we investigate two plasticity mechanisms that may produce correlates of tinnitus: homeostatic and Hebbian plasticity. Computational models predict that after peripheral damage, homeostatic plasticity in the central auditory system (Schaette and Kempter, 2006) and specific to the primary auditory cortex (Chapter 2) can contribute to neural correlates of tinnitus such as increased spontaneous firing and synchrony. These theoretical accounts have received some empirical support. For example, a recent study of hearing loss induced via acoustic trauma suggests that homeostatic synaptic scaling

may contribute to the tinnitus percept (Yang et al., 2011). Moreover, more complex forms of plasticity may explain some of the changes seen after peripheral auditory damage, including tonotopic reorganization (Robertson and Irvine, 1989; Rajan et al., 1993; Eggermont and Komiya, 2000), which has been linked to tinnitus (Mühlnickel et al., 1998; but see Langers et al., 2012). Theoretical predictions and empirical observations (Chapter 2; Chapter 3) indicate that homeostatic mechanisms may be involved in the broadening of receptive fields after acoustic trauma but that they cannot account for cortical reorganization after hearing loss. It is possible that cortical reorganization is mediated by Hebbian plasticity (Dahmen et al., 2008; Noreña, 2011). Since neural tuning can be shifted towards a desired frequency when tones at the original CF rapidly (within 12 ms) follow tones at the desired frequency (Dahmen et al., 2008), spike-timing-dependent plasticity (STDP) may be a more accurate model of the Hebbian plasticity underlying tonotopic reorganization after hearing loss. A better understanding of how plasticity mechanisms contribute to the development of tinnitus correlates and of how they interact with sound therapies may be essential in the development of more successful interventions.

The ideal way to investigate the plasticity mechanisms underlying tinnitus would be to monitor cortical network connections and dynamics over the long-term following acoustic trauma. However, this is not feasible in large scale neural circuits. Alternatively, computational models can provide insights into potential cortical mechanisms underlying tinnitus perception, and how these mechanisms interact with tinnitus treatments. In order to pursue this strategy, however, it is first necessary to establish that a computational

model exhibits the known behavioural correlates of tinnitus. Some of the most referenced correlates of hearing loss-related tinnitus include tonotopic reorganization (Mühlnickel et al., 1998; but see Langers et al., 2012), increased spontaneous firing (Seki and Eggermont, 2003; Noreña et al., 2003) and increased spontaneous synchrony (Seki and Eggermont, 2003) (for a review see Eggermont and Roberts, 2004). In addition, EEG and MEG recordings indicate that there may be a causal link between increased delta-band and gamma-band activity and tinnitus (Weisz et al., 2005; Dohrmann et al., 2007; Weisz et al., 2007, Kahlbrock and Weisz, 2008), based on the observation that when people can modulate activity within these bands they can suppress their tinnitus (Dohrmann et al., 2007) and that tinnitus suppression results in reduced delta-band activity (Kahlbrock and Weisz, 2008). It is possible that aberrant delta- and gamma-band activity in the auditory cortex can develop after hearing loss, and when it does develop, it may be responsible for the perception of tinnitus.

Our previous work (Chapter 2; Chapter 3) suggested that homeostatic plasticity could induce aberrant synchrony and spontaneous firing after hearing loss. Here, we extend our model to investigate its ability to capture increases in the amplitudes of delta- and gamma-band oscillations and tonotopic map reorganization, along with the features captured by our previous model, namely, changes in spontaneous firing and synchrony. Our computational model of the primary auditory cortex (AI) includes two forms of plasticity, homeostatic scaling (like the previous model) and Hebbian plasticity. These plasticity mechanisms respond to normal and hearing loss activity, when driven by input generated by a realistic model of the auditory periphery (Zilany et al., 2009). Thus, we

aim to capture all of the generally agreed upon cortical correlates of tinnitus within a unified theoretical framework. Having established that our model accounts for most major correlates of tinnitus, we investigate the potential for the model to predict tinnitus treatments.

Effective tinnitus treatments are aimed at transiently or permanently ameliorating one or more correlates of tinnitus. One such treatment is through acoustic stimulation. This treatment is particularly aimed at tinnitus associated with hearing loss. It is important to note that while tinnitus is most often associated with hearing loss (Eggermont and Roberts, 2004), it also occurs in individuals with no detectable hearing loss (Schaette and McAlpine, 2011); some of these cases may reflect very mild and/or ultra-high-frequency loss not picked up on a standard audiogram, but tinnitus may also have other origins. Whether tinnitus caused by other factors could be reduced by acoustic therapy is unclear. That being said, tinnitus reduction through acoustic stimulation provides an important avenue for studying the underlying correlates of tinnitus in the central auditory system. For example, even a simple constant acoustic stimulus, lasting seconds to minutes, can temporarily reduce or eliminate the perception of tinnitus in some by purportedly disrupting aberrant activity (i.e. synchrony) in the auditory cortex, a phenomenon referred to as residual inhibition (RI) (Eggermont and Roberts, 2004; Osaki et al., 2005; Roberts et al., 2006; Kahlbrock and Weisz, 2008). Whereas RI is a transient pheonomenon lasting seconds to minutes, more complex acoustic stimulation paradigms are used to attempt to permanently undo the central auditory changes contributing to tinnitus (Schaette et al., 2010) or to prevent the kind of cortical reorganization (Noreña

and Eggermont, 2005) that has been associated with tinnitus (Mühlnickel et al., 1998). Engineer et al. (2011) focus on cortical reorganization that has occurred after damage to the auditory periphery, and attempt to re-establish normal tonotopic organization in AI by coupling specific tone ensembles with vagus nerve stimulation. While this treatment provides a significant improvement in silent gap detection (a reduced ability to detect silent gaps is thought to indicate tinnitus in animal models; for details see Turner et al., 2005), its long-term effect on other tinnitus correlates was not characterized. Thus, acoustic stimulation along with vagus nerve stimulation may have been effective in improving gap detection because it also normalized tinnitus correlates other than tonotopic reorganization. Indeed, recent evidence indicates that tonotopic reorganization is not required for tinnitus perception in those with near-normal hearing (Langers et al., 2012). Regardless, an acoustic stimulus that acts on multiple correlates of tinnitus may be more likely to target the underlying cause of the tinnitus, and therefore have a greater treatment success rate. Designing such a stimulus in general is a complex task in and of itself, but in addition, characteristics of the optimal stimulus are likely to vary between individuals. In order to improve the success rate of acoustic treatments for tinnitus, we must improve our understanding of how the same neural mechanisms that are activated by hearing loss can react to an acoustic therapy in a way that reduces or eliminates conditions necessary for tinnitus perception.

With this in mind, we describe a computational model that captures the established correlates of tinnitus at the level of the auditory cortex (increased spontaneous firing, synchrony and delta- and gamma-band activity), along with tonotopic

reorganization, which requires further study with respect to its potential link to tinnitus. We then use this model to predict how strategies for tinnitus reduction may alter tinnitus correlates in the presence of cortical plasticity. In our model, tinnitus correlates at the level of the auditory cortex are the aberrant consequences of homeostatic and Hebbian-type spike-timing-dependent plasticity that responds to damage at the auditory periphery. In terms of the development of tinnitus correlates, our model makes three main predictions: severe hearing loss is not required for the development of established tinnitus correlates, homeostatic plasticity can account for most tinnitus correlates but not tonotopic reorganization, and generally agreed upon tinnitus correlates can develop in a model of homeostatic plasticity and spike-timing-dependent plasticity even when hearing loss is not sufficient to induce tonotopic reorganization, suggesting that reorganization is not necessary for tinnitus. Our model also makes an important prediction about successful long-term acoustic tinnitus treatments: they should take into account characteristics of the entire hearing loss region.

Methods

Network model

Our computational model is a network consisting of a cortical layer and an input layer (see Figure 1), where input activity is first generated by a model of the auditory periphery (Zilany et al., 2009) and then processed further to produce thalamocortical input activity (this process is explained in the next section). The input layer is therefore a simplification as there are actually several sub-cortical levels of processing between the

auditory nerve and the cortex in the mammalian brain. The behaviour of the cortical units is described by the Izhikevich neural model (Izhikevich, 2003). The layout of the cortical layer is similar to that of our previously described model (Chapter 2) except that in the current model, excitatory and inhibitory connections are co-tuned, consistent with empirical evidence (Wehr and Zador, 2003) and we include both feedforward and feedback inhibition (Figure 1). Cortical neural units (400 excitatory regular spiking units and 80 fast spiking inhibitory units) are organized tonotopically with characteristic frequencies spaced logarithmically, according to the relationship between basilar membrane position and characteristic frequency (Greenwood, 1990); we restrict our analysis to frequencies between 100 Hz and 15 kHz. The input layer, which consists of 400 distinct inputs, is organized in the same way. The model is simulated with 0.2-ms resolution; 4th order Runge-Kutta numerical estimation is used to determine firing rates (for homeostatic learning rules).

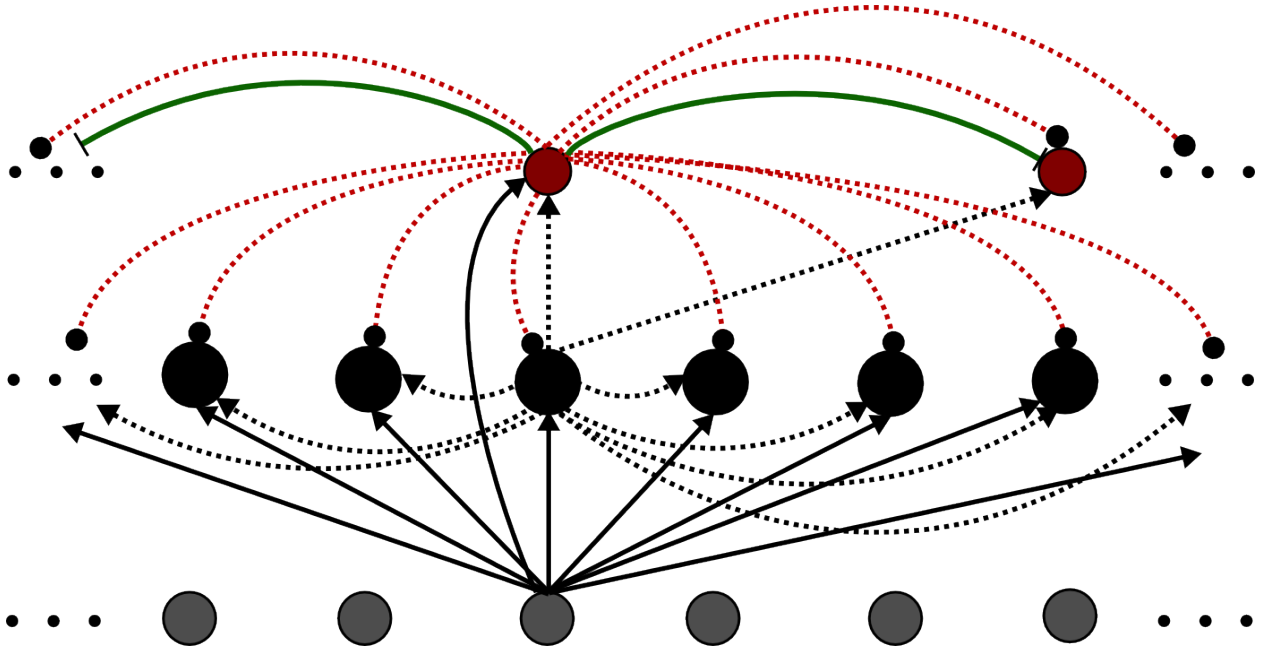

Figure 4.1: Connection layout of cortical model. The grey, black and red circles represent thalamic units, cortical regular-spiking units and inhibitory fast-spiking units, respectively. Solid black lines are thalamocortical projections, while dashed black and red lines are lateral excitatory and inhibitory connections, respectively. Solid green lines represent gap-junction coupling between neighbouring fast-spiking units.

In general, weight vectors (**w**) between source (s) and destination (d) neural units (e.g. input weights, excitatory and inhibitory lateral connections) are described by the following equation:

$$\mathbf{W_{s,d}} = A \cdot \exp\left(-\left(\frac{|s-d|}{\sigma}\right)^{c}\right), \text{ for } s, d \in \{1, 2, 3, \ldots, 400\}, \ |s-d| \leq x, \qquad (1)$$

where A is the initial peak value for the weight, s and d represent the positions of the source and destination units, respectively, σ and c determine how fast the weight function decays as a function of the distance between the two units, $c = 1$ only for lateral excitatory connections, which act to sharpen the tuning curve (Wu et al., 2008), otherwise $c = 2$. The weight function is non-zero only for connections between neurons within x units of each other. All above parameter values are the same as those in our previous work (Chapter 3).

In previous modeling work (Chapter 2; Chapter 3) we did not quantify changes in the amplitude of oscillatory activity after hearing loss. Since oscillatory activity may be strengthened by gap junctions between fast-spiking inhibitory neurons (Galarreta and Hestrin, 1999; Gibson et al., 1999), we include electrical coupling via gap junctions in the current instance of the model. Based on empirical observations (Galarreta and Hestrin,

1999), we set the coupling ratio of neighboring neurons to be 6.4%, falling off geometrically with distance between inhibitory neurons and dropping to zero for neurons more than three neighbors apart on either side. In our model, removing gap junctions reduces the amplitude of gamma-band oscillations by as much as 50%, suggesting that including electrical coupling may be required to capture elevated gamma-band activity that is associated with tinnitus (Weisz et al., 2007).

Normal, hearing loss and acoustic treatment inputs

In our previous model we used mutually independent Poisson processes to generate inputs for our cortical model. Here, we aim to generate inputs that more accurately reflect a realistic acoustic environment. To do this, we use a model of the auditory periphery up to the level of the auditory nerve (Zilany et al., 2009) to generate neural responses to speech and other natural sounds. The wav files we input into the peripheral model are taken from the TIMIT database (male and female voices) and from www.soundjay.com/nature-sounds.html (natural sounds). The sound waves are scaled to 65 dB SPL before being input into the peripheral model. We use the generated auditory nerve fiber (ANF) responses to train the cortical model during initialization, after simulated hearing loss, and with inputs modified by hearing aid gain profiles.

The peripheral model simulates responses of single auditory nerve fibers to input wave forms. To obtain inputs to our cortical network model, we simulate the response of auditory nerve fibers with 400 characteristic frequencies spaced logarithmically and

ranging from 20 Hz to 15 kHz. While the stimuli contain higher frequencies, we restrict our analysis to activity and hearing loss within this frequency range. Given an input waveform, a characteristic frequency, and (optionally) a threshold shift at this frequency, the peripheral model first generates inner hair cell potentials, which are then modulated by an outer hair cell function and post-synaptic transformation to obtain auditory nerve fiber responses to the stimulus. An audiogram characterizing the hearing loss region (e.g. Figure 2A) is used in this model to determine how peripheral activity will be altered across frequencies; we assume that two thirds of the threshold shift is accounted for by damage to outer hair cells and one third by damage to inner hair cells (Plack et al., 2004). The peripheral model also allows for simulating low-, medium-, and high-threshold fibers. Based on empirical evidence of the proportion of these fibers in the cat auditory periphery (Liberman, 1978), for each relevant characteristic frequency, the peripheral firing rate is obtained by aggregating responses of 3, 1 and 1 low-, medium-, and high threshold fibers, respectively. The output activity of each fiber is represented as a post-stimulus time histogram (PSTH), with 10-μs time bins; we re-bin these into 0.2-ms time bins for our cortical model. At each simulated frequency, we then attempt to account for the temporal jitter and reduced firing rates prior to this output reaching AI by randomly removing spikes from the PSTH (Figure 2C). This way, the overall input profile across frequencies and the temporal pattern of simulated peripheral responses are preserved (Figure 2B and C), while the firing rates of the thalamic inputs are similar to those observed empirically (Aitkin and Webster, 1972; Rose and Metherate, 2005).

A

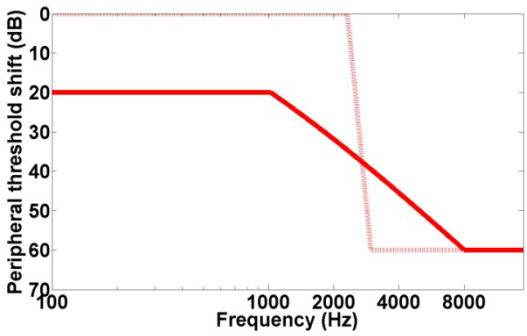

B

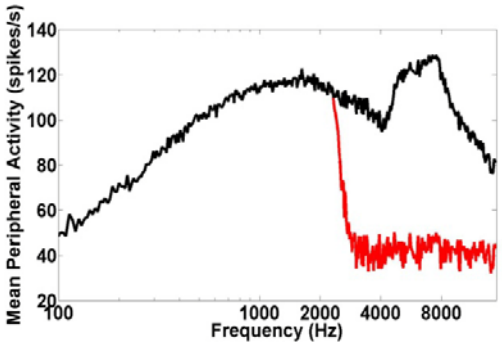

C

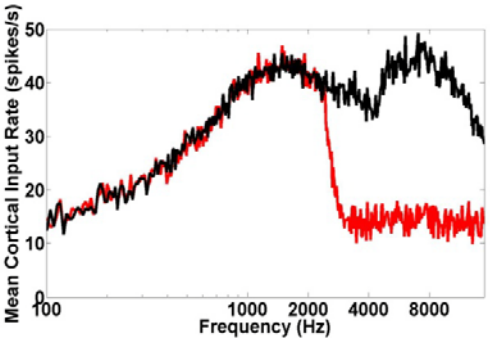

Figure 4.2: Inputs from peripheral model. A, Hearing loss profiles for severe (60-dB) hearing loss with a steep hearing loss edge (dashed red line) and sloping hearing loss with a maximum threshold shift of 60 dB (solid red line). B, Mean peripheral activity across the tonotopy during training stimuli; normal activity is represented by a solid black line, while the solid red line represents activity after severe (60-dB) hearing loss. C, Cortical input activity after random removal of spikes from peripheral PSTH to account for processing in intermediate stages of the auditory system; normal activity is

represented by a solid black line, while the solid red line represents activity after severe (60-dB) hearing loss. The profile of mean activity across the tonotopy is preserved after spike removal.

To initialize the cortical model we generate input firing patterns for a normal hearing profile such that thresholds are not elevated at any frequency. After the model is initialized, we generate peripheral responses after hearing loss, to determine resulting changes in the cortical model. We simulate two types of hearing loss, a steep hearing loss curve (large hearing loss region starting at 2.94 kHz or at the neural unit at location 225 in the network) and a more gradually sloping hearing loss curve (Figure 2A). For sloping hearing loss, the threshold shift starts at 20 dB (at 1.0 kHz) and gradually increases to 60 dB (by 8 kHz), while for the steep hearing loss case we simulate three levels of hearing loss: mild (20 dB), moderate (35 dB) and severe (60 dB) loss across all frequencies above 2.3 kHz. We are thus able to investigate how these hearing loss profiles may differentially affect tonotopic organization and other correlates of tinnitus. Importantly, even 20 to 30 dB threshold shifts have been shown to induce cortical reorganization in cats (Noreña and Eggermont, 2005).

In the results section, we discuss two instances of this model: the HSP (homeostatic plasticity) model, in which spike-timing-dependent plasticity STDP is not included, and the HSP+STDP model, which captures the behaviour of STDP along with HSP. We compare the behaviour of the HSP model to that of the HSP+STDP model for

the case of mild, moderate and severe steep hearing loss. We also investigate the behaviour of the HSP+STDP model in response to a gradually sloping hearing loss curve.

Finally, we also simulate the HSP+STDP model's response to long-term hearing aid use and potential acoustic therapies for tinnitus. Our simulated sound therapy is similar to the acoustically enriched environment used by Noreña and Eggermont to prevent tonotopic reorganization in a cats exposed to acoustic trauma (2005, 2006). Namely, we create a tone ensemble consisting of randomly generated tones with frequencies spanning our frequency range of interest (20 Hz to 15 kHz); tone loudness is set to 65 dB SPL in the normal hearing region and to 90 dB SPL in the hearing loss region. Similar stimulus paradigms immediately after acoustic trauma seem to prevent tonotopic reorganization (Noreña and Eggermont, 2005) and the development of other tinnitus correlates (Noreña and Eggermont, 2006) in cats. This is in accordance with data from humans with tinnitus: acoustic stimulation from noise devices is more effective in reducing self-rated tinnitus measures when the stimulus frequency range encompasses the perceived tinnitus frequency, which lies within the hearing loss region (Davis et al., 2008; Schaette et al., 2010). Inputs to the cortical model are generated as described above.

HSP learning rules

To make baseline weights more biologically plausible, and to prevent uniform learning via STDP (discussed below), we first randomly jitter each of the weights $\mathbf{W_{s,d}}$ within 20% of its initial value. We then initialize the model by training it according to our homeostatic learning rules (Chapter 2). Briefly, we set target firing rates for excitatory

and inhibitory cortical neurons to be 10 spikes/s and 20 spikes/s, respectively. The spontaneous firing rate in our inhibitory neurons is higher than that of regular spiking neurons, in agreement with empirical observations in V1 and S1 of awake animals (Swadlow, 2003). The learning rules for homeostatic plasticity, described in Chapter 2, dynamically re-scale synaptic strengths of excitatory and inhibitory inputs to the neural units to maintain target neural firing rates of 10 and 20 spikes/s for excitatory and inhibitory units, respectively. Rather than using Poisson distributed noisy inputs as in our previous work, the model described here is trained using simulated auditory nerve (AN) responses (generated by a peripheral model of the cochlea and auditory nerve developed by Zilany et al., 2009) to natural sounds. This allows our network to calibrate itself according to a natural acoustic environment that humans encounter on a daily basis. In subsequent simulations (simulating hearing loss or tinnitus treatments), HSP mechanisms only re-scale inputs to excitatory neural units to maintain their target firing rate (10 spikes/s), as this restricted homeostatic response is more likely to occur in the adult auditory cortex (Chapter 3).

STDP learning rules

Our earlier model included only a limited form of plasticity, HSP, and was unable to capture cortical reorganization, suggesting that an additional plasticity mechanism was necessary. We therefore add a spike-timing-dependent form of plasticity (STDP), which has been shown to lead to tonotopic reorganization in a tone pairing paradigm (Dahmen et al., 2008). We include STDP on excitatory connections within the cortical network

with STDP weight updates defined as anti-symmetric exponentials (as per Masquelier et al., 2008):

$$\Delta \boldsymbol{w}_{s,d} = \begin{cases} a_{LTP} \cdot \exp\left(\frac{t_s - t_d}{\tau_{LTP}}\right), & \text{if } t_s \leq t_d \\ a_{LTD} \cdot \exp\left(-\frac{t_s - t_d}{\tau_{LTD}}\right), & \text{if } t_s > t_d \end{cases} \quad (2)$$

We set τ_{LTP} = 16.8 ms and τ_{LTD} = 16.8 ms. As in the model described by Masquelier et al., (2008), we also use small values for the coefficients a_{LTP} (= 0.003125) and a_{LTD} (= $0.4 \cdot a_{LTP}$). Figure 3 illustrates how relative spike timing affects weight changes in the network. Our homeostatic plasticity rules help to prevent runaway excitation or complete elimination of weights in the presence of the STDP learning rule.

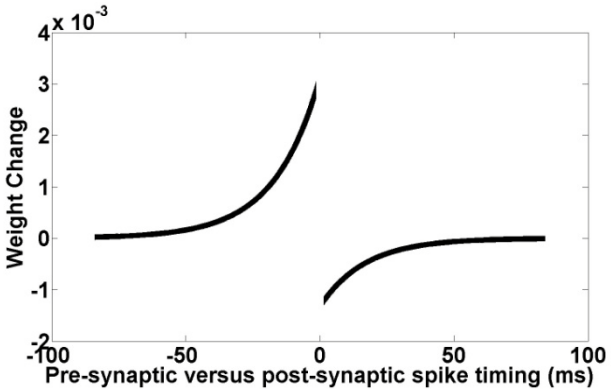

Figure 4.3: Weight changes induced by spike-timing-dependent plasticity. Potentiation of the synaptic connection occurs if the pre-synaptic spike occurs prior to the post-synaptic spike. The synaptic weight is decreased if the pre-synaptic spike occurs after the post-synaptic spike.

Tinnitus correlates in computational model

We run simulations to assess measures of our tinnitus correlates in the model after initial training, after the model responds to damage at the auditory periphery, as well as after either the application of a simulated hearing aid or an acoustic therapy for tinnitus.

To characterize changes in tuning and tonotopic organization in the model, we assess frequency receptive fields of the cortical excitatory units. To produce these we generate peripheral model responses to 50-ms tones with frequencies spanning 100 Hz to 6 kHz and sound levels from 0 to 90 dB SPL. As in empirical work, the tone level and frequency are selected pseudo-randomly with 2 repetitions for each level and frequency combination. The restricted frequency range is selected for computational efficiency and because it is sufficient for our purposes (hearing loss begins at 2.3 kHz); this frequency range is also sufficient to capture receptive-field changes at sound levels of interest. We then look at the excitatory receptive field for a neuron within the hearing loss region (5.2-kHz CF), and for a neuron near the edge of hearing loss (2.7-kHz CF), before and after hearing loss. We also look at the receptive fields of these units after the simulation of an acoustic therapy and after prolonged use of a hearing aid.

In addition to changes in tuning, elevated spontaneous firing and synchrony are implicated in tinnitus (Eggermont and Roberts, 2004); we therefore also look at how these aspects of activity are affected in our cortical model. As in our previous work (Chapter 2), we measure spontaneous synchrony by looking at peak cross-correlation values between neurons throughout the network in response to spontaneous input activity

(20 spikes/s). The peak cross-correlation value between neural units i and j (with a separation of 25 units) is the maximum (over time lag *d*) of the cross-correlation coefficients for the spike trains of these two units, where the cross-correlation coefficients are defined as (see Seki and Eggermont, 2003):

$$p_{i,j}(d) = \frac{(\sum_t x_i(t)x_j(t-d) - N_i N_j/N)}{(N_i \cdot N_j)^{0.5}}, \quad (3)$$

where *x* represents the spike train for the neural unit, *d* is the time lag (-50 ms to 50 ms), N_i and N_j are the total number of spikes for units *i* and *j*, respectively, and *N* is the number of bins (we use 2-ms bins). During simulations of spontaneous activity, we also look at levels of spontaneous firing, since this is a potential correlate of tinnitus that has been investigated at various levels of the auditory pathway, including at the level of the cortex (Eggermont and Roberts, 2004).

In addition to changes in tuning and spontaneous firing, changes in oscillatory activity in the delta and gamma range have been strongly implicated in tinnitus in humans (Weisz et al, 2007). Therefore, lastly, we look at changes in delta- and gamma-band activity in our model. We define delta-band oscillations as those falling between 1 and 4 Hz (inclusive), and gamma-band oscillations as those between 30 and 50 Hz (inclusive), consistent with previous studies (Weisz et al., 2007; Kahlbrock and Weisz, 2008). To look at the potential relationship between hearing loss, plasticity and changes in oscillatory activity, we determine the mean amplitude of these oscillatory bands in the spontaneous activity of neural units within the hearing loss region. Namely, we summate postsynaptic potentials of neural units across the hearing loss region and calculate the

discrete Fourier transform of this summed activity using a fast Fourier transform algorithm available in MATLAB. We then calculate mean amplitude of frequency components between 1 and 4 Hz (delta-band), and between 30 and 50 Hz (gamma-band).

All measures of tinnitus correlates based on spontaneous activity are averaged across 30 repetitions, each starting from a different initial random seed

Results

Overview

The current version of our model built on our previous work (Chapters 2 and 3) by incorporating three novel features: more realistic inputs (derived from a model of the auditory periphery), gap junctions between inhibitory units, and spike-timing-dependent plasticity (STDP). It was important to evaluate the impact of each of these additions on our model's ability to account for the main correlates of tinnitus. Therefore, we first ran simulations to compare several measures of tinnitus in a model with HSP alone (hereafter referred to as the HSP model) to one with both HSP and STDP (hereafter referred to as the HSP+STDP model). In these initial simulations, we applied a steep simulated hearing loss (a steep hearing loss curve with a maximum threshold shift of 20 dB, 35 dB and 60 dB, to simulate mild, moderate and severe hearing loss, respectively). The validity of using cortical inputs derived from simulated auditory nerve (AN) responses was also tested by comparing our overall results to those found empirically and to our previous observations (Chapter 2). The results discussed below indicate that the HSP+STDP model produces behaviour that is in agreement with empirical observations, and can

explain additional data (i.e. receptive field shifts and tonotopic map reorganization) not accounted for by the HSP model.

To further validate the HSP+STDP model, we simulated different levels of hearing loss (steep hearing loss curves with 35-dB and 20-dB maximum threshold shifts), and assessed whether tonotopic reorganization depended on the level of peripheral damage, as has been observed empirically. We also quantified changes in spontaneous activity under these hearing loss scenarios in order to shed light on how tinnitus correlates linked to aberrant spontaneous activity were affected by different levels of hearing loss. These simulations were in agreement with empirical observations and indicated that major cortical correlates of tinnitus can arise after mild hearing loss in the absence of tonotopic reorganization.

Having validated a theoretical framework of major tinnitus correlates via the HSP+STDP model, we simulated potential treatment strategies for tinnitus: the use of a hearing aid and acoustic therapy. We simulated the NAL-R linear gain prescription (Dillon, 2001) for the most severe hearing loss described here: a steep hearing loss curve with a maximum threshold shift of 60 dB SPL. We also simulated an acoustic therapy consisting of a tone ensemble. In both cases we evaluated all tinnitus correlates that are captured by the HSP+STDP model in light of these potential treatment strategies. The HSP+STDP model predicted that, depending on when they are administered and how they are designed, both treatment strategies may reduce correlates of tinnitus to varying degrees.

We focused on the main potential correlates of tinnitus: (increased) spontaneous synchrony, (increased) spontaneous firing, and (increased) delta- and gamma-band amplitudes. We also simulated tonotopic reorganization that can arise after hearing loss and that has been linked to tinnitus; because of the debate as to whether tonotopic reorganization is necessary for tinnitus perception (Langers et al., 2012), we simulated different hearing loss profiles to determine if the other tinnitus correlates arose even when reorganization did not occur. At the end of the results section, we summarize simulation results for spontaneous firing rates and oscillatory activity amplitude, for ease of comparison.

Simulation of the HSP model

Simulations of our previous models indicated that homeostatic plasticity was sufficient to elevate spontaneous synchrony and firing rates after hearing loss. While the way in which we modeled hearing loss here differs from that of our previous simulations (namely, we included more realistic inputs to our cortical model that were derived from simulated AN responses), HSP was still sufficient to elevate peak cross-correlation values (Figure 4) after simulation of a steep hearing loss curve of varying severity, with maximum threshold shifts of 20 (mild hearing loss), 35 (moderate hearing loss) and 60 (severe hearing loss) dB SPL. If elevated cortical synchrony underlies tinnitus perception, this result suggested that the tinnitus pitch should fall within or span the hearing loss region, rather than being represented by the edge of hearing loss. This finding was in agreement with empirical observations (Roberts et al., 2006; Yang et al., 2011).

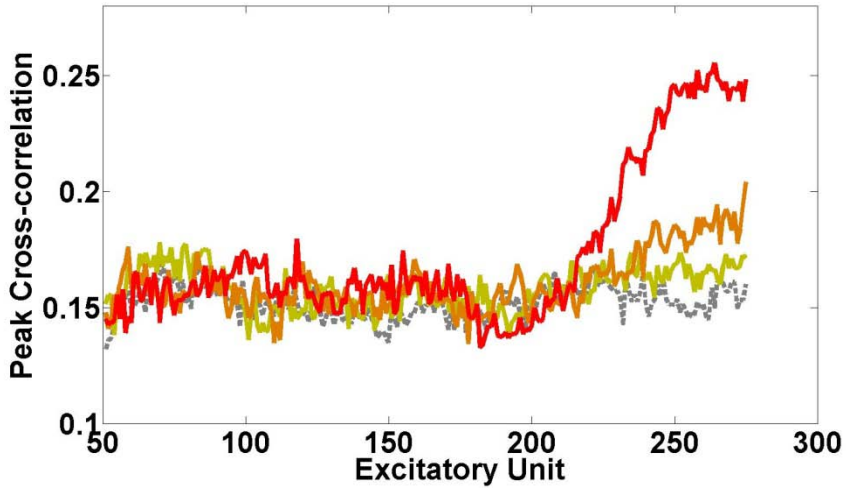

Figure 4.4: Peak cross-correlation values in HSP model. Normal peak cross-correlation values are indicated by the dashed grey line, while the yellow, orange and red lines indicate peak cross-correlation values after mild (20-dB), moderate (35-dB) and severe (60-dB) hearing loss. When HSP responds hearing loss, spontaneous synchrony in the model increases in the hearing loss region. Peak cross-correlation values were calculated for cortical neural units separated by 25 units of space (neighbouring units have a distance of 1 unit) in the network. Hearing loss started at unit 200 and reached maximum threshold shift at unit 225.

Similar to our previous HSP model (Chapter 2), this HSP model exhibited increases in spontaneous activity that were proportional to the level of hearing loss: spontaneous firing rates increased from 10.7 spikes/s at baseline to 13.0 spikes/s after

mild hearing loss, 17.6 spikes/s after moderate hearing loss and 32.3 spikes/s after severe hearing loss. The mean amplitude of delta- and gamma-band activity in the hearing loss region also increased monotonically with the severity of simulated hearing loss. Mean delta-band amplitudes rose from 1.0 to 1.03 after mild hearing loss, to 1.11 after moderate hearing loss, and to 1.44 after severe hearing loss. Mean gamma-band amplitudes rose from 0.29 to 0.43, 0.54, and 1.32, for mild, moderate and severe hearing loss, respectively. The substantial increases in oscillatory amplitudes after simulation of severe hearing loss were likely due to significant reductions in the strength of inhibitory connections via HSP and the resulting extreme hyperactivity in the network, as we observed in our previous model after simulation of severe hearing loss (Chapter 2). Thus, with the exception of the marginal increase in delta-band activity after simulated mild hearing loss, the HSP model captured the increases in oscillatory bands that have been linked to the presence of the tinnitus percept (Weisz et al., 2007).

The model with HSP alone exhibited changes in thresholds, spontaneous firing and synchrony consistent with our previous model (Chapter 2), but no tonotopic reorganization (Figure 5). Furthermore, we observed increased levels of driven activity in the frequency receptive field after hearing loss as a result of homeostatic up-regulation of excitatory inputs and down-regulation of inhibitory inputs to cortical neural units. The overall increase in weight distribution functions for excitatory units after hearing loss (Figure 5C) further illustrated why there was hyperexcitability but no receptive field shift and hence no cortical reorganization. Thus, for the HSP model, the only major changes in the receptive field after a severe (60-dB) peripheral threshold shift were a cortical

threshold shift (50 dB) at the characteristic frequency and a hyperactive response to sound levels above the new threshold.

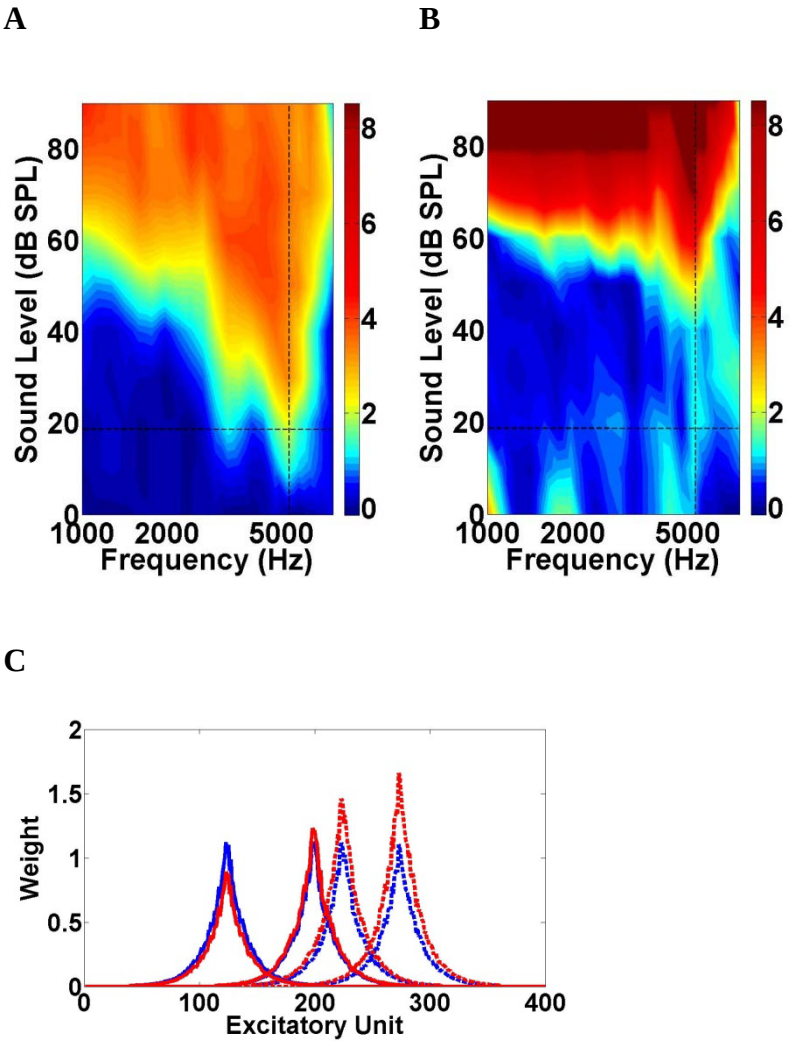

Figure 4.5: Frequency receptive fields after severe (60 dB) hearing loss with homeostatic plasticity but no Hebbian plasticity. A, Receptive field for normal hearing (model trained with only HSP). B, Receptive field after hearing loss. Note that while the threshold was elevated, the characteristic frequency did not change. Also, the receptive field indicated hyperexcitability. C, Weight functions for lateral excitatory (i.e. cortical) inputs to neural

units at locations 125 (no hearing loss), 200 (beginning of steep loss), 225 (at the edge of deepest hearing loss) and 275 (at deepest hearing loss region). Blue lines show weight functions before hearing loss, in a network trained with HSP only; red lines represent the same weight functions after severe hearing loss and HSP-mediated recovery. As the level of deafferentation increased (towards the hearing loss region), homeostatic scaling of excitatory inputs became more pronounced. Intersecting dashed lines in frequency receptive fields indicate the characteristic frequency and the sound level at which it was determined in the normal network. Dashed lines in weight functions indicate that the respective units were within the hearing loss region.

Thus, the results of simulations with the HSP model suggested that a shift in the balance between excitation and inhibition, even without tonotopic reorganization, may be sufficient to induce other tinnitus correlates. These results were very pertinent to our understanding of tinnitus as some empirical work indicates that the tinnitus pitch is not necessarily represented by frequencies that are overrepresented within a reorganized region of the primary auditory cortex (Yang et al., 2011), but rather, by frequencies that previously spanned the hearing loss region (Roberts et al., 2006; Yang et al., 2011). Furthermore, tonotopic reorganization may not even be necessary for tinnitus perception (Langers et al., 2012). Our simulations of the HSP model suggested that homeostatic plasticity may be a sufficient plasticity mechanism for generating cortical correlates of tinnitus, while STDP may capture additional phenomena (i.e. receptive field expansion and tonotopic reorganization) that may occur after hearing loss but may not underlie tinnitus.

Simulation of the HSP+STDP model

Motivated by the inability of the HSP model to capture cortical reorganization that is evident after moderate peripheral damage (Robertson and Irvine, 1989), we included spike-timing-dependent plasticity (STDP) that may underlie tonotopic reorganization (Dahmen et al., 2008), and may also be important in the cortical response to tinnitus therapies. The HSP+STDP model predicted that STDP can drive cortical reorganization after severe hearing loss (steep hearing loss curve with a maximum threshold shift of 60 dB SPL). However, before we outline changes in receptive fields in the HSP+STDP model, we look at how adding STDP affected changes in spontaneous activity after severe hearing loss.

Consistent with the HSP model and empirical observations, the HSP+STDP model exhibited several correlates of tinnitus after severe hearing loss. Peak cross-correlation values (Figure 6) and spontaneous firing (15.2 spikes/s in the hearing loss region versus 10.2 spikes/s in the normal network) were both elevated in the hearing loss region, as in our previous model (Chapter 2); the drop in peak cross-correlation values near the edge of hearing loss may be explained by lower rescaling of input weights in this partially deafferented region. Furthermore, as in the HSP model, and in agreement with empirical observations (Weisz et al., 2005; Weisz et al., 2007), our HSP+STDP model exhibited elevated amplitudes in the delta and gamma bands for neural units within the hearing loss region: mean delta-band amplitude in the hearing loss region increased from 1.43 to 1.63 while mean gamma-band amplitude increased from 0.67 to 0.93. Including

STDP increased baseline values for both delta-band and gamma-band amplitude relative to the HSP model, which may be the case because connections between distant neural units are stronger in the HSP+STDP model (Figure 7C) than in the HSP model (Figure 5C).

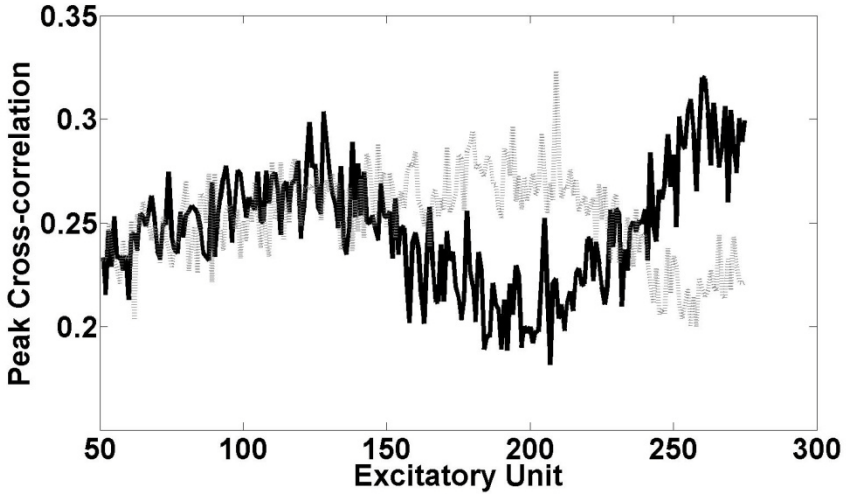

Figure 4.6: Peak cross-correlation values for normal hearing and severe hearing loss. The synchrony measure appeared to be elevated deeper in the hearing loss region; similar to simulations where only HSP is present after severe hearing loss, there was a drop in synchrony near the hearing loss edge. Peak cross-correlation values were calculated for cortical neural units separated by 25 units of space (neighbouring units have a distance of 1 unit) in the network. Hearing loss started at unit 200 and reached maximum threshold shift at unit 225. The dashed grey line indicates peak cross correlation values for normal hearing while the solid black line represents peak cross-correlation values after severe hearing loss.

Whereas both the HSP and the HSP+STDP models exhibited changes in spontaneous activity levels, synchrony, delta- and gamma-band amplitudes, only the HSP+STDP model exhibited cortical reorganization and only after sufficient peripheral damage. This was clearly observed when comparing frequency receptive fields for corresponding neural units before (Figure 7) and after (Figure 8) severe (60-dB) hearing loss. The weight functions after severe hearing loss indicated that there was a large-scale shift in cortical (lateral) excitatory inputs to units near the edge of hearing loss and within the hearing loss region. Specifically, the STDP mechanism weakened synapses on inputs that were driven by frequencies higher than the neural unit's original CF, and it strengthened those driven by lower frequencies. This large shift meant that lower frequency sounds could drive the reorganized neural unit at lower sound levels, while sounds at the former CFs required higher sound levels to drive the neural unit. The result was tonotopic reorganization: a shift in the characteristic frequency of cortical neural units. STDP in our model shifted the CF of a neural unit within the hearing loss region (Figure 7B and 7B) from 5.2 kHz to 1.6 kHz; the threshold for responding to the new CF dropped from 50 dB to 30 dB, while the threshold for responding to sounds at the former CF rose from 10 dB to 60 dB SPL. This large shift was significantly greater than the shift observed in a unit closer to the edge of hearing loss. The input weight functions for a unit deep in the hearing loss region and one for a unit that was near the hearing loss edge (Figure 8C) indicated very similar shifts towards lower frequency inputs. The more drastic change in the receptive field of the unit deeper in the hearing loss region could be explained by the much larger peripheral threshold shifts for most inputs to this unit.

Regardless, the HSP+STDP model suggested that STDP could account for overrepresentation of lower frequencies throughout the hearing loss region after severe hearing loss. Thus, the HSP+STDP model characterized a potential mechanism through which cortical reorganization could develop after damage to the auditory periphery.

A **B**

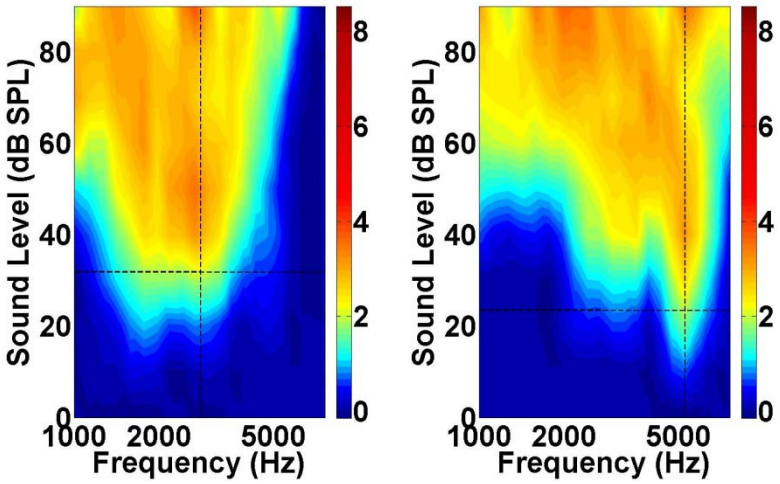

C

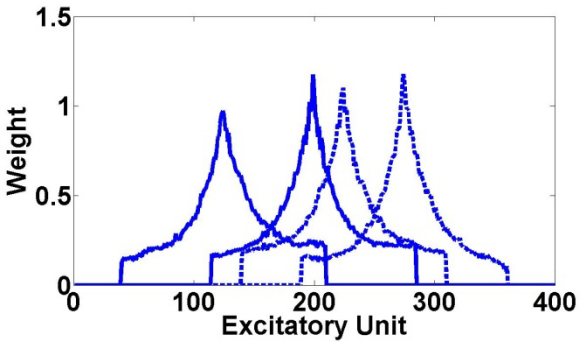

Figure 4.7: Normal frequency receptive fields. A, Receptive field for unit close to edge of hearing loss (CF approximately 2.7 kHz). B, Receptive field for unit deeper in hearing loss region (5.2 kHz). While there is some variance, weight functions were fairly similar across the tonotopy. Intersecting dashed lines in frequency receptive fields indicate the characteristic frequency and the sound level at which it was determined in the normal network. Dashed lines in weight functions indicate that the respective units would be within the hearing loss region after simulated peripheral threshold shifts.

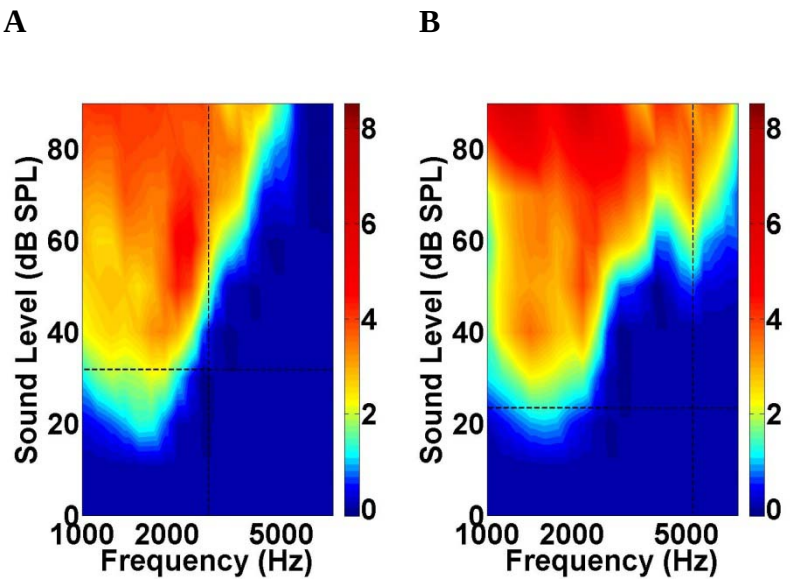

C

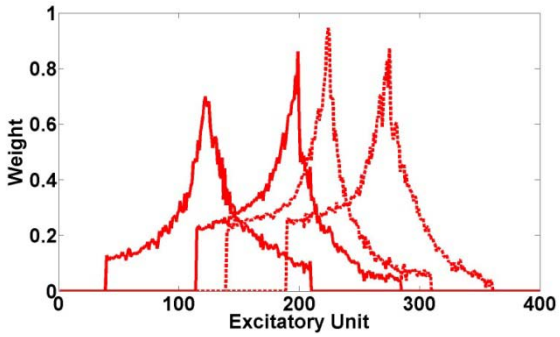

Figure 4.8: Frequency receptive fields after severe (60-dB) hearing loss. A, A receptive field with a CF that shifted from 2.7 kHz to 1.7 kHz. B, A receptive field with a new CF at 1.6 kHz (formerly at 5.2 kHz). Note that the receptive fields were not residuals of the normal receptive fields. C, For neural units near or within the hearing loss region, input weight distributions shifted to lower frequencies (those below the hearing loss edge), while the input weight function in the normal hearing region (centered at the excitatory unit at position 125 or 1 kHz) was unaffected. Note that even the neural unit at position 200, which is the start of the hearing loss region, had a shift in weight distribution after severe hearing loss. Intersecting dashed lines in frequency receptive fields indicate the characteristic frequency and the sound level at which it was determined in the normal network.

The HSP+STDP model constituted a novel and comprehensive theoretical framework of the major cortical correlates of tinnitus. The same model that captured cortical reorganization also accounted for tinnitus correlates exhibited by our previous

model: elevated spontaneous firing and synchrony, along with increased delta- and gamma-band activity.

Simulating milder hearing loss in the HSP+STDP model

Audiograms vary from person to person, and different levels of peripheral damage have distinct effects on tonotopic organization in the auditory cortex (Rajan, 1998; Eggermont and Komiya, 2000; Seki and Eggermont, 2002). Furthermore, tinnitus may be experienced by those with mild hearing loss or near-normal hearing without evidence of tonotopic reorganization (Langers et al., 2012). Therefore, we assessed tinnitus correlates in the HSP+STDP model after moderate (35-dB) and mild (20-dB) hearing loss with steep hearing loss edges, as well as after severe hearing loss that slopes gradually (starting at 20 dB to a maximum of 60 dB). We wanted to determine how these other hearing loss profiles would influence cortical reorganization in our model, and additionally, whether other tinnitus correlates would develop even if there was no tonotopic reorganization.

Peak cross-correlation values were elevated in the hearing loss region for all simulated hearing loss profiles (Figure 9). Our simulations indicated that even small-scale homeostatic responses and shifts in cortical weight distribution would increase spontaneous synchrony. If increased spontaneous synchrony is a necessary and sufficient condition for tinnitus, then the HSP+STDP model suggests that a person who does not appear to have hearing loss (up to the 8-kHz range tested by audiologists) may still

develop tinnitus if there is mild hearing loss at higher frequencies; this observation is in agreement with observations of tinnitus in those with hearing loss limited to frequencies above 8 kHz (e.g. Langers et al., 2012).

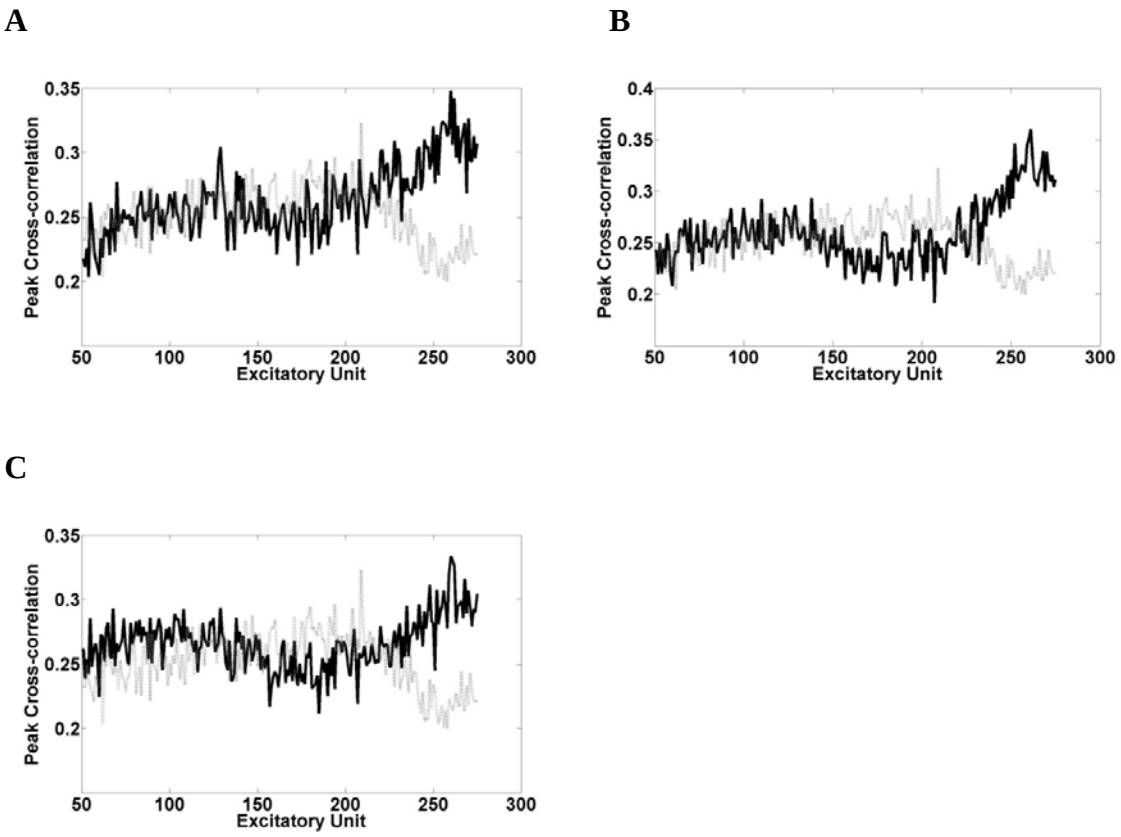

Figure 4.9: Peak cross-correlation values for mild (A), moderate (B) and sloping (C) hearing loss. Spontaneous synchrony increased for each hearing loss case, with the greatest increase occurring after hearing loss (mild or moderate) with a steep hearing loss edge. Dashed gray line indicates baseline levels for peak cross-correlation values.

Other tinnitus correlates in spontaneous activity also increased after simulation of these three hearing loss profiles. The HSP+STDP model exhibited slightly elevated spontaneous firing rates for mild to moderate hearing loss and a larger increase in spontaneous firing for sloping severe hearing loss; relative to a baseline of 10.2 spikes/s spontaneous activity increased to 11.7 spikes/s after mild loss, 11.3 spikes/s after moderate loss, and a substantially elevated rate of 16.9 spikes/s after a sloping severe hearing loss. Oscillatory activity amplitudes also increased for each type of hearing loss simulated, but in agreement with empirical observations (Weisz et al., 2005) and unlike results from the HSP model, these increases were not necessarily proportional to the threshold shift. Namely, average gamma-band amplitudes changed non-monotonically with increasing hearing loss: rising from 0.67 (normal network) to 0.88 after a mild hearing loss, 0.76 after a moderate hearing loss and 1.29 after sloping severe hearing loss. Delta-band amplitude also rose for each hearing loss condition we simulated: relative to baseline (1.43), delta-band activity increased to 1.54 after mild hearing loss, to 1.85 after moderate hearing loss, and to 1.90 after sloping severe hearing loss. If tinnitus occurs with only mild hearing loss, our model would suggest that increased gamma-band activity plays a more important role in the tinnitus percept than delta-band activity, since delta-band activity only increased slightly after simulating mild hearing loss. However, the slight increase in delta-band amplitudes after simulation of mild hearing loss was still more pronounced than the marginal increase exhibited by the HSP model, suggesting that plasticity mechanisms additional to HSP may have a role to play in tinnitus arising after mild hearing loss. The above results demonstrated the development of major tinnitus

correlates after simulation of different hearing loss profiles and permitted the use of the HSP+STDP model to determine how changes in cortical tonotopy relate to the development of generally agreed upon tinnitus correlates.

In the HSP+STDP model, simulations of moderate (35-dB) hearing loss with a steep audiometric edge still produced tonotopic reorganization (Figure 10A and 10B). However, for a unit deeper in the hearing loss region, a residual of the original receptive field remained (Figure 10B), which was not the case after severe (60-dB) hearing loss (Figure 8B). In our model, mild (20-dB) hearing loss did not lead to cortical reorganization; this was in agreement with empirical observations, where threshold shifts of 20 dB or less did not lead to shifts in receptive fields (Rajan 1998, 2001). Thus, the development of tinnitus correlates in spontaneous cortical activity in our model did not necessarily go hand in hand with cortical reorganization.

A **B**

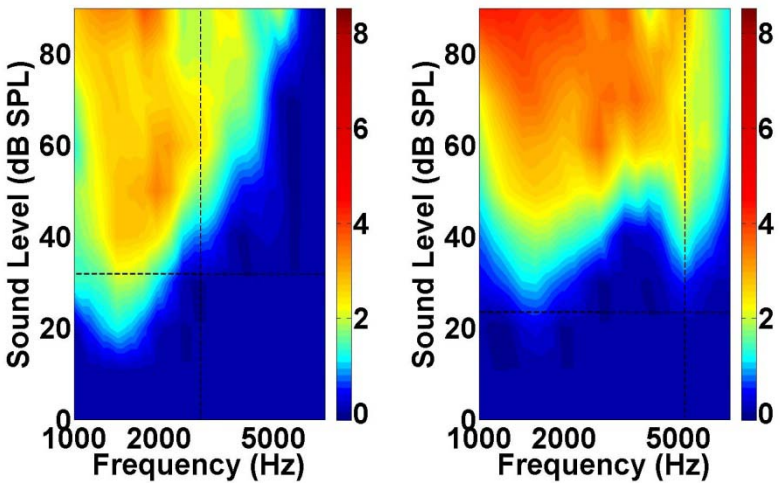

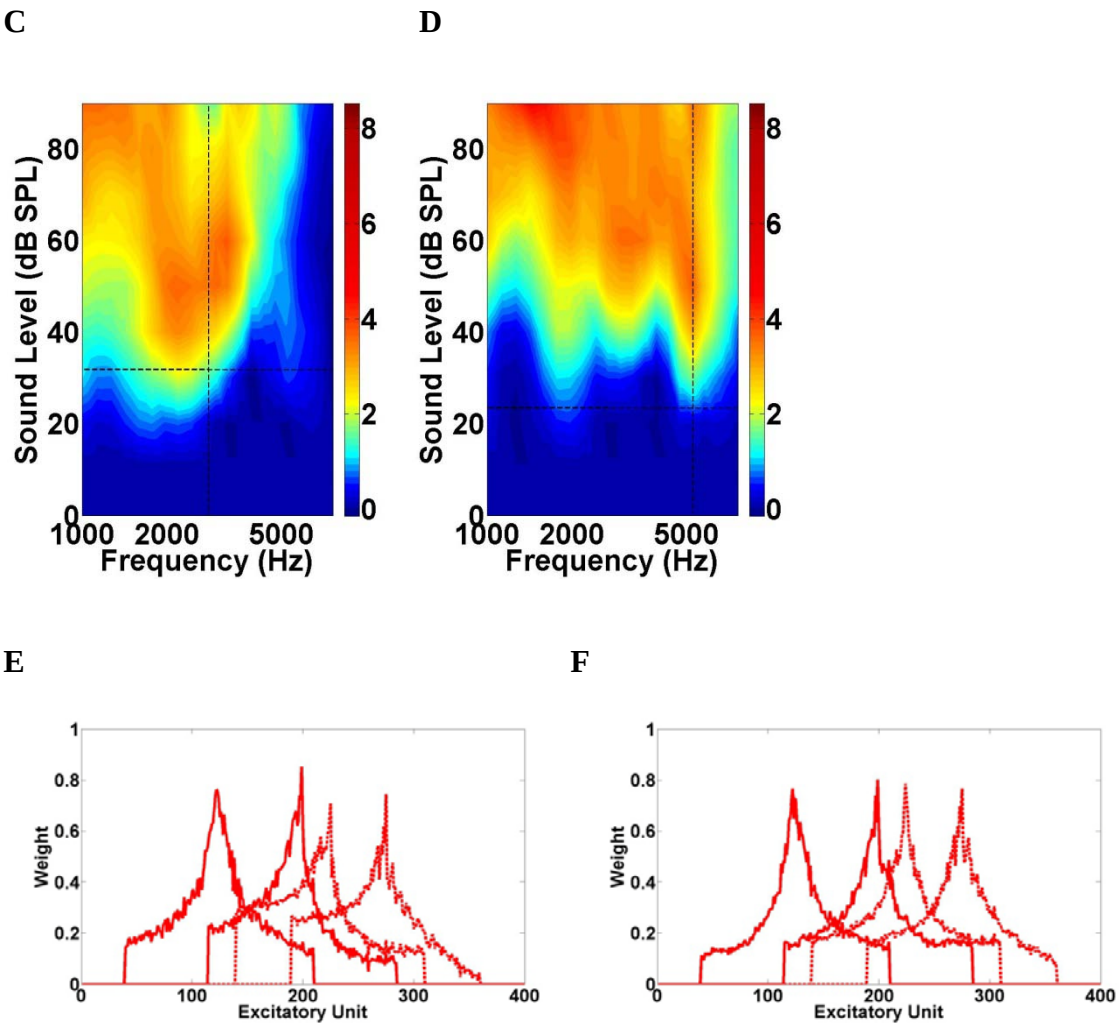

Figure 4.10: Frequency receptive fields after moderate (35-dB) and mild (20-dB) hearing loss. A, For the unit with a normal CF of 2.7 kHz, the CF shifted to 1.4 kHz after moderate hearing loss. B, The CF for one unit shifted to 1.6 kHz from 5.2 kHz after moderate hearing loss. C and D, Frequency receptive fields were affected by mild hearing loss, but reorganization did not occur. E, Weight distribution changes for lateral connections indicated a significant change after moderate hearing loss. F, Mild hearing loss did not greatly alter weight distributions in the hearing loss region.

A hearing loss profile with gradually increasing threshold shifts is representative of audiograms observed in many people with hearing loss. Therefore, we wanted to determine if this form of hearing loss would also lead to tonotopic reorganization. Our simulations indicated that a steep hearing loss profile was not necessary for cortical reorganization, as input weight distributions were biased towards lower frequencies (Figure 11C) after we simulated a sloping hearing loss. Reorganized receptive fields had higher thresholds than when we simulated severe and moderate hearing loss with a steep audiometric edge (Figure 8 and 10), but this was to be expected given that the audiogram for the sloping hearing loss also had 20-dB peripheral threshold shifts at lower frequencies (Figure 11D). Importantly, the threshold shifts at lower frequencies did not prevent receptive fields from shifting to regions with less peripheral damage; the magnitude of the CF shifts was similar to that seen in our simulations after steep hearing loss curves.

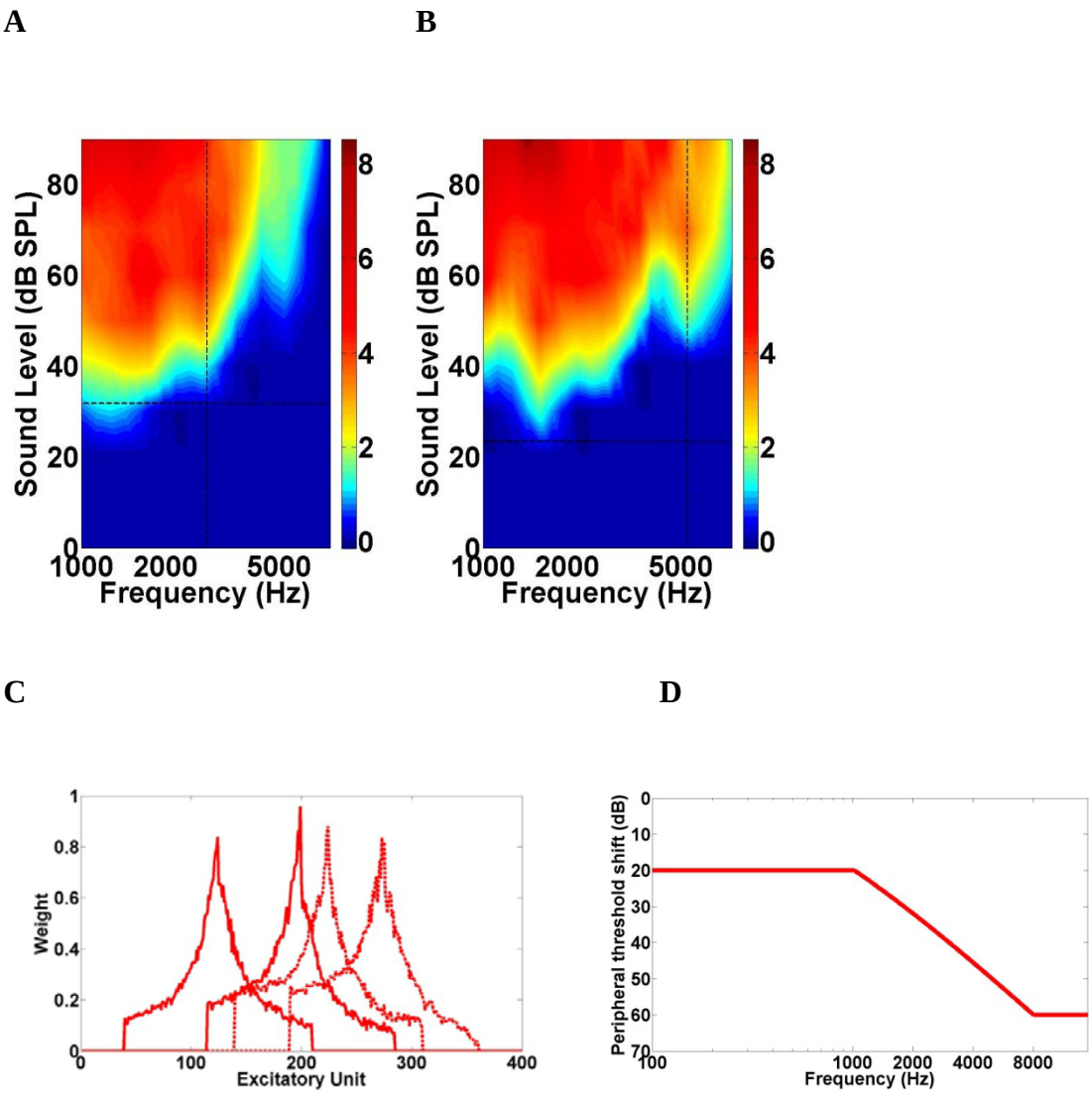

Figure 4.11: Frequency receptive fields after sloping hearing loss. A, The CF shifted from 2.7 kHz to 1.8 kHz for a unit close to the beginning of the sloping hearing loss region. B, The CF of a unit deeper in the hearing loss region also shifted from 5.2 kHz to 1.8 kHz. Thresholds after reorganization were higher than for other forms of hearing loss since this hearing loss case had a minimal 20-dB threshold shift across the tonotopy, with the sloping portion of the audiogram beginning at 2.3 kHz. C, Weight distribution

functions support a redistribution of input strength towards lower frequencies. D, Threshold shifts for sloping hearing loss.

The HSP+STDP model supported empirical observations that reorganization may depend on the level of damage at the auditory periphery; this observation provided further validation for this instance of the model. With respect to tinnitus, this model made an important prediction about tonotopic reorganization, a recently questioned tinnitus correlate. Namely, while cortical reorganization could occur after simulating moderate to severe hearing loss, major tinnitus correlates arose in simulations irrespective of the presence of cortical reorganization. Therefore, the HSP+STDP model provided novel insights into the conditions that may be necessary for the development of tinnitus after hearing loss and shed light on which changes in the auditory cortex may not be necessary for tinnitus to arise.

Simulating tinnitus treatments with the HSP+STDP model: hearing aids

Having validated the HSP+STDP model against empirically observed correlates of hearing loss and tinnitus, we next used this model to make novel predictions with respect to how acoustic treatment strategies affect cortical correlates of tinnitus. Since little is known about the mechanisms through which acoustic therapies may alleviate or eliminate tinnitus, this model could provide important insights as to how HSP and STDP in the primary auditory cortex may interact with strategies for tinnitus reduction.

We began by simulating a NAL-R linear hearing aid amplification prescription (Dillon, 2001) for severe (60-dB) hearing loss with a steep hearing loss edge. We compared the result of immediate hearing aid use with that of late hearing aid use. Late hearing aid use was simulated by training the HSP+STDP model with NAL-R amplified sounds after the network was first altered by severe (60-dB) hearing loss with a steep audiometric curve. The results indicated that hearing aid use can reduce some tinnitus correlates, but that it is not a cure. Furthermore, early hearing aid use did not provide greater benefits than late hearing aid use. The fact that we used a simple linear gain scheme that only addresses threshold shifts at frequencies up to 6 kHz may limit the generalizability of these results.

The effects of applying a hearing aid amplification scheme on tinnitus correlates in spontaneous cortical activity were marginal in our model. While synchrony was still elevated after simulating early hearing aid use (Figure 12A), the elevation in peak cross-correlation values was not as pronounced as it was without hearing aid use (Figure 6). On the other hand, simulating late hearing aid intervention did not meaningfully reduce synchrony in the HSP+STDP model (Figure 12B). Spontaneous firing rates after simulations of early (15.7 spikes/s) and late (15.1 spikes/s) hearing aid use were relatively unchanged compared to no hearing aid use (15.2 spikes/s), and were substantially higher than the firing rate (10.2 spike/s) in a normal network. The effect on oscillatory activity was mixed: simulation of early hearing aid use led to an increase in mean delta-band amplitude (1.83) relative to values for severe hearing loss with no hearing aid use (1.63), while simulation of late hearing aid use resulted in a decrease in mean delta-band

amplitude (1.44). On the other hand, mean gamma-band amplitude increased relative to its levels without hearing aid use (0.93) for early hearing aid use (0.98) and even more for late hearing aid use (1.06). The increases in oscillatory activity may have resulted from a plasticity-mediated response to a gain amplification scheme that only affected part of the tonotopy. Namely, threshold shifts at frequencies above 6 kHz were not addressed, potentially resulting in more variable and complex changes in oscillatory activity; this issue may be partly addressed by a sound therapy that accounts for the entire hearing loss region (discussed in the next section). Thus, in agreement with empirical observations (Moffat et al., 2009), our model suggested that a hearing aid prescription that cannot fully address the hearing loss region (but is characteristic of currently prescribed hearing aids) may not be an effective strategy for tinnitus reduction.

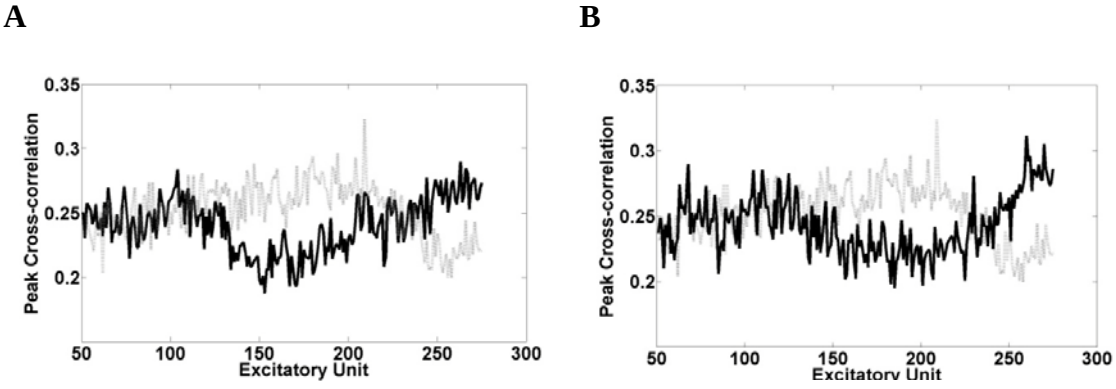

Figure 4.12: Peak cross-correlation values after early and late hearing aid interventions for severe hearing loss. A, Peak cross-correlation values after early hearing aid use. B, Peak cross-correlation values after late hearing aid use.

A novel prediction of the HSP+STDP model was that even a simple linear hearing aid could reduce cortical reorganization. With no hearing aid use (Figure 8) receptive fields shifted to a greater degree than with early (Figure 13A and 13B) or late (Figure 13C and 13D) hearing aid use. While the CF of a unit deep in the hearing loss region shifted from 5.2 kHz to 1.6 kHz without a hearing aid, the shift could be reduced by almost an octave with early hearing aid use (Figure 13B), and to a lesser extent if the hearing aid was simulated after changes to the network had occurred (Figure 13D). In addition to a reduction in the CF shift, it was also clear that inputs from higher frequency regions were more effective at driving activity with hearing aid use (i.e. there is increased excitability in the high-frequency region of the receptive field). If tonotopic reorganization underlies tinnitus (Mühlnickel et al., 1998), our model would suggested that early hearing aid use will be more effective at preventing cortical changes that contribute to tinnitus generation. However, if tinnitus exists without tonotopic reorganization (Langers et al., 2012) our model predicted that the main benefit of a hearing aid with a linear gain prescription would be the reduction of aberrant spontaneous synchrony.

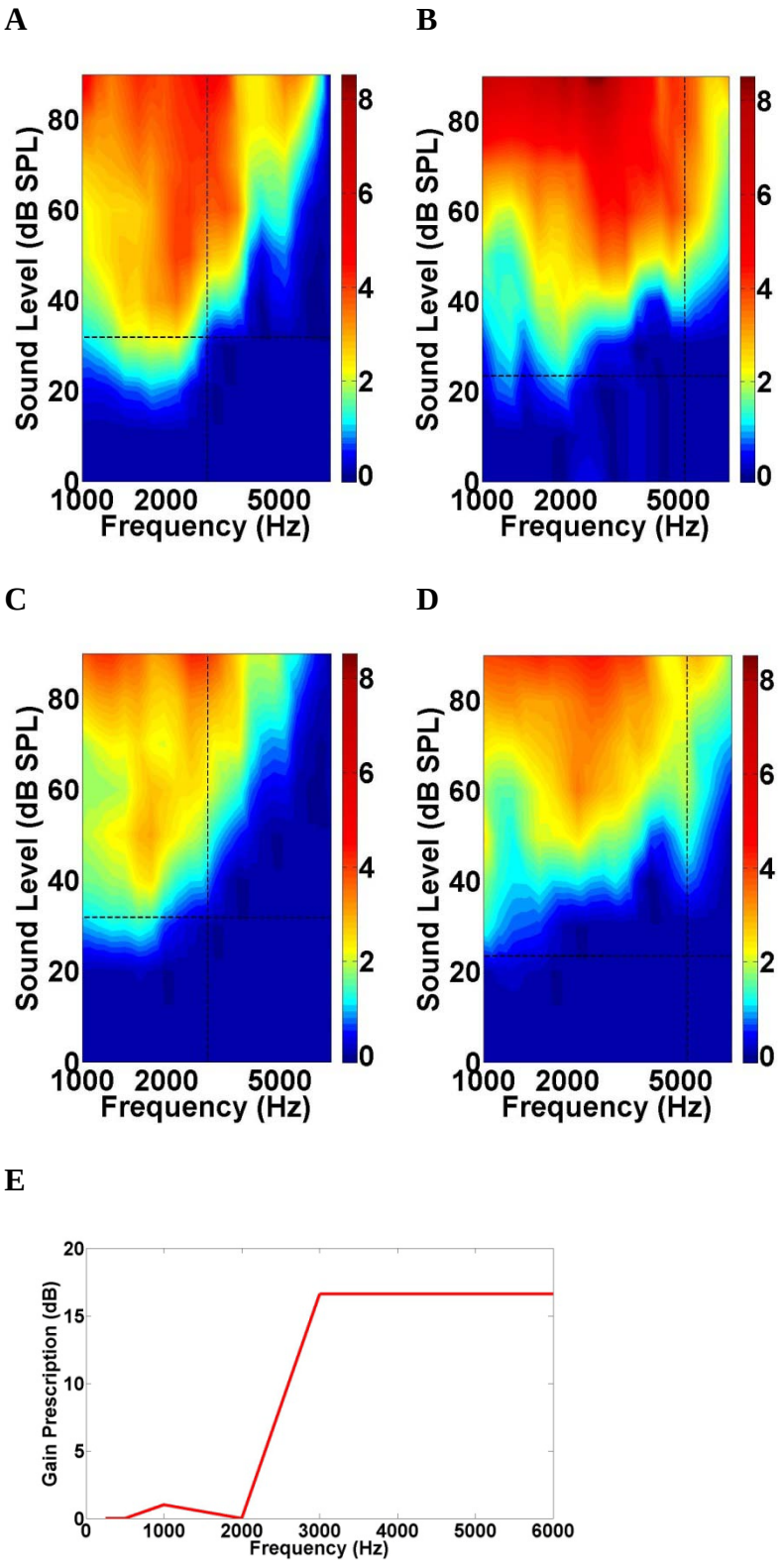
A
B
C
D
E
Sound Level (dB SPL)
Frequency (Hz)
1000
2000
5000
0
20
40
60
80
0
2
4
6
8
Gain Prescription (dB)
0
5
10
15
20
1000
2000
3000
4000
5000
6000

Figure 4.13: Frequency receptive fields after severe (60-dB) hearing loss and hearing aid use. A, With early hearing aid use, the model exhibited a slight shift of the receptive field of a unit close to the hearing loss region; the CF shifts from 2.7 kHz to 2.2 kHz. B, A unit deeper in the hearing loss region had an elevated threshold and a CF shift to 2.9 kHz, which was less than that observed without hearing aid use. C, With late hearing aid use, the CF was still shifted from 2.7 kHz to 1.8 kHz. D, Even with late hearing aid use, the CF of this unit shifted to 2.2 kHz which is closer its original value (5.2 kHz). E, NAL-R gain prescription for the severe hearing loss.

The HSP+STDP model suggested that oscillatory activity mediated by the cortical circuit may increase with hearing aid use, and that other tinnitus correlates are only marginally affected. Furthermore, the model did not suggest additional benefits are possible through early hearing aid use; empirical studies on this subject have not been conducted. The exception is tonotopic reorganization, which was mitigated more effectively in our simulations of early hearing aid use. However, whether this would have an effect on tinnitus perception is unclear. While the role of hearing aids as a tinnitus therapy has been previously investigated (Moffat et al., 2009; Schaette et al., 2010), this was the first attempt to understand their interaction with cortical plasticity and to predict what this meant in terms of the intervention time point.

Simulating tinnitus treatments with the HSP+STDP model: acoustic stimulation

Given the limited benefit of hearing aid use predicted by our model for reducing cortical tinnitus correlates, we sought to investigate the interaction between acoustic

stimulation and cortical plasticity in the context of the HSP+STDP model. Namely, we simulated a sound therapy consisting of exposure to an acoustically enriched environment in which tones (50-ms duration) with frequencies that fall within the hearing loss region were amplified (90 dB SPL versus 65 dB SPL for tones that did not fall into the hearing loss region). We applied this treatment to a network trained with severe (60-dB) steep hearing loss. We observed that while this treatment did not have a large effect on cortical reorganization (Figure 14), it did reduce other correlates of tinnitus. Namely, in our simulations, synchrony (Figure 15), spontaneous firing (dropped from 15.2 spikes/s to 12.1 spikes/s), and average gamma-band amplitude (dropped from 0.93 to 0.83) were all affected by the simulated treatment in a way that should reduce the tinnitus percept. In fact, the effects of simulated sound therapy on these other correlates were more promising than the effects of simulated hearing aid use. While both hearing aids and the sound therapy we simulated increased the gain for frequency content in the hearing loss region, the sound therapy was not constrained to the 6-kHz frequency limit that was embedded in the hearing aid amplification scheme. Therefore, the HSP+STDP model predicted that sound therapies that take into account the full hearing loss profile may reduce tinnitus severity more effectively.

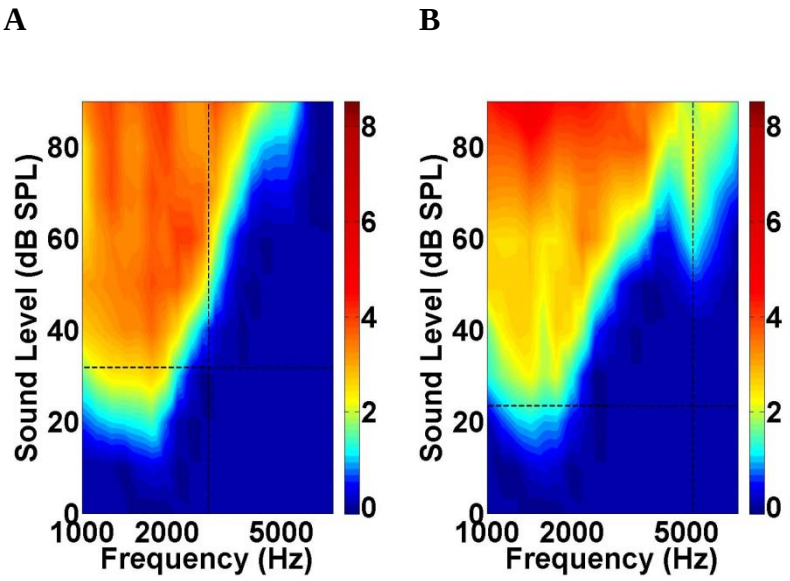

Figure 4.14: Frequency receptive fields after acoustic therapy of network trained on severe hearing loss. A, The CF of a unit near the edge of hearing loss was shifted negligibly from 1.7 kHz (see Figure 8A) to 1.8 kHz. B, The CF of a unit deep in the hearing loss region, did not change.

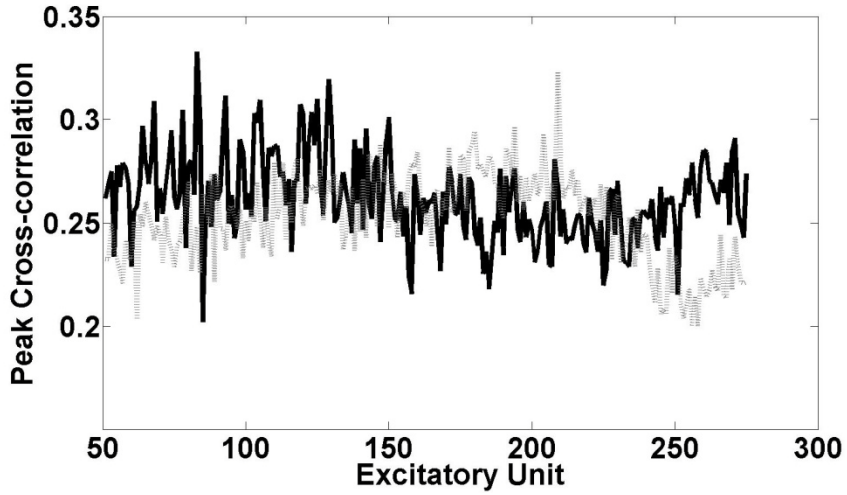

Figure 4.15. Peak cross-correlation after acoustic therapy of network trained on severe hearing loss. While elevated relative to baseline (gray line), the peak cross-correlation values appeared to be near normal levels.

Gap Junctions

As stated in the Methods section, the presence of gap junctions increased the amplitude of gamma-band oscillations in both models. Simulations of normal and hearing loss HSP+STDP models without gap-junction coupling indicated that these connections accounted for approximately half of the amplitude in the gamma-band; they did not have an effect on the amplitude of delta-band oscillations. This was likely due to the increased synchrony between electrically-coupled inhibitory neural units (Galarreta and Hestrin, 2001), which had higher spontaneous firing rates in our model. The amplitude of both oscillatory bands was linked to the spontaneous firing rates in the model: inhibitory neuron firing contributed mostly to gamma-band amplitude, while excitatory neuron firing contributed to the delta-band amplitude. Both firing rates were dependent on the target firing rates used to initiate the cortical model; however we did not analyze this in detail.

Summary of spontaneous firing and oscillatory results

The results from the simulations of the effect of hearing loss on changes in spontaneous firing and oscillatory activity described above are summarized in Figures 16 and 17, and Table 1. The figures capture the differences between the HSP and HSP+STDP models, as well as changes in the HSP+STDP model after various types of

hearing loss and treatment strategies. There was a clear increase in spontaneous firing (Figure 16) and both delta- and gamma-band activity (Figure 17) regardless of the severity of hearing loss. The HSP+STDP model predicted that these tinnitus correlates could be slightly mitigated by hearing aid use and more effectively mitigated through an appropriate acoustic therapy. Table 1 directs the reader to preceding figures that are related to the simulation category labels used in Figures 16 and 17.

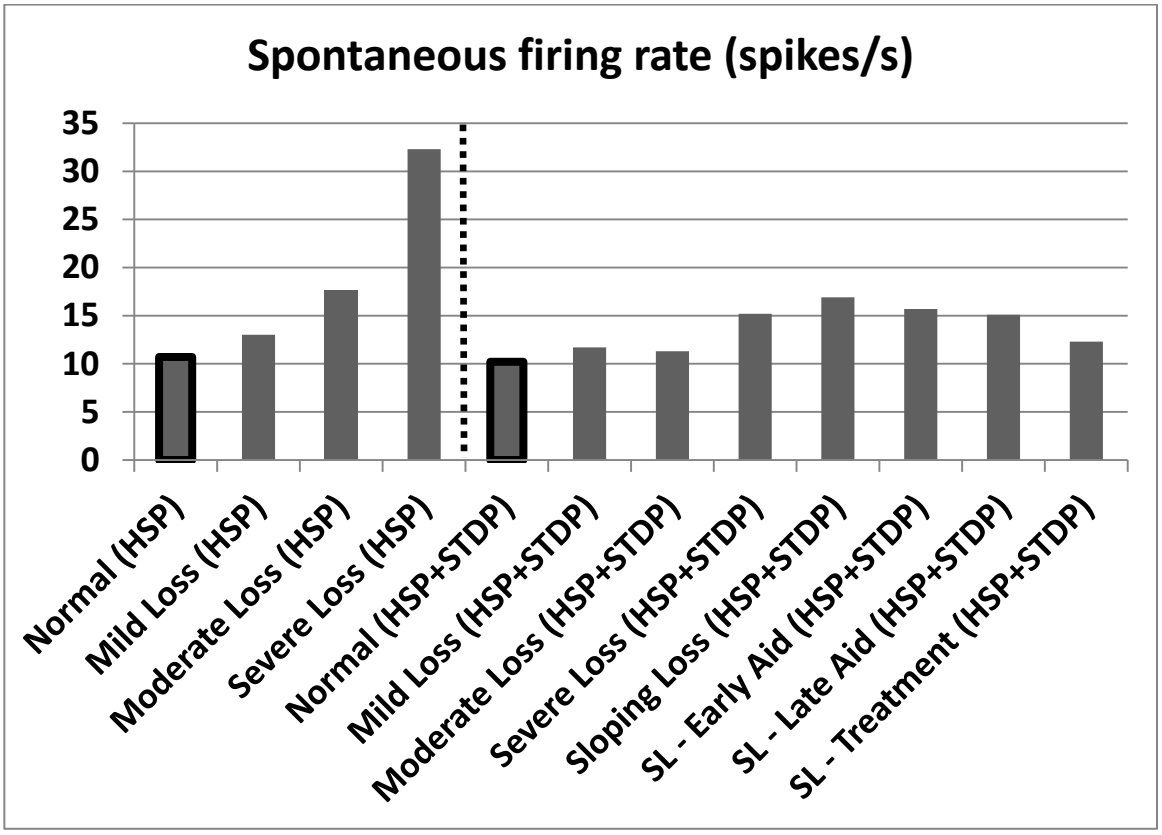

Figure 4.16: Summary of spontaneous firing rates for the scenarios discussed above. The normal spontaneous firing rate when both HSP and STDP were present is highlighted with a black outline for easier comparison. SL: severe loss. The dashed line separates values from simulations of the HSP model from values from the HSP+STDP model.

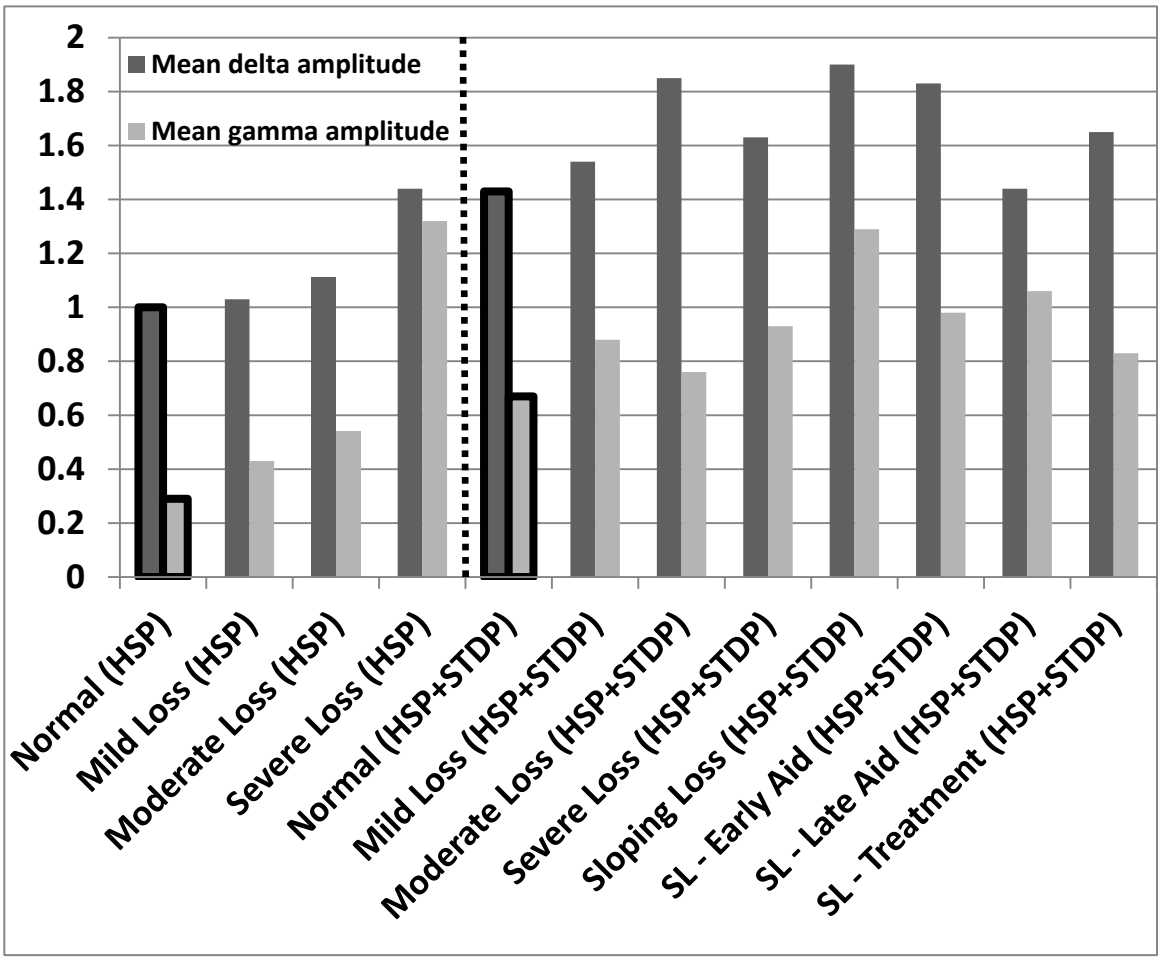

Figure 4.17: Summary of results for average delta-band and gamma-band oscillatory amplitudes. Normal values when both HSP and STDP were present are highlighted with a black outline for easier comparison. SL: severe loss. The dashed line separates values from simulations of the HSP model from values from the HSP+STDP model.

Simulation Category	Related Figures
Normal (HSP)	4, 5
Mild Loss (HSP)	4
Moderate Loss (HSP)	4
Severe Loss (HSP)	4, 5
Normal (HSP+STDP)	6, 7
Mild Loss (HSP+STDP)	9, 10
Moderate Loss (HSP+STDP)	9, 10
Severe Loss (HSP+STDP)	6, 7
Sloping Loss (HSP+STDP)	9, 11
SL - Early Aid (HSP+STDP)	12, 13
SL - Late Aid (HSP+STDP)	12, 13
SL - Treatment (HSP+STDP)	14, 15

Table 4.1: Related figures. This table directs the reader to figures pertaining to each class of simulations summarized in Figures 16 and 17.

Discussion

We have described how plasticity mechanisms can alter tuning and activity in the primary auditory cortex (AI) after different types of hearing loss; the focus was on changes that may be pertinent to tinnitus generation. Our HSP+STDP model (where both homeostatic and Hebbian-type plasticity are present), consistent with empirical data, indicates that with sufficient hearing loss (greater than 20-dB threshold shift), tonotopic reorganization can occur in AI. In addition, the model predicts that cortical reorganization can occur with a steep or gradual hearing loss edge. In this model, the addition of spike-timing-dependent plasticity (STDP) was necessary for reorganization to occur (Figure 8); this is a novel prediction that has not been previously investigated in the context of hearing loss or tinnitus. When homeostatic plasticity (HSP) was active but Hebbian plasticity was removed from our model (referred to as the HSP model), we did not

observe shifts in receptive fields (Figure 5). However, the HSP model did capture other changes in cortical activity correlated with tinnitus: increased spontaneous firing rates and synchrony, along with increases in the amplitudes of delta- and gamma-band oscillations. Including STDP did not affect simulated changes in spontaneous activity qualitatively, but did lead to quantitative differences. Furthermore, the HSP+STDP model suggests that while tonotopic reorganization requires moderate (35-dB) to severe (60-dB) hearing loss, generally agreed upon tinnitus correlates can develop even if hearing loss is mild (20 dB).

Adding a realistic model of the auditory periphery to our cortical model allowed us to compare changes in AI that may result from different hearing loss profiles. Furthermore, we were able to simulate hearing-aid use and an acoustic therapy to determine if these interventions could reduce correlates of tinnitus in our model. We simulated the use of the National Acoustics Lab (NAL) linear gain hearing aid prescription (NAL-R) at the initiation of hearing loss and after a period of hearing loss during which a hearing aid was not used. We found that with this type of hearing aid, the extent of cortical reorganization could be reduced, particularly if used immediately after hearing loss (Figure 13). Simulations of an acoustic treatment paradigm consisting of randomly generated tones, where tones that fall within the hearing loss region were louder, also altered tinnitus correlates in our model. While cortical reorganization was not undone, spontaneous firing, synchrony and gamma oscillation amplitude dropped closer to baseline than with the linear gain hearing aid scheme (Figure 15, 16 and 17). As both treatment strategies involve increasing gain within the hearing loss region, the model

prediction that sound therapy is more effective treatment likely stems from the fact that the hearing aid prescription did not address hearing loss above 6 kHz. If tinnitus is perceived irrespective of whether tonotopic reorganization has occurred (Langers et al., 2012), then sound therapies (and potentially hearing aids) that take into account the full hearing loss region may hold promise as a means to reduce tinnitus severity.

While tinnitus may be mediated by many brain regions, there is evidence that changes in the auditory cortex play an important role in generating this phantom sensation (for review see Eggermont and Roberts, 2004). Previous empirical work also indicates that hearing loss after acoustic trauma can lead to increased spontaneous firing rates (Kimura and Eggermont, 1999) and increased spontaneous synchrony (Seki and Eggermont, 2003; Noreña and Eggermont, 2003) in AI. As in our previous work (Chapter 2), we also looked at these potential tinnitus correlates in our extended model. In simulations of the HSP model we observed that as the peripheral threshold shift increased, so did post-plasticity spontaneous firing rates (SFR) (Figure 16). In the HSP+STDP model SFRs increased to similar levels for mild to moderate hearing loss, and substantially more after simulating severe hearing loss; these increases were all lower in magnitude than corresponding increases in the HSP model. Recordings from cat primary auditory cortex after noise trauma suggest that the elevation in spontaneous activity within hours of trauma (Noreña and Eggermont, 2003) is larger than the increase observed weeks or months after trauma (Komiya and Eggermont, 2000; Seki and Eggermont, 2003). If HSP and STDP are both active in adult AI after hearing loss, it is possible that spontaneous activity that is substantially elevated soon after hearing loss

(due to inhibitory unmasking or rapid HSP) will still be elevated but to a lesser degree once peak input weights drop as STDP mediates a shift in the overall weight distribution towards the normal hearing region (Figure 5C versus Figure 8C). Perhaps transient tinnitus develops when excessive noise exposure can temporarily elevate peripheral thresholds (Clark, 1991), reduce ascending input activity and subsequently lead to inhibitory unmasking and a rapid HSP response (Chapter 3), but whether a resulting tinnitus percept becomes permanent will depend on further HSP- and STDP-mediated changes in the auditory cortex.

We used peak cross-correlation as a measure of neural synchrony during spontaneous activity (see Seki and Eggermont, 2003; Noreña and Eggermont, 2003). The HSP+STDP model predicts that mild (20-dB) hearing loss is sufficient to elevate neural synchrony in AI (Figure 9A). Furthermore, the elevation in peak cross-correlation values was not necessarily proportional to the level of hearing loss: levels of neural synchrony for mild, moderate and sloping hearing loss were similar (Figure 9) and slightly higher than levels after severe hearing loss (Figure 6). Therefore, greater cortical reorganization, which was evident after simulations of severe hearing loss (Figure 8), did not always equate to increased neural synchrony between units. The ability to drive units in the hearing loss region when louder sounds are being processed (as during receptive field mapping) may not necessarily translate to synchrony in spontaneous activity that occurs in a quieter environment. However, it is important to consider that we looked at cross-correlation between units separated by a distance of 25 in our network, and that here we used only 5-ms time bins. It is possible that there was greater correlation between more

distant units after severe hearing loss, but we did not investigate this here. Regardless, the key observation here is that neural synchrony can be elevated after simulating a wide range of hearing loss profiles. This prediction may shed light on the presence of tinnitus when audiometric thresholds appear to be normal but deafferentation may still be present (Weisz et al., 2006) as well as on empirical observations indicating that the tinnitus percept may not require tonotopic reorganization (Langers et al., 2012).

A more recently proposed neural correlate of tinnitus is altered oscillatory activity: increases in delta-band and gamma-band activity (Weisz et al., 2005; Weisz et al., 2007). Our HSP model indicates that after hearing loss, multiplicative synaptic scaling contributes to the increased amplitude of delta (1-4 Hz) and gamma (30-50 Hz) oscillatory bands. While the HSP+STDP model also exhibited these changes, for the highest level of hearing loss simulated (60 dB) increases in delta- and gamma-band amplitudes were notably larger in the HSP model than in the HSP+STDP model (Figure 17). Empirical observations do not indicate such large increases in gamma-band activity (Weisz et al., 2007) in those with tinnitus, but do support the large increase in delta-band amplitude in the HSP model (Weisz et al., 2005). However, after simulating mild hearing loss, the increase in delta-band activity was marginal in the HSP model but much more pronounced in the HSP+STDP model (Figure 17), which suggests that Hebbian-type plasticity may also play a role in the development of aberrant oscillations. Finally, the relationship between the level of hearing loss and changes in oscillatory activity differed between the two models: while delta- and gamma-band amplitudes increased for all hearing loss simulations in both models, the increase was proportional to the severity of

hearing loss in the HSP model but not in the HSP+STDP model (Figure 17). The latter finding is in agreement with empirical observations of no significant correlation between hearing loss depth and changes in oscillatory activity or tinnitus distress scores (Weisz et al., 2005). Thus, both models account for different empirical observations, indicating that more work needs to be done in order to simulate changes in oscillatory activity after hearing loss within one theoretical model. Indeed, a cortical model that does not characterize changes in the thalamus or the dynamics of the thalamocortical system (Llinas et al., 1999) will not be able to fully characterize oscillatory behaviour, especially delta-band oscillations. That being said, the models presented here can still shed light on how neural plasticity operating in a cortical network can contribute to increased power within the delta and gamma bands of oscillatory activity and thus play a role in tinnitus perception (Weisz et al., 2007).

Plasticity-mediated decreases in inhibition within the central auditory system have been implicated in tinnitus (Wang et al., 2011; Yang et al., 2011). Homeostatic plasticity is one mechanism that may respond to deafferentation by reducing the strength of inhibitory synapses (Rutherford et al., 1997; Rutherford et al., 1998; Kilman et al., 2002) as well as increasing the strength of excitatory synapses (Turrigiano, 1999) in the cortex. Recently it has been observed that when HSP reduces inhibition in a region of adult rat AI after hearing loss, there is an increased likelihood of a tinnitus percept characterized by frequencies represented in that region (Yang et al., 2011). Simulations of our HSP model suggest an explanation for these observations: after hearing loss the action of homeostatic mechanisms on inhibitory synapses (down-regulation) and excitatory

synapses (up-regulation) leads to the development of tinnitus correlates (Figure 16, Figure 17). While the HSP+STDP model can also exhibit these behaviours, we suggest that HSP, perhaps with contributions from an STDP mechanism, plays a critical role in the emergence of tinnitus after hearing loss.

While HSP on its own can contribute to most neural correlates of tinnitus in our model (see Figure 4, 16 and 17), it cannot account for tonotopic reorganization (Figure 5; Chapter 2; Chapter 3). Tonotopic reorganization in the primary auditory cortex is evident after mechanical cochlear lesions (Robertson and Irvine, 1989; Rajan et al., 1993), after acoustic trauma in juvenile and adult cats (Eggermont and Komiya, 2000; Seki and Eggermont, 2002) and in aged mice with high frequency hearing loss (Willot et al., 1993). Furthermore, tonotopic reorganization was initially implicated in tinnitus generation in an MEG study (Mühlnickel et al., 1998), but a recent high-resolution fMRI study suggests that tonotopic reorganization is not required for tinnitus perception (Langers et al., 2012). Our simulations indicate that an STDP mechanism operating in concert with HSP mediates cortical reorganization after hearing loss. Thus, we used our HSP+STDP model, which captures both tonotopic reorganization and cortical correlates of tinnitus to predict whether the conditions sufficient for the development of established tinnitus correlates necessarily induce tonotopic reorganization.

The action of STDP after hearing loss can be explained as follows: if a neuron is normally strongly driven by a particular frequency, while another cortical neuron is partially driven by the same frequency, once hearing loss reduces activity driving the first

neuron, spiking in the partially driven neuron will often precede spiking in the deafferented neuron. This would strengthen intracortical inputs from a neuron outside the hearing loss region to the deafferented neuron, and contribute to reorganization. The same argument holds for thalamocortical inputs representing frequencies outside the hearing loss region, which would now more effectively drive neurons within the hearing loss region than inputs representing their normal CFs. In addition, a concurrent HSP response to peripheral damage increases the efficacy of excitatory inputs and reduces inhibition, possibly accelerating STDP-mediated reorganization.

Spike-timing-dependent plasticity has been observed at excitatory synapses in neural circuits throughout the neocortex (for review see Caporale and Dan, 2008). In addition to evidence of the involvement of STDP mechanisms in barrel cortex reorganization after whisker trimming (Caporale and Dan, 2008), paired tone paradigms indicate that STDP may mediate reorganization in AI (Dahmen et al., 2008). We suggest that STDP may also contribute to aberrant shifts in auditory cortical receptive fields after deafferentation. Plastic reorganization that occurs after mechanical lesions (Rajan et al., 1993) is also evident in the HSP+STDP model (Figure 8, Figure 10A,B and Figure 11) in which we use STDP as a candidate mechanism for cortical reorganization after hearing loss. Our model also indicates that cortical reorganization can occur with more moderate hearing loss (35-dB threshold shift), but not for mild hearing loss (20-dB threshold shift). Both results are in agreement with empirical observations: reorganization seems to occur after moderate hearing loss (minimum 30-dB threshold shift in one study and 20- to 25-dB threshold shift in another study) caused by noise trauma (Eggermont and Komiya,

2000; Seki and Eggermont, 2002), while a bandwidth increase but lack of reorganization seems to be present after mild (20-dB or lower) threshold shifts (Rajan, 1998; Rajan 2001). Furthermore, our HSP+STDP model indicates that even mild hearing loss that does not lead to cortical reorganization can lead to an increase in tinnitus correlates (Figure 9A and Figure 17). This constitutes an important prediction of the HSP+STDP model: in agreement with recent empirical observations (Langers et al., 2012), simulations of mild hearing loss in the HSP+STDP model suggest that tonotopic reorganization may not be required for the perception of tinnitus.

We also investigated whether reorganization in our model occurs after a sloping hearing loss curve. There is evidence that progressive hearing loss is sufficient for cortical reorganization in adult AI (Komiya and Eggermont, 2000). With a sloping hearing loss, the expectation is that after reorganization, neurons throughout the hearing loss region will be tuned to frequencies closer the hearing loss edge and that their thresholds will be lower than simple residual thresholds from the original receptive field. In our HSP+STDP model, this is indeed the case (Figure 11) after simulation of sloping hearing loss. Furthermore, simulations of this type of hearing loss also indicate the development of established tinnitus correlates (Figure 9C, Figure 16 and Figure 17).

While characterizing an STDP mechanism in our model enabled us to simulate cortical reorganization after various hearing loss profiles, this does not mean that HSP did not play a role in these model behaviours. Spike-timing-dependent plasticity enables networks of neurons to evolve in response to patterns of inputs without unduly disrupting

network stability (Abbott and Nelson, 2000). In our model multiplicative synaptic scaling (HSP) further ensures that activity-dependent plasticity occurs without destabilizing the network. However, HSP also increases competition within the network to a greater degree than STDP alone (Abbott and Nelson, 2000). Namely, stronger connections can drive the neural unit above its homeostatic set-point and result in a reduction in all excitatory inputs to that unit; this effect further reduces weaker connections and the likelihood that they will be strengthened via STDP. Our simulations indicate that the combined action of these two plasticity mechanisms in AI can lead to cortical reorganization after sufficient damage at the periphery.

Although simulations of our HSP+STDP model are in agreement with many empirical observations, our model has several limitations with respect to capturing the behaviour of plasticity mechanisms in the cortex and in the auditory system as a whole. In our model, single-compartment neural units cannot account for the underlying mechanisms of HSP or STDP, or differences in their behaviours that may depend on synapse location within the dendritic tree (Goel and Lee, 2007; Caporale and Dan, 2008). For our purposes, we are more concerned with network-level effects of these forms of plasticity and whether they can contribute to the development of tinnitus correlates in the auditory cortex after hearing loss. We also do not model detailed non-linear interactions that may occur when multiple post-synaptic spikes follow a pre-synaptic spike, since such interactions would not prevent the strengthening of the associated synaptic connection (Carporale and Dan, 2008). Furthermore, we do not include STDP on inhibitory synapses (for review see Bi and Poo, 2001; Caporale and Dan, 2008), though this may be an

interesting avenue for future model development. Finally, neuromodulators such as acetylcholine that may play an important role in altering the magnitude of STDP (Kilgard and Merzenich, 1998) are not captured by our model. These neuromodulators may play an important role in the efficacy of tinnitus treatments that involve vagus nerve stimulation (Engineer et al., 2011), as well as in normal attention, learning and memory processes. A limitation of our model with respect to simulating the role of neural plasticity in tinnitus is that we do not include the numerous sub-cortical auditory nuclei (the cochlear nucleus, superior olivary complex, inferior colliculus, medial geniculate body), most of which demonstrate changes in spontaneous firing (for review see Eggermont and Roberts, 2004) and down-regulation of inhibition after hearing loss (Milbrandt et al., 2000; Wang et al., 2011). That being said, our simulations of HSP and STDP provide important insights into the role of neural plasticity in the development and mitigation of cortical correlates of tinnitus.

Sound therapies and hearing aid use can both reduce tinnitus symptoms to varying degrees in anywhere from 50 to 66% of cases (Schaette et al., 2010). While there is still debate over how helpful hearing aids can be to tinnitus patients (Moffat et al., 2010), some of the variability in findings may be a result of hearing aids not amplifying sufficiently high frequencies to cover the frequency range representing the tinnitus percept (Schaette et al., 2010). There is also evidence that acoustic treatments are more effective when the frequency content of the treatment encompasses the patient's tinnitus frequency (Schaette at al., 2010); this may explain why acoustic treatments incorporating sounds at frequencies above those produced by traditional hearing aids and noise devices

(i.e. greater than 6 kHz) successfully reduce tinnitus-related distress in a greater proportion of tinnitus patients (Davis et al., 2008). These findings are in agreement with our model predictions, as plasticity-induced changes in AI were only mitigated meaningfully by providing compensation at frequencies spanning the hearing loss region. Thus, successful treatments may be those that undo the effects of aberrant plasticity in high-frequency regions of AI where threshold shifts are most likely and where the tinnitus pitch may be represented (Roberts et al., 2006; Yang et al., 2011). Although the NAL-R linear gain prescription (Dillon, 2001) we simulated amplifies sounds at frequencies of up to 6 kHz, we simulated hearing loss that began at 2.3 kHz and extended to 15 kHz. Our simulations suggest that early hearing aid adoption can slightly reduce tonotopic reorganization (Figure 13A and 13B) and neural synchrony (Figure 12A), but that late adoption may not. However in both cases, elevations in the amplitude of gamma-band oscillations, which may underlie tinnitus perception (Weisz et al., 2007), were not mitigated, and the effects on the amplitude of delta-band oscillations were mixed (Figure 17). The HSP+STDP model did not predict any other benefits of hearing aid use with respect to the tinnitus correlates we focused on. In agreement with empirical observations, our model suggests that a hearing aid prescription that does not take into account high-frequency hearing loss may provide little benefit for tinnitus sufferers if their tinnitus percept is generated by neurons throughout the hearing loss region.

An alternative tinnitus treatment strategy that can take into account the entire hearing loss region is sound therapy. While a very diverse range of acoustic treatments have been developed for tinnitus reduction, there is no one-size-fits-all stimulus ensemble

that consistently alleviates symptoms for tinnitus patients. However, acoustic treatments are more successful when they cover frequencies that match the tinnitus pitch (Schaette et al., 2010). Because the tinnitus spectrum seems to lie within or span the hearing loss region (Roberts et al., 2006; Yang et al., 2011), it is likely that acoustic therapies will be more successful when customized for each patient. While the acoustic treatment that we simulated did not undo cortical reorganization, it did reduce neural synchrony (Figure 15), spontaneous firing rates (Figure 16) and the amplitude of gamma-band activity (Figure 17). These results may provide insight into why sound therapies are sometimes but not always effective in tinnitus reduction (Davis et al., 2008; Schaette et al., 2010) or in the reduction of tinnitus correlates (Noreña and Eggermont, 2005; Noreña and Eggermont, 2006). The HSP+STDP model predicted that some tinnitus correlates could be reduced by using an enriched stimulus ensemble that covered the entire spectrum and accounted for the hearing loss region through increased sound levels for tones with frequencies throughout this region. The greater reduction of tinnitus correlates relative to simulated hearing aid use was likely a result of addressing the entire hearing loss region rather than providing a gain scheme for frequencies up to 6 kHz. The fact that our model did not predict normalization of the tonotopy is not necessarily a limitation of the model, as such effects seem to require driving cholinergic inputs while applying a sound therapy (Engineer et al., 2011) or perhaps immediate exposure to an enriched acoustic environment after hearing loss (Noreña and Eggermont, 2005). We only trained the HSP+STDP model with the simulated acoustic therapy after changes due to severe (60 dB SPL) steep hearing loss had already occurred. Our simulations of early hearing aid use

(Figure 13A and 13B) suggest that increased input activity within the hearing loss region can reduce the shift in receptive fields towards the normal hearing region.

While we leave simulation of more sophisticated sound therapies in conjunction with more advanced gain prescriptions for future work, we are able to use our simulation results to make important predictions about tinnitus treatment strategies. Firstly, it is important to take into account that while we do not know which tinnitus correlates are ultimately responsible for the tinnitus percept, our HSP+STDP model predicts that most tinnitus correlates can develop even with mild hearing loss, and for different hearing loss profiles; the exception is tonotopic reorganization, which did not occur in simulations of mild (20-dB) hearing loss and may not be necessary for tinnitus perception (Langers et al., 2012). Fortunately, the same model predicts that even after severe (60-dB) hearing loss, as long as auditory nerve fibers can still be driven, the development of tinnitus correlates can be mitigated by sound therapies that are tailored toward a full audiogram. These approaches are motivated by taking into account HSP and STDP and understanding how their aberrant effects can be minimized by altering their actions on synaptic connections in AI after hearing loss.

References

Abbott LF, Nelson SB (2000). Synaptic plasticity: taming the beast. *Nat Neurosci* 3 Suppl:1178-83.

Aitkin LM, Webster WR (1972). Medial geniculate body of the cat: organization and responses to tonal stimuli of neurons in ventral division. *J Neurophysiol* 35(3):365-80.

Bennett MV, Zukin RS (2004). Electrical coupling and neuronal synchronization in the mammalian brain *Neuron* 19;41(4):495-511.

Bi G, Poo M (2001). Synaptic modification by correlated activity: Hebb's postulate revisited. *Annu Rev Neurosci* 24:139-66.

Caporale N, Dan Y (2008). Spike timing-dependent plasticity: a Hebbian learning rule. *Annu Rev Neurosci* 31:25-46.

Chrostowski M, Stolzberg D, Becker S, Bruce IC, Salvi RJ (in revision). A potential role for homeostatic plasticity in adult primary auditory cortex. *J Neurophys* JN-00205-2012.

Chrostowski M, Yang L, Wilson HR, Bruce IC, Becker S (2011). Can homeostatic plasticity in deafferented primary auditory cortex lead to traveling waves of excitation? *J Comput Neurosci* 30:279-299.

Clark WW (1991). Recent studies of temporary threshold shift (TTS) and permanent threshold shift (PTS) in animals. *J Acoust Soc Am* 90(1):155-63.

Dahmen JC, Hartley DE, King AJ (2008). Stimulus-timing-dependent plasticity of cortical frequency representation. *J Neurosci* 28(50):13629-39.

Davis PB, Wilde RA, Steed LG, Hanley PJ (2008). Treatment of tinnitus with a customized acoustic neural stimulus: a controlled clinical study. *Ear Nose Throat* 87, 330e339.

Dillon, H. (2001). *Hearing Aids*. New York, NY: Thieme Medical Publishers.

Dohrmann K, Weisz N, Schlee W, Hartmann T, and Elbert T (2007). Neurofeedback for treating tinnitus. *Prog Brain Res* 166: 473-485.

Eggermont JJ (2008). Role of auditory cortex in noise- and drug-induced tinnitus. *Am J Audiol* 17: S162-169.

Eggermont JJ, Komiya H (2000). Moderate noise trauma in juvenile cats results in profound cortical topographic map changes in adulthood. *Hear Res* 142:89 –101.

Eggermont JJ, Roberts LE (2004). The neuroscience of tinnitus. *Trends Neurosci* 27:676-682.

Engineer ND, Riley JR, Seale JD, Vrana WA, Shetake JA, Sudanagunta SP, Borland MS, and Kilgard MP (2011). Reversing pathological neural activity using targeted plasticity. *Nature* 470: 101-104.

Fröhlich F, Bazhenow M, Sejnowski T (2008). Pathological effect of homeostatic synaptic scaling on network dynamics in diseases of the cortex. *J Neurosci* 28(7): 1709–1720.

Galarreta M, Hestrin S (1999). A network of fast-spiking cells in the neocortex connected by electrical synapses. *Nature* 4;402(6757):72-5.

Galarreta M, Hestrin S (2001). Electrical synapses between GABA-releasing interneurons. *Nat Rev Neurosci* 2:425– 433.

Gibson JR, Beierlein M, Connors BW (1999). Two networks of electrically coupled inhibitory neurons in neocortex. *Nature* 402(6757):75-9.

Goel A, Lee H-kyoung (2007). Persistence of experience-induced homeostatic synaptic plasticity through adulthood in superficial layers of mouse visual cortex. *J Neurosci* 27:6692- 6700.

Greenwood DD (1990). A cochlear frequency-position function for several species--29 years later. *J Acoust Soc Am* 87(6):2592-605.

Izhikevich EM (2003). Simple Model of Spiking Neurons. *IEEE Trans Neural Netw* 14:1569-1572.

Kilgard MP, Merzenich (1998). Cortical map reorganization enabled by nucleus basalis activity. *Science* 279(5357):1714-8.

Kilman V, Rossum MCW van, Turrigiano GG (2002). Activity Deprivation Reduces Miniature IPSC Amplitude by Decreasing the Number of Postsynaptic GABA A Receptors Clustered at Neocortical Synapses. *J Neurosci* 22:1328-1337.

Kimura, M, Eggermont JJ (1999). Effects of acute pure tone induced hearing loss on response properties in three auditory cortical fields in cat. *Hear Res* 135:146-162.

Langers DR, de Kleine E, van Dijk P (2012). Tinnitus does not require macroscopic tonotopic map reorganization. *Front Syst Neurosci* 6:2.

Liberman MC, Kiang NYS (1978). Acoustic trauma in cats. Cochlear pathology and auditory-nerve activity. *Acta Otolaryngol suppl* 358:1-63.

Llinás RR, Ribary U, Jeanmonod D, Kronberg E, Mitra PP (1999). Thalamocortical dysrhythmia: A neurological and neuropsychiatric syndrome characterized by magnetoencephalography. *Proc Natl Acad Sci* 96(26):15222-7.

Londero A, Langguth B, De Ridder D, Bonfils P, and Lefaucheur JP (2006). Repetitive transcranial magnetic stimulation (rTMS): a new therapeutic approach in subjective tinnitus? *Neurophysiol Clin* 36: 145-155.

Masquelier T, Guyonneau R, Thorpe SJ (2008). Spike timing dependent plasticity finds the start of repeating patterns in continuous spike trains. *PLoS One*, 2;3(1):e1377.

Milbrandt JC, Holder TM, Wilson MC, Salvi RJ, Caspary DM, (2000). GAD levels and muscimol binding in rat inferior colliculus following acoustic trauma. *Hear Res* 147, 251-260.

Moffat G, Adjout K, Gallego S, Thai-Van H, Collet L, Noreña AJ (2009). Effects of hearing aid fitting on the perceptual characteristics of tinnitus. *Hear Res* 254(1-2):82-91.

Mühlnickel W, Elbert T, Taub E, and Flor H (1998). Reorganization of auditory cortex in tinnitus. *Proc Natl Acad Sci U S A* 95: 10340-10343.

Noreña AJ (2011). An integrative model of tinnitus based on a central gain controlling neural sensitivity. *Neurosci Biobehav Rev* 35(5):1089-109.

Noreña AJ, Eggermont JJ (2005). Enriched acoustic environment after noise trauma reduces hearing loss and prevents cortical map reorganization. *J Neurosci* 25(3):699-705.

Noreña AJ, Eggermont JJ, (2006). Enriched acoustic environment after noise trauma abolishes neural signs of tinnitus. *Neuroreport* 17, 559-563.

Noreña AJ, Tomita M, Eggermont JJ (2003). Neural changes in cat auditory cortex after a transient pure-tone trauma. *J Neurophysiol* 90:2387-401.

Osaki Y, Nishimura H, Takasawa M, Imaizumi M, Kawashima T, Iwaki T, Oku N, Hashikawa K, Doi K, Nishimura T, Hatazawa J, Kubo T (2005). Neural mechanism of residual inhibition of tinnitus in cochlear implant users. *Neuroreport* 16(15):1625-8.

Plack CJ, Drga V, Lopez-Poveda EA (2004). Inferred basilar-membrane response functions for listeners with mild to moderate sensorineural hearing loss. *J Acoust Soc Am* 115(4):1684–1695.

Rajan R (1998). Receptor organ damage causes loss of cortical surround inhibition without topographic map plasticity. *Nat Neurosci* 1(2):138-43.

Rajan R (2001) Plasticity of excitation and inhibition in the receptive field of primary auditory cortical neurons after limited receptor organ damage. *Cereb Cortex* 11(2):171-82.

Rajan R, Irvine DR, Wise LZ, Heil P (1993). Effect of unilateral partial cochlear lesions in adult cats on the representation of lesioned and unlesioned cochleas in primary auditory cortex. *J Comp Neurol* 338:17– 49.

Rauschecker JP (1999). Auditory cortical plasticity: a comparison with other sensory systems. *Trends Neurosci* 22:74–80.

Roberts LE, Moffat G, Bosnyak DJ (2006). Residual inhibition functions in relation to tinnitus spectra and auditory threshold shift. *Acta Oto-Laryngologica Supplementum* (556), 27–33.

Robertson D, Irvine DRF (1989). Plasticity of frequency organization in auditory cortex of guinea pigs with partial unilateral deafness. *J Comp Neurol* 282:456–471.

Rutherford LC, DeWan A, Lauer HM, Turrigiano GG (1997). Brain-derived neurotrophic factor mediates the activity-dependent regulation of inhibition in neocortical cultures. *J Neurosci* 17:4527- 4535.

Rose HJ, Metherate R (2005). Auditory thalamocortical transmission is reliable and temporally precise. *J Neurophys* 94:2019-2030.

Rutherford LC, Nelson SB, Turrigiano GG (1998). BDNF Has Opposite Effects on the Quantal Amplitude of Pyramidal Neuron and Interneuron Excitatory Synapses. *Neuron* 21:521-530.

Seki S, Eggermont JJ (2002). Changes in cat primary auditory cortex after minor-to-moderate pure-tone induced hearing loss. *Hear Res* 173(1-2):172-86.

Seki S, Eggermont JJ (2003). Changes in spontaneous firing rate and neural synchrony in cat primary auditory cortex after localized tone-induced hearing loss. *Hear Res* 180:28-38.

Schaette R, Kempter R (2006). Development of tinnitus-related neuronal hyperactivity through homeostatic plasticity after hearing loss: a computational model. *Eur J Neurosci* 23(11):3124-38.

Schaette R, Konig O, Hornig D, Gross M, and Kempter R (2010). Acoustic stimulation treatments against tinnitus could be most effective when tinnitus pitch is within the stimulated frequency range. *Hear Res* 269: 95-101.

Stolzberg D, Chrostowski M, Salvi R, Allman B (in press). Intracortical circuits amplify sound-evoked activity in primary auditory cortex following systemic injection of salicylate in the rat. *J Neurophys* JN-00946-2011R1.

Swadlow HA (2003). Fast-spike interneurons and feedforward inhibition in awake sensory neocortex. *Cereb Cortex*. 13(1):25-32.

Turner JG, Brozoski TJ, Bauer CA, Parrish JL, Myers K, Hughes LF, Caspary DM (2006). Gap detection deficits in rats with tinnitus: a potential novel screening tool. *Behav Neurosci* 120(1):188-95.

Turrigiano GG (1999). Homeostatic plasticity in neuronal networks: the more things change, the more they stay the same. *Trends Neurosci* 22:221-227.

Wang H, Brozoski TJ, Caspary DM (2011). Inhibitory neurotransmission in animal models of tinnitus: maladaptive plasticity. *Hear Res* 279(1-2):111-7.

Wehr M, Zador AM (2003). Balanced inhibition underlies tuning and sharpens spike timing in auditory cortex. *Nature* 426:442-446

Weisz N, Hartmann T, Dohrmann K, Schlee W, Noreña A (2006). High-frequency tinnitus without hearing loss does not mean absence of deafferentation. *Hear Res* 222 (1–2): 108-114.

Weisz N, Moratti S, Meinzer M, Dohrmann K, Elbert T (2005). Tinnitus perception and distress is related to abnormal spontaneous brain activity as measured by magnetoencephalography. *PLoS Med* 2(6):e153.

Weisz N, Müller S, Schlee W, Dohrmann K, Hartmann T, Elbert T (2007). The neural code of auditory phantom perception. *J Neurosci* 27(6):1479-84.

Willott JF, Aitkin LM, McFadden SL (1993). Plasticity of auditory cortex associated with sensorineural hearing loss in adult C57BL/6J mice. *J Comp Neurol* 329(3):402-11.

Wu GK, Arbuckle R, Liu BH, Tao HW, Zhang LI (2008). Lateral sharpening of cortical frequency tuning by approximately balanced inhibition. *Neuron* 58:132-143.

Yang S, Weiner BD, Zhang LS, Cho S-J, Bao S (2011). Homeotatic plasticity drives tinnitus perception in an animal model. *Proc Natl Acad Sci* 108:14974-14978.

Zilany MSA, Bruce IC, Nelson PC, Carney LH (2009). A phenomenological model of the synapse between the inner hair cell and auditory nerve: Long-term adaptation with power-law dynamics. *J Acoust Soc Am* 126(5):2390–2412.

Postscript

This chapter outlined a novel and more complete computational model that tied together the earlier work I have presented with insights into correlates of tinnitus that have not been modeled before. A more complete model of plasticity and tinnitus correlates in AI enabled me to justify simulating methods of treatment for tinnitus. The findings discussed in this chapter not only shed light on how aberrant plasticity in AI can contribute to tinnitus, but also provide an important step towards developing more informed tinnitus treatment strategies.

General Discussion

Tinnitus is a neurological disorder that disrupts the lives of 10-15% of the population (Eggermont and Roberts, 2004). Unfortunately, the underlying neural mechanisms of tinnitus have not been fully characterized, and treatment success rates are underwhelming (Hoare et al., 2011). While some progress has been made in understanding the neural basis of tinnitus, a wide array of different brain regions has been implicated, with tinnitus research suggesting a role for auditory structures including the dorsal cochlear nucleus (Baizer et al., 2012; Wang et al., 2011), inferior colliculus (Chen and Jastreboff, 1993; Wang et al., 2011) and auditory cortex (Hoke et al., 1991; Mühlnickel et al., 1998; Eggermont and Roberts, 2004), as well as evidence of limbic system involvement (Kraus and Canlon, 2012); it has therefore become difficult to form a complete picture of the causes of this disorder. Improving our understanding of how a phantom auditory percept develops will require an integrative approach that includes studies of tinnitus in humans and in animal models, as well as the creation of a comprehensive theoretical framework that can explain the complex brain changes correlated with tinnitus. A critical and understudied part of this process is to understand how cortical mechanisms contribute to tinnitus. While changes in spontaneous activity after hearing loss develop at several levels of the central auditory system (for review see Eggermont and Roberts, 2004), aberrant activity at the level of the auditory cortex may be responsible for the perception of tinnitus (Stolzberg et al., 2012). To understand how

aberrant auditory cortical activity and processing could develop after hearing loss, it is necessary to take into account the role of cortical plasticity.

Neural plasticity is important during development, and it persists into adulthood (Goel and Lee, 2007; Caporale and Dan, 2008; Feldman, 2009). However, while plasticity is necessary for the formation and maintenance of functional neural circuits, it can also have undesired effects. Homeostatic plasticity (HSP) is meant to maintain balance in cortical circuits (Turrigiano et al., 1998; Turrigiano 1999), but a homeostatic response reduced input activity may actually create aberrant activity and cortical processing (e.g. Fröhlich et al., 2008). Furthermore, recent empirical work (Yang et al., 2011) provides evidence suggesting that HSP contributes to the perception of tinnitus. Hebbian plasticity is also a potential mechanism contributing to tinnitus (Noreña, 2011). It has been suggested that spike-timing-dependent plasticity (STDP), which is a Hebbian-type plasticity mechanism, may underlie cortical reorganization in adult primary auditory cortex (Dahmen et al., 2008). Tonotopic reorganization and overrepresentation are common developments after hearing loss due to noise trauma (Calford et al., 1993; Seki and Eggermont, 2002; Noreña et al., 2003) and mechanical lesions at the periphery (Robertson and Irvine, 1989; Rajan et al., 1993). In addition, tonotopic reorganization in the auditory cortex is a potential tinnitus correlate (Mühlnickel et al., 1998) that has recently been called into question (Langers et al., 2012). Therefore, a theoretical framework of the cortical correlates of tinnitus could benefit from a computational model that captures the response of both HSP and STDP to hearing loss.

The work described here has focused on developing and validating a theoretical framework for central tinnitus, specifically focusing on the role of the auditory cortex in tinnitus generation and perception. By developing a computational model of the primary auditory cortex and capturing the network-level effects of homeostatic and Hebbian plasticity after hearing loss, we have furthered our understanding of how plasticity mechanisms can contribute to the emergence of tinnitus correlates after hearing loss and how they can inform tinnitus treatments. The major contributions of this thesis are as follows: 1) homeostatic plasticity is active in the adult auditory cortex and can affect processing therein within hours, 2) the actions of HSP after hearing loss can lead to increased spontaneous firing, synchrony and oscillatory activity, each of which is a potential correlate of tinnitus, 3) STDP working in concert with HSP can explain tonotopic reorganization in the auditory cortex along with the same cortical correlates of tinnitus captured by an HSP model, and thus sheds light on whether cortical reorganization is necessary for tinnitus perception, and 4) by taking into account the triggers for these plasticity mechanisms, acoustic therapies for tinnitus can be made more effective. We elaborate on each of these main results in the next three sub-sections, after which we discuss limitations of the work and directions for future research.

5.1 Homeostatic Plasticity and the Development of Tinnitus Correlates (Chapters 2-3)

The initial model of homeostatic plasticity acting in the primary auditory cortex predicted that when HSP is triggered in response to different levels of hearing loss, there

may be undesired changes including elevated spontaneous activity, a potential tinnitus correlate. By increasing excitatory inputs and reducing inhibition to restore a target level of activity in an acoustically rich environment, HSP mechanisms created a hyper-excitable state in the auditory cortical network. These theoretical observations were in agreement with empirical evidence suggesting that HSP may be active in developing (Kotak et al., 2005) and adult (Yang et al., 2011; Chapter 3) auditory cortex after peripheral damage. Furthermore, simulations indicated that when homeostatic plasticity was triggered in response to hearing loss, it could also produce short-range traveling waves of activity, as discussed in Chapter 2. However, the distance over which such activity could spread through the cortex seemed to be limited by the increase in spontaneous activity, which also induced more frequent refractory periods in the hearing loss region. Therefore, the model predicted that after hearing loss, homeostatic plasticity may not only create aberrant activity in the auditory cortex, but that it can also contribute to increases in spontaneous firing and synchrony that are thought to underlie tinnitus.

An unresolved issue in the literature, up until now, has been the time course over which neural mechanisms can induce various correlates of tinnitus and reorganization after the onset of hearing loss. Elevated spontaneous firing rates and synchrony are potential neural correlates of tinnitus (Eggermont and Roberts, 2004) that can develop very soon after hearing loss induced by acoustic trauma (Seki and Eggermont, 2003; Noreña and Eggermont, 2003). However, our cortical model suggested that HSP could also contribute to the development and persistence of these tinnitus correlates over a longer time scale (Chapter 2; see also the synaptic level model of Schaette and Kempter,

2006, which also predicts increased spontaneous firing). Furthermore, we obtained evidence indicating that HSP in the auditory cortex responded to hearing loss within 8 hours of peripheral damage in adult animal studies of acoustic trauma (Chapter 3); this was a significant observation, as no prior research had attempted to characterize rapid HSP within the auditor cortex. This implied that homeostatic plasticity could indeed contribute to the development of tinnitus correlates on a timescale of hours to days (Chapter 2; Chapter 3; see also Yang et al., 2011). Evidence of rapid HSP does not imply that synaptic scaling can completely restore normal firing rates within hours of peripheral damage, but rather, that synaptic scaling during this time is sufficient to adversely affect processing and activity in the auditory cortex. Such rapid action is not unexpected, given that it has been observed in other cortical regions (Hartmann et al., 2008; Ibata et al., 2008). Simulations suggested that a broad range of homeostatic mechanisms could induce aberrant activity and tuning in the primary auditory cortex. However, synaptic scaling acting on intracortical connections in superficial layers was the strongest candidate since simulations with this mechanism most accurately predicted empirical results. The predicted development of tinnitus correlates in primary auditory cortex after hearing loss via HSP implicates homeostatic plasticity in this auditory disorder. It is critical to understand the rate at which cortical networks can change via synaptic scaling since such changes seem to contribute to the emergence of tinnitus correlates and may be important in cortical reactions to various tinnitus therapies.

Understanding the potential importance of homeostatic plasticity in the development and persistence of tinnitus will be important for future treatment prospects.

Indeed, accounting for homeostatic plasticity may not only improve treatments but also ensure greater care in the development of any future drug therapies for tinnitus that may unexpectedly trigger homeostatic responses by acting on synaptic transmission (Schaette and Kempter, 2012). Refined computational models will enable the testing of various treatment strategies in the context of aberrant neural plasticity.

5.2 Hebbian Plasticity, Tinnitus correlates and Treatments (Chapter 4)

While the simulation results discussed in Chapters 2 and 3 suggest that homeostatic plasticity plays an important role in the development of aberrant spontaneous activity that is linked to tinnitus, cortical reorganization did not occur after simulated hearing loss. However, there is evidence that damage to the auditory periphery can result in tonotopic reorganization at the level of the primary auditory cortex (Robertson and Irvine, 1989; Calford et al., 1993; Rajan et al., 1993; Seki and Eggermont, 2002; Noreña et al., 2003). Furthermore, while there is debate as to whether tonotopic reorganization is necessary for tinnitus perception (Mühlnickel et al., 1998; Langers et al., 2012), normalizing the tonotopic map is used as the basis for recent tinnitus therapies (Engineer et al., 2011). Therefore, it is important to capture this phenomenon in a theoretical model of central tinnitus.

The primary auditory cortex model described in Chapter 4 built on the empirically validated theoretical model discussed in Chapter 3. This more comprehensive model included both spike-timing-dependent plasticity and homeostatic plasticity, and provided

two important contributions to our understanding of how plasticity mechanisms in the auditory cortex react to hearing loss. Firstly, by including a realistic model of the auditory periphery (Zilany et al., 2009) as input, the model could more accurately reflect how cortical plasticity mechanisms respond to hearing loss. Secondly, including the behaviour of spike-timing-dependent plasticity in the model provided a more complete picture of changes in primary auditory cortex after hearing loss. The model predicted cortical reorganization after threshold shifts that exceeded 20 dB SPL and a lack of reorganization for lower threshold shifts. These predictions are in agreement with empirical findings (Rajan 1998; Seki and Eggermont, 2002). In addition to making novel predictions about how STDP can mediate tonotopic reorganization in the primary auditory cortex, this model also captured other tinnitus correlates, namely, increased spontaneous firing, synchrony and increased oscillatory activity.

Elevated delta-band (1-4 Hz) and gamma-band (>30 Hz) oscillatory activity is correlated with the presence of tinnitus (Weisz et al., 2005; Weisz et al., 2007). Furthermore, reducing delta-band amplitude through neurofeedback training reduces or even eliminates tinnitus (Dohrmann et al., 2007), while tinnitus reduction after sound masker presentation results in reduced delta-band activity (Kahlbrock and Weisz, 2008). Therefore, we also included gap junctions between inhibitory neurons in the model described in Chapter 4; without gap junctions, the amplitude of gamma-band (30-50 Hz) oscillatory activity was substantially weaker. Simulations of this model exhibited elevated delta- and gamma-band amplitudes after hearing loss. While removing STDP from the model indicated that only homeostatic plasticity was necessary for the elevated

oscillatory activity, including STDP did not qualitatively affect these predictions. More importantly, the model that captured both HSP and STDP suggested that tinnitus correlates in spontaneous activity could develop irrespective of the presence of tonotopic reorganization. This result constitutes an important insight into tinnitus correlates and is in agreement with empirical work (Langers et al., 2012) indicating that reorganization is not required for tinnitus perception.

Since predictions of the model with respect to the development of tinnitus correlates after hearing loss were in agreement with empirical data, the model could provide important insights into why and how cortical activity and processing can become aberrant after hearing loss. Namely, homeostatic plasticity would create hyperactivity in the cortex by reducing inhibitory synaptic transmission and increasing excitation to compensate for reduced ascending input activity. Spike-timing-dependent plasticity may operate at the same time, and shift the distribution of synaptic input strength towards frequencies below the hearing loss region. While simulations indicated that the magnitude of resultant changes increased with greater peripheral damage, the model also predicted that relatively mild hearing loss could lead to tinnitus. This may help explain why tinnitus may develop even when clinical audiograms do not indicate hearing loss but deafferentation may still be present (Weisz et al., 2006). Computational modeling elucidates how easily plasticity mechanisms can evoke aberrant cortical activity, and potentially, a phantom auditory percept. Capturing a wide range of tinnitus correlates allowed us to predict how cortical plasticity could lead to tinnitus; the next step was to understand if this knowledge could inform acoustic tinnitus treatments.

A comprehensive cortical model of tinnitus is important because it sheds light on neural mechanisms underlying tinnitus, but it also presents an exciting opportunity to determine which tinnitus treatments may be effective. This is critical because of the time usually invested in tinnitus therapies, which do not always succeed. Using a computational model that accounts for the actions of STDP and HSP while simulating realistic peripheral damage provides a novel method for testing treatments; if validated, this approach would permit the investigation of the efficacy of a tinnitus treatment without human participation. Simulations discussed in Chapter 4 suggested that tinnitus treatments would be more effective when they address the full frequency profile of peripheral threshold shifts, since these changes eventually drive aberrant plasticity. Namely, the computational model predicted that while compensating for elevated thresholds in the hearing loss region with a hearing aid prescription can mitigate cortical reorganization, a prescription that does not account for high frequency hearing loss to the normal frequency limit of human hearing, will do little to mitigate increased spontaneous firing, synchrony or oscillatory activity. On the other hand, acoustic therapies can effectively reduce many tinnitus correlates if they encompass the tonotopy and also take into account the hearing loss profile by delivering louder sounds at frequencies in the hearing loss region. These results are in agreement with empirical work comparing the greater effectiveness of acoustic treatments that address the hearing loss region and tinnitus pitch with those that do not (Davis et al., 2008; Schaette et al., 2010; Pantev et al., 2012). The simulation results described in Chapter 4 suggest that these treatment strategies are more effective when they can drive neural firing rates in the hearing loss

region closer to their homeostatic set-point as this would reduce HSP- and STDP-mediated responses to hearing loss. Therefore, the computational models described here have not only shed light on underlying neural mechanisms of tinnitus, but have also provided a much needed starting point from which to develop a better understanding as to why certain tinnitus treatment strategies are more likely to succeed than others.

5.3 Limitations of the presented models

The outlined work has focused on neural plasticity mechanisms at the level of the cortex and how these may contribute the development of tinnitus. However, the effects of neural plasticity after damage to the auditory periphery have been observed in subcortical auditory structures (Milbrandt et al., 2000; Wang et al., 2011; Browne et al., 2012). Furthermore, correlates of tinnitus manifest themselves in altered spontaneous activity at most structures along the auditory pathway (for review see Eggermont and Roberts, 2004). In other cases, more complex tinnitus correlates like increased oscillatory activity develop through interactions between two auditory stages, such as the auditory thalamus and the primary auditory cortex (Llinás et al., 1999). If hearing loss induces changes in subcortical structures as well as at the level of the auditory cortex, it becomes difficult to determine to what extent the development of cortical correlates of tinnitus is due to cortical plasticity versus it being a phenomenon inherited from subcortical auditory nuclei. While some inheritance is likely, there is also evidence of homeostatic responses at the level of the auditory cortex after hearing loss (Kotak et al., 2005; Yang et al., 2011). Furthermore, because the auditory circuit contains corticofugal projections, it can

be argued that some of the changes in subcortical activity are influenced by changes in the primary auditory cortex (see Eggermont, 2008). Thus, while the cortical models described in this dissertation cannot fully explain tinnitus without being extended to include other brain regions, they do elucidate the contributions of cortical plasticity to tinnitus generation and perception.

Importantly the description of neural plasticity within this framework also has limitations. While extensive simulations permitted a comparison of the various possible types and loci of homeostatic plasticity and how these can explain empirical observations from animal models of hearing loss, the same extensive investigation was not applied with respect to Hebbian-type plasticity. Namely, the spike-timing-dependent plasticity mechanism that was described in Chapter 4 is a simplified model, and is unlikely to capture the full complexity of activity dependent plasticity in the brain. However, this model was able to capture cortical reorganization, and thus provided important insights into what kind of hearing loss profiles could affect the cortical tonotopy. Furthermore, we were able to investigate which treatments could mitigate the effect of a form of plasticity that is dependent on correlated or synchronous activity, which may be especially pertinent to tinnitus. That being said, more work can be done to elaborate on the richness and complexity of neural plasticity in order to provide a more precise understanding of the mechanisms that contribute to tinnitus.

5.4 Future work: extending the model

As was stated earlier, understanding tinnitus requires a comprehensive and integrative approach that takes into account a vast array of empirical and theoretical studies. The work described in this thesis has provided major contributions towards our understanding of the role of cortical plasticity in the development of tinnitus correlates and of how plasticity mechanisms can interact with acoustic treatment strategies. However, more can be done to capture other cortical correlates of tinnitus and to simulate non-acoustic tinnitus treatments. To accomplish this, the existing model should take into account additional neural mechanisms that can modulate or lead to tinnitus correlates. Furthermore, the comprehensive model outlined here could also be integrated into a larger computational model of the overall tinnitus network in the brain.

Synaptic plasticity is not the only means of inducing functional changes in the auditory cortex nor is it the only phenomenon that can contribute to cortical correlates of tinnitus. Damage at the auditory periphery can very rapidly reduce outgoing activity (Liberman and Dodds, 1984) that ultimately drives cortical inhibition. The result is inhibitory unmasking (Rajan et al., 1993; Rajan, 2001; Wehr and Zador, 2003) that may contribute to tinnitus correlates in the same way as a homeostatic reduction in inhibition (Chapter 2; Chapter 3). Investigating this rapid effect of hearing loss on activity in the auditory cortex may shed light on how tinnitus can arise from acute noise exposure. Understanding the difference between immediate and long-term effects of hearing loss

would help delineate which central mechanisms can induce transient tinnitus versus those that can lead to chronic tinnitus.

In addition to extending the model to gain a more complete picture of cortical mechanisms that can contribute to tinnitus, we can also build on the present model in order to capture other tinnitus correlates at the level of the auditory cortex. Some of these correlates can be investigated with the model in its present state, but others may also require an extended cortical model. Namely, after sensory training, there are differences in the 40-Hz auditory steady state response (ASSR) in tinnitus subjects versus controls (Roberts et al., 2012), which is thought to reflect changes in the way neural plasticity behaves in the primary auditory cortex of those with tinnitus. The model described here has only been used to calculate mean oscillatory amplitudes but could also be extended to capture the ASSR. A more ambitious extension of the type of models discussed in this dissertation would be to capture functional coupling in oscillatory bands between different brain regions (Schlee et al., 2009). Since the current model predicts increases in gamma-band oscillations, it is possible that it could also provide insight into increased long-range coupling of gamma-band activity between brain regions during chronic tinnitus (Schlee et al., 2009). In essence, this dissertation describes a comprehensive model of cortical correlates of tinnitus, but this model is also amenable to placement within a larger framework that integrates changes in other auditory and non-auditory brain structures that are pertinent to tinnitus.

Other modalities may also affect tinnitus correlates in the auditory cortex. There is already evidence of crossmodal inputs being able to modulate tinnitus through inputs to the dorsal cochlear nucleus (for review see Shore et al., 2007), but perhaps crossmodal inputs that become functional during adult-onset deafness (Allman et al., 2009), can also influence tinnitus that arises after hearing loss. An extended cortical model could investigate tinnitus modulation through other modalities by simulating intracortical crossmodal inputs or by capturing subcortical crossmodal information. While such model extensions are ambitious, they may be a necessary step towards creating a complete framework of the entire brain circuit implicated in tinnitus.

Finally, while we have used the model to simulate sound therapies, other potential tinnitus treatments also benefit from a better understanding of their effect on the cortical network. For instance, there is a very limited understanding of why transcrannial magnetic stimulation (TMS) (Lehner et al., 2012) and transcrannial direct current stimulation (tDCS) (Garin et al., 2011) can reduce tinnitus for some but not for others. These top-down treatments can vary in terms of the positing of a magnetic coil (TMS) or electrodes (tDCS) as well as in terms of the actual stimulation parameters. Simulating these treatments in a cortical model could lead to more informed parameter selection and greater treatment success. While the current model could predict how these treatments interact with active neural plasticity, the model can also be extended to capture short-term and long-term adaptation that may be very relevant for these acute treatment strategies.

Tinnitus is complex and it is highly unlikely that only one neural mechanism or brain region is responsible for the emergence of the phantom percept. Therefore, future tinnitus studies should take into account various lines of research and determine where commonalities exist so that an overall theoretical framework can be developed. An integrative theoretical model of tinnitus will shed further light on underlying mechanisms, and it can also drive the development of promising treatment strategies. Knowledge of neural mechanisms of tinnitus has come a long way in recent years, and with an increasing understanding of this auditory disorder, we may be close to developing effective treatments. The contributions discussed in this dissertation are meant to further this knowledge by focusing on the role of cortical plasticity in tinnitus. A more complete understanding of aberrant plasticity in adult auditory cortex is an important piece of the puzzle and is likely to be essential in eventually developing methods to reduce or eliminate the phantom auditory percept.

References

Abbott LF, Nelson SB (2000). Synaptic plasticity: taming the beast. *Nat Neurosci* 3 Suppl:1178-83.

Allman BL, Keniston LP, Meredith MA (2009). Adult deafness induces somatosensory conversion of ferret auditory cortex. *Proc Natl Acad Sci* 106(14):5925-30.

Baizer JS, Manohar S, Paolone NA, Weinstock N, Salvi RJ (2012). Understanding tinnitus: The dorsal cochlear nucleus, organization and plasticity. *Brain Res* 2012 Mar 27.

Bi G, Poo M (2001). Synaptic modification by correlated activity: Hebb's postulate revisited. *Annu Rev Neurosci* 24:139-66.

Browne CJ, Morley JW, Parsons CH (2012). Tracking the expression of excitatory and inhibitory neurotransmission-related proteins and neuroplasticity markers after noise induced hearing loss. *PLoS One* 7(3):e33272.

Caporale N, Dan Y (2008). Spike timing-dependent plasticity: a Hebbian learning rule. *Annu Rev Neurosci* 31:25-46.

Chen GD, Jastreboff PJ (1995). Salicylate-induced abnormal activity in the inferior colliculus of rats. *Hear Res* 82(2):158-78.

Chrostowski M, Stolzberg D, Becker S, Bruce IC, Salvi RJ (in revision). A potential role for homeostatic plasticity in adult primary auditory cortex. *J Neurophys* JN-00205-2012.

Chrostowski M, Yang L, Wilson HR, Bruce IC, Becker S (2011). Can homeostatic plasticity in deafferented primary auditory cortex lead to traveling waves of excitation? *J Comput Neurosci* 30:279-299.

Dahmen JC, Hartley DE, King AJ (2008). Stimulus-timing-dependent plasticity of cortical frequency representation. *J Neurosci* 28(50):13629-39.

Davis PB, Wilde RA, Steed LG, Hanley PJ (2008). Treatment of tinnitus with a customized acoustic neural stimulus: a controlled clinical study. *Ear Nose Throat* 87, 330e339.

Dohrmann K, Weisz N, Schlee W, Hartmann T, Elbert T (2007). Neurofeedback for treating tinnitus. *Prog Brain Res* 166:473-85.

Eggermont JJ, Roberts LE (2004). The neuroscience of tinnitus. *Trends Neurosci* 27:676-682.

Engineer ND, Riley JR, Seale JD, Vrana WA, Shetake JA, Sudanagunta SP, Borland MS, and Kilgard MP (2011). Reversing pathological neural activity using targeted plasticity. *Nature* 470: 101-104.

Feldman DE (2009). Synaptic mechanisms for plasticity in neocortex. *Annu Rev Neurosci* 32:33-55.

Garin P, Gilain C, Van Damme JP, de Fays K, Jamart J, Ossemann M, Vandermeeren Y (2011). Short- and long-lasting tinnitus relief induced by transcranial direct current stimulation. *J Neurol* 258(11):1940-8.

Goel A, Lee H-kyoung (2007). Persistence of experience-induced homeostatic synaptic plasticity through adulthood in superficial layers of mouse visual cortex. *J Neurosci* 27:6692- 6700.

Hartmann K, Bruehl C, Golovko T, Draguhn A (2008). Fast Homeostatic Plasticity of Inhibition via Activity- Dependent Vesicular Filling. *PLoS ONE* 3:e2979.

Hoare DJ, Kowalkowski VL, Kang S, Hall DA. (2011). Systematic review and meta-analyses of randomized controlled trials examining tinnitus management. *Laryngoscope* 121(7):1555-64.

Hoke M, Pantev C, Lütkenhöner B, Lehnertz K (1991). Auditory cortical basis of tinnitus. *Acta Otolaryngol Suppl* 491:176-81.

Ibata K, Sun Q, Turrigiano GG (2008). Report Rapid Synaptic Scaling Induced by Changes in Postsynaptic Firing. *Neuron* 819-826.

Kahlbrock N, Weisz N (2008). Transient reduction of tinnitus intensity is marked by concomitant reductions of delta band power. *BMC Biol.* Jan 16;6:4.

Kotak VC, Fujisawa S, Lee FA, Karthikeyan O, Aoki C, Sanes DH (2005). Hearing loss raises excitability in the auditory cortex. *J Neurosci* 25:3908-18.

Kraus KS, Canlon B. (2012). Neuronal connectivity and interactions between the auditory and limbic systems. Effects of noise and tinnitus. *Hear Res* 288(1-2):34-46.

Lehner A, Schecklmann M, Landgrebe M, Kreuzer PM, Poeppl TB, Frank E, Vielsmeier V, Kleinjung T, Rupprecht R, Langguth B (2012). Predictors for rTMS response in chronic tinnitus. *Front Syst Neurosci* 6:11.

Milbrandt JC, Holder TM, Wilson MC, Salvi RJ, Caspary DM, (2000). GAD levels and muscimol binding in rat inferior colliculus following acoustic trauma. *Hear Res* 147, 251-260.

Mühlnickel W, Elbert T, Taub E, and Flor H (1998). Reorganization of auditory cortex in tinnitus. *Proc Natl Acad Sci* 95: 10340-10343.

Noreña AJ, Tomita M, Eggermont JJ (2003). Neural changes in cat auditory cortex after a transient pure-tone trauma. *J Neurophysiol* 90:2387-401.

Noreña AJ, Eggermont JJ (2003). Changes in spontaneous neural activity immediately after an acoustic trauma: implications for neural correlates of tinnitus. *Hear Res* 183:137-153.

Noreña AJ (2011). An integrative model of tinnitus based on a central gain controlling neural sensitivity. *Neurosci Biobehav Rev* 35(5):1089-109.

Pantev C, Okamoto H, Teismann H. (2012). Tinnitus: the dark side of the auditory cortex plasticity. *Ann N Y Acad Sci* 1252:253-8.

Rajan R, Irvine DR, Wise LZ, Heil P (1993). Effect of unilateral partial cochlear lesions in adult cats on the representation of lesioned and unlesioned cochleas in primary auditory cortex. *J Comp Neurol* 338:17– 49.

Rajan R (1998). Receptor organ damage causes loss of cortical surround inhibition without topographic map plasticity. *Nat Neurosci* 1(2):138-43.

Rajan R (2001) Plasticity of excitation and inhibition in the receptive field of primary auditory cortical neurons after limited receptor organ damage. *Cereb Cortex* 11(2):171-82.

Roberts LE, Bosnyak DJ, Thompson DC (2012). Neural plasticity expressed in central auditory structures with and without tinnitus. *Front Syst Neurosci* 6:40.

Robertson D, Irvine DRF (1989). Plasticity of frequency organization in auditory cortex of guinea pigs with partial unilateral deafness. *J Comp Neurol* 282:456–471.

Schaette R, Kempter R (2006). Development of tinnitus-related neuronal hyperactivity through homeostatic plasticity after hearing loss: a computational model. *Eur J Neurosci* 23(11):3124-38.

Schaette R, Konig O, Hornig D, Gross M, and Kempter R (2010). Acoustic stimulation treatments against tinnitus could be most effective when tinnitus pitch is within the stimulated frequency range. *Hear Res* 269: 95-101.

Schaette R, Kempter R. (2012). Computational models of neurophysiological correlates of tinnitus. *Front Syst Neurosci* 6:34.

Seki S, Eggermont JJ (2002). Changes in cat primary auditory cortex after minor-to-moderate pure-tone induced hearing loss. *Hear Res* 173(1-2):172-86.

Seki S, Eggermont JJ (2003). Changes in spontaneous firing rate and neural synchrony in cat primary auditory cortex after localized tone-induced hearing loss. *Hear Res* 180:28-38.

Stolzberg D, Chrostowski M, Salvi R, Allman B (2012). Intracortical circuits amplify sound-evoked activity in primary auditory cortex following systemic injection of salicylate in the rat. *J Neurophys* 108(1):200-14.

Turrigiano GG, Leslie KR, Desai NS, Rutherford LC, Nelson SB (1998). Activity-dependent scaling of quantal amplitude in neocortical neurons. *Nature* 391:892-895.

Turrigiano GG (1999). Homeostatic plasticity in neuronal networks : the more things change, the more they stay the same. *Trends Neurosci* 22:221-227.

Wang H, Brozoski TJ, Caspary DM (2011). Inhibitory neurotransmission in animal models of tinnitus: maladaptive plasticity. *Hear Res* 279(1-2):111-7.

Wehr M, Zador AM (2003). Balanced inhibition underlies tuning and sharpens spike timing in auditory cortex. *Nature* 426:442-446

Weisz N, Moratti S, Meinzer M, Dohrmann K, Elbert T (2005). Tinnitus perception and distress is related to abnormal spontaneous brain activity as measured by magnetoencephalography. *PLoS Med* 2(6):e153.

Weisz N, Müller S, Schlee W, Dohrmann K, Hartmann T, Elbert T (2007). The neural code of auditory phantom perception. *J Neurosci* 27(6):1479-84.

Yang S, Weiner BD, Zhang LS, Cho S-J, Bao S (2011). Homeotatic plasticity drives tinnitus perception in an animal model. *Proc Natl Acad Sci* 108:14974-14978.

Zilany MSA, Bruce IC, Nelson PC, Carney LH (2009). A phenomenological model of the synapse between the inner hair cell and auditory nerve: Long-term adaptation with power-law dynamics. *J Acoust Soc Am* 126(5):2390–2412.